FOREIGN
BROADCAST
INFORMATION
SERVICE

JPRS Report

Science & Technology

Japan
32nd Space S&T Conference

19980129 103

Science & Technology

Japan

32nd Space S&T Conference

CONTENTS

Development of Rail Gun Reported

*43062505a Tokyo PROCEEDINGS OF THE 32ND
SPACE SCIENCES & TECHNOLOGY
CONFERENCE in Japanese 26-28 Oct 88, No 1A12,
pp 34-35*

[Article by Keiichi Satoh of the Institute of Space and
Astronautical Science: "Mass Driver"]

[Text] 1. Preface

An electromagnetic launch technology is used to accel-
erate objects with mass by means of electromagnetic
force. When this technology is used for transportation in
space, it is referred to as a "mass driver." It has generally
been used in linear motors up to now, but recently, the
development of accelerators based on a rail gun system
has been carried out enthusiastically. Since fiscal 1986,
the Institute of Space and Astronautical Science [ISAS]
has been developing a rail gun for application to scien-
tific fields. In this paper, I will report the results of the
development-related work.

2. Principle of Rail Gun

In the rail gun, an object called a "projectile," which will
be accelerated, is put between two rails, and a portion
called an "armature," which conducts electricity, is at
the back of the projectile. As shown in Figure 1, electric
current passes through the rails, and the projectile and
armature are accelerated by the magnetic field generated
by the electric current in the rails and Lorentz's force
caused by the electric current in the armature.
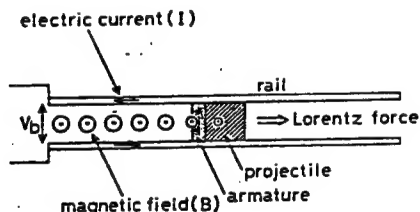
Figure 1. Principle of Rail Gun

3. Rail Gun System

3.1 Rail Gun

Figure 2 shows a cross section of the rail gun used by the
ISAS. Two copper rails are surrounded by insulators,
clipped longitudinally and laterally with steel blocks, and
tightened with bolts.

3.2 Projectile

The projectile is a block of polycarbonate resin weighing
about 1 gram, and is shaped to fit into the bore snugly.
The projectile has an aluminum or phosphor bronze fuse
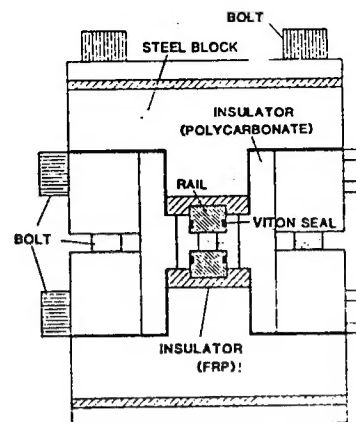
Figure 2. Cross Section of Rail Gun
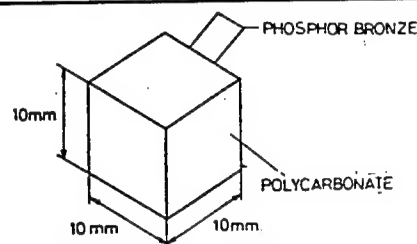
Figure 3. Projectile

on its back side and, as soon as the fuse discharges
electricity, it melts, turns to plasma, and conducts elec-
tricity as an armature.

3.3 Power Source

As shown in Figure 4, the power source of the ISAS
consists of a 4:1 pulse transformer, main switch, crowbar
switch, and six-stage-pulse-forming network. Each stage
of the six-stage-pulse-forming network consists of a
capacitor and inductor. The power of the capacitor at
each stage is 1 millifarad, and the maximum charging
voltage is 10 kilovolts. Therefore, the total capacity is 6
millifarads and the maximum charging energy is 300
kilojoules. The power of the inductor can be changed
from 0 to 24 microhenrys, and the waveform of the
electric current can also be changed.
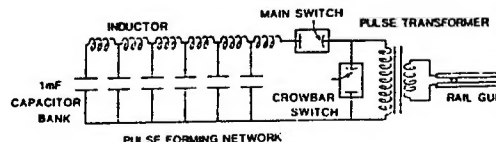
Figure 4. Circuit Diagram of Power Supply

4. Results

Figure 5 [not reproduced] is a streak photograph showing the plasma luminescing state in the rail gun. The left side of the plasma luminescing state is a curve, and is represented by a trace at the inside of the rail gun. Figure 6 shows examples of the electric current waveform, velocity and acceleration at the inside of the rail gun. The velocity and acceleration are calculated on the basis of the streak photograph shown in Figure 5
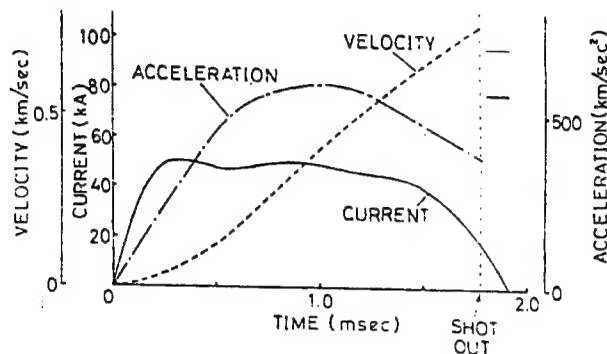
Figure 6. Performance of Low Energy Rail Gun

The ISAS has successfully accelerated a projectile weighing approximately 1 gram to about 3.7 kilometers per second. The charging velocity at that time was 7 kilovolts. Assuming that the efficiency of the entire system is (kinetic energy)/(energy charged in capacitor), the efficiency of the entire system at that time is about 5 percent.

Transportation System After H-II Rocket, HOPE

43062505b Tokyo PROCEEDINGS OF THE 32ND SPACE SCIENCES & TECHNOLOGY CONFERENCE in Japanese 26-28 Oct 88, No 1A13, pp 36-37

[Article by Yoji Shibafuji of the National Space Development Agency of Japan]

[Text] 1. Preface

The National Space Development Agency of Japan [NASDA] has been conducting the development of the H-II rocket smoothly so that the first rocket can be launched in 1992. The advent of the H-II rocket represents a means of transportation at the international level in terms of launching performance, reliability and cost. In addition, HOPE, which is an unmanned space plane, will be launched with the H-II rocket and, similarly to the space shuttle, will return to earth. NASDA is currently conducting research on HOPE, and has scheduled its first flight for sometime around 1996. The space transportation of the 1990s will be carried out by the H-II rocket and HOPE. Accordingly, the demand for space transportation will increase, and an economical

launching means will be required for the space transportation. In this paper, I will present a concept of the space transportation system after the H-II rocket and HOPE.

2. H-II Rocket (Improved Model) and HOPE

The H-II rocket has a launching capacity of 4 tons to geostationary transfer orbits and of about 10 tons to low altitude orbits, and it is possible that the H-II rocket can be used to simultaneously launch a number of small satellites. The most important points in the development of the H-II rocket are as follows: 1) the H-II rocket must be developed only by using completely independent technologies, 2) the development cost must be at the same level as the cost required for satellites which will be launched using international rockets in the 1990s, and 3) the H-II rocket must offer high reliability and minimum failure when launching satellites. The H-II rocket will be used to supply materials to the space station and to launch HOPE, as well as to launch platforms and satellites for communications, broadcasting, earth observation and space experiment missions.

HOPE, an unmanned space plane, is being researched so that it can be launched without having to make any
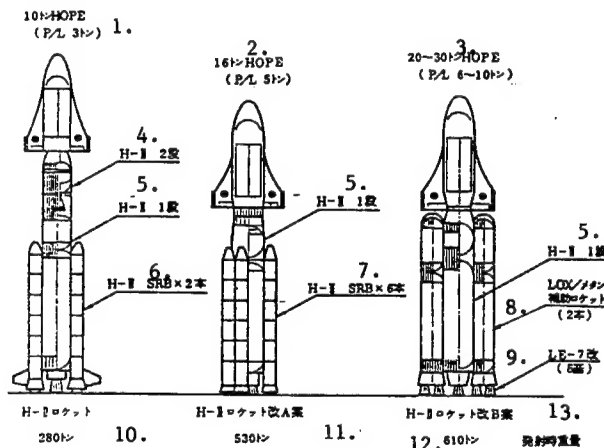
Figure 1. Examples of H-II Rocket (Including Improved Model) and HOPE

Key:
1. 10-ton HOPE (P/L 3 tons)
2. 16-ton HOPE (P/L 5 tons)
3. 20- to 30-ton HOPE (P/L 6 to 10 tons)
4. H-II two stages
5. H-II one stage
6. H-II SRB x 2
7. H-II SRB x 6
8. LOX/two methane strap on boosters
9. 8 LE-7s (improved)
10. 280-ton H-II rocket
11. 530-ton H-II rocket version A plan
12. 610-ton H-II rocket version B plan
13. Weight at launch time
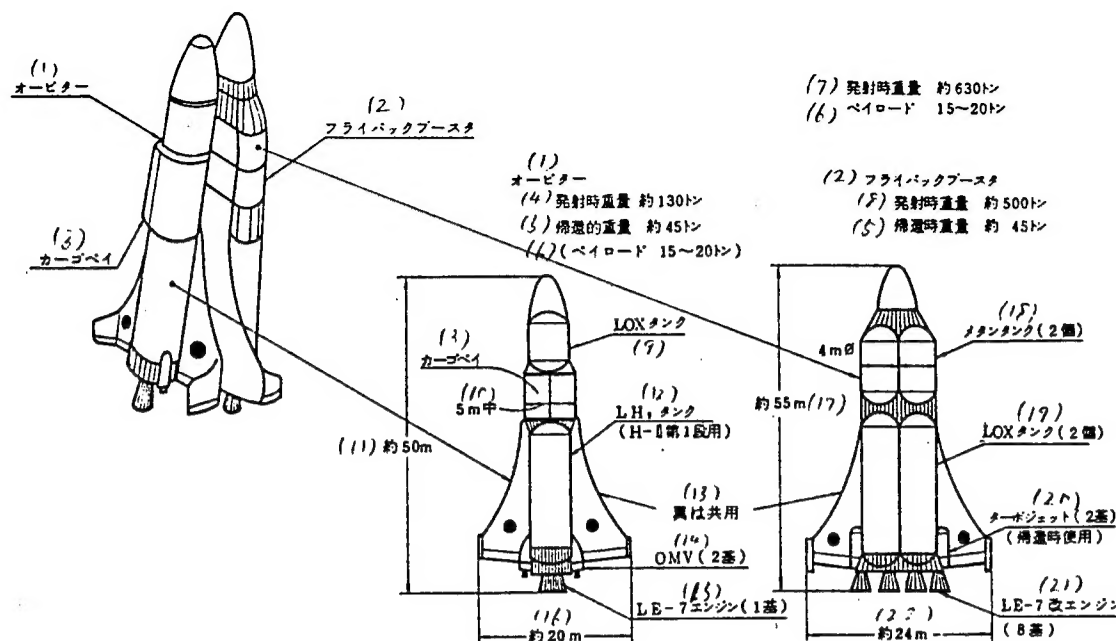
Figure 2. Vertical Take-off Reusable Two-Stage Rocket (Plan)

Key:
1. Orbiter
2. Flyback booster
3. Cargo bay 4. Weight at launch time: approximately 130 tons
5. Weight at returning time: approximately 45 tons
6. Payload: 15 to 20 tons
7. Weight at launch time: approximately 630 tons
8. Weight at launch time: approximately 500 tons
9. LOX tank
10. Within 5 meters
11. Approximately 50 meters

12. LH$_2$ tank (for the first stage of H-II)
13. Wings are for common use
14. Two OMVs
15. One LE-7 engine
16. Approximately 20 meters
17. Approximately 55 meters
18. Two methane tanks
19. Two LOX tanks
20. Two turbojets (used upon returning)
21. Eight LE-7 version engines
22. Approximately 24 meters

substantial improvements on the H-II rocket. Therefore, the weight of HOPE when launched will be approximately 10 tons, while that of the cargoes will be about 3 tons. It should be possible for HOPE to stay in space for approximately 1 week.

In the late 1990s, a further improved version of the H-II rocket could be used to meet the increase in demand for launching satellites and the decrease in the cost of rockets. The H-II rocket has a characteristic that makes it relatively easy to raise its performance. As shown in Figure 1, if the number of solid rockets is increased to six, the satellite launching capacity will be doubled, increasing to 4 tons. Also, even if two stages are removed from the H-II rocket due to a low altitude orbit, it will still be possible to launch cargoes weighing 16 tons, and the launching capacity will be increased by 60 percent following almost the identical course. There is an idea whereby liquid auxiliary rockets would be used instead of solid rockets. Figure 1 shows an example of using methane instead of liquid hydrogen by improving the

LE-7 at the first stage of the H-II rocket. If the size of the liquid auxiliary rockets is determined, it will be possible to transport cargoes weighing 20 to 30 tons to low altitude orbits and to decrease the cost per unit weight to from one-half to one-third.

3. Completely Reusable-Type Rocket

By the year 2000, Japan will have no choice but to meet her needs based on the H-II rocket and with a transportation systems augmented by HOPE. Throw-away-type rockets have their limits in respect to cost reduction. In order to meet the demand anticipated for the rockets which will be used subsequent to the year 2000, it will become necessary to reuse rockets. The single-stage-type horizontal take-off and landing plane can be cited as the ultimate completely reusable rocket, but it involves problems with funding as well as serious technical problems, such as with the air breathing engine and high heat resistant, lightweight materials. Accordingly, it will be impossible to use such completely reusable rockets before 2010. In addition, it will become necessary to use a stopgap transportation system

while the technologies obtained from the development of the H-II rocket, HOPE, etc., are being extended, until the single-stage-type horizontal take-off and landing plane is realized. The two-stage vertical launching and horizontal landing-type rocket system shown in Figure 2 is regarded as a candidate for this stopgap transportation system. This idea is based on the idea of the H-II rocket (conceptual type) and HOPE shown in Figure 1, and can be realized by using the above technologies. The use of this system will enable transportation costs to be sharply reduced.

4. Postface

I have described an example of a completely reusable rocket which will meet the demands of space transportation around the year 2000. This rocket can be realized by fully utilizing the technologies obtained from the development of the H-II rocket and HOPE. I think that this concept is indispensable not only for meeting the demands of space transportation, but also for realizing future space planes and developing intermediate-stage technologies.

Solid Rocket Booster with Increased Performance Studied

43062505c Tokyo PROCEEDINGS OF THE 32ND SPACE SCIENCES & TECHNOLOGY CONFERENCE in Japanese 26-28 Oct 88, No 1A14, pp 38-39

[Article by Akihiro Eguchi and Hiroshi Miyama of NASDA; Noboru Onojima and Yoichi Yamamoto of Nissan Motor Co., Ltd.; and Toru Mitani of the National Aerospace Laboratory]

[Text] 1. Preface

The solid rocket booster [SRB] has been adopted for the H-II rocket, Titan and the space shuttle, which are used to launch large artificial satellites, and is scheduled to be used in ARIANE-5 in the future.

Most of the rockets make their flights in the atmospheric phase in which such SRBs are operated, and when these SRBs breathe air, it is possible to increase the thrust.

This manuscript describes a study of the validity of the following two systems: One is a system whereby thermal energy is generated from the air breathed by the SRB by mixing the air with high-temperature-rocket discharging gas, and is injected by accelerating this thermal energy, and the other is a system whereby air is accelerated and injected by positively and secondarily buring the air together with the rocket discharging gas.

2. Performance of Propulsion

The thrust to air-breathing-type rockets is given by the following equations: $F = (m_p + m_a)V_j - m_aV_a + A_e(P_e - P_a)$, where F is the thrust, m_a is the inflow rate of air, V_j is the jet injection relative velocity, m_p is the flow rate of the propellant, V_a is the flying speed, P_e is the nozzle outlet pressure and P_a is the atmospheric pressure, and
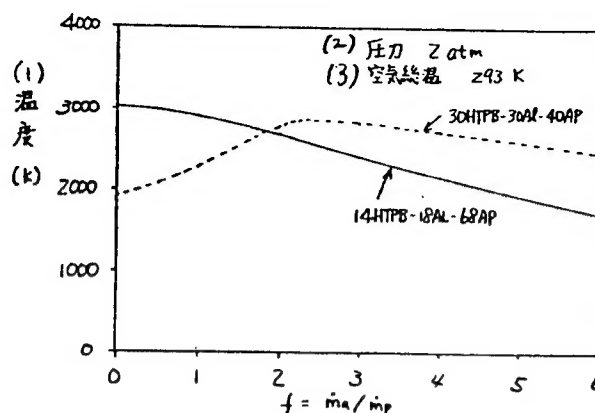
Figure 1. Secondary Combustion Gas Mixing with Air/Temperature

Key:
1. Temperature (Kelvin)
2. Pressure: 2 atm
3. Overall atmospheric temperature: 293 K

where V_j can be expressed as follows: $V_j = [2C_{p3}T_{o3}(1-P_e/P_{o3})(\gamma-1)/\gamma)]^{1/2}$. The index 3 shows the quantity of state of a throat which injects mixed gas. [In this paragraph, m has a dot over it; this is: first derivative with respect to time].

T_{o3} in the only mixing case is quite different from that in the secondary combustion case. A typical calculation example is shown in Figure 1. In the secondary combustion case, the amount of oxidizer for the solid propellant is decreased, while the amounts of HTPB and Al as fuels are increased. P_{o3} depends on the shapes of the air intake and of the mix/secondary combustion chamber.

$f = m_a/m_p$ refers to the air inflow ratio. Figure 2 shows the results obtained from a specific impulse calculated for the condition $P_e = P_a$ by regarding the air inflow ratio
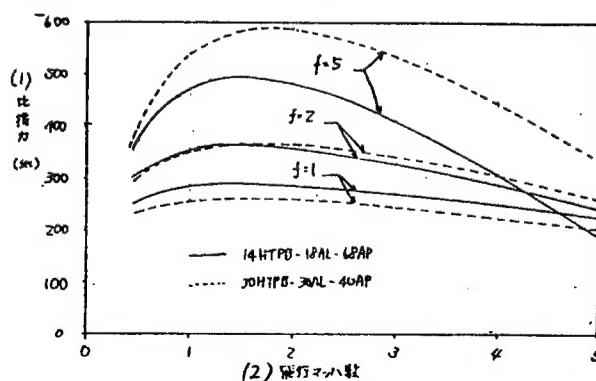
Figure 2. Flight Mach Number and Specific Impulse

Key:
1. Specific impulse (seconds)
2. Flight Mach number

as a parameter. In the secondary combustion case, the specific impulse is increased in proportion to the increase in f. However, when f is low, the specific impulse is lower than that in the mixing case.

Accordingly, the combustion system appropriate for f is regarded as effective.

3. Launching Orbit

The performance of air-breathing-type rockets also changes since the atmospheric density and Mach number change with time during actual orbit launchings. It is necessary to comprehensively evaluate the gravity loss, air resistance, etc., when launching, but it is preferable that such rockets make their flights at a Mach number that will cause the highest specific impulse to occur at each altitude. Rockets in which no lift can be used have limits when approaching the ideal since orbits cannot but be changed slightly by the thrust profile.

Figure 3 shows results obtained by calculating orbits on the assumption that a nozzle of the SRB of the H-II rocket is converted into an air-mixing-type nozzle. These results show a flight profile in which the thrust can be increased, and it has been confirmed that this flight profile contributes to an increase in capacity when launching satellites. In addition, it is believed that this capacity can be increased further by studying the slot ring of core rockets, the thrust profile of the SRB, etc.

Figure 4. Conceptual Drawing of Basic Test

Key:
1. Load cell
2. Air plenum chamber
3. Mixing/secondary combustion chamber
4. Solid motor

Study of Weight of AOTV Aerobrake

[Article by Tsutomu Iwata of National Space Development Agency of Japan; Sumio Kato, Hiroshi Oda and Nobuyoshi Muroi of Kawasaki Heavy Industries, Ltd.]

[Text] 1. Preface

The orbital transfer vehicle [OTV] is one of the most important elements of the future space infrastructure. When orbits at high altitudes are changed to ones at low altitudes through atmospheric control by means of an aerobrake, it is possible to sharply economize the transfer of orbit fuel. The aero-assisted orbital transfer vehicle [AOTV] refers to an OTV equipped with an aerobrake to utilize the atmospheric braking power. Recently, research involving the AOTV has been conducted enthusiastically. In this paper, we will describe the results of parametrically studying the load of aerobrakes, etc., based on the load and heating conditions, etc., upon entering the atmosphere on the assumption that an OTV is returning from geostationary transfer orbit [GEO] to a low earth orbit [LEO].

Figure 3. Launch Orbit and Increase in Thrust

Key:
1. Altitude (kilometers)
2. Increase in thrust
3. Flight Mach number

4. Conclusion

It has been confirmed that the use of air-breathing-type rockets would raise the performance of the SRB. In the future, we are scheduled to continue analyses and studies of rises in performance of such SRBs, while examining the increase in thrust by the basic test shown in Figure 4.

2. Validity of Aerobrake

Figure 1 shows the relationship between the structure and difference of the fuel ratio ($\mu_2 - \mu_1$) and the fuel weight ratio of the AOTV and an all-propulsion-type OTV for three kinds of missions—GEO delivery, round-trip transportation, and retrieval. When an aerobrake is used to control the atmosphere, it can be appreciated that if the $\mu_2 - \mu_1$ is less than approximately 0.1 for the GEO round-trip transportation and GEO retrieval missions, the fuel weight will be less than half that of the all-propulsion-type OTV.
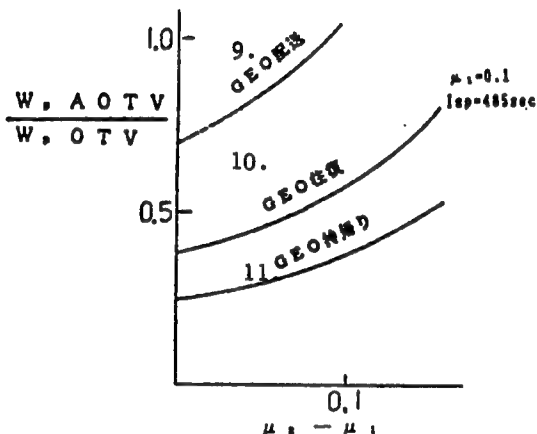
Figure 1. Fuel Weight Ratio of AOTV/OTV

Key:
1. Delivery to GEO: P/L is positioned from LEO to GEO, and the sole OTV returns to LEO at an altitude of 500 km.
2. Round trip to GEO: P/L is transported from LEO to GEO, and OTV, with P/L, returns to LEO at an altitude of 500 km.
3. Return to GEO: The sole OTV transfers from LEO to GEO and, with P/L, returns from GEO to LEO.
4. μ_1: W_s/W_p of total-propulsion-type OTV
5. μ_2: W_s/W_p of AOTV
6. W_s: Fuel, structure, etc., except for P/L 7. W_p: Weight of fuel
8. P/L: Weight of payload
9. Delivery to GEO
10. Round-trip to GEO
11. Return to GEO

3. Load Conditions at Atmospheric Entry

Studies were conducted involving the loads, such as acceleration, g and aerodynamic heating, imposed on the aerobrake when the AOTV passes through the atmosphere. As an example, Figure 2 shows that results of calculating g.

4. Study of Weight of Aerobrake

(1) Study Conditions

An aerobrake employing a lifting brake system is circular, and consists of a thermal protection system [TPS]
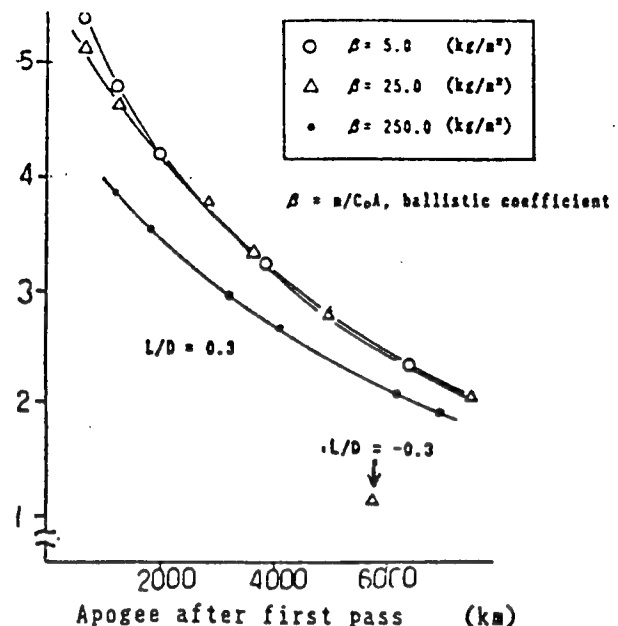
Figure 2. G and Apogee Altitude After Passing Through Atmosphere

and a supporting structure. The supporting structure is a tetrahedral truss, and is made of Al or Gr/Pi. Table 1 shows the above conditions as well as other ones.

(2) Weight of TPS

Figure 3 shows the results obtained by simulating thermal environments when the OTV enters the atmosphere, conducting non-stationary thermal analyses of two kinds of TPS materials, and finding the relationship between the weight of the TPS and the maximum heat flux. It can be appreciated that the weight of the TPS when Gr/Pi is used in the supporting materials is about half that of the TPS when Al is utilized in such materials.

(3) Weight of Aerobrake

When the rocket enters the atmosphere, the supporting structure (truss) of the aerobrake will be subjected to a bending load according to the acceleration, g, and the buckling of each member will be critical. The weight of the aerobrake was determined by selecting the dimensional accuracy of the truss on the basis of this buckling load, calculating the weight, and adding the TPS weight to the calculated weight. The diameter, height of the truss, acceleration, etc., are taken as parameters. Figure 4 shows an example of calculating the brake weight when the diameter of the brake is measured on the transverse axis.

(4) Policy of Aerobrake Lightening

The load conditions (load and heating quantity), operation methods (number of passages through the atmosphere, etc.), aerodynamic characteristics, aerobrake

Table 1. Conditions of Aerobrake Weight Study

Key:
1. Support structure material
2. Aerobrake
3. Progressive direction
4. Bus
5. Payload
6. Item
7. Contents
8. Standard form
9. Lifting brake system
10. Aerobrake specifications
11. Form
12. Circle (diameter Dmφ)
13. Constitution
14. TPS + support structure material
15. Support structure
16. Structural system
17. Material
18. Tetrahedral truss
19. Al or Cr/Pi
20. ACC + insulator, ceramic tile (LI-900), Lightweight TPS
21. Payload/propulsion system
22. Orbit
23. Return orbit from GEO to LEO at altitude of 500 km
24. Load (α)
25. Approx. 0 to 4 grams
26. Thermal load

Figure 3. Relationship Between TPS Weight and Maximum Heat Flux

Key:
1. TPS weight (kg/m^2)
2. Maximum heat flux Q_{max} (W/cm^2)
3. ACC + insulation
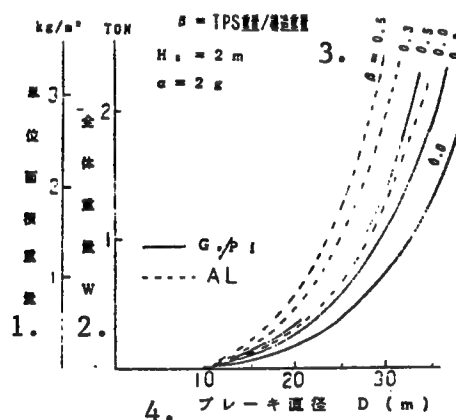
Figure 4. Relationship Between Aerobrake Weight and Diameter

Key:
1. Unit area weiht
2. Overall weight
3. β = TPS weight/structural weight
4. Brake diameter D (meters)

system, structural design (dimensional accuracy, etc.), TPS, etc., can be cited as items which should be studied in order to lighten the aerobrake.

(5) Postface

The validity of the aerobrake has been shown, and the weight studied parametrically. Importance is attached to the structure and weight of the aerobrake and, in order to realize the AOTV in the future, it is essentially necessary to study the aerodynamic, thermal protective, and guidance and control technologies, etc.

Solar Thermal Rocket Studied as Transfer Between Orbit Propulsion Systems

43062505e Tokyo PROCEEDINGS OF THE 32ND SPACE SCIENCES & TECHNOLOGY CONFERENCE in Japanese 26-28 Oct 88, No 1A16, pp 42-43

[Article by Morio Shimizu, Katsuya Ito and Yasuo Watanabe of the National Aerospace Laboratory]

[Text] 1. Preface

Recently, the solar thermal rocket has been reviewed as a propulsion system for OTVs. This rocket possesses

characteristics midway between those of conventional chemical rockets and ion rockets. The AFAL (formerly AFRPL [Air Force Rocket Propulsion Laboratory]) has conducted research on high performance rockets.[1, 2] Such rockets have a specific impulse of 800 seconds or more and a hydrogen temperature of 2,300 K or more.

The NAL [National Aerospace Laboratory] has completed a rocket with a hydrogen temperature of 1,100 K and a specific impulse of 500 second-class, as a preliminary stage,[3] and has begun researching a higher performance rocket with a specific impulse of 650 to 800 seconds. The specific impulse of this rocket is more than twice that of conventional apogee propulsion system rockets. If the new rocket is used for OTVs, it can be expected that the performance will increase sharply. We will now describe the advantages and problems involved in its use for OTVs, and its development for application to AOTVs.

2. System and Performance of Solar Thermal Rocket

The solar thermal rocket has a simple structure, i.e., a system is employed whereby propellants are concentrated from the sun, heated and injected. It involves no special technical problems other than measuring for high temperatures for the heat collecting portion. As shown in Figure 1, the merits of this rocket are as follows: 1) the specific impulse is 500 to 1,000 seconds, which is higher than that of chemical propulsion system rockets, 2) the efficiency when using solar energy is 10 times that of electric propulsion system rockets, 3) relatively large thrust (1 to 10 newtons) can be obtained, and 4) the rocket is not contaminated in space. On the other hand, the main disadvantages of the rocket are as follows: 1) there is a limit to the degree of freedom of the relationship between the solar direction
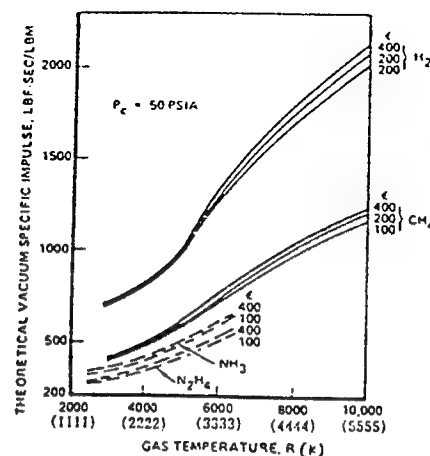
Figure 1. Theoretical Vacuum Specific Impulse Variation[1]

and the injecting direction, and 2) the rocket must be equipped with a large liquid hydrogen tank and a solar concentrator.

3. Use of Solar Thermal Rocket in OTVs, etc.

Table 1 compares performances of propulsion systems for various OTVs according to AFAL and based on the space shuttle. There is little difference between the solar thermal rocket and liquid oxygen/hydrogen rocket in terms of spiral lasing (solar No 1), but for the case of multi-burn (solar No 2), the geostationary payload capacity (47 percent of LEO mass) of the solar thermal rocket is increased by 42 percent, which is two or three times that (18 percent of LEO mass) of the current solid rockets and monomethyl hydrazine-nitrogen tetra oxide [MMH-NTO] rockets.

Table 1.
Comparison of Various OTV Propulsion System Performances[1]

Parameter	Solar #1	LO_2-LH_2	N_2O_4-MMH	Ion	Solar #2
V, m/s	5,850	4,270	4,270	5,850	4,800
Trip time	14 days	5 hours	5 hours	180 days	40 days
Isp, sec	872	475	320	2,940	872
Mass Fraction	0.85	0.90	0.92	0.68	0.85
Payload, kg	9,300	9,250	4,990	19,960	13,150

Figure 2 shows a Japanese 16 ton-class geostationary platform.[5] It has two large antennas with diameters of 30 meters which, if used as solar concentrating parabolic antennas with the solar thermal rocket, will enable the solar thermal rocket to be lightened. It also appears that, if the solar cells are attached to the back of these solar concentrating parabolic antennas, they can be used with solar cell paddles. In this case, the propulsion system would be assembled on the platform. It is also preferable to use the concentrator for generating solar heat as the propulsion

system for a space station. These are shown in Table 2. In addition, if the round-trip-type OTV is used as an AOTV system, it could be possible to employ an altitude of approximately 150 kilometers with a very small amount of aerodynamic heating as a perigee and the back side of the solar concentrating parabolic antenna as an aerodynamic brake. In this case, the OTV would return from the geostationary transfer orbit [GTO] to the LEO over a period of approximately 20 days as a multi-pass system passing through the perigee 100 times.

Table 2.
Performance of Solar Heat Rocket at Stationary Platform, etc.

	Stationary Platform (GPF)	Common Orbit Platform (ATP)	SS
Launch period	1995	1995	1993 to 1996 (phase I)
Weight (kg)	16	8.3 (PM 0.7, F 0.8)	260 (phase II)
Large parabolic antennas	30 m in diameter, 2	Nil (1 m in diam, 2)	15 m in diameter, 2 (for generating solar heat)
Orbit	GEO	Approx. 500 km	Approx. 500 km
Solar ray input	Approx. 2,000	(2.2)	513
Thrust (Newton) of solar heat rocket (Isp = 650 s)	300	(0.33)	77
Others	LED → GEO 20 days	Uncontaminated thruster preferable to high Isp and large thrust	Satisfies a maximum thrust of 45 Newtons or more as an SS propulsion system
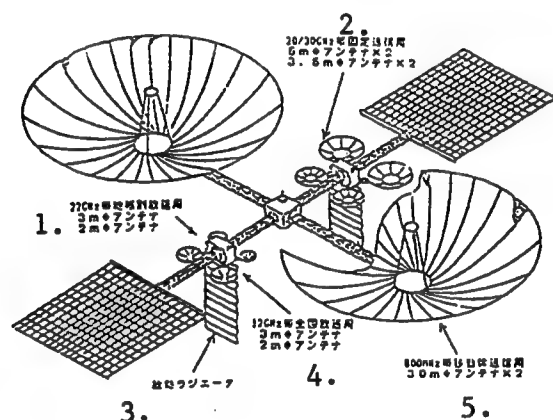
Figure 2. An Example of 16-Ton-Class GPF[5]

Key:
1. Antennas with diameters of 2 and 3 meters for broadcasting by 22 Cmz band areas
2. Two antennas with diameters of 6 meters and two antennas 3.5 meters in diameter for 20/30 Cmz-band-fixed communications
3. Heat radiator
4. Antenna with a diameter of 3 meters and antenna with diameter of 2 meters for 12Cmz-band nationwide broadcasting
5. Two antennas with diameters of 30 meters for 800 MHz-band vehicular communications

References

1. Etheridge, F., "Solar Rocket System Analysis," AD-A0792117, Dec 1979

2. Shoji, J.M., "Solar Thermal Propulsion for Orbit Transfer," AIAA-88-3171

3. Shimizu, et al., "Trial Manufacturing of Solar Thermal Thruster," Part 1, Space Transportation Symposium held in fiscal 1987, p 24

4. Shimizu, et al., "Solar Thermal Rocket as an Upper State Propulsion System," Proceedings of the 31st Space Sciences and Technology Conference, p 520

5. Takashi Hamasaki, "Papers of the Third Space Station Lecture Meeting," 1987 p 97

Superhigh Accuracy Sun Sensor Mounted on SOLAR-A

43062505f Tokyo PROCEEDINGS OF THE 32ND SPACE SCIENCES & TECHNOLOGY CONFERENCE in Japanese 26-28 Oct 88, No 1D3, pp 116-117

[Article by Keiken Ninomiya, Yoshiaki Ogawahara and Eiji Hirokawa of the Institute of Space and Astronautical Science; Fumihiko Okamoto, Katsuhiko Tsuno, Satoru Akabane and Yoshihiko Kameda of Toshiba Corporation]

[Text] 1. Preface

The development of a sun sensor is being conducted as an attitude sensor mounted on the SOLAR-A, a scientific satellite. The accuracy of this sensor is higher than that of conventional sensors. This is attributable to the fact that high control performance is required for the attitude system so that the view direction of the mission equipment can be turned toward the solar center. This mission equipment will be used to observe solar flares. Research on the sun sensor is being carried out so that an accuracy of at least 0.0035° can be obtained for a view of 2° x 2°. Therefore, a system in which repeated reticles and a linear-charged coupled device [CCD] are used as the sensors was adopted for use in the scientific satellite. This report introduces the outline and main data of a sun sensor (two-dimensional fine sun sensor [TFSS]), as well as the test results of its trial-manufactured product.

2. Outline and Main Data on Sensor

The TFSS is a two-axial sensor, consisting of a sensor section and an electronic circuit section. It differs from that employing a wide-view-type system (see Ref. 1) in its performance raising capability, and a linear CCD is installed at the lower portion ofthe repeated reticles.

CCD signals which detect repeated patterns of solar images are compared with replica signals synchronized with reticles, as shown in Figure 1. The distance of the replica transferred when the phase difference = 0 is found as an incidence angle α by moving the replica so that the phase difference between signals is 0. Figure 2 shows a functional block diagram according to this phase difference feedback method. Additional details are given in Reference 2.
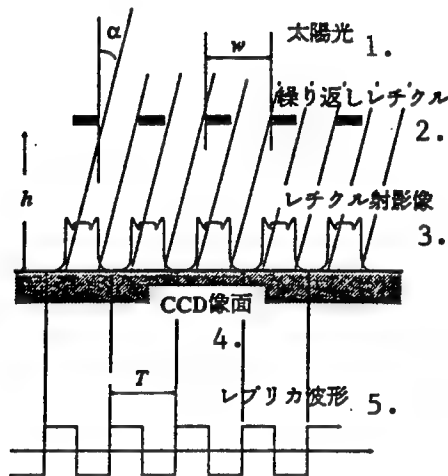
Figure 1. Principle Drawing

Key:
1. Solar beam
2. Repeated reticle
3. Reticle projecting image
4. CCD image surface
5. Replica waveform
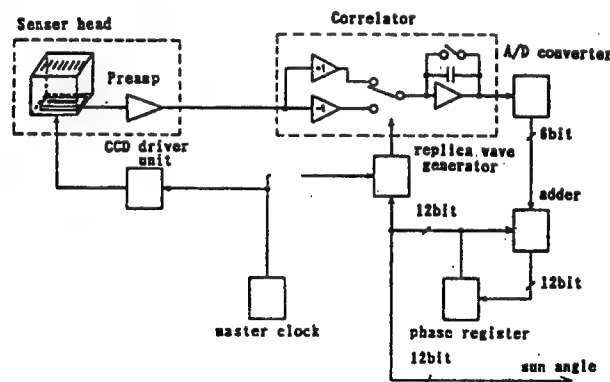
Figure 2. Functional Block Diagram

Features of this method are as follows:

• The processing is not affected by any profiles of diffraction images.
• The processing is not affected by any off-set signals (dark current, etc.,) of the CCD.

• The following influences can be reduced:
(1) Slit dimensions of reticles and deviation among slit intervals
(2) Sensitivity among CCD picture elements and unevenness of dark current

Main data on the TFSS are shown in Table 1.

Table 1. Main Data	
Visual field	plus/minus 1° x plus/minus 1°
Resolving power	0.00054°
Accuracy	Bias error: 0.0035°
	Random error: 0.003°
Weight	Sensor: 0.6 kg
	Circuit: 1.8 kg
External dimensions (mm)	Sensor: 65 x 116 x 76
	Circuit: 100 x 180 x 130
Power consumption	3.1 W

3. Trial Manufacturing and Testing

The sensor section shown in Photograph 1 [not reproduced] and an electronic circuit section were trial manufactured, and their characteristics were evaluated. The CCD was set by using the 2048 picture element so that one cycle w was the 128 picture element. The test was conducted by fixing the sensor section on the two-axial gimbals, and transfer characteristics of the TFSS were measured by the incident beams of a solar simulator in the sensor section.

Results are shown in Figure 3 (a) and (b). This figure confirms that the linearity (accuracy of approximately 0.001°) was excellent in linear areas and the random error was one least significant bit [LSB] (5.4 x 10^{-40} or less.

4. Postface

We have confirmed the propriety of the performance increase when using this method, and have seen our way clear to carrying out the development. In the future, we plan to conduct more detailed design and study projects, and to fully utilize the results obtained from this work in a flight model.

References

1. Ninomiya, K., et al., "CCD Fine Sencor for Scientific Satellites," ESA SP-255, Dec 1986

2. Ninomiya, K., et al., "High Accuracy Sun Sensor Using CCDs," Proceedings of AIAA GN&C Conference, Aug 1988
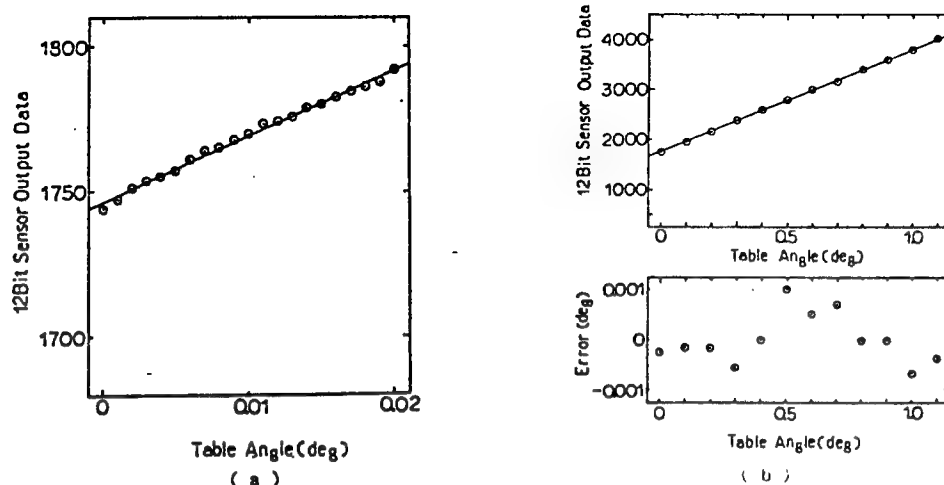
Figure 3. Transfer Characteristic Rate

MUSES-A Optical Navigation Sensor Developed

[Article by Keiken Ninomiya and Eiji Hirokawa of the
Institute of Space and Astronautical Science; Ryoichi
Chiba and Kazuhide Noguchi of NEC Corporation]

[Text] 1. Preface

The optical navigation sensor [ONS] reported below has
been mounted on the 13th scientific satellite, MUSES-A,
for the purpose of conducting device development tests.
A pulse frequency modulation [PFM] device is currently
being developed and manufactured. We have obtained
partial data on the performance tests conducted for the
ONS by simulating the moon and background fixed
stars, and will report it here.

2. Outline

Optical navigaton, as well as radio navigation, is impor-
tant for deep space exploration. Optical navigation is
used to photograph planets and their satellites together
with background fixed stars by means of television
cameras, etc., and to increase the relative position and
accuracy of probes for these planets and their satellites.
The ONS is mounted on the MUSES-A to aid in the
development of devices for use in optical navigation in
future deep space exploration and, after image data on
the moon and stars of the second magnitude or more are
obtained and converted into digital data, it is capable of
transferring the digital data to computers in the attitude
orbit control system. A schematic flow diagram of the
ONS is shown in Figure 1.

The ONS consists of a hood, optical section and electric
circuit section. The hood prevents the ONS from being
affected by solar beams, the optical section consists of
CCDs, lenses, etc., and the electric circuit section con-
verts the image data sent from the CCDs into digital
serial signals and transmits the digital serial signals to the
attitude orbit control system.

The time delay and integration [TDI] system was
adopted as a CCD driving system since the MUSES-A is
a spin satellite. In addition, separate CCDs for the moon
and stars have been installed independently in the
optical section and, after the image data obtained from
the optical section is A/D (analog-to-digital)-converted,
they are transmitted as pulse-code-modulation [PCM]
signals by means of optical fiber cables by way of the
processor and memory in the attitude orbit control
system to the ground and will be used as data for
controlling the satellite orbits.

3. Function, Performance, Appearance

Since the ONS employs the TDI system, the charge
transfer clock (V-CLOCK) corresponding to the spin rate
is input from the attitude orbit control system, the CCDs
for both the moon and stars are driven by synchronizing
them with this clock, and video signals sent from both
CCDs are selected using moon/star switching signals sent
from the attitude orbit control system. Dark current
components are removed by applying offset voltage to
this CCD output since the dark current is overlapped by
the CCD output. Subsequently, four-bit A/D conversion
is carried out in pixel units, image data obtained from
the four-bit A/D conversion is converted into serial PCM
signals by adding synchronous patterns to the image
data, and the image data is transmitted, using optical
fiber cables, to the attitude orbit control system by
driving a light emitting diode [LED] for transmitting
light. In addition, the electric circuit section employs a
power strobe control system which serves as a power
source for the circuits and is necessary only when image
data are obtained since power consumption must be
reduced. Table 1 presents the ONS specifications.

Figure 1. Schematic Flow Diagram of ONS

Key: 1. Hood   2. Optical section   3. Electrical circuit

Table 1. ONS Specifications

Angle of field	V direction: 7.3°
	H direction: 10.1°
Sensitivity	Moon image, detection of stars of the second magnitude or greater
Image data gradient	16 gradation (4-bits/pixel)
Conceivable spin rate scope	10.0 to 20.5 rpm
Image data transfer bit rate (ONS → attitude orbit control system)	14.96 MBPS (PCM data transmitting system according to optical fiber cables)
Performance maintaining temperature range	-20 to +45°C
Power consumption	OP: 11.5W
	STBY: 11.0W
	OFF: 0.1W
Weight	4.7 kg
ONS - O (Optical Section)	
Weight	1.75 kg
Form (exterior)	Shown in Figure 2 [not reproduced]
Lens aperture	40 mm
Focal length	50 mm
Detector	CCDI system for photographing moon
	CCDI system for photographing stars
ONS - H (Hood)	
Weight	0.65 kg
Form (exterior)	Shown in Figure 3 [not reproduced]
Solar ray interference angle	60° or greater (nominal)

Table 1. ONS Specifications (Continued)

Attenuation factor	10^{-8} or less (nominal)
ONS - E (Electric Circuit)	
Weight	2.3 kg

4. Results of Ground Tests

Figure 4 presents data (without TDI operation, use of shutter) obtained by inputting pseudo data equivalent to stars of the second and one-half magnitude from the background fixed star simulator. The data are almost the same as the design values in terms of the expansion of star images and levels. In the future, we plan to obtain detailed data by conducting spinning tests in which data will be obtained while spinning a three-axis motion table and by conducting field tests, etc., through which actual images of stars and the moon will be obtained.

Figure 4. Example of Obtained Data

5. Postface

This device has been subjected to vibration and impact tests and is being subjected to further detailed performance tests so that it can be mounted on the MUSES-A before its flight. We acknowledge our appreciation to the staff members concerned at Matsushita Research Institute Tokyo, Inc., and Mitaka Koki Co., Ltd., for their cooperation in respect to manufacturing the device.

Accurate Earth Sensor Research Model Developed

43062505h Tokyo PROCEEDINGS OF THE 32ND SPACE SCIENCES & TECHNOLOGY CONFERENCE in Japanese 26-28 Oct 88, No 1D5, pp 120-121

[Article by Fumio Takahashi, Toshihiro Kurii and Kenji Hiraishi of NEC Corporation; Norio Kimura and Kunio Nakamura of Matsushita Research Institute Tokyo, Inc.; Yasushi Wakabayashi and Hiroyuki Nakamura of the National Space Development Agency of Japan]

[Text] 1. Introduction

We have manufactured and evaluated an accurate earth sensor research model (BBM, shown in Figure 1 [not reproduced]) which is being developed as a main attitude sensor for the earth-oriented three-axis stable missile. The following outlines the results of our evaluations and tests of the BBM.

2. Outline of Accurate Earth Sensor

The accurate earth sensor is a scan-through type which detects roll and pitch attitude angles by scanning two instantaneous fields of view [IFOV]s of the earth, separated by 7.64°, in the east and west directions. This sensor has been designed based on the specifications shown in Table 1.

Table 1.
Main Specifications

Type	Scan-through system
Detection element	Lead titanate pyroelectric element
Wave band	14 to 16 μm
Scanning system	Mirror vibrating system
Data updating cycle	125 ms
Exterior dimensions	122 x 164 x 125 mm^3 (except for tube)
Weight	Approx. 2 kg
Power consumption	Approx 5 W
Designed life	10 years in orbit
Attitude angle detecting accuracy	0.03°

Figure 2 shows the functional block configuration of the accurate earth sensor broadly consisting of a vibration mechanism system, infrared photoelectric system, electronic circuit systemand power source circuit system.
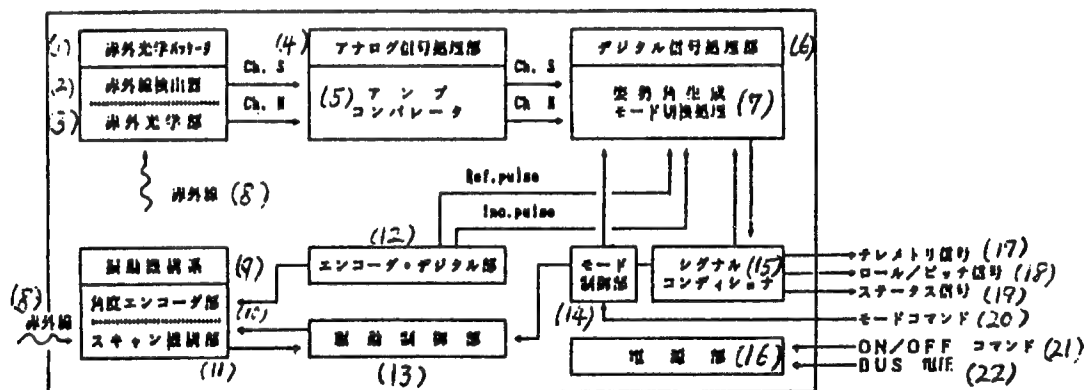
Figure 2. Functional Block Configuration

Key:
1. Infrared optical package
2. Infrared detector
3. Infrared optical section
4. Analog signal processing section
5. Amplifying converter
6. Digital signal processing section
7. Attitude angle formation mode switching
8. Infrared ray
9. Vibration mechanism
10. Angle encoder
11. Scan mechanism
12. Encoder and digital section
13. Driving control section
14. Mode control section
15. Signal conditioner
16. Power source
17. Telemetry signal
18. Roll/pitch signal
19. Status signal
20. Mode command
21. ON/OFF command
22. BUS voltage
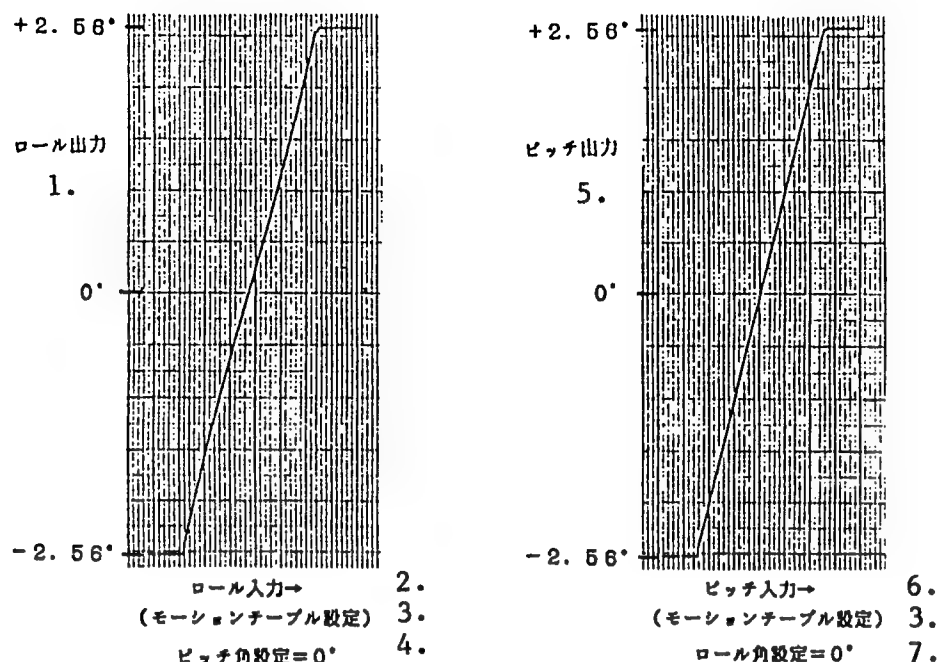
Figure 3. Roll/Pitch Transfer Characteristics (Geostationary Altitude)

Key:
1. Roll output
2. Roll input
3. (Establishment of motion table)
4. Establishment of pitch angle = 0°
5. Pitch output
6. Pitch input
7. Establishment of roll angle = 0°

The vibration mechanism system detects scan mirror supporting and rotating angles, the infrared photoelectric system converts and amplifies infrared photoelectrons, the electronic circuit system processes roll and pitch angle producing signals and carries out scan mirror driving control, etc., and the power source circuit system supplies electric power.

The evaluation and test checklist covers the following items: 1) function and performance, 2) environmental resistance, and 3) reliability. Items 1) and 2) are evaluated by using the BBM. Item 3) is checked using a program for developing parts prepared in parallel with the development of the BBM. As for the contents of the program, see References (1) and (2).

3. Results of Evaluation

3.1. Functional and Performance Tests

Figure 3 shows examples of results of roll and pitch transmitting characteristic tests. The relationship between the relative position of the scan pass and earth and the output of the accurate earth sensor has been confirmed by this figure. In addition, Table 2 presents an example of results of an evaluation of roll and pitch angle detection accuracy.

Table 2.
Results of Evaluating Roll/Pitch Angle Detection Accuracy (Common Use of Test Results and Those from Numerical Simulation)

	Zero point bias error (°)		Random error (°-3 σ ordinary temperature)	
	Steady mode	Admission mode	Steady mode	Admission mode
Roll	0.037	0.067	0.023	0.030
Pitch	0.028	0.079	0.013	0.017

3.2. Environmental Resistance Test

Table 3 shows the level of environmental resistance tests conducted by using the BBM. Of these tests, interference has been partially recognized in an electromagnetic compatibility test, but it has been confirmed that no problems occur in other tests. In addition, an impact test, conducted using a test model, has confirmed that the test model can withstand an impact of 610 G (Q = 10, SRS).

Table 3.
Environmental Resistance Test Level

Sine wave vibration test	5-30 G_{O-P}
Random vibration test	22.2 G rms
Thermal vacuum test	-30 - +60°C (base plate temperature)

Table 3.
Environmental Resistance Test Level (Continued)

Electromagnetic compatibility test	RS03: 5-20 V/m
	CS01, 02: 1-3 V_{p-p}

Postface

We have introduced partial results of evaluating the accurate earth sensor, BBM. In the above trial manufacturing and testing of the BBM, it has been confirmed that the BBM possesses performance sufficient for use as a main attitude sensor for future earth-oriented three-axis stable missiles. We have finished manufacturing an experimental model [EM], and are currently conducting developmental tests with the goal of applying the EM to the VI type engineering test satellite [ETS-VI].

References

1. "Development of Parts of Infrared Photoelectric System for Accurate Earth Sensor," Proceedings of the 32nd Space Sciences and Technology Conference

2. "Development of Parts of Vibration Mechanism System for Accurate Earth Sensor," Proceedings of the 32nd Space Sciences and Technology Conference

Research, Development of Guidance, Control Equipment for HOPE

[Article by Shunsuke Tanaka, Yoshisada Takizawa, Tomokazu Sato, Tatsuji Izumi and Tsunekazu Kimura of the National Space Development Agency of Japan]

[Text] 1. Preface

The National Space Development Agency of Japan [NASDA] is conducting the research and development of guidance and control equipment as part of its research involving HOPE, which is an H-II-rocket-launched-type of space plane. This guidance and control system consists of various equipment, and is being developed so that all flight phases, from the launching of the rocket to the take-off of the space plane, are unmanned and automatic. The research and development of this equipment requires the application of technologies for equipment mounted on conventional rockets, satellites, aircraft, etc. In addition, the equipment involves many new problems. We are going to take the first step toward steadily mastering the fundamental technologies for future space planes, etc., by utilizing Japan's capabilities for developing the equipment mounted on rockets, satellites, aircraft, etc. This paper describes the components and configuration of guidance and control equipment, the status of research and development, and other main subjects.

2. Equipment Components

As shown in Figure 1, the guidance and control equipment broadly consists of a guidance and control computer, navigation sensor, control sensor, electronic control equipment, a data interface unit and remote-controlled equipment. Except for the remote-control equipment, all are based on the data bus (MIL-STD-1553B) interface and basically have 1-fail-operative configurations.

Figure 1. Guidance and Control Equipment

Key:
1. Control sensor
2. Navigation sensor
3. Remote-control equipment
4. Electronic control equipment
5. ADS: Air Data System
6. CAR: C-band Angle Receiver
7. C-band Tr: C-band Transponder
8. DIU: Data Interface Unit
9. DME: Distance Measuring Equipment
10. E-PKG: Electronic Package
11. GCC: Guidance and Control Computer
12. GPSR: Global Positioning System Receiver
13. IMU: Inertial Measurement Unit
14. LAR: L-band Angle Receiver
15. OMS: Orbit Maneuvering System
16. RA: Radio Altimeter
17. RCS: Reaction Control System
18. ST: Star Tracker
19. TV.TX: TV Camera Transmitter

3. Outline of Research and Development

We have already conducted a feasibility study of all equipment and have investigated the main elements of technical development, etc. The following describes the main functions, features and technical subjects of the respective equipment: GCC [Guidance and Control Computer]: carries out the navigation, guidance, control calculations, data transmission control, system control, redundancy control, etc. The target specifications have been established based on the guidance and control system design and a study of the software. Subjects include the high-speed arithmetic circuit, redundant interface, etc. IMU [Inertial Measurement Unit]: is a strapped-down type of IMU based on the IMU of the H-II rocket and detects angular velocity and acceleration. Subjects include reducing the angular velocity noise and acceleration noise. GPSR [Global Positioning System Receiver]: is used in the updated system as a high-accuracy navigation sensor when the rocket returns to earth subsequent to a black-out in orbit. A TTFF [time to first fix] capability of less than or equal to 150 seconds will be obtained in the future by using a five channel receiver corresponding to high maneuverability. The code tracking loop and coastal loop comprise the main subjects. ST [Star Tracker]: is used to determine the high-accuracy attitude in orbit, observes fixed stars in the view direction specified with a sensor employing two-dimensional solid-state image elements, and outputs the position vector of the stars. Optical systems and centroid star identifying technologies are important. CAR [C-band Angle Receiver] and DME [Distance Measuring Equipment]: constitute the microwave landing system [MLS], and are used in the updated system to support the landing phase navigation. Pulse wave formation and the differential phase-shift keying [DPSK] demodulation circuit comprise the technical subjects.

The target specifications shown in Table 1 have been established and studies are being conducted since it has

been deemed necessary to accumulate technologies through tests during the trial manufacture of the BBM, particularly at the research and development stage of the above six kinds of equipment.

It is basically believed that technologies for equipment mounted on rockets can be fully utilized in the DIU [Data Interface Unit], which functions as a discrete and analog signal interface, the E-PKG [electronic package], which controls the respective actuators, and the C-band Tr [C-band transponder], which is used to measure the distance from a landing area. However, it is accepted that there is room for further development of the E-PKG, depending on the actuator system. It is also believed that technologies for equipment mainly mounted on aircraft can be fully utilized in the RA [Radio Altimeter], which measures the altitude upon landing time, the ADS [Air Data System], which analyzes data involving pneumatic pressure, etc.

4. Postface

In the future, we plan to adjust the relationship between the accuracy required for the guidance and control system and the equipment performance, and to continuously conduct the requisite research and development. In addition, an important concern will involve minimizing the dimensions, weight and power consumption, which have large impacts on the entire HOPE system.

References

1. Tanaka, S., et al., "Guidance, Navigation and Control System Study of H-II Orbiting Plane, HOPE," ISTS 88

2. Tanaka, et al., "Study of Guidance and Control Systems of HOPE," Proceedings of the 32nd Space Sciences and Technology Conference, 1988

Study of Guidance, Control System for HOPE

[Article by Shunsuke Tanaka, Yoshisada Takizawa, Tomokazu Sato, Tatsuji Izumi and Tsunekazu Kimura of the National Space Development Agency of Japan]

[Text] 1. Preface

The National Space Development Agency of Japan [NASDA] is continuing to conduct research on HOPE, which is an H-II-rocket-launch-type of space plane, with the intention of launching HOPE in the 1990s. HOPE will be unmanned, and will be launched with the H-II rocket. Subsequently, it will carry out such missions as supplying and recovering materials to and from space stations. After that, it will change its orbit, exit the orbit, and re-enter the atmosphere. After re-entry, it will

Table 1. Target Specifications for Each Equipment Item

Equipment	Summary of the aimed specification		Value
GCC	Processing Data		Fixed point data / Floating point data
	Word Length		32bit
	Performance		more than 1MIPS
IMU	Accuracy of Angular Velocity (60days,3σ)	residual bias error	0.096(μg)
		scale factor error	33(ppm)
	Accuracy of Acceleration (60days,3σ)	residual bias error	130(μg)
		scale factor error	150(ppm)
GPSR	Pseudo-range error(3σ)		50(m)
	Pseudo-range rate error(3σ)		0.25(m/s)
	TTFF		less than 150(sec)
ST	Field of View		8 X 6(deg²)
	Sensitivity		-2 ~ 4(mag/V)
	Max Tracking rate		0.5(deg/s)
	Bias(3σ)		60(arcsec)
MLS	Distance Measurement(2σ) IAM(12~37km)	bias error	±30(m)
		noise error	±15(m)
	FAM(0~12km)	bias error	±15(m)
		noise error	±10(m)
	Angle Measurement(2σ)	bias error	0.017(deg)
		noise error	0.01 (deg)

```
┌─────────────────────────────┐  ┌─────────────────────────────────┐
│      Remote pilot system    │  │        Automatic system         │
│  ┌───────────────────────┐  │  │  ┌─────┐    ┌──────────────┐     │
│  │     On-board system   │  │  │  │ GCC │    │  Nav. Sons.  │     │
│  │  ┌─────────────┐      │  │  │  │ ┌─┐ │    │              │     │
│  │  │ G & N       │      │  │  │  │ │N│ │    │ LAR   CAR    │     │
│  │  │ TV·Tx       │      │  │  │  │ └─┘ │    │ ST    IMU    │     │
│  │  │ C-band TR   │      │  │  │  │ ┌─┐ │    │ GPSR  RA     │     │
│  │  └─────────────┘      │  │  │  │ │G│ │    │ DME          │     │
│  │                       │  │  │  │ └─┘ │    └──────────────┘     │
│  │          ┌──────┐     │  │  │  │ ┌─┐ │    ┌──────────────┐     │
│  │          │Comm. │     │  │  │  │ │C│ │    │ Flight Cont. │     │
│  │          │ Rx   │─────┼──┼──┼──│ └─┘ │    │   Sons.      │     │
│  │          └──────┘     │  │  │  └─────┘    │ IMU*    ADS  │     │
│  │  ┌────────┐           │  │  │             └──────────────┘     │
│  │  │ Ground │           │  │  │  ┌────────────┐                  │
│  │  │ Station│           │  │  │  │Cont. Equip.│                  │
│  │  └────────┘           │  │  │  │ OMS  E-PKG │                  │
│  └───────────────────────┘  │  │  │ RCS  E-PKG │                  │
└─────────────────────────────┘  │  │ WING E-PKG │                  │
                                  │  └────────────┘                  │
          Guidance Command        │  ┌──────────┐                    │
                                  │  │ Effectors│                    │
                                  │  └──────────┘                    │
                                  └─────────────────────────────────┘
```

ADS   Air Data Sensor
CAR   C-band Angle Receiver
C-band TR C-band Transponder
Comm. Rx   Command Receiver
DME   Distance Measurement Equipment
E-PKG   Electronic Package
GCC   Guidance Control Computer
GPSR   Global Positioning System Receiver
IMU   Inertial Measurement Unit
LAR   L-band Angle Receiver
OMS   Orbital Maneuvering System
RA   Radio Altimeter
RCS   Reaction Control System
RVD   Rendezvous and Docking
ST   Star Tracker
TV·Tx   TV Camera Transmitter
*   common to the IMU for Navigation

Figure 1. Guidance and Control System Configuration (Except for RVD Phase

reduce its speed by means of aerodynamic force, automatically reach a landing site, and land horizontally on the specified runway. This guidance and control system is important if the HOPE is to carry out its missions, and there are many technical subjects involved in the development of this system.

This paper briefly describes the study of the configuration and equipment of this guidance control system, as well as guidance and control law.

2. System Configuration

Figure 1 shows the system configuration currently regarded as the base line.

This system broadly consists of an automatic system and a remote-controlled system. With regard to the base line, the automatic system is composed of a triplex redundant system and is devised so that it will not lose its function upon a single failure.

In addition to the base line, the duplex and single system configurations are being studied. Basically, it is possible to carry out all missions by means of the automatic system alone.

It is also believed that the remote control system should be backed up at the landing phase, etc.

The respective guidance and control-based equipment are connected via the MIL-STD-1553B, the main guidance and control computer [GCC]. The GCC is used to navigate, guide and control HOPE, to control this data

bus, to manage the redundancy and to control the airframe and other systems.

As shown in Figure 1, the equipment used in the guidance and control system consists of a navigation control sensor, control electronic equipment, a GCC, and remote-control equipment. For details of the equipment, see Reference (4).

3. Navigation, Guidance and Control System

The software of the guidance and control system generally consists of navigation, guidance, control and system management. In addition, the navigation, guidance and control are classified for every flight phase.

(1) Navigation

Composite navigation according to the Karman filter is used for navigation. As shown in Figure 2, the renewal sensor is switched according to the flight phase.

(2) Guidance

Lambert's orbit transferring method has been adopted as the orbit transferring guidance system at orbital phases.

The closed form system has been adopted for the re-entry phase. It is a guidance system devised so that the re-entry phase can be classified into parts, with a standard orbit provided for each part, and HOPE can make its flight along the standard orbit.
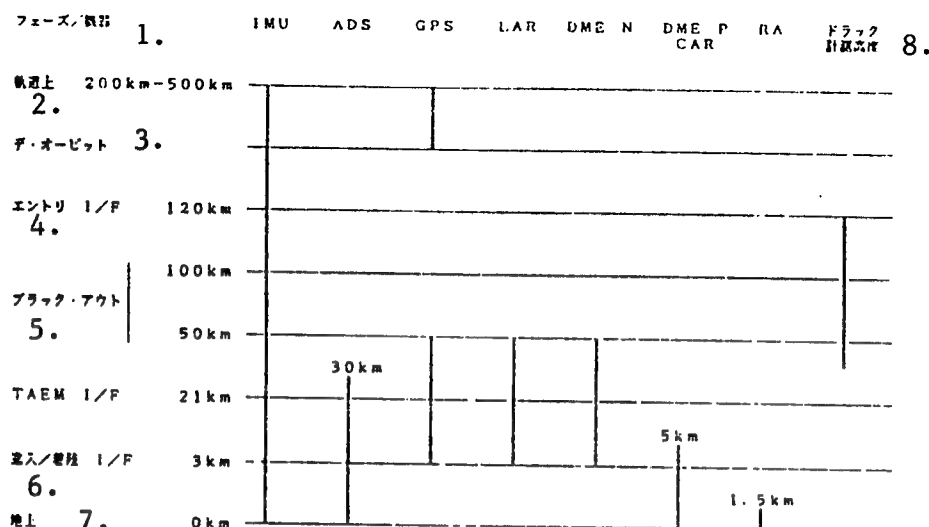
Figure 2. Navigation Support Equiopment Use Phase

Key:
1. Phase/equipment
2. In orbit
3. De-orbit
4. Entry I/F 5. Blackout
6. Approach/landing I/F
7. Ground
8. Drag measuring altitude

During the TAEM phase, potential and kinetic energies of HOPE are controlled so that they conform to approach and landing interface conditions.

A flare system that is resistant to disturbances is currently being studied since, during the landing phase, because HOPE does not have a cruising engine, it is greatly affected by the disturbance generated after the flare.

(3) Control

The gas jet [RCS] and aerodynamic control surface can be cited as control actuators. The former is mainly used in orbit, while the latter is generally used when HOPE returns to earth. The "bang-bang control system," in accordance with the RCS, is used to control the attitude of HOPE while in orbit.

Both the RCS and the aerodynamic control surface are used during the re-entry phase. The ON-OFF switching system and the linear control system are currently being studied as a combined system.

(4) System Management

The system management consists of data transfer, mode control of the equipment, redundancy control, airfram system control, etc.

4. Summary

We have studied the basic functions, specifications and constitution of the guidance and control system of HOPE. In the future, we will determine the system configuration, adjusting it with the airframe system.

References

1. Tanaka, et al., "Space Plane Guidance and Control," MEASUREMENT AND CONTROL, Vol 26 No 6

2. Takizawa, "Guidance and Control of H-II Rocket Launching Type Winged Recovery Plane (HOPE)," SICE '88

3. Tanaka, S., et al., "Guidance, Navigation and Control System Study of H-II Orbiting Plane, HOPE," ISTS 88

4. Tanaka, et al., "Research and Development of Guidance and Control Equipment of HOPE," Proceedings of the 32nd Space Sciences and Technology Conference, 1988.

Guidance, Analysis of HOPE Re-entry

[Article by Shunsuke Tanaka, Yoshisada Takizawa, Tomokazu Sato, Tatsuji Izumi and Tsunekazu Kimura of the National Space Development Agency of Japan]

[Text] Outline

The National Space Development Agency of Japan [NASDA] is currently conducting research on HOPE (H-II Orbiting Plane) as a space transportation system. Some conditions involving the guidance of the HOPE re-entry phase are restricted, particularly the aerodynamic heating conditions during the initial stage of the re-entry, which are critical. The following is a report of

an example of guidance and analysis of the HOPE re-entry phase, particularly regarding the aerodynamic heating problems.

1. Analysis of Guidance Error

We have analyzed the safety margin that should be anticipated in satisfying aerodynamic heating conditions in order to guide HOPE during the re-entry phase. A drag profile is established during the critical aerodynamic heating phase so that the aerodynamic heating rate is constant as a nominal orbit, and the aerodynamic heating rate is estimated by measuring the drag acceleration. HOPE is guided during the re-entry phase by using a closed form method, and the aerodynamic heating control is carried out through the control of bank angles based on the results obtained from comparing the above-mentioned estimate and a preset value. The following items can be cited as error factors involving the aerodynamic heating rate that are actually caused during such a control process: 1) initial state errors (position and velocity errors at the re-entry point), 2) airframe characteristic errors (errors caused by estimating the aerodynamic coefficient, wing loading, etc.), and 3) environmental condition errors (atmospheric density errors, etc.). As a result of analyzing the sensitivity of the aerodynamic heating rate against these error factors, it is concluded that approximately 15 percent of the aerodynamic heating rate control level should be estimated as the safety margin rate against aerodynamic heating.

2. Theory of Control of Aerodynamic Heating Rate

As mentioned above, aerodynamic heating is controlled through the control of the bank angles and, in order to maintain the aerodynamic heating rate at a constant level, it is necessary to control bank angle φ so that the angle satisfies the following equation. This fact is introduced analytically. (approximate expression) $\cos(\varphi) = (C_L/C_D)^{-1} \times [-6.3(C/U)^{-6.3} + F^{-1} \times (1 - (U^2/gr)) \times (C/U)^{-4.3}]$ (bank angle control law), where $F = \frac{1}{2} C_D \times (W/S)^{-1} \times ((Q_{CL} \text{ square root } R)/K_O)^2 C^{-4.3}$, R is the radius of curvature of the stagnation point, Q_{CL} is the aerodynamic heating rate control level, and C has a velocity dimension and is expressed as $C^{-2} = (1/6.3g) \times (\delta/(\delta r))\ln(\rho/\rho_0)$ (r is the geocentric radius).

When the absolute value of the right side of the equation exceeds 1, bank angle solutions satisfying the equation will not exist. This fact introduces the limits of the aerodynamic heating rate control. Also, it can be appreciated that the minimum value of bank angle φ can be regarded as a scale for the severity of the aerodynamic heating restrictions. Figure 1 shows a profile simulation of the bank angle following the re-entry of HOPE. The control limit is shown by the curve in which bank angle φ has reached 0°.

3. Limits of Aerodynamic Heating Rate Control

From the above theory, the control limits of the aerodynamic heating rate can be expressed by the fact that the maximum value of the right side of the equation is 1 or
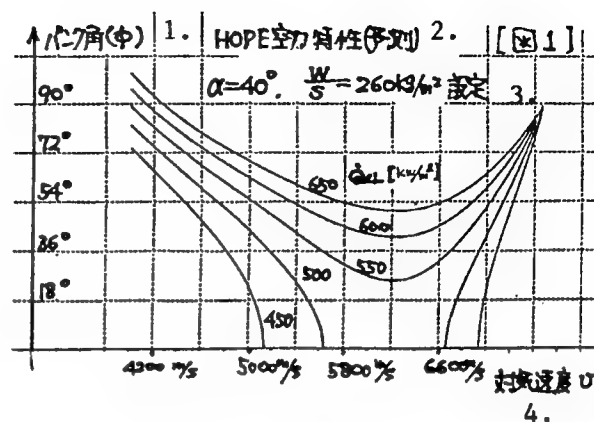
Figure 1.

Key:
1. Bank angle (φ)
2. Aerodynamic characterists of HOPE (expected)
3. Establishment of $\alpha = 40°$ and w/s = 260 kg/m^2
4. Air speed v

less. The maximum value of the right side is expressed by $(C_L/C_D)^{-1} \times$ (the function of F), and the results of simulating some aerodynamic data and the input angle of attack were plotted to verify that the maximum value of $\cos(\varphi)$ is actually of such a functional type. Figure 2 shows the results. The validity of the above theory is thus confirmed.
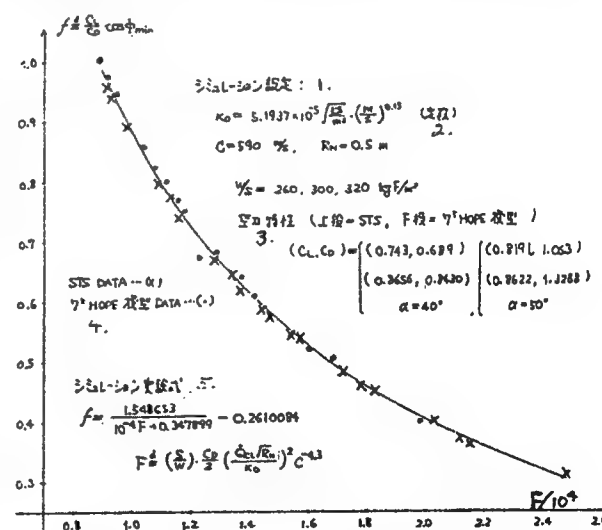
Figure 2.

Key:
1. Establishment of simulation
2. (constant)
3. Aerodynamic characteristics (upper stage = STS, and lower stage = 7^5 HOPE lateral)
4. 7^5 HOPE lateral DATA ...(.)
5. Experimental simulation formula

4. Aerodynamic Heating Restrictions Against Design of HOPE

The current thought is that when HOPE is designed, the leading edge of the main wing must undergo the most severe aerodynamic heating conditions. Integrating the temperature restrictions of the structural members and the above-mentioned aerodynamic heating rate controllable conditions, the following expression can be obtained as a restrictive condition for designing HOPE: $K_1(W/S)((1-a \times (C_L/C_D)/(1+b \times (C_L/C_D))) \times C_D^{-1}$ is equal to or less than $[((\text{square root of } 2R_e)\varepsilon\sigma T_C^4)/(1000 \times \eta(\alpha)(1+MS))]^2$, where a, b and K are positive constants, $\eta(\alpha)$ is a function of the effective sweepback angle (Λ_e) of the main wing $(\sin (\Lambda_e) = \sin (\Lambda) \times \cos (\alpha))$, ε is a heat radiation coefficient (it is estimated that most of the heat dissipation is caused by heat radiation), and MS is the safety margin rate.

C/C materials have been proposed for use in the nose and leading edge of the main wing of HOPE. C/C materials are currently being developed, and it is estimated that the upper temperature limit (T_e) will be about $1,700°C$. As an example, Figure 3 presents a graph of the above-mentioned design restrictions with respect to wing loading. In the future, we will optimize the design parameters while referring to the above analytical results.
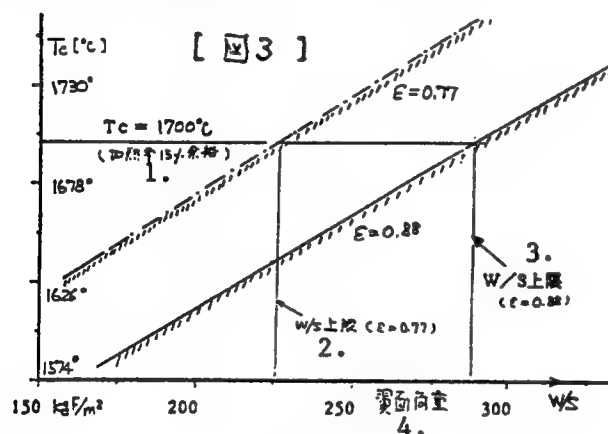
Figure 3.

Key:
1. (15 percent margin heating rate)
2. W/S upper limit $(\varepsilon = 0.77)$
3. W/S upper limit $(\varepsilon = 0.88)$
4. Wing loading

References

1. Harpard, J.C., Graves, C.A. Jr., "Space Shuttle Entry Guidance," AAS-78-147

Concept of Space Power Reactor as Extension of FBR Technologies

[Article by Kazuo Haga and Hisashi Nakamura of the Power Reactor and Nuclear Fuel Development Corporation]

[Text] 1. Preface

The following items can be cited as conditions involving the large-scale supply of energy sources in space: 1) it is not necessary to supply fuel to space at all times, 2) oxygen is not necessary in space, 3) space does not depend on the sun and 4) radioactive resistance is high.

It may be safely said that the nuclear reactor is the energy supply means that meets these conditions and, therefore, it is regarded as a technology indispensable for future space development. Of the various nuclear reactors, lightweight, compact and long-life nuclear reactors are required for this future space development. Of the reactors that have already been constructed and operated on the ground, the liquid metal-cooled fast breeder reactor [FBR] best satisfies the above-mentioned conditions. This is due to the following reasons: 1) the liquid metal-cooled FBR does not require any moderators, but instead requires only a reactor with little high-density output since fast neutrons generated just after nuclear fission are used in the following nuclear reaction, 2) the liquid metal-cooled FBR can be constructed as a compact system since the liquid metal used in this system has excellent properties as a heat transfer working fluid with high thermal conductivity and a high saturation temperature, and 3) stable output over a long period of time can be obtained without replacing any of the fuel because the reactivity change caused by combustion is small.

Accordingly, when studying space power reactors on the basis of current FBR technologies, we will determine to what extent the demonstrated technologies have been realized and what subjects remain to be explored.

2. Difference Between Nuclear Reactor Installation Environments on Ground and in Space

An FBR employing liquid sodium as the coolant has been developed over the past 30 years and, in late 1986 in France, a demonstration reactor, the "Super Phenix," with an electric output of approximately 1,242 MW, was put into operation at the rated output. The nuclear reactor design, control and technologies for handling liquid metal, etc., used in FBRs can be applied, without any changes, to space

power reactor systems, but it will be necessary to cope with the many new matters caused by the differences between the nuclear reactor installation environments. Table 1 shows the influences of the above differences on the design and operation of systems.

Table 1.
Influence of Environment on Specifications of Nuclear Reactors

Item	Ground	Space
Weight and size	Unrestricted	Very lightweight and compact
Waste heat treatment	Heat transfer to water and air	Only radiation to space
Plant temperature	Rankine cycle (Water is used in the generating system because the heat transfer releases a large amount of heat.) A steam temperature of 483°C is used in Monju. The outlet temperature of nuclear reactors is 500-550°C, while that of Monju is 529°C.	The outlet temperature of nuclear reactors should be increased as much as possible, going back to the fluid temperature of generation systems, in order to increase the efficiency of heat release caused by radiation.
Effect of gravity	Natural circulation power is used	Unusable in orbit
Maintenance and control	It is relatively easy to access plants. Plants can be monitored and operated at all times by humans.	It is difficult to access plants. Strong demand that human monitoring and operation be minimized.
Fuel replacement	Generally replaced every 2-3 years	Fuel should not have to be replaced for 10-30 years.
Aseismatic design	Necessary	Not necessary

3. Concept of Space Power Reactor

When the space power reactor system is studied by developing current FBR technologies, the following matters can be cited: Reactor core: (thermal output is 10 MW) Capacity is 20 liters, and fuel is uranium nitride. Primary system: Working fuel is liquid metal lithium, reactor core outlet temperature is approximately 1,000K, the difference between the reactor core outlet temperature and reactor core inlet temperature is about 150K, and electromagnetic pumps are used in the primary system. Secondary system and power generating system: Rankine cycle electromagnetic pumps with potassium are used in these systems, and the power generating efficiency is about 35 percent. Waste heat treatment: Radiation radiator using a heat pipe, or liquid-drop radiation-type system. Control system: Self-working-type control rod. System control: Autonomous dispersion control system with failure resistance and function persistence, to which importance is attached.

4. Conditions Necessary for Space Power Reactors and Applicability of FBR Technologies

Table 2 compares the levels required by each technical field for space power reactor systems and those of the current technologies in relation to the development of FBRs. This table indicates that the current levels are almost satisfactory in heat transferring technologies and fuel development capacities. Carbide and nitride fuels

Table 2. Current Status and Level Required by Each Elemental Technology in Space Power Reactor System

技術分野 1.	要求水準 9.	23. 現状				
			はとんど手付かず 24.	開発むにかかっているが不十分 25.	ほぼ十分 26.	十分 27.
炉心燃料 2.	被覆材温度 約1000℃ 10. 長寿命性 (～30年) 11. 燃料製造 (開発能力) 12.	約700℃ 28.		○—○ ○———○		○
遮蔽 3.	軽量 13.	重コンクリート 29.	○			
熱制御 4.	廃熱：放射ラジエータ 14. 蓄熱：相変化 15. 熱輸送：液体金属 16.	熱伝導 30.	○—○ ○	○———○		
エネルギー変換・輸送 5.	直接変換 17. (熱電対、熱電子) 18. 熱機関 マイクロ波、レーザ 19.	レーザ加工技術 31.	○ ○	○—○		
系統制御 6.	自律制御 (人工知能) 20.	原子炉診断システム 32.	○ ○—○			
構造材 7.	軽量・高温構造 21.	高温構造設計 33.	○———○			
振動 8.	柔軟構造 (減衰、免震) 22.	免震構造 34.	○———————○			

Key:
1. Technical field
2. Reactor core fuel
3. Shield
4. Heat control
5. Energy conversion and transportation
6. System control
7. Structural material
8. Vibration
9. Required level
10. Temperature of cladding materials: approx. 1,000°C
11. Long working life (up to 30 years)
12. Manufacturing of fuel (development capability)
13. Lightweight
14. Waste heat: Radiator
15. Heat reserve: Phase change
16. Thermal transportation: Liquid metal
17. Direct conversion (thermocouple and thermal electron)
18. Heat engine
19. Microwave and laser
20. Autonomous control (artificial intelligence)
21. Lightweight and high temperature structure
22. Flexible structure (attenuation and earthquake isolation)
23. Current Status
24. Barely started
25. Development started, but insufficient
26. Nearly sufficient
27. Sufficient
28. Approx. 700°C
29. Heavy concrete
30. Heat transfer
31. Laser beam machining technology
32. Nuclear reactor diagnostic system
33. High temperature structural design
34. Earthquake isolation structure

are scheduled for development in the future. They will be regarded as fuels with satisfactory specifications for use in high temperature environments. Many technologies will be obtained from the FBR technologies currently being developed in other fields.

5. Postface

We have studied the concept of space power reactors based on the accumulated FBR technologies. We have made a comparison between the current technical level and the technical level required for space power reactor systems, and have confirmed which technologies can be used in the space power reactor systems without making any changes and which ones will have to be further developed.

Some of the technical fields involving space power reactor systems are not included in the developmental items comprising the current FBR technologies, but will be handled as part of the development of fundamental technologies from the standpoint of further increasing the safety of FBRs and diversifying their use.

Control of Space Manipulator Used to Recover Satellites

[Article by Keiken Ninomiya, Ichiro Nakatani, Junichiro Kawaguchi and Koichi Harima of the Institute of Space and Astronautical Science]

[Text] 1. Preface

The Institute of Space and Astronautical Science [ISAS] is studying an autonomous satellite recovery experiment using a space flyer unit [SFU]. This report proposes a method for controlling a manipulator and automatically recovering satellites, and demonstrates the validity of this method by means of simulations.

2. Control Law[1],[2]

The following is an equation which expresses the movement of the manipulator in space. The report indicates that the degree of freedom of the manipulator is 7.

$$^Ar = {^AJ\theta} + {^AS^Aq} \ (1)$$

where, r is the position of the end effector, vector (6 x 1), which expresses the attitude; J is the Jacobian matrix (6 x 7) in space, used in consideration of the reaction to which the SFU is subjected; θ stands for each joint angular velocity vector (7 x 1); S is the mass of the system consisting of a SFU and manipulator [system], with matrix (6 x 6) consisting of the moment of inertia; and q is the momentum of the system, with the vector (6 x 1) expressing angular momentum.

In addition, the A to the upper left of the symbols indicates an inertial coordinate system, while an E at that position would indicate an end effector coordinate system. Let the target value of the moment of the end effector denote the following ^Ar_d:

$$^A = {^Ar_T} + K_p({^Ar_T} - {^Ar}) \ (2)$$

where, r_T is the position of capture of a target satellite [TS] which should be recovered, with vector (6 x 1) expressing attitude; and K_p is the gain matrix (6 x 6).

As shown in the following equation, the only joint angular velocity of the manipulator is controlled without controlling the SFU proper.

$$\theta_d = {^AJ^+}[{^Ar_T} + K_p({^Ar_T} - {^AR}) - {^AS^Aq}] \ (3)$$

where, θ_d is the target joint angular velocity vector (7 x 1); and $^AJ^+$ is the affine inverse matrix (7 x 6) found so that the sum of the squares of each joint angular velocity is minimal.

The error vector $\Delta\theta$ (7 x 1) is shown below:

$$\Delta\theta = \theta - \theta_d = {^AJ^+}[{^Ar} - {^AS^Aq}] - {^AJ^+}[{^Ar_T} + K_p({^Ar_T} - {^Ar}) - {^AS^Aq}] = {^AJ^+}[{^Ar} - {^Ar_T} + K_p({^Ar} - {^Ar_T}] \ (4)$$

Using the transformation matrix T (6 x 6) defined by $^Ar - T({^Er} - {^E\varepsilon})$, and the position vector $^E\varepsilon$ (6 x 1) of the A coordinate system origin expressed in the E coordinate system, equation (4) can be expressed using the following end effector coordinate system:

$$\Delta\theta = {^EJ^+}[{^Er} - {^Er_T} + (T^{-1}T + T^{-1}K_pT)({^Er} - {^Er_T})] \ (5)$$

where, $T^{-1}T$ is expressed only with the angular velocity of the E coordinate system. Assuming θ (7 x 1) in the following equation, the control torque is calculated by using the Newton-Euler law, and the results obtained from the calculation is impressed on each joint.

$$\theta = -K_v\Delta\theta \ (6)$$

where, K_v is the gain matrix (7 x 7).

3. Results of Simulation

Simulations were carried out to confirm the validity of the above control law. Figure 1 shows the results when the angular momentum of the system is zero and the manipulator is moved slowly, and also shows an example enabling the TS to be captured by means of the above control law. In addition, suppose it is possible to measure the attitude, relative position of the end effector and the TS necessary for the control. Data used for the simulations are as follows: 1) The SFU has a diameter of 3 meters, 2) it is cylindrical and has a height of 2 meters and a mass of 1 ton, 3) the manipulator has an elongation of 5.6 meters and 4) the overall mass is 150 kg. The TS capture occurs 1 meter ahead of its center of gravity, and rotates at an angular velocity of approximately 1 rpm around the angular momentum vector. Also, the relative distance between the end effector and the TS capture is 2.5 meters at the start of the movement of the manipulator.
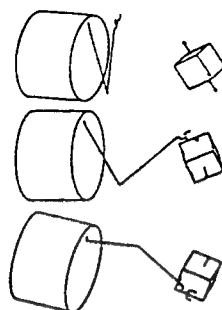
Figure 1. When Angular Momentum of System Is Zero

4. Summary

This report describes a method of controlling the sole joint angular velocity without controlling the SFU, in consideration of the capture of satellites by means of a manipulator mounted on the SFU. This method is characterized by the following points: 1) it is not necessary to take the angular momentum of the system into consideration, and 2) satellites can be controlled solely with the relative value obtained from the TS and the end effector by changing equation (5) to K_p = diag (K, ..., K). Figure 2 shows the results obtained by applying this control law to the case when the system has an angular momentum rotating at approximately 1 rpm in the same direction as that of the TS at the start of operation of the manipulator. Compared with the results shown in Figure 1, those shown in Figure 2 indicate a smooth capture process. In the future, we plan to study a method for use with controlling the attitudes of the SFU.
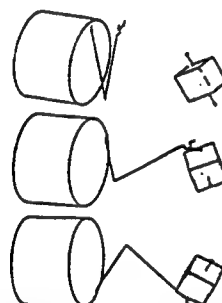
Figure 2. When System Has Angular Momentum

References

1. Umetani, Y., Yoshida, K., "Continuous Path Control of Space Manipulator Mounted on OMV," 37th IFAC, 1986

2. Ninomiya, et al., "Control of Capture of Space Manipulator in Which the Changes of Self-Attitude are Considered," Papers of SAIRAS, 1987, pp 11-14

Processing of Visual Information Necessary for Autonomously Recovering Tumbling Satellites

[Article by Keiken Ninomiya, Ichiro Nakatani, and Shinsuke Higashi of the Institute of Space and Astronautical Science]

[Text] 1. Preface

Vision is important for robots since, through it, a large amount of information regarding environments can be obtained. However, such a large amount of information must be processed efficiently. The Institute of Space and Astronautical Science [ISAS] is studying an experiment whereby passive target satellites are captured and recovered autonomously with a manipulator mounted on the space flyer unit [SFU].[1] Laser radar equipment will be used with the vision to perform this experiment, and such vision will be regarded as an important means of obtaining information on target satellites. The authors, et al., have studied a method of determining the position and attitude from the pattern images of a corner cube reflector [CCR] installed four at a time on each face of a target satellite with a nearly cubic shape as a means of processing the visual information that will be used to analyze the rotation and translation of the target satellite.[2] This method is promising for the rendezvous phase since the burden imposed on the image processing is small, but during the capture phase, the method involves the following problems: 1) when the CCR hides behind the manipulator, it cannot be identified, and 2) the error of the information on depth is large. This paper proposes a new method for processing visual information taking into consideration its use during the capture phase, and briefly describes the current status of this study.

2. Vision and Capture Operation in Satellite Recovery Experiment

The principal axis of the maximum inertia of the target satellite is equipped with a capture bar marked with stripes (as the interval approaches the center of the capture, the closer it is). In addition, seals with high reflecting efficiency are attached to the edges of two faces equipped with capture bars so that the edges of the target satellite proper can be detected readily. The edges (quadrangles) are recognized by a camera installed on the SFU proper, and the position and attitude of the target satellite are calculated. An end effector is brought closer to the center of the capture bar by elongating the manipulator based on the information obtained from the above calculation. At this time, stripes marked on the capture bar are detected using a camera installed on top of the manipulator, and the capture is conducted while correcting errors in the depth direction, which is included in the information obtained from the camera installed on the SFU proper.[3] (See Figure 1.)
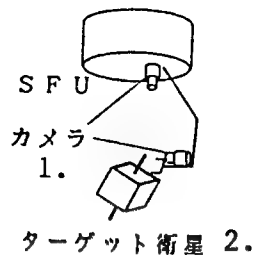
Figure 1. Conceptual Drawing of Satellite Recovery

Key: 1. Camera   2. Target satellite

3. Detection of Position and Attitude from Visual Information

A coordinate with four vertices is necessary for indentifying quadrangles, but it is difficult to find the vertices directly from images. Accordingly, an intersection point obtained by finding four straight lines is calculated. As shown in Figure 2, screens are divided into n x n (the figure shows 4 x 4), and the straight lines are found and extracted within each small screen by using a method of least squares. Even if the straight lines are broken or vertices project from the screen, it is possible to identify quadrangles by using this method.
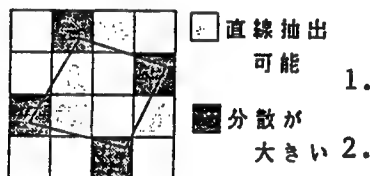
Figure 2. Recognition of Quadrangle of Screen Division

Key:
1. Possible to extract straight line
2. Dispersion is large

The position and attitude of the target satellite in three-dimensional space are found by using a coordinate with intersection points between diagonal lines and four vertices of a quadrangle obtained through the above-mentioned method, and by using the double ratio theorem of projective geometry.

4. Simulation

Simulations were carried out to confirm the operation of the above-mentioned method of identifying the position and attitude and to investigate detection errors. The target satellite executes a tumbling motion based on Euler's equation of motion, and the estimated parameters are as follows: 1) coordinate of center of mass of target satellite, 2) angle θ formed by the principal axis of maximum inertia and the angular momentum vector, and 3) ψ, which expresses the rotation around the angular momentum vector. The attitude was originally
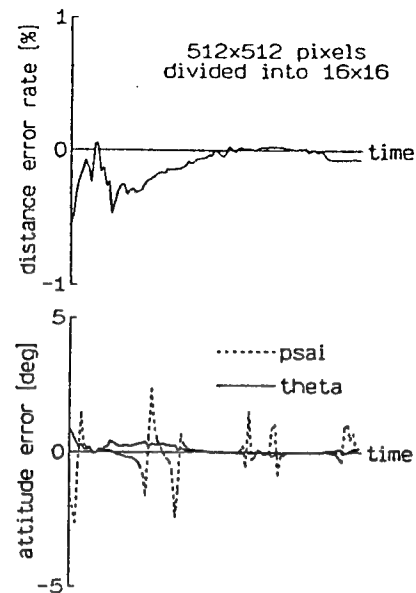
Figure 3. Simulation Results

expressed with three degrees of freedom, and information on the phase of rotation around the capture bar is not taken into consideration since it is not required for the capture itself. Figure 3 shows an example of an error obtained from simulations. The time required to process a screen was approximately 0.5 second. (The CPU was the MC68020 + MC68881.)

5. Summary

The result of simulations indicates that the position is found at the required accuracy since simple filtering is conducted, but many errors occur when the attitude is determined. We are studying the filtering of attitude angles in order to increase the extraction accuracy. We intend to establish a method to process the images obtained from a camera installed on top of the manipulator and to verify this method through experimentation.

References

1. Ninomiya, et al., "Satellite Recovery Experiment Utilizing Free Flyer," Space Artificial Intelligence/Robot/Automation Symposium, Nov 1987

2. Nakatani, Tanamachi, Ninomiya, "Satellite Motion Analysis via Laser Reflector Pattern Processing for Rendezvous and Docking," 37th Congress of IAF, Innsbruck, Austria, Oct 1986, IAF-86-06

3. Ninomiya, Nakatani, Higashi, "Autonomous Capture and Recovery of Tumbling Satellites," the 2nd Space Artificial Intelligence/Robot/Automation Symposium, Nov 1988 (scheduled to lecture)

Simulator for Capture, Operation Utilizing Space Manipulator

43062505o Tokyo PROCEEDINGS OF THE 32ND SPACE SCIENCES & TECHNOLOGY CONFERENCE in Japanese 26-28 Oct 88, No 2A3, pp 254-255

[Article by Ryojiro Akiba, Junichiro Kawaguchi and Shuuichiro Fukuzawa of the Institute of Space and Astronautical Science]

[Text] 1. Preface

Space station-related research is mainly being conducted by the National Aeronautics and Space Administration [NASA], and this space station will initially operate in 1992. Thanks to this research, it will become possible for humans to observe phenomena in space and to perform experiments in space that have previously been impossible. However, automation technologies will become increasingly important in proportion to the expansion of advances in space and the complexity of the systems that must be handled by humans. The space manipulator is one automation technology that will lighten the work burden imposed on crewmen and will support and expand the working capabilities. It will be widely used to assemble large structures, supply materials, repair and replace malfunctioning parts and to remove meteorites and debris from the periphery of the space station. In other words, it is of high utility value.

Japan is currently performing physical experiments in space, and is developing an SFU [space flyer unit] to perform some technical experiments. Study is being conducted on a simulation satellite recovery experiment using an autonomous manipulator as one of the technical experiments. Research on a space manipulator has been conducted experimentally based on the above experiment.

When a manipulator is operated in space, it is characterized by the fact that the base is not fixed. Therefore, in order to conduct experiments on the ground, it is necessary to construct a simulator that changes the attitude and relative distance between the base and target in accordance with the reaction of the arms. According to the previous report, the mass of an actual manipulator is approximately 5 percent of the total weight of the SFU. A simulation of the rotation of the base, generated by means of the inertia of the arms, has been conducted independent of the translation of the base.[1] This report describes the results of simulations in which translation is studied by using a device constructed by adding a simulator system to a previously-fabricated space manipulator system.

2. Space Manipulator System[1]

The following is a brief outline of the space manipulator system. The system used in this experiment consists of a manipulator equipped with a video camera as an external sensor. This manipulator has four degrees of freedom. The basic expression used to move arms consists of an expression which shows the geometric relationship among the arms and an expression of conservation of momentum and angular momentum, and is formulated as shown in equation (1). The formulation is carried out by giving a degree of freedom to the basic expression as a Jacobian matrix of a manipulator with three degrees of freedom around the position. The system is fed back and controlled so that the relative position between the end effector and the target obtained from the visual sensor is zero. (See Figure 1.)

$$\delta r = J \delta \theta \quad (1)$$

where, J is the formulated Jacobian matrix, and $\theta = (\theta_1, \theta_2, \theta_3, \theta_4)$.
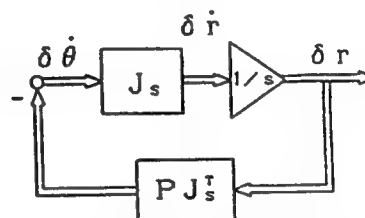
Figure 1. Example of Control Law Used in Experiment

3. Simulator System

Agravity, the gravity gradient torque of earth, solar wind, etc., can be regarded as factors which affect the manipulator in space environments in the vicinity of earth from the dynamic standpoint. Here, the influence of agravity on the manipulator is discussed. Methods of realizing a gravity-free state on the ground can be broadly classified into two types.[3] One involves physically realizing the gravity-free state, while the other utilizes software. The latter method has been adopted for this research since it not only enables a gravity-free state to be realized comparatively easily, but it also makes it possible to realize a state quite close to that of actual space environments by taking other influences into consideration by means of software.

Figure 2 shows the simulator used in this research. This device is used to realize the fluctuation of the relative position between the base and target by moving the target side. This fluctuation is generated by the fluctuation of the base (manipulator side). In other words, an observer watches the movement by regarding the base-fixed coordinate system as a visual point. In addition, it is not necessary to take the change in the relative attitude between the target and base into consideration because the target is regarded as a mass point. The target can be moved three-dimensionally around the position by using a combination of three linear moving actuators in the mutually orthogonal direction.

The computer at the manipulator control side transmits data on joint driving angles to the simulator side. The simulator calculates the fluctuation of the base based on
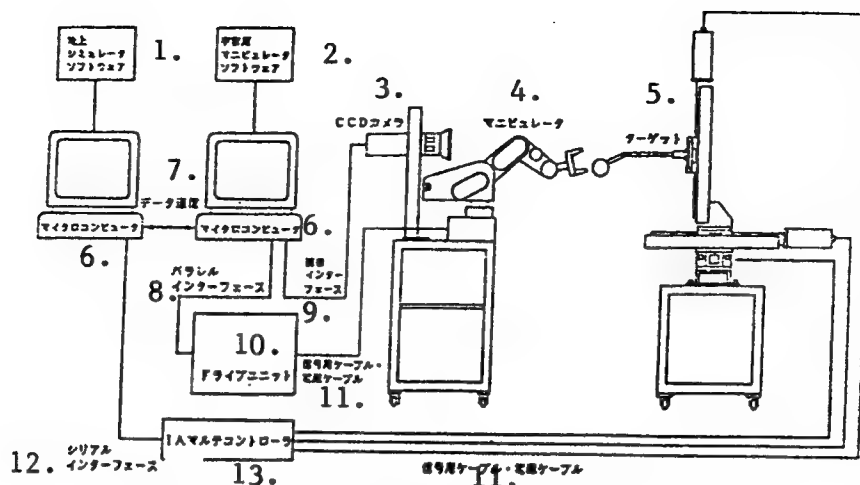
Figure 2. Block Flow Diagram of Ground Simulator System

Key:
1. Ground simulator software
2. Space simulator software
3. CCD camera
4. Manipulator
5. Target
6. Microcomputer
7. Data communications
8. Parallel interface
9. Image interface
10. Drive unit 11. Signal cable
12. Serial interface
13. 1A multi-controller

the data, and drives the target only while changing the relative position between the target and base which is generated by the translation and rotation of the base. When the target moves relatively against the base, the simulator drives the target for the change, to which the fluctuation generated by the movement is added.

4. Experimental Method

According to the references,[4],[5] the manipulator mounted on the SFU has a reach of 5.6 meters and a weight of 150 kg. The total weight of the fully-equipped SFU is about 3 tons. On the other hand, the reach of the manipulator used in the experiment is 595 mm, almost one-tenth that of an actual manipulator. Therefore, the manipulator was used as a one-tenth-scale simulator in the experiment, and target capture was simulated for some cases.

5. Summary

A target in space can be captured autonomously by using a manipulator. This concept is new and unprecedented. For this reason, many problems must be solved and confirmed. The manipulator and target used in this experiment have smaller degrees of freedom than the actual one will, but the authors believe that they constitute an effective means of extracting essential parts of the solutions. In the future, we intend to increase the degrees of freedom of the manipulator and target, to reduce the remaining problems, and to solve them.

References

1. Ryojiro Akiba, et al., "Simple Satellite Recovery Simulation Using Space Manipulator," Proceedings of the 31st Space Sciences and Technology Conference, 1987

2. Umetani, Y., Yoshida, K., "Continuous Path Control of Space Manipulator Mounted on OMV," IAF-86-13, 1986

3. Inoue, et al., "Space Recovery Ground Simulator Facility," Space Artificial Intelligence/Robot/Automation Symposium Papers, 1987

4. Toshimitsu Nishimura, "Space Experiment/Guidance and Control of Observation Free Flyer/Measurement and Control," 26-6, 503/506, 1987

5. Small Space Platform Working Group," Automatic Satellite Retrieval Experiment," ISAS Report EXP-R-i013-0, 1987

Evolution of Scientific Exploration of Moon by Japan

43062505p Tokyo PROCEEDINGS OF THE 32ND SPACE SCIENCES & TECHNOLOGY CONFERENCE in Japanese 26-28 Oct 88, No 2A4, pp 256-257

[Article by Nobushige Kawashima of the Institute of Space and Astronautical Science]

[Text] It is generally thought that the moon has already been explored sufficiently by the Apollo project, but

actually, only a small number of landing points have been found and only a very few places explored, mainly in the vicinity of what planetary science refers to as the moon's equator.

Twenty years have passed since the Apollo Age. Japan currently has the capability to explore the moon scientifically. It is now thought necessary to study how this exploration should be promoted. Several years ago, the Institute of Space and Astronautical Science [ISAS] of the Ministry of Education formed a working committee within the space scientific committee. Leading Japanese scientists and researchers of planets participate in the working committee and discuss methods of promoting the Japanese lunar exploration and research. The essential aspects are shown below. These plans have resulted from the working committee's current study, and will now be combined with other plans selected by ISAS. The combined plan will then be proposed as ISAS' formal proposal.

The First Stage: Path Finding Mission

This is a mission that will open the way for Japan's full-scale exploration of the moon and will be promoted by using a next generation large launching rocket, the development of which is currently demanded by ISAS. The following three missions are being studied:

Preconditions for launching rocket (see Table 1) Possible missions (see Table 2, Figures 1 and 2 and Figure 3 [not reproduced])

Table 1

Constraints	
To be launched by upgraded M-3S	
Weight:	
Low earth orbit	1.8 ton
Moon flyby	455 kg
Moon orbiter (1.2 Re x 10 Re)	408 kg
Moon orbiter (1.2 Re circular)	328 kg
Size	
Diameter	< 2 m
Height	< 2 m

Table 2. Candidate Missions

Lunar Polar Orbiter
  m100 km polar circular orbit
  mPassive remote sounding using IR, X-rays, gamma rays, etc.

Penetrator
  mMore than 2 penetrators on the back side of moon
  mSeismometer/Heat flow meter

Lander
  mEngineering test of landing on the back side of moon
  mTV camera

The working committee has determined that first two rockets, equipped with penetrators and remote-control probes in pairs, must be launched successively within 6 months to 1 year. The feasibility of this requirement is dependent on the development of the rocket to be launched and the competition with other missions that will be proposed within the ISAS, but it is hoped that this requirement is realized early, preferably in the mid-1990s.

The Second Stage: Overall Direct Lunar Exploration

It is hoped that the overall lunar scientific exploration will be realized in the late 1990s using the powerful and unmanned lunar vehicle shown in Figure 4 [not reproduced]. This exploration will be carried out by using the above lunar vehicle, remote-control probe, and penetrator, and will form the foundation of the lunar base construction project in the 21st century. This exploration will be carried out together with the exploration of resources, such as helium 3, etc. In addition, it will serve as a significant mainstay of Japan's space development involving international cooperation, as well as constituting a mission promoted solely by the ISAS.

The Third Stage: Participation in Lunar Base Construction

A lunar base will be constructed in the 21st century. This project will include the construction of a telescope to be used in the study of new astronomical matters, such as gamma rays, neutrinos, gravity waves, etc.

Moon Exploration Project Using Penetrator

[Article by Hitoshi Mizutani, Masahiro Takano and Nobushige Kawashima of the Institute of Space and Astronautical Science; Isao Yamada of Nagoya University]

[Text] 1. Preface

The Institute of Space and Astronautical Science [ISAS] of the Ministry of Education is planning to execute its exploration of the moon in the mid-1990s. Moon exploration employing a penetrator is regarded to be a focus of this project. It can be said that the penetrator is an instrument carrier used to hard-land measuring instruments, including seismometers and heat flowmeters, on the lunar surface from a satellite orbiting the moon. Such a penetrator has not yet been put to practical use abroad, but it appears that the penetrator will become very useful in exploring the internal structure of planets and in forming networks of scientific stations on the surfaces of these planets. Therefore, it can be said that the development of a moon-exploring penetrator is very significant for the future exploration of solid planets, as well as for the exploration of the moon. This paper outlines the moon-exploring penetrator project being studied by the ISAS, and introduces the developmental status of the penetrator.

2. Outline of Moon Exploration Project Using Penetrator

In the Project Apollo, several rocks were collected from the lunar surface and narrow areas along the equator were explored using a remote sensor. However, information on the internal constitution of the moon is insufficient, and global data on the chemical composition and configuration of the surface have not been obtained. These data are indispensable for clarifying the origin and evolution of the moon. This matter has been increasingly recognized in the research which has been conducted since the Apollo project. In addition, the primary purpose of moon exploration using penetrator will be to obtain data on the internal constitution of the moon. If this data is obtained, the internal constitution will be clarified. This clarification will generate information about the materials constituting the interior of the moon, and will lead to the generation of data regarding key points to account for the origin and evolution of the moon.

Three penetrators will be mounted on an oblong polar orbit satellite orbiting the moon, and will be discharged to three sites, including ones on the back side of the moon, in order to set a seismometer and a heat flowmeter. The seismometer will be used to observe the deep earthquakes reported by the Project Apollo, and data indispensable for interpreting the depth constitution of the moon will be obtained. Data obtained from the seismometer and the heat flowmeter will be transmitted to earth via a satellite. Judging from the capacity of the batteries that will be incorporated in the penetrators, the observation period is predicted to last approximately 1 year.

3. Development of Penetrator

It is necessary that all the basic parts, such as the measuring instrument, battery, transmitter-receiver, etc., incorporated in the penetrator be able to withstand an impact of approximately 10,000 grams, since the penetrator will collide with the lunar surface at a speed of 200 to 300 meters per second. It is also necessary that the optimum shape, etc., of the penetrator be investigated since, from the scientifically significant standpoint, it will be required to go from 1 to 3 meters beneath the lunar surface. In order to investigate these items, an experiment in which an almost full-size penetrator with a diameter of 120 mm and a length of 800 mm is driven is being conducted using a penetrator launching device at ISAS' Noshiro Testing Ground. Sand similar to regolith in respect to particle size and hardness is being used as the target. In addition, impact experiments involving model penetrators with diameters of 15 and 50 mm are being conducted utilizing impact devices at Nagoya University and the ISAS. As a results of these experiments, it has been confirmed that the scientific equipment incorporated in the penetrator can sufficiently withstand large impacts caused by collisions. It has also been confirmed that the proper selection of the shape of the tip of a penetrator will cause it to penetrate the sand to the depth satisfying scientific requirements. From the above-mentioned items, it appears that there is a strong possibility that the penetrator will be used as a general and useful equipment item in exploring the interiors of planets as well as the moon.

Japanese Project to Explore Venus

[Article by Koichiro Koyama, Mikio Shimizu, Hironori Matsuo and Yasunori Matokawa of the Institute of Space and Astronautical Science; Hiroshi Oya of the Department of Science, Tohoku University]

[Text] 1. Preface

The United States and the Soviet Union have been competing in [space] exploration since 1961. As a result, much of the mystery surrounding Venus has at last been revealed. However, although the exploration activities are not yet finished, the road for future exploration is becoming increasingly open. Japan's science and engineering joint research group is now in third place in planet observation, and is attempting to develop research on planets through international, minute and full-scale research.

2. Purpose and Academic Significance

Venus, with a radius of 6,073 km, is very similar to the earth, with a radius of 6,375 km, and is the largest of the earth-type planets. On the other hand, there are great differences between the earth and Venus in terms of the atmospheres and magnetic fields covering them. In short, the earth is blessed with abundant seas and proper temperatures and, filled with water and oxygen, represents a paradise for life, while Venus, which exists under complete cloud cover, is exposed from the lower portion of the cloud to a shower of undiluted sulfuric acid filled with high pressure carbon dioxide gas and is just like a hell, with temperatures of from 350 to 400 degrees C and higher. Venus is a planet without a magnetic field. Therefore, even now, solar winds drive against its atmosphere and Venus continues to lose the oxygen that has separated from the carbon dioxide gas. This state does not exist at all on the earth, which is covered with intensive magnetic fields and which stops solar winds at a distance of at least 10 times the radius of the earth. The relationship between Venus' atmosphere and solar wind is a problem quite significant academically. For this reason, the exploration and research of Venus will be promoted in accordance with the "Clarification of the Process of the Mutual Action of Solar Wind and Venus' Atmosphere," which is a basic theme.

Also, according to present observations, the mutual action of the solar wind and Venus' atmosphere is related to aspects involving the disappearance of O-atoms and ions, but judging from the history of the solar

system, there is no doubt that the escape of Venus' atmosphere to the solar system has continued since Venus' birth. Research on the disappearance of atoms and ions generated in the past will be conducted in parallel with the research on the long-time fluctuation generated by the mutual action of Venus' atmosphere and the solar wind.

3. Scientific Observation Equipment

Research on the following themes will be carried out definitively to clarify the process involving the mutual action of solar wind and Venus' atmosphere: 1) behaviors and wave phenomena of particles in the vicinity of ionopose, 2) behaviors including the scale, velocity, characteristics, etc., of the plasma cloud and plasma streamer that seems to be related to the dissipation of Venus' atmosphere, and 3) the nocturnal ionosphere-maintaining mechanism. The observation equipment apparently useful for these tasks include an energy particle measuring instrument, magnetic field measuring instrument, plasma sounder, electric field measuring instrument, plasma energy measuring instrument, ultraviolet measuring instrument, etc. In addition, S- and X-band transmitters can be used to obtain information on Venus' atmosphere and ionosphere.

4. Tentative Mission Plan

4.1 Probe

The weight of the probes currently being considered is 250 kg after having been launched into orbit around Venus. The perihesperian, aphesperian and orbital inclinations of the orbiter will be 300 km, 6 Rv (36,000 km) and 28 degrees, respectively. The period is 11.64 hours. The S- and X-bands will be used in combination as communications systems so that all of the data transmitted from both bands (2 k bits per second) can be ensured at 2 AU. The offset parabolic antenna, with a diameter of 1.2 meters, has been adopted as a despun antenna. When the diameter is larger than 1.2 meters, the widths of the beams of electric waves will be reduced and the attitude control of the probe will be increasingly required since such electric waves are received on the earth. Judging from the capabilities of Japanese launchers, it will be difficult to increase the amount of transmitted data over 2 k bits per second, although 10^{-11} per second would be required for the frequency stability of the S- and X-bands in order to obtain information on Venus' atmosphere and ionosphere. A spin stable-type probe will be used to minimize the weight, and thrusters will be installed in the axial, radial and tangential directions to control the attitude. It is believed that 23 kg of hydrazine will be carried on the probe.

4.2 Rocket and Orbit

A total of 410 kg of Venus fly-by weight are required to ensure 250 kg for the Venus orbiter. Therefore, it is necessary to develop a rocket that can be used to launch a satellite weighing at least 1.8 tons into orbit around the earth. Assuming that, for example, the rocket can be launched in March 1996, it will reach Venus between July and September 1996.

Conclusion

We have studied the Venus mission in cooperation with NEC Corporation, and we acknowledge our appreciation to this company for its cooperation. We want to mention that the Venus mission has not yet been recognized officially, and the figures are presented in the tentative plan prepared by the "Earth-type Planet Exploration Working Committee."

SOCCER Project (Comet Coma Sample Return Mission)

[Article by Kuninori Uesugi of the Institute of Space and Astronautical Science]

[Text] 1. Preface

Solar system exploration projects for the 1990s have attracted worldwide attention. One of them is a comet coma sample return mission in which an unmanned probe will approach a short period comet, collect dust from the comae, and bring the dust to earth. Basically, this is a comet fly-by mission, similar to the "Sakigake" and "Suisei" used to investigate Halley's Comet," and it will be be possible to accomplish the mission by using a comparatively small probe. A working group, consisting of ISAS [Institute of Space and Astronautical Science] and NASA staff members, has been formed. This group has tentatively named the above project "Sample of Comet Coma Earth Return [SOCCER] Project," and is studying this project since it is thought that, except for the dust collector and recovery method upon return, the above mission can be realized using existing technologies. NASA is also studying the CRAF Project[1] and NSR Project.[2] This paper outlines the current status of the SOCCER Project.

2. Mission Analysis

It is impossible to regard the long-period comet as a target in this mission since the appearance of such a comet is uncertain. Accordingly, when the object is narrowed to a short-period comet which seems certain to return to the earth from 1994 to 1999, 35 such comets exist.[3] The mission has been described as "Dust will be collected from comet comae in the intact state by means of the fly-by, and will be brought back to earth," and the mission has been analyzed under the tentative conditions that the relative speed when the probe and comet meet will be 10 km/sec or less and that the launching energy C_3 will be 5 km²/sec² or less. As a result, it has been determined that it will be possible to launch a mission in 1995 to either the Churyumov-Gerasimenko
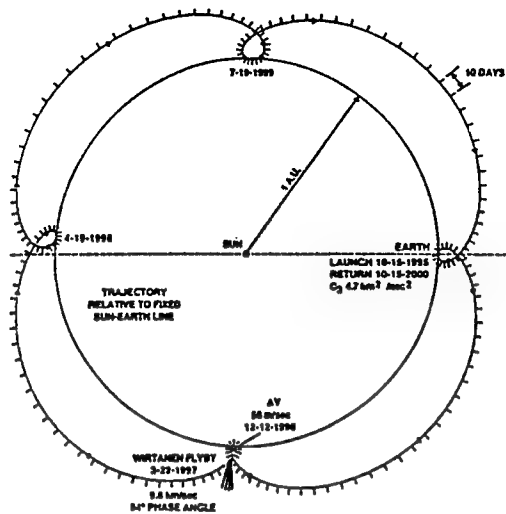
Figure 1. Orbit of Wirtanen Mission

Comet or the Wirtanen Comet, returning to earth in 2000, or to launch one to the same Wirtanen Comet in 1996, returning to earth in 2001.[3] Figure 1 shows an orbit of the Wirtanen Comet Mission in 1995 as a typical example. This orbit is expressed with a rotation coordinate system in which the line linking the sun and the earth is fixed.

3. Concept of Probe

The maximum allowable weight of the SOCCER probe is currently uncertain since the rocket used to launch the probe has not yet been selected. However, the concept of this probe has been studied on the assumption that the weight will be 400 kg. First, the speed-changing capability required by propulsion systems is estimated. Even if the probe is recovered by one of NASA's orbital maneuvering vehicles [OMV] in order for it to return to earth, a large amount of fuel will be required to reduce the speed of the probe upon approaching its orbit. At this time, all propulsion systems of probes must be capable of doing so. Therefore, after the probe has entered into an oblong orbit around the earth, it is necessary to use the so-called "aerobrake technology" in order to lower apogee. It is estimated that the ΔV capability of the propulsion system should be approximately 850 meters per second and the fuel weight about 100 kg, and it is thought that approximately 50 kg-drag cones can be manufactured for the aerobraked. Japan and the United States are currently carrying out the joint research and development of a low density material for a dust collector that can be used to completely catch comet dust flying at approximately 10 km per second. It will be necessary for the dust collector to have a frontal area of at least 5 square meters and a weight of approximately 40 kg. An imaging device and a gamma-ray burst detector, etc., have been proposed as observation equipment in addition to the dust collector and, assuming their weight

totals 20 kg, the weight allowable for other equipment on the probe will be 190 kg. Basically, the probe will be cylindrical and will have a stable system based on a spin or momentum wheel. Also, solar cells will be installed around the probe. The dust collector will be folded and mounted on the upper portion of the probe. It will be elongated only when the probe encounters a comet. This method appears to be good. A drag cone for the aerobrake will be mounted on the lower portion of the probe. On the other hand, a problem involving the communications systems is what shape should be selected for the antennas. One proposal is that electric despun antennas be set linearly on the peripheries of the probe, but it is necessary to study whether or not the probe's necessary attitudes can be ensured and, particularly, whether the circuit between the probe and the earth can be ensured when the probe enters a comet coma. On the other hand, it will be necessary to mount mechanical despun antennas, such as parabolic antennas, etc., on the lower portion of the probe in order to prevent it from colliding with comet dust. In addition, the probe must be able to avoid interference with the aerobrake's drag cones.

References

1. Draper, R.F., "The Comet Rendezvous Asteroid Flyby Project," IAF-87-446, 38th IAF Congress, Brighton, United Kingdom, Oct 1987

2. Kerridge, S.J., et al., "A Comet Nucleus Sample Return Mission," IAF-87-447, 38th IAF Congress, Brighton, United Kingdom, Oct 1987

3. Uesugi, K., et al., "Comet Coma Sample Return Mission," J OF SPACE TECHNOLOGY AND SCIENCE, Vol 3 No 2, 1988 pp 1-11

4. Shimizu, Mikio, et al., "Comet Sample Return Project," Scientific Satellite Symposium Lecture Papers in Fiscal 1988, ISAS, 1988.

MUSES-A Planet Exploration Mission

[Article by Kuninori Uesugi of the Institute of Space and Astronautical Science]

[Text] 1. Preface

The MU Space Engineering Satellite [MUSES-A] was recognized as the Space Activities Commission [SAC]'s 13th scientific satellite in fiscal 1984. The MUSES-A is mainly used to perform engineering experiments in orbit. It has the following main purposes intended to acquire and establish technologies considered to be indispensable for the moon and planet exploration missions in the near future:

(1) A double moon swing-by orbit using the moon is achieved, and high accuracy orbit standardizing and

operating technologies are developed in order to acquire orbit changing technologies using the gravity fields of celestial bodies.

(2) Experiments on the delivery of an artificial micro-miniature satellite around the natural satellite in orbit are performed to acquire the necessary technologies for delivering an orbiter into orbits around celestial bodies.

(3) Telemetry in the X-band is adopted for the first time to transmit data with high efficiency. In addition, experiments on lead Solomon, bucket telemetry, etc., are performed by using new computers mounted on the satellite.

(4) The optical navigation system is important for increasing the accuracy when approaching a target satellite in interplanetary navigation. An experiment involving this system is performed for the first time using a spin stable satellite.

(5) Very slight space dust is observed using a dust counter developed by Technische Universitat Munchen in West Germany. This observation represents a kind of environmental instrumentation for use in space around the moon and the earth.

A flight model is currently being manufactured so that the MUSES-A can be launched by the M-3S 11 Type No 5 rocket from Kagoshima Space Observatory in January or February 1990.

2. Plan for Orbit of MUSES-A

Figure 1 shows a typical example of an orbit of the MUSES-A. This example is expressed by a rotation coordinate system in which lines linking the sun with the earth are fixed. A and S shown in this figure represent an apogee and a swing-by point, respectively. The so-called "Double Moon Swing-by Orbit" is adopted in the MUSES-A so that as many experiments as possible involving swing-by can be performed. As shown by S1 in the figure, the change from a
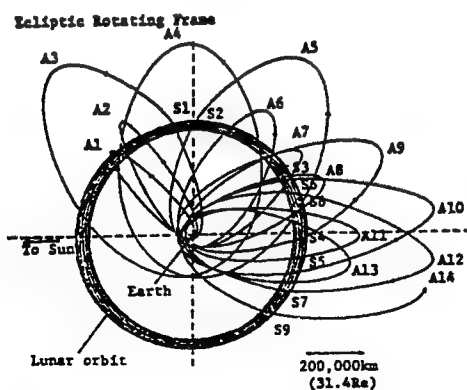
Figure 1. Example of Orbit of MUSES-A

small orbit to a large one is repeated and, as shown by S2, the change from a large orbit to a small one is also repeated.

The lunar orbiter is separated from the satellite proper just prior to the first swing-by, starts a reduction motor, and begins lunar orbit, as shown in Figure 2.
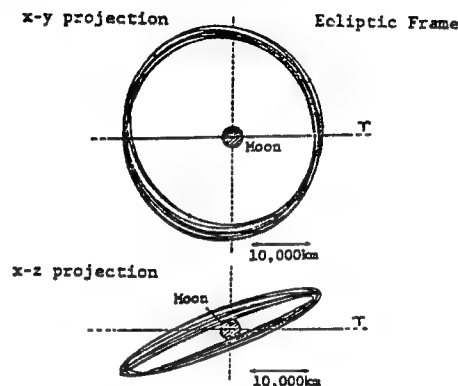
Figure 2. Example of Orbit of Lunar Orbiter

3. Outline of MUSES-A Satellite

As shown in Figure 3, the MUSES-A is a cylindrical spin-stable-type satellite with a diameter of 1.4 meters, a height of 80 cm and a weight of approximately 195 kg. The weight includes about 40 kg of hydrazine fuel for controlling the attitude and orbit and about 13 kg for the weight of the lunar orbiter mounted on the upper portion of the satellite. Also, solar cells are attached to the outside of the satellite. The satellite has an S-band transmitter-receiver and an X-band transmitter as its communications system, and can communicate with Usuda and Kagoshima stations through two low gain antennas for the S-band and middle gain antennas for the S- and X-bands. The satellite is equipped with three accelerometers, as well as a spin-type solar sensor, star scanner and earth sensor as attitude sensors. The actuators consist of an annular-type new station damper and a reaction control system [RCS] consisting of eight 23N thrusters and four 3N thrusters, and have a control capability of 400 meters/second or more in terms of ΔV. The mission equipment includes an optical navigation system, fault tolerant-type mounting computer and dust counter, as well as the previously-mentioned lunar orbiter. The lunar orbiter is of an icosahexahedral shape with a facing length of 40 cm. The power control unit, transponder, data processing unit, measuring instrument, timer and decelerating solid motor are incorporated in the lunar orbiter. Also, 1,000 newly-developed In-P solar cells are attached to the outside of the lunar orbiter. After being separated from the MUSES-A proper, the lunar orbiter will communicate directly with Usuda Station through the two S-band low gain antennas installed on the head of the lunar orbiter.

1.　リアクションコントロールシステム（RCS）

2.　ルナーオービター（LO）

太陽電池パネル（SCP）

3.

オムニアンテナ（LGA）

4.

中利得アンテナ（MGA）

5.
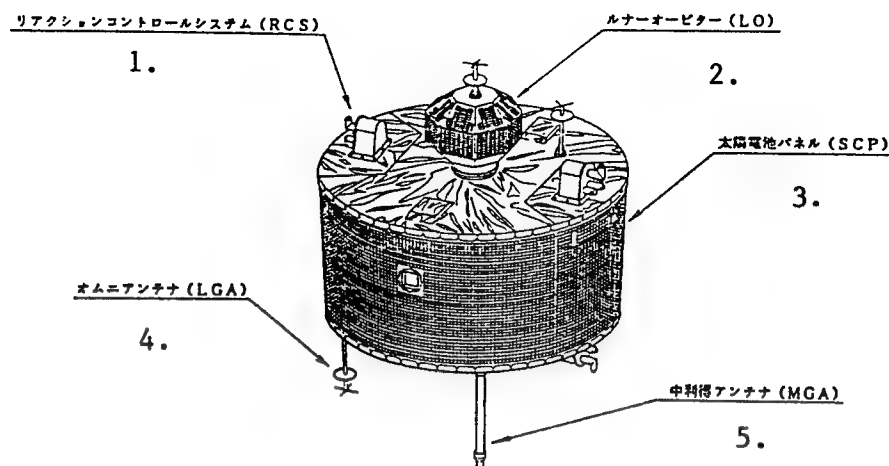
Figure 3. Appearance of MUSES-A

Key:
1. Reaction control system [RCS]
2. Lunar orbiter [LO]
3. Solar cell panel [SCP]
4. Omnidirectional antenna (low gain antenna [LGA])
5. Middle gain antenna [MGA]

Scenario of Lunar Development

43062505u Tokyo PROCEEDINGS OF THE 32ND SPACE SCIENCES & TECHNOLOGY CONFERENCE in Japanese 26-28 Oct 88, No 2A10, pp 274-275

[Article by Tsutomu Iwata of the National Space Development Agency of Japan; Shunsuke Tanaka, Masaya Yamamoto, Toshihide Maeda and Suguru Nakajima of Hitachi, Ltd.]

[Text] 1. Preface

The moon is the celestial body nearest to the earth, and has been investigated scientifically by various missions, including Project Apollo. In recent years, the utility value of the moon has been evaluated from practical aspects involving the procurement of materials necessary for constructing space infrastructures and and advanced space base. In this paper, we will discuss a scenario for lunar development, including dividing it into four phases and carrying them out.

2. Use of the Moon

It is thought that lunar development will be carried out for various purposes, and the following matters can be cited as lunar characteristics which will serve as preconditions for this development: 1) Gravity is low, approximately one-sixth that of the earth. 2) There is no atmosphere on the moon. 3) Mineral components are abundant in the soil and rock. 4) Day and night are long (each continues for approximately 15 days, respectively). 5) Compared with the earth, it is possible to use wide spaces on the moon.

Energy is required to place lunar objects into orbit around the moon or to escape from the moon. However, because of items 1) and 2) above, this energy is smaller than that required on the earth. From the standpoint of the degree of acceleration, i.e., the amount of propellant necessary for carrying a constant payload, compared with that required on the earth's surface, the lunar surface is very close to the lower earth orbits, geostationary orbit, etc. In addition, with regard to item 3), metals such as Al, Fe and Ti are useful as materials for structures on the moon and those orbiting the earth, and the oxygen obtained from separating these metals can be used for propellants and breathing aids. From the above-mentioned lunar characteristics, the following matters can be studied as uses for the moon: 1) Plant for producing materials for use in space 2) Advanced space base 3) Base for experimentation, investigation and observation for scientific purposes 4) Sightseeing and medical purposes

3. Scenario of Lunar Development

The lunar development will be divided into the four phases shown in Table 1 and carried out. Each phase is described below.

Table 1.
Lunar Development by Phase

	Explanation	Kind of Space Planes in Moon Periphery			Manned/Unmanned
		In Orbit Around Moon	Lunar Face (fixed)	Lunar Face (moving)	
Phase 1	Remote sensing by using lunar resource probe, exploration of internal constitution by using lunar penetrator, and analysis of surface soil by using lunar vehicle	Lunar resource probe	Lunar penetrator (Seismometer)	Lunar vehicle (Collection and analysis of surface soil)	Unmanned
Phase 2	Objects of exploration are narrowed down from Phase 1, and the exploration is carried out in detail	Lunar resource probe; Relay satellite	Lunar base (Pressurized module and power source)	Lunar vehicle (Excavation and analysis)	Partially manned
Phase 3	Excavation of lunar resources, and small-scale lunar plant for handling the lunar resources	Relay satellite; station orbiting moon; lunar landing plane	Lunar base development type; small-scale lunar plant	Excavator; Transporter	Partially manned
Phase 4	Full-scale production activities are carried out on the moon	Relay satellite; station orbiting moon; lunar landing plane	Lunar base development type; lunar plant; lunar power plant	Excavator; transporter; other robots	Partially manned

(1) Phase 1

A lunar resource probe is launched into lunar orbit, and is remote-controlled with sensors so that it can smoothly investigate resources and conditions for locating a lunar base, lunar plant, etc. In addition, surface soil is collected by a lunar vehicle and is analyzed.

It is necessary to investigate the mystery surrounding the moon for scientific purposes. A penetrator is placed in the moon to observe earthquakes and the artificial earthquakes generated by the lunar vehicle. The internal constitution of the moon is investigated based on this observation.

(2) Phase 2

The only locations promising as sites for resource digging are explored continuously based on the exploration results gained from Phase 1. As in the case of Phase 1, a lunar resource probe and lunar vehicle are used to investigate the moon. In addition, a simple lunar base is constructed on the moon so that humans can conduct a detailed investigation of the moon.

The lunar base consists of a cylindrical module close to the pressurization module of the space station and a power source system using solar cells.

The lunar vehicle has excavation capabilities in addition to the ability to collect surface soil shown in Phase 1, and can collect underground samples.

(3) Phase 3

The lunar base is expanded, and a small-scale lunar plant is constructed as an extension of Phase 2.

In addition, a lunar landing plane flies between the moon and the lunar orbit in order to raise the efficiency, and a lunar-orbiting station is constructed as a relay base as the frequency of flying between the earth and the moon increases.

(4) Phase 4

Phase 4 is a further developed version of Phase 3. The lunar plant is operated on a full scale, a lunar power plant is also constructed, and electric power is supplied to the various facilities.

Although solar energy is plentiful on the moon during the day, the procurement of energy during the night represents a problem. The following items can be considered as means for procuring nighttime energy: (1) Secondary battery In this case, night activities should be minimized. (2) Fuel cell This system has the advantage whereby water, which is a product of fuel cells, can be used by the humans on the moon. (3) Heat reservation With this method, energy obtained during the day can be reserved in the form of heat, and power can be generated by this heat during the night. Solar energy can be used highly efficiently by combining this method with the temperature difference power generating method mentioned below. (4) Temperature difference power generation Although the lunar surface temperature increases and decreases sharply, the temperature of areas approximately 2 meters below the lunar surface remains constant, about -30 degrees C at all times. Therefore, it may be possible to generate power by using the temperature difference between the lunar surface and internal areas. (5) Atomic battery Atomic batteries are used in American deep space probes, but are inappropriate as large capacity power supply sources. (6) Nuclear power generation Nuclear power generation is promising as a means

of supplying a large amount of energy night and day. It is excellent as a means of generating power on the moon since electric power can be supplied by a small amount of fuel over a long period of time, but, in order to realize this means, the following problems must be solved: a) The procurement of materials on the moon to reduce the transportation costs b) Developing a cooling system suitable for lunar operation c) Ensuring the safety of fuel transportation

(7) Developing a power plant network

Power plants using solar beams or solar heat are constructed at several sites (at least three) on the moon's equator, and if facilities, such as plants, etc., which consume electric power are linked with these power plants via a network, it will become possible to supply electric power to these facilities at all times. In this case, the problem involves transmitting energy from the power plants to the electric power consuming areas and vice versa.

4. Postface

This report describes a scenario of lunar development as divided into four phases taking lunar characteristics into consideration. In the future, we plan to study the trade-off between transporting materials from the earth and procuring them on the moon from the standpoint of cost, as well as a more economical and realistic scenario of lunar development.

Lunar Base Concept

43062505v Tokyo PROCEEDINGS OF THE 32ND SPACE SCIENCES & TECHNOLOGY CONFERENCE in Japanese 26-28 Oct 88, No 2A11, pp 276-277

[Article by Tsutomu Iwata of the National Space Development Agency of Japan; Katsutoshi Omura and Kazuo Aida of Mitsubishi Electric Corporation]

[Text] 1. Preface

According to a recent NASA report, the lunar base concept has suddenly entered into the limelight, symposiums have been held successively in the United States, and study meetings have been held increasingly in Japan. The lunar base is still at the conceptual stage and lunar base scenarios are being prepared enthusiastically. This report describes the philosophy of realizing the lunar base concept, and presents ideas for the conceptual and developmental plans of the lunar base.

2. Coping with South Pole Base and Lunar Base

The South Pole Base is very instructive as an example in that several to several dozen humans live under severe environmental conditions in order to conduct scientific observations. Table 1 was prepared by summarizing previously-collected information. There are significant differences between the conditions found at the South Pole Base and a lunar base, but it is generally thought that the two bases will have many things, such as the construction of buildings and living areas, a few people living in an enclosed space, etc., in common. It is believed that the rules, etc., already drawn up can be used for the lunar base since it will be absolutely necessary to construct this base through international cooperation. The problem lies in the significance of lunar use (practical and scientific observation) and its supporting system. Would a strong tendency toward constructing a lunar base emerge if a kind of pioneering boom were promoted? It seems important that a plan be made so that global support can be obtained.

Table 1.
Summary of Lunar Base and South Polar Base

	South Polar Base	Lunar Base	Remarks
Purpose	IGY	Astronomical earth observation site, testing ground	
	Earth observation site	Human living areas other than earth	
	International cooperation (territory/resources)	Advanced base toward solar system	
		Use of resources/international cooperation	
Environment	Very cold, blizzards	1/6 gravity	
	Nights with midnight sun, snow, ice	Vacuum (no air), exposure to radiation	
		24 hours, 14 days (temperatures of 100 to -140°C)	
Transportation means	Icebreaker, helicopter, etc.	(1) Ground → SS (Shuttle, HOPE)	
	Snowmobile, dog sled	(2) SS → SS orbiting moon (special purpose OTV)	
		(3) SS orbiting moon → lunar surface (special-purpose taking-off and landing ship)	
		(4) Lunar vehicle and working vehicle	
Construction	Three buildings, power generation/communications building	Various plans	
	Increase in construction work	1. Use of SS modules	

**Table 1.
Summary of Lunar Base and South Polar Base
(Continued)**

	South Polar Base	Lunar Base	Remarks
		2. Use of lava tube/precipices	
		3. Use of concrete	
Developmental form	11 to 20 wintering members	Initial Period: several to 10 wintering members	
	Observation base strictly specified	Developmental period: Several dozen to several hundred wintering members	
		Mature period: Several thousand wintering members (Lunar city)	
International cooperation	IGY and calling	Mainly NASA	
	Participation of 64 countries	Soviet Union, ESA, Canada, Japan	
	Participation of up to 100 countries(?)	Only advanced countries(?)	
Use	Permanent observation base	Use of resources	
	Tourist and resource development	Others	
		Testing ground and waste disposal area	
Cost	¥ 200 to 300 billion (FY 1988 conversion)	¥ 2 to 6 trillion (FY 1992 conversion)	ROM

3. Conceptual Plan for Lunar Base

The lunar base concept can be broadly classified into the following four items, and it is thought necessary to use the base properly in accordance with the initial, developmental and mature stages: (1) Use of pressurized section, node, etc., of space station (2) Use of caves, lava tunnels, etc., on the moon (3) Construction of unit-type buildings made of concrete (4) Use of robots, linear motor cars, unmanned plants, mass drivers, etc.

Some think that the surface of the moon is covered with regolith, about 2 meters in thickness, as a measure against radiation and to control temperatures. However, this idea is problematical in respect to workability and effectiveness. Accordingly, it is believed to be most practical to use the caves of precipices for permanent facilities. For this reason, it will become important to probe the lunar surface by means of a remote sensing satellite in order to select a site for base construction, and it will become necessary to observe the moon with higher accuracy than that found in the age of the Project Apollo. Figure 1 shows a lunar base concept at the developmental stage. Features of this idea include living spaces employing the caves of precipices, dome-type farms to supply food, a plant using minerals to collect oxygen, traveling linear motor cars, a mass driver using resources, etc. Atomic batteries, etc., will supply electric power during the night. In the future, at the mature stage, unit living quarters made of concrete will be constructed in the living areas apart from the production areas.

4. Developmental Plan, etc.

It is necessary to make a plan and prepare an idea for allotment, taking international cooperation into consideration, so that national support for transportation means, residential modules, life sustaining equipment, experimental means, etc., can be obtained. The United States, and the Johnson Space Center in particular, is planning a lunar base (some claim it will be an expedition to Mars) as a target of the space station. The following scenarios can be regarded as forms of international cooperation, but it will be necessary to make a careful study of how to execute these cases. A: Each country participates equally in each working group, from system design to construction, and discharges completely equal duties (international working group, UN system). B: A certain country is in charge of the system design, with other countries in charge of hardware, software, and subsystem design generated from the system design in accordance with their expertise. C: A certain country carries out such design work as the system design, subsystem design and hardware, with other countries manufacturing products based on the specifications obtained from the design work, performing tests on the products, and delivering the products to the United States. D: Each country carries out similar development work independently while exchanging information on its status and engaging in proper international cooperation.
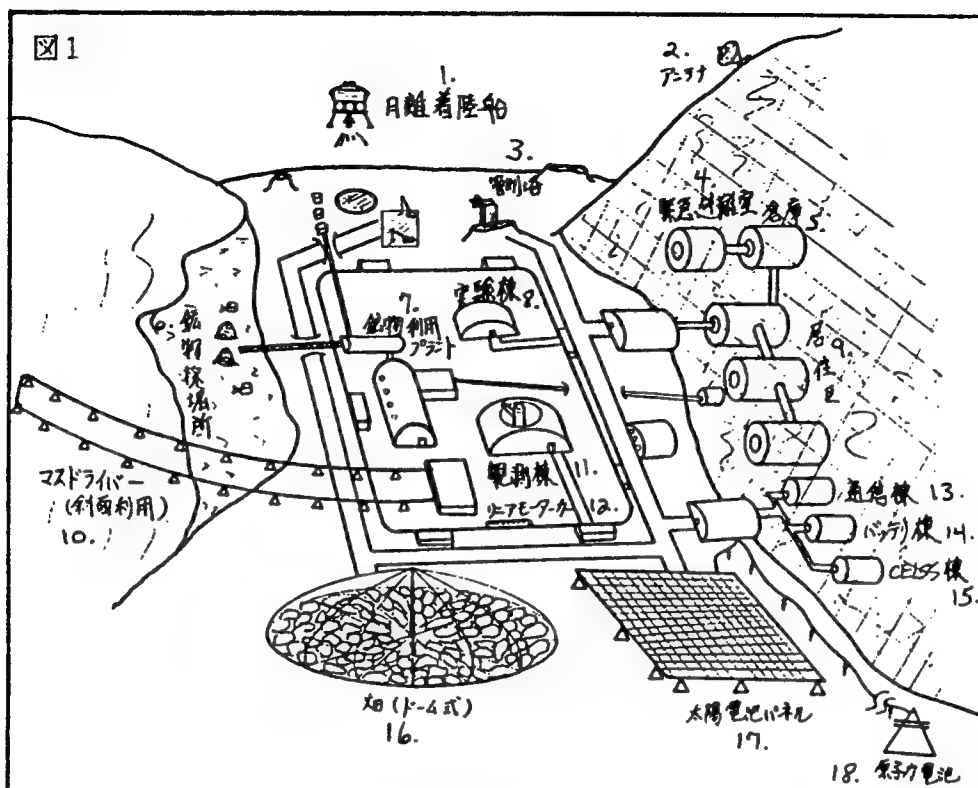
Figure 1.

Key:
1. Lunar take-off and landing ship
2. Antenna
3. Control tower
4. Emergency evacuation site
5. Warehouse
6. Mineral slope
7. Mineral-using plant
8. Experiment building
9. Living quarters
10. Mass driver (using slope)
11. Observation building
12. Linear motor car
13. Communications building
14. Battery building
15. CELSS building
16. Farm (dome)
17. Solar cell panel
18. Atomic battery

References

1. "Lunar Bases and Space Activities in 21st Century,"
NASA, Mendell, 1986.

Study of Lunar Flight System, Necessary Technical Subjects

[Article by Yasuo Kano and Hitoshi Takatsuka of the National Space Development Agency of Japan; Akira Nakajima of Mitsubishi Space Software Co., Ltd.]

[Text] 1. Preface

Artificial satellites are launched into orbit so that they can be used for various purposes. In the past, Japan's space development has attached importance to the launching of such artificial satellites. It is anticipated that, in the future, the scope of human activities will be rapidly extended in proportion to the progress of space base construction involving international cooperation and that the scope of activities of the respective countries, including Japan, will be extended to the moon at the end of the 20th century or the beginning of the 21st century. In consideration of this tendency, we have studied the trajectory of the H-II rocket to the moon (around the moon for the time being), have ascertained the possibility of lunar missions and have taken up the technical developmental subjects which will become necessary in the future.

2. Establishment of Trajectory to the Moon

A flying probe is affected by the gravitation of the sun and planets as well as that of the earth and the moon. In order to establish a definite trajectory to the moon, it is necessary to handle this matter as an n-body problem. Celestial bodies other than the earth and the moon have not been taken into consideration since importance has been attached to obtaining the overall tendency for the trajectory. Also, the problem has been handled as a two-body problem on the assumption that the probe is affected only by the gravitation of the earth until it enters the gravisphere of the moon, and is affected only by the gravitation of the moon once it enters the moon's gravisphere.

The basic flight system is as follows: After the H-II rocket lifts off, a probe is place in orbit around the earth (parking orbit) at the second-stage engine cut-off [SECO]-1, the speed is increased to the required speed by re-starting the second stage, and the probe is moved to an oblong lunar transfer orbit. After the probe reaches the gravisphere of the moon, its trajectory generally becomes a hyperbolic orbit and, after the probe passes through the perilune, it escapes the gravisphere of the moon. Accordingly, it is necessary to reduce the speed of the H-II rocket at the specified altitude and lower the speed of the probe to the lunar circulating speed. Figure 1 shows a conceptual drawing of the above-mentioned matter.

The lunar transfer orbit is established as follows: the perigee altitude is established in consideration of the orbit transferring efficiency from the parking orbit, and the apogee altitude is determined by giving a proper oribtal period to the time, approximately 180 hours (in the standard case). This time has been established as the flight time of the probe which is placed into lunar transfer orbit and which passes through the perilune,
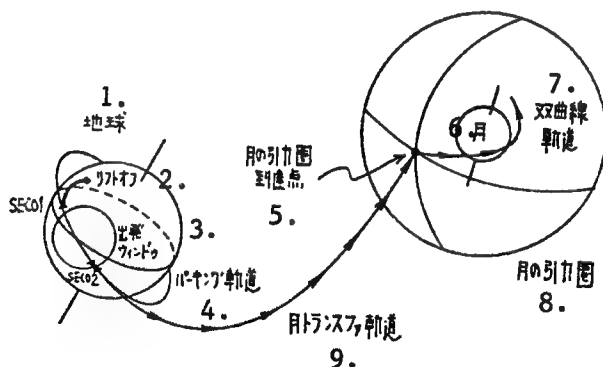
taking into consideration the observability, etc., of earth stations. It is necessary to establish the proper longitude and latitude when the probe reaches the orbit inclination and the lunar gravisphere, in accordance with the H-II rocket launching date (relative relationship between position of earth and lunar coordinate systems) and the required mission, since the above-mentioned longitude and latitude directly affect the hyperbolic orbit elements when the probe approaches the moon. The launching azimuth and launch time when the H-II rocket leaves the earth are determined so that the speed loss is minimized when the rocket moves from the parking orbit to the above-mentioned transfer orbit. However, the yaw rate is required during combustion in the main engine since the launching azimuth is restricted by other conditions involving flight safety. Therefore, the launching capabilities are lowered to some extent.

The following shows an example of calculations for the case of an H-II rocket being launched on 1 August 1996, with a perilune altitude of 100 km and a 90-degree inclination of orbit in the lunar approaching orbit:

Launching azimuth: 130 degrees

Lunar gravisphere reaching condition: Longitude of 14 degrees and latitude of 10 degrees

Parking orbit around the earth: Circle with a radius of 6,578 km, inclination of orbit of 61.1 degrees, and circular orbit speed of 7.784 km/sec

Lunar approaching orbit: Perilune altitude of 100 km, hyperbola with eccentricity of 1.45, inclination of orbit of 87.3 degrees, and perilune speed of 2.555 km/sec

Lunar transfer orbit: Ellipse with a radius of 6,578 x 382,000 km, inclination of orbit against the earth of 61.1 degrees, perigee speed (starting speed) of 10.915 km/sec, and $\Delta V_1 = 3.131$ km/sec

Flight time up to perilune: 107.4 hours

Launching capability: Approx. 2,800 kg (use of H-II rocket)

The H-II rocket moves from the hyperbolic orbit to the lunar orbit when it approaches the moon. It is possible to regard this movement as an orbital transfer in planes. When the final orbit is a circular orbit with an altitude of 100 km and an inclination of orbit of 90 degrees, as shown below, the effective weight of the probe is approximately 2 tons.

Perilune speed: 2.555 km/sec

Propulsion system: Hydrazine/NTO system (Isp = 320 s)

Circular speed at altitude of 100 km: 1.633 km/sec

Amount of propellant: 710 kg

ΔV_2: 0.922 km/sec

Weight of propulsion system: 90 kg

Figure 1. General Conceptual Drawing

Key:
1. Earth
2. Lift off
3. Start window
4. Parking orbit
5. Lunar gravisphere arrival point
6. Moon
7. Hyperbolic orbit
8. Lunar gravisphere
9. Moon transfer orbit

Effective weight of probe: 2,000 kg

3. Necessary Technical Development Subjects

(1) Star Sensor (Canopus Star Tracker) and Attitude Determining System

This is an on-board system which determines or corrects the attitude of the probe in the lunar transfer orbit, and consists of a star sensor and compact computer recording information on an all-weather map.

(2) Real-Time Orbit Determining System

This is an earth station system which measures the range and range rate of the probe, determines the real-time orbit and calculates the amount of correction for various orbits if these orbits are to be transferred.

(3) Orbit Transferring Engine System

This is an on-board system which corrects orbital errors in the lunar transfer orbit, moves this orbit toward the lunar orbit, starts the maneuver engine on the basis of the orbit correction determined on the ground, and controls the increased speed.

Study of Conditions Required for Soft Landing on Moon

43062505x Tokyo PROCEEDINGS OF THE 32ND SPACE SCIENCES & TECHNOLOGY CONFERENCE in Japanese 26-28 Oct 88, No 2A16, pp 286-287

[Article by Akira Nakajima of Mitsubishi Space Software Co., Ltd.; Yasuo Kano of the National Space Development Agency of Japan]

[Text] 1. Preface

Japan has not accumulated any lunar or planet exploring technologies, or soft landing technologies in particular, from experience. Therefore, when Japan works out her own lunar soft landing plan in the future, it will be necessar for her to design the systems and develop the technologies based on the Project Apollo, etc., executed in the past. In this paper, we will describe the results of analyzing orbital errors occurring when a landing plane conducts inertial navigation using an inertial measuring unit [IMU], and will study the requirements determined by this initial analysis.

2. Standard Orbit and Landing Plane System

The standard orbit used in the above analysis of the landing was designed with reference to Project Apollo. The details are as follows: (1) Standard orbit: A landing plane is transferred from a lunar orbit at an altitude of 100 km to an elliptic orbit with an apolune altitude of 100 km and a perilune altitude of 15 km. When the landing plane passes through the perilune, it will begin to
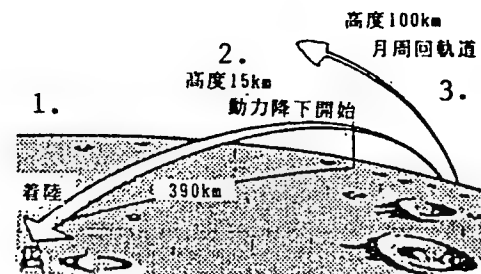
Figure 1.1 Outline of Descent Orbit

Key:
1. Landing
2. Start of decrease in power at altitude of 15 km
3. Orbiting moon at altitude of 100 km

lower its power and make a soft landing. The orbit is outlined in Figure 1.1 and Table 1.1. (2) Landing plane system: The landing plane is launched with the H-II rocket and its initial weight is estimated to be 1,500 kg. The inertial navigation system [INS] mounted on the landing plane is strapped down as is the IMU on the H-II rocket. Table 1.2 presents details of the landing plane system.

**Table 1.1
Sequence of Events**

Time (sec)	Event
0.0	Placing of Hohmann transfer orbit
3412.5	Start of decrease in power upon passing through perigee
4050.9	Touch down

**Table 1.2
Details of Landing Plane System**

Initial weight of landing plane	1,500 kg
INS to be mounted	Strapped-down-type IMU mounted on H-II rocket
Thrust system for descent	Three-stage step-type thrust
	Specific impulse: approx. 350 sec
	Thrust at first stage: approx. 476 kg
	Thrust at second stage: approx. 277 kg
	Thrust at third stage: approx. 135 kg

3. Analytical Conditions

After the landing plane is placed into transfer orbit, IMU errors will be generated. The influence of these errors on the orbit until the landing time is analyzed by using the above-mentioned standard orbit. With regard to the IMU 3σ main error sources, see Table 1.3.

Table 1.3
Results of Analyzing Errors**

Error upon landing (T = 4,050 sec)		Position error (meters)			Speed error (m/sec)		
		X	Y	Z	X	Y	Z
IMU Main Error Source	Acceleration system x	-886	151	0	-1.11	-0.42	0.00
	Bias (130 μg) y	0	0	-427	0.00	0.00	0.15
	z	2820	-1310	0	3.80	0.79	0.00
	Gyro-bias (0.12)	0	0	-527	0.00	0.00	-1.64
	y	1440	584	0	3.93	2.21	0.00
	z	0	0	641	0.00	0.00	1.46
	Gravity (J3)	229	-203	-2	0.33	0.09	0.00
	3 σ RSS value	3175	1326	678	5.48	2.35	1.64
	(*)	(2799)	(2001)	(698)	(4.82)	(3.51)	(1.64)

(*) 3 σ RSS value in the directions of altitude, down range, and cross range, respectively.

4. Results of Analysis

Table 1.3 shows the results of analyzing the errors caused by the IMU 3 main error sources.

This table indicates that it is difficult for the landing plane to make a soft landing solely on the basis of the navigation calculation results using the INS. The altitude directional error is generated by the IMU main error sources (3σ) upon landing. The altitude directional error, at about 3 km, is particularly remarkable. Therefore, it is necessary to conduct composite navigation using inertial navigation equipment and an altimeter when landing. Navigation of higher accuracy requires a speedometer.

As mentioned in 3 above, this analysis was conducted under the assumption that, prior to the landing plane being placed in transfer orbit, IMU errors will not exist, i.e., an ideal state will exist. This means that, in actual missions, it will be necessary to initialize the IMU before placing the landing plane into transfer orbit.

The conditions required as a result of this analysis are as follows: 1. composite navigation, 2. initialization of the IMU.

5. Postface

The above analysis is basic, and has been conducted taking only IMU errors into consideration. In the future, it will be necessary to carry out orbit analysis by taking the initial position, speed, attitude error, etc., into consideration, as well as to set the required conditions over a wider area. It will also be necessary to carry out analysis with respect to the direct transferring of a landing plane from the lunar transfer orbit as well as the landing of the landing plane from the lunar orbit.

References

1. "Apollo 11 Mission Report," No NASA SP-238.

Instrumentation Data Processing System for Testing Large Artificial Satellites

[Article by Senjiro Iide and Ken Nozawa of the National Space Development Agency of Japan; Masahiro Soura, Katsura Kawate, Yoichi Takegawa and Kazuo Momose of Toshiba Corporation]

[Text] 1. Preface

The National Space Development Agency of Japan [NASDA] is constructing a facility at the Tsukuba Space Center. This facility will be used to comprehensively perform tests on an engineering test satellite, type VI, a space station experimental module and various space planes which will become increasingly larger from now on. Regarding this comprehensive testing facility, in this paper we will outline the instrumentation data processing system used to collect, analyze and control various data on specimens and to control the operation of the overall facility.

2. Outline of System

Figure 1 shows an outline of the instrumentation data processing system. This system consists of four sets of processing units (high speed data collector/measuring instrument and super minicomputer: TOSBAC G-8000), a set of computers (super minicomputer: TOSBAC G-8000), work station (EWS: AS-3000) and a personal computer (PASOPIA) as a data terminal. These computers are connected by means of a local area network [LAN]. The four sets of processing units are used to process the data sent from various facilities for tests involving the space chamber, vibration, sound, and impact. The set of computers is used to store and control the test data, data base, etc., and to analyze the data. The
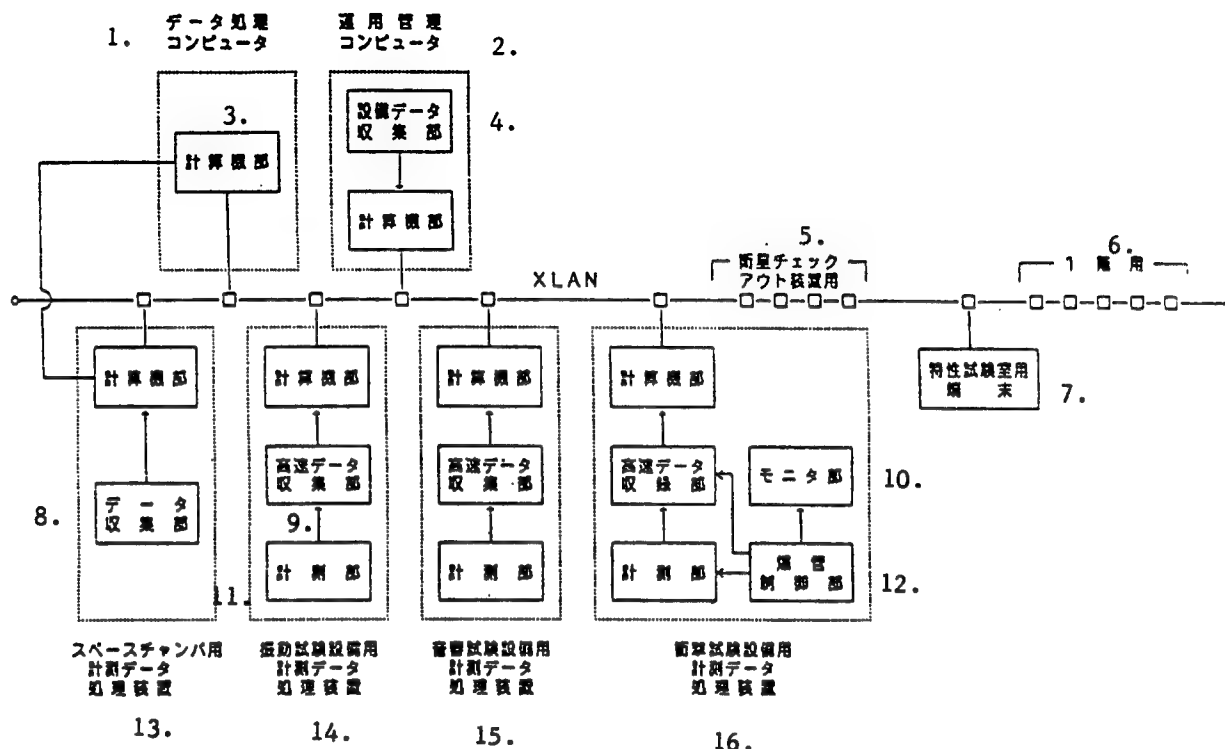
Figure 1. Outline of System

Key:
1. Data processing computer
2. Operation control computer
3. Computer section
4. Facility data collecting section
5. For satellite check-out unit
6. For first floor
7. Terminal for characteristic testing room
8. Data collection section
9. High speed data collecting section
10. Monitoring section
11. Measuring instrument section
12. Explosion tube control section
13. Instrumentation data processing unit for space chamber
14. Instrumentation data processing unit for vibration test facility
15. Instrumentation data processing unit for acoustic test facility
16. Instrumentation data processing unit for impact test facility

work station is used to one-dimensionally control the operation of the overall test facility.

3. Function

Table 1 shows the function and performance of this system. The system possesses the following features:

1) High speed processing (real-time collection/high speed analyzing) Data used to be recorded on tapes, etc., and was then input by means of a processing unit. However, in this system, data can be input directly to a processing unit by means of a high speed data inputting function and, immediately after being collected, it will be fast-Fourier-transformed [FFT]ed by means of a high speed arithmetic processor (DSP 9506). With this method, the work, extending from data input to the required analysis, can be carried out in less than one-tenth the time previously required.

2) Back-up processing Thermal vacuum tests using a space chamber require a long period of time (45 days maximum). Even if an accident occurs in the system during the testing, no problems result since the system's hardware and software enable the data processing computer to gain control instead of the system.

3) Comprehensive control The system one-dimensionally controls all testing states as well as the water, electric power and room entrance. Data can be shared since the respective computers are connected through the system's LAN. In addition, the system is constructed so that it can cope flexibly with its future extension, etc., since a standard LAN has been adopted.

4. Postface

Space planes will become increasingly larger from now on. This system is currently being installed at Tsukuba Space Center and wil be completed as part of the

Table 1.
Function and Performance of System

	Instrumentation Data Processing Unit for Space Chamber	Instrumentation Data Processing Unit for Vibration Test Facility	Instrumentation Data Processing Unit for Acoustic Test Facility	Instrumentation Data Processing Unit for Impact Test Facility of measuring points
	Temperature of specimens, etc., approx. 1,360 points	Acceleration, strain, etc., approx. 370 points	Sound pressure, acceleration, strain, etc., approx. 250 points	Acceleration, etc., approx. 200 points
Continuous instrumentation period	45 days (max)	Sine wave for 6 minutes, random wave for 3 minutes	4 minutes	160 milliseconds
Data processing	Quick look (temperature graph indication)	Quick look	Quick look	Quick look
Analyzing		Transfer function; f-g curve; PSD analysis; mode analysis	PSD analysis; 1/1, 1/3 octave; effective value time history	SRS analysis; FFT analysis; indication of waveform

comprehensive environment testing facility for use in launching four space planes annually. After tests on the relationship between the system and the respective test facilities are conducted, the system is scheduled to be completed around June 1989. Finally, we thank all the persons concerned for their help with this system.

Analysis of ETS-VI Contamination

43062505z Tokyo PROCEEDINGS OF THE 32ND SPACE SCIENCES & TECHNOLOGY CONFERENCE in Japanese 26-28 Oct 88, No 2B2, p 294

[Article by Koji Terada of the National Space Development Agency of Japan; Kimitsune Akai and Hiromichi Kochi of Toshiba Corporation]

[Text] 1. Preface

It may become impossible to maintain the initial performances of artificial satellites since the surfaces of these satellites are contaminated due to various factors and optical characteristics change. In order to prevent the surfaces from becoming contaminated and the optical surfaces from changing, it is necessary to analyze the contamination in advance and to take effective measures against the contamination.

It is becoming increasingly important to analyze the contamination since the ETS-VI has a long life, many kinds of thrusters serve as contamination sources, and many types of mission equipment and sensors are readily affected by contamination.

Table 1. 1N in Control of E/W Orbit; Amount of Thruster Plumes Attaching

		付着量 1. (A) *1	許容温度範囲 (℃) 2.
3. 東	精太陽センサ 6. (FSSH3)	1.4	-40～65
	Sバンドアンテナ (S-ANT2)	170	-155～90
	イオンエンジン放熱面 (OSR)	9300	-13～ *2
	イオンエンジン本体 (ITRS)	610	-100～ *2
4. 西	精太陽センサ 10. (FSSH1)	1.6	-40～65
	(FSSH2)	2.0	〃
	粗太陽センサ (CSSH2PA)	1.1	-55～95
	(CSSH2PB)	1.2	
	(CSSH2YA)	1.2	
	(CSSH2YB)	1.2	〃
	放射線計測装置 11. (SRU)	1.5	-30～60
	イオンエンジン放熱面 (OSR)	9300	-13～ *2
	イオンエンジン本体 (ITRS)	610	-100～ *2
5. アンテナ	20GHz主反射鏡(裏面: MLI) 12.	95	-180～100
	30GHz主反射鏡(裏面: MLI) 13.	240	TBD

*1 スラスタ噴射60秒当りの値 14.   *2 解析による予測最低温度 15.

Key:
1. Amount of Thruster Plumes Attaching (A) *1
2. Allowable Temperature Range (°C)
3. East side
4. West side
5. Antenna
6. Accurate solar sensor
7. S-band antenna
8. Ion engine heat radiating surface
9. Ion engine proper
10. Accurate solar sensor
11. Dosage meter
12. 20 GHz main reflecting mirror (back side: MLI)
13. 30 GHz main reflecting mirror (back side: MLI)
14. *1: Value per 60 seconds of thruster injection
15. *2: Lowest temperature anticipated with analyses

This report describes contamination of the ETS-VI, specifically that caused by RCS 1N thruster plumes and ion engine (IES) electrical discharge chamber wearing substances. It seems that the contamination caused by these plumes and substances greatly affects the ETS-VI.

CONTAM is used as the standard software for analysis in the West. This CONTAM was used to analyze the contamination of 1N thruster plumes.

2. Results of Analysis

(1) Amount of RCS 1N Thruster Plumes Attaching

Table 1 shows the amount of thruster plumes becoming attached to the surface of each satellite in the case of E/W orbit control. Substances attaching to the surface include NH_3 and H_2O, and the volumetric ratio is approximately 20:1. The allowable temperature ranges of the respective components are different from the actual surface temperatures, but, for reference purposes, Table 1 shows these allowable ranges. It is anticipated that NH_3 and H_2O will not attach to many components except for the solar cell paddle and the heat insulating blanket (MLI) since, when the surface temperature is greater than -90 degrees, these substances will not attach to these components. It is also believed that even if the substances become attached to the components, they will not exert any large influences on the components since they will evaporate when the temperature rises.

Study of Platform-type Earth Observation Satellite System

43065012a Tokyo PROCEEDINGS OF THE 32ND SPACE SCIENCES & TECHNOLOGY CONFERENCE in Japanese 26-28 Oct 88, No 2B9, pp 308-309

[Article by Tatsuna Kawashima, Kojiro Ikuta and Noriaki Oka of Toshiba Corporation]

[Text] 1. Preface

This report describes the platform-type earth observation satellite system, specifically the satellite configuration. This satellite is scheduled to be launched as Japan's earth observation satellite. The system was also studied in fiscal 1987.

2. Mission of Platform-type Earth Observation Satellite

The object of the study of this system is a satellite used to conduct two missions, i.e., earth observation and platform technical development. Therefore, as shown in Table 1, this satellite must have the equipment/functions appropriate for platform technical development as well as earth observation equipment.

Table 1. Example of Missions for Platform-type Earth Observation Satellite

Mission Requirement	Equipment to be Mounted/Function
	Name
Earth observation	Sea water color-sea water temperature scanning radiometer (OCTS)
	Advanced visible near infrared radiometer (AVNIR)
	Wide collection sensor (AO sensor)
	Data collecting system (DCS), or:
	Direct broadcasting system(DB)
Earth observation and development of platform technology	Data relay tracking satellite communications function
	High accuracy attitude orbit control function
Development of platform technologies	Technologies for modularization/unit
	Automation/autonomous operating function
	Long life two-liquid-type propulsion system

3. Main Items Required for Platform-type Earth Observation Satellite System

Table 2 shows the main items required for the platform-type earth observation satellite system. The dual launch utilizing the H-II rocket is assumed in this study. The launching weight must be 2,500 kg or less, and this satellite must be incorporated in the lower portion of the fairing with an inside diameter of 4.6 meters.

Table 2. Example of Main System Requirements

Item	Requirements
Launching period	Winter of fiscal 1993
Launch rocket	H-II rocket
	Stored in lower portion of dual fairing
	Inside diameter of dual fairing is 4.6 meters
Launch weight	2,500 kg or less
Launch site	Tanegashima Space Center
Orbit altitude	799.8 km (stationary observation orbit)
	703.3 km (orbit transfer experimental orbit)
Inclination of orbit	98.6° (stationary transfer experimental orbit)
	98.2° (orbit transfer experimental orbit)
Descending node local hour	10:30 am +/- 15 min
Placed orbit	Apogee altitude: 800 km +/- 180 km
	Perigee altitude: 250 km +/- 180 km
	Inclination of orbit: 98.6° +/- 0.2°
Design life	3 years

4. Modularization and Unit

The system was studied based on the following: 1) the platform-type earth observation satellite shall consist of three modules, i.e., mission module, bus module and propulsion module, and 2) in principle, the dimensions of the respective units shall be unified through a subsystem unit.

With regard to the mission module, the shape and basic dimensions of the mission main body structure have been determined so that all mission equipment can be mounted on the satellite in order to satisfy the requirements of modularization.

With regard to the bus module, the unit has been adopted and the dimensions unified based on the bus equipment data which satisfies the subsystem requirements.

Also, the constitution and basic dimensions of the propulsion module have been determined by analyzing the amount of propellant and requiring that thrusters be installed for orbit conversion.

5. Satellite Configuration

Figures 1 and 2 show examples of satellite configurations obtained from results of basic dimensions of each module and unit, as well as from system design and analysis.

The three modules are positioned in the following order: propulsion module, bus module and mission module,

Figure 2. Example of Configuration in Orbit

Key:
1. Mission module   3. Propulsion module
2. Bus module

from the satellite separation side, taking into consideration the combining with a rocket, ensuring the visual field of each equipment item, evading the influence of plumes, etc. The solar cell paddle is designed to be a one-wing type due to the electric power requirement value and orbit conditions.

The height (axial direction of the rocket) of the main body structure of the mission module is approximately 2.1 meters, and the observation equipment is mounted on the +Z face (earth directional face) of the main body structure. The space at the -Z side is mainly used to store antennas for data relay transmission.

According to the unit dimensions, the main body structure of the bus has a height of approximately 1.4 meters. A bus unit is properly placed in relation to each of the four sides of the bus main body structure in accordance with the requirements involving the visual field, the amount of discharged heat, etc.

The equipment based on the gas jet propulsion system includes the propellant tank, individual thrusters, etc., and is used to convert the orbit, retain the orbit, and control the attitude. All equipment items are installed on the propulsion module in accordance with the principle of modularization.

6. Conclusion

We were able to plan a satellite configuration which satisfies the requirements of unit, modularization and installation of mission equipment imposed on the platform-type earth observation satellite.

Figure 1. Example of Configuration at Launch

Key:
1. Mission module   3. Propulsion module
2. Bus module

Construction of Lunar Structure Using Concrete

43065012b Tokyo PROCEEDINGS OF THE 32ND SPACE SCIENCES & TECHNOLOGY CONFERENCE in Japanese 26-28 Oct 88, No 2C14, pp 356-357

[Article by Hiroshi Kanamori, Shinji Matsumoto, Noboru Ishikawa, Haruyuki Nanba, Yoshiro Kai and Kunihiko Sugihara of Shimizu Construction Co., Ltd.]

[Text] 1. Preface

It is expected that concrete will represent an effective building material when a permanent lunar base is constructed. Reasons for its effectiveness are as follows: 1) most of the necessary raw materials already exist on the moon, 2) the manufacturing process is comparatively simple, and 3) concrete has been used in many situations as a structural material on the earth.

This report outlines a lunar structure for which concrete is employed as the main structural material.

2. Manufacturing of Concrete on the Moon

The following preconditions are required in order for a lunar structure to be constructed of concrete: 1) a transportation system used to carry necessary materials must be established to some extent, 2) various material production plants must be in operation on the moon, and 3) materials of the required quality must be in stable supply.

In order to supply the water necessary for the concrete hardening process, it will be necessary to transport hydrogen from the earth. It has been pointed out that, basically, the concrete-constituting materials other than hydrogen can be obtained from lunar sources.[1] Also, with regard to the influence of the lunar environment on the concrete manufacturing process, an experimental study has already been carried out and results obtained. The results indicate that low gravitational acceleration (1/6 G) does not greatly affect the quality of the concrete, but the decrease in the strength of the concrete caused by a vacuum environment cannot be ignored.[2] Accordingly, it is thought that precast members manufactured in a pressurized chamber will be practical temporarily. It is apparent that the technology for manufacturing concrete in a vacuum will be developed in the future, with the author, et al., having already proposed a method for doing so.[2]

3. Shape and Structure of Module

In addition to the use of the above-mentioned precast members, we have taken the following matters into consideration: 1) the lunar structure shall be pressure tight, 2) the lunar structure shall be combined with modules for reasons of safety and workability, and 3) the lunar structure can be expanded in the future. As a result, a module in the shape of a hexagonal prism was devised. Figure 1 shows the module. The module consists of a frame, ceiling, wall and floor panels. When all panels are
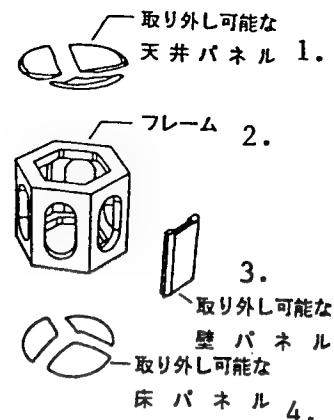
Figure 1. Module Shape

Key:
1. Removable ceiling panel
2. Frame
3. Removable wall panel
4. Removable floor panel

installed on the module and the inside of the module is pressurized, internal pressure will eventually be imposed on the frame. The frame is made of pre-stressed concrete, with side, horizontal and perpendicular cables laid in the frame. The side cable resists internal pressure, while the horizontal and perpendicular cables connect adjacent modules in the longitudinal and lateral directions. The end of the cables is anchored inside the module, and the cable tautening and maintenance can be carried out inside the pressurized module.

4. Production and Assembly of Module

Facilities for manufacturing cement, aggregate, oxygen, fibers, concrete plants, etc., are installed in the pressurized factory, and pre-stressed concrete, frames and panels can be assembled there. Modules with pressurized interiors are shipped from the factory and carried by means of a drawing crane and a mobile crane which travel on the upper face of the existing module. Modules set in their specified positions are connected by tautening cables from the inside of the existing modules. Zones for various functions can be laid out by positioning wall panels in modules. Figure 2 shows such zones. It is also possible to provide comparatively large spaces within the modules by using these modules as structural materials. As mentioned previously, the modules are built to cope with the future expansion of a base and can be separated from each other in arbitrary positions in case of an emergency.

5. Future Tasks

This report describes our study of a lunar structure made of concrete from the standpoint of design, material, structure and assembly. It is apparently necessary to study these items further and to evaluate them, including their economic efficiency, in a comprehensive manner.
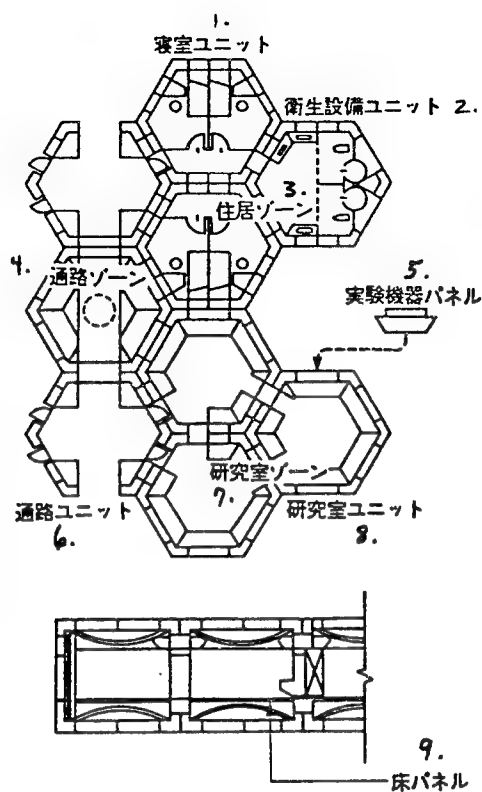
Figure 2. Module Layout

Key:
1. Bedroom unit
2. Sanitation unit
3. Living zone
4. Path zone
5. Experimental equipment panel
6. Path unit
7. Research laboratory zone
8. Research laboratory unit
9. Floor panel

References

1. Lin, T.D., "Concrete for Lunar Base Construction," CONCRETE INT, July 1987

2. Ishikawa, Kanamori, Okada, "Possibility of Concrete Production on the Moon," Houston, Symposium on Lunar Bases and Space Activities in 21st Century, April 1988

Plan for Geostationary Meteorological Satellite No 4

[Article by Shinichi Ishikawa and Atsushi Noda of the National Space Development Agency of Japan; Masao Koichi of NEC Corporation; Shigeru Usuda, Nobuyuki Hirata, Kazuko Owada and Yasunori Toyoda of NEC Aerospace System Co., Ltd.]

[Text]

1. Preface

The H-I rocket is used to launch the Geostationary Meteorological Satellite No 4 [GMS-4]. The rocket-placing error and AMF [apogee motor fire] attitude error are larger than those of the GMS-1 to GMS-3 since the second apogee AMF is executed. The drift rate following the AMF has increased, and it has become difficult to make a plan for a geostationary satellite in accordance with the above substantial errors. It is judged that this is because there were problems with the methods used to estimate the drift rate when the plan was made. We have again studied the influence on the drift rate of the transfer-orbit-placing error and the AMF error immediately following the AMF. This paper reports our results obtained in regard to devising the above plan.

2. Error Processing

2.1 Transfer Orbit Placing Errors

Of the transfer orbit placing errors, we have studied the processing of the apogee altitude error (Δha) and the inclination of orbit error (Δi) which affect the drift rate.

Up to now, cases of very low probability were also objects of analysis since the range of errors extended from -3σ to $+3\sigma$, regardless of the correlation between Δha and Δi. Generally, all that is necessary is to regard the normal distribution as a model of accidental errors, and when the number of variables is two, the model is two-dimensional normal distribution. We have decided to study the two-dimensional normal distribution concerning Δha and Δi, taking the correlation ρ between two errors (Δha and Δi) into consideration.

A 3σ error ellipse has been selected from the elliptic group for the study of Δha and Δi up to +/-3σ, since ellipses[1] consist of coordinates with a constant probability density in two-dimensional normal distribution. The coordinate at the inside of this error ellipse indicates a class of errors that becomes the object of analysis. Then, all that is required is to analyze the section as a form of processing the transfer orbit placing error.

Figure 1 shows an error ellipse and the status of the error range which becomes the object of analysis.

2.2 AMF Error

When the AMF error is large, it greatly affects the drift rate following the AMF. Therefore, when a plan for a geostationary satellite is devised, it is necessary to take this influence into consideration.

We will divide the speed incremental errors accompanying the AMF into two kinds, i.e., the speed incremental error caused by attitude and that caused by thrust, and will study them.

The speed incremental error vector quantity: ΔV_{ATT} caused by the attitude has components which meet at
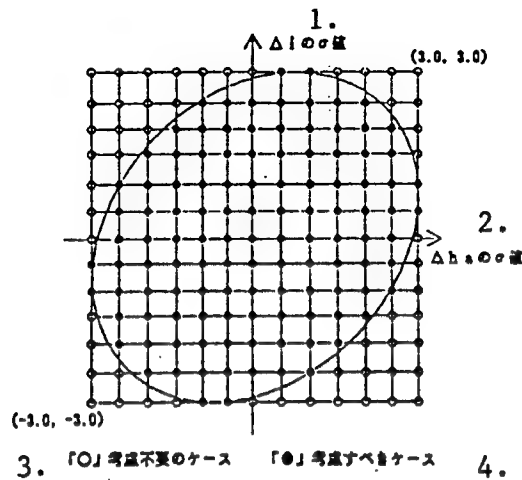
Figure 1. Error Ellipse

Key:
1. Value of σ of Δi
2. Value of σ of Δha
3. Case that does not need to be studied
4. Case that should be studied

right angles with the thrust vector out of the AMF speed incremental error, and the magnitude is as follows:

absolute value of vector quantity: $\Delta V_{ATT} = V_{AMF}$ x tan $(\Delta\theta)$, where V_{AMF}: Nominal value of increase in AMF speed $\Delta\theta$: AMF attitude error

The speed incremental error vector quantity: ΔV_{Pro} caused by the thrust has components parallel to the thrust vector out of the AMF speed incremental error, and the magnitude is as follows:

absolute value of vector quantity: $\Delta V_{Pro} = V_{AMF}$ x $\Delta F/100$, ΔF: Thrust error of AKM [apogee kick motor] (percent)

The correlation between the two errors is zero since they are independent. The influence of this speed incremental error on the drift rate can be obtained from the magnitude when this error is projected on the drift orbit plane.

Figure 2 outlines the processing of the AMF error.

3. Plan for Geostationary Satellite

A plan for a geostationary satellite has been made taking the error processing explained in 2 into consideration.

In order to formulate the plan, it is necessary first to find the longitude λ just under the point immediately following the AMF and the drift rate (first derivative with regard to time) λ. λ and λ_{TR} (first derivative with regard to time) are found immediately after the AMF about the orbit with an error (inside of error ellipse shown in Figure 1) whose range has become an object of analysis, taking the correlation in paragraph 2.1 into consideration. Next, the speed incremental error accompanying the AMF studied in paragraph 2.2 is converted into the drift rate (first derivative with
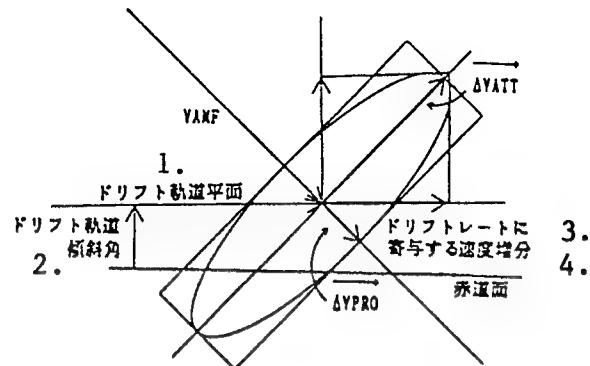
Figure 2. AMF Error Processing

Key:
1. Drift orbit plane
2. Drift inclination of orbit
3. Increase in speed contributing to drift rate
4. Equatorial face

regard to time) λ_{AMF}. The sum of (first derivative with regard to time) λ_{TR} and (first derivative with regard to time) λ_{AMF} will become the drift rate when the geostationary satellite plan is studied.

Figure 3 shows the results obtained by plotting the drift rate and the longitude immediately under the point found by the above-mentioned method on a graph. As can be seen from this figure, when the drift rate in point A and that in point B are positive and negative, respectively, they demonstrate the worst cases. Therefore, when the plan is formulated, all that is generally necessary is to analyze points A and B. Figure 4 shows an example of a planfor a geostationary satellite when point A exists.
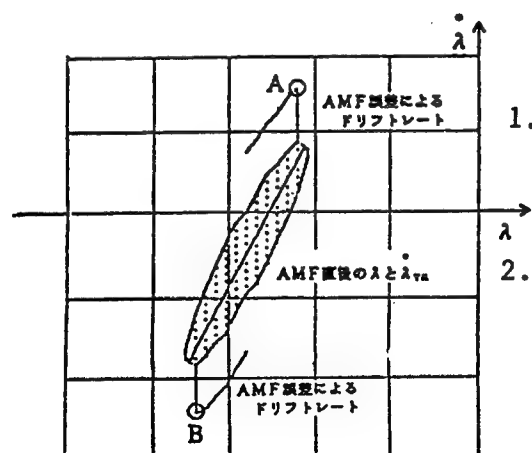
Figure 3. Drift Rate and Longitude Directly Under Point Immediately After AMF

Key:
1. Drift rate according to AMF error
2. λ and λ_{TR} immediately after AMF

1. 目標静止経度

○で静止化のための軌道制御を行う 2.
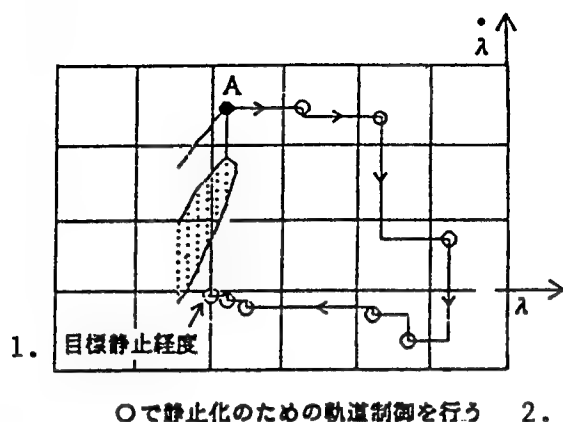
Figure 4. Plan for Geostationary Status When Point A Is Involved

Key:
1. Target geostationary longitude
2. Geostationary orbital control is carried out at O

4. Summary

The influence of the transfer orbit placing error and that of the AMF error on the drift rate are found. The drift rate immediately following the AMF is estimated by adding the two influences. In this case, cases barely realized can be removed by carrying out analyses taking the correlation between Δha and Δi of the transfer orbit into consideration. The use of this drift rate will validate the plan.

References

1. NASDA's Design Standard, "Propulsion System Performance Calculation Standard for Controlling Geostationary Satellite Orbit" (NDC-2-2-1).

Determination of Geostationary Satellite Laser Range Finding, Precision Orbit

43065012d Tokyo PROCEEDINGS OF THE 32ND SPACE SCIENCES & TECHNOLOGY CONFERENCE in Japanese 26-28 Oct 88, No 2D6, pp 374-375

[Article by Masaaki Murata of National Aerospace Laboratory; Ryoji Deguchi of Taiko Electronic Communication Co., Ltd.; Naoki Yanagisawa of Otsuka Computer Research Institute Co., Ltd.]

[Text]

1. Preface

The 11th Japan-European Space Agency [ESA] Executive Official's Conference was held in the ESA headquarters, located in Paris, France, on 16-17 April 1986. It was recognized at this conference that the National Aerospace Laboratory [NAL] would participate in the Laser Synchronization of Atomic Clocks from Stationary Orbit [LASSO], which is one of ESA's projects. The main purposes of LASSO are to determine precision orbits and to establish an intercontinental time synchronizing technology using the geostationary satellite laser range finding. The ESA has manufactured two orbits, i.e., LASSO-A and LASSO-B, as space sections (LASSO packages). In 1979, the ESA issued an A.O. [Announcement of Opportunity] calling for participation in experiments involving LASSO and, in 1982, it utilized the ARIAN-L5-type rocket to launch the SIRIO-2 satellite equipped with the LASSO-A, but it resulted in failure. Subsequently, the ESA was scheduled to modify the LASSO and to use the ARIAN-4-L1, a new type of rocket, in order to launch the METECOSAT-P2, a meteorological satellite equipped with the LASSO payload (LASSO-B), from mid- to late-1986. However, it was decided that the launching of the METECOSAT-P2 would be postponed to after July 1987 because a test flight of the ARIAN-4 rocket, which was carried ahead of the above schedule, failed. As mentioned previously, the postponement was repeated, but the ESA finally launched a rocket successfully on 15 June 1988, and the rocket became stationary in the vicinity of 10 degrees West longitude on 17 July. The system is currently being checked and, if all goes well, it is scheduled to enter the operational stage from late September to October, and an experiment involving the LASSO will be started. The following is an outline of the LASSO project and a description of the results of simulation analyses carried out preliminarily in preparation for determining the precision orbit according to the geostationary satellite laser range finding.

2. Preliminary Analysis for Determining Precision Orbit

The LASSO payload consists of retro-reflectors, photo-detectors, and an ultra-stable oscillator and counter [USO] for indicating time-tags on the pulse reaching time. These time-tags are encoded by dividing multiple times and are transmitted, with other information, to the ground by means of a telemeter. (They are used for time comparison.) Each station measures the two-way or one-way propagation time. A total of 10 European and American stations are currently scheduled to participate in the measurement. An orbit-determining program, "Cosmos-V," is vectored and operated with the supercomputer "V-400," made by the NAL, and is used to determine the orbit. The standard model adopted is the Merit Standards (J2000.0 system). First, the influence of a force model on the satellite position errors is investigated (see Table 1). Obviously, in addition to the earth's gravitational field and lunar and solar attractions, the influence of the solar radiation pressure is large, and if this large influence is ignored, a positional error will be generated in the long-track direction of a maximum of 2.4 km for 7 days. It is permissible to end the degree and the order of the earth gravity potential at six, respectively, and to ignore the marine tide-producing force. However, it can be appreciated that the solid earth tide, earth albedo (earth radiation pressure), and the attraction of the main planets should be taken into consideration when studying the above influence. A preliminary

experiment involving orbit selection was performed taking these results into consideration. Simulative observation data on the gravity field GEM-L2 and solar radiation pressure were obtained from a precision model in which the attitude, shape and thermal characteristics of the surface of the satellite were taken into consideration, with those on thers obtained from the Merit Standards, those on earth rotation (polar movement and UT1) obtained from the values estimated by the IERS, and those on local positional coordinates obtained from the NAL-8701 solution (six locations) by the NAL (only at night). The observation noise is assumed to be 10 cm (1σ). On the other hand, the coefficient of reflection (one parameter) is taken as an unknown in the usual models. Then, the usual model, the earth's tide, earth's albedo and the attractions of the three main planets are studied in the gravity field GEM-T1 and with the solar radiation pressure in order to determine the orbit. The values estimated by the IERS have been adopted for the earth's rotation, and the solution CSR8702, formulated by the Space Research Center, University of Texas, has been adopted for local positional coordinates.

**Figure 1. Orbit Positional Error
(Estimated Value - True Value) (unit: meters)**

Table 1.
Influence of Perturbative Acceleration on Satellite Positional Error (Unit: meters)

Error Source	ΔR	ΔT	ΔN
Total solar radiation pressure	1000	2400	1.8
diffuse	160	500	0.1
specular	60	150	1.3
Earth's gravity error	0.4	16	-
(GEM-L2 vs GEM-T1)			
GEM-L2 truncated (6x6)	-	0.25	-
GEM-L2 truncated (4x4)	1.4	56	0.05
Earth's albedo	0.6	2.6	-
Solid earth tide	0.02	0.9	0.2
Planets (Mars, Jupiter, Saturn)	0.02	0.45	0.08
Ocean tide	-	0.09	0.02

Six elements of the orbit and seven parameters of the coefficient of solar radiation pressure have been estimated using a batch filter by assuming an arc length of seven days. As a result, 1.4, 2.1 and 10 meters were obtained in the epoch as estimated errors of position in the radial, along-track and normal directions, respectively. Also, 1.3845 has been obtained as the coefficient of radiation pressure. Deviations from the true orbit are found by propagating them to the orbit. These deviations are shown in Figure 1. These results suggest that it is quite difficult to determine the orbit to the submeter level. Results obtained from other experiments involving numerical values indicate that the maximum error is not caused by the force model, but instead is caused by the local positional error which is estimated to be within 10 cm. Space does not permit us to present an explanation of the above-mentioned matters, but details will be given at the conference.

Control of Orbit of MOS-1

[Article by Mikio Sawabe, Masao Hirota, Hideji Araki and Mayumi Tomura of the National Space Development Agency of Japan]

[Text]

1. Preface

An oceanographic observation satellite, the "MOS-1," was launched on 19 February 1987. The MOS-1 is Japan's first solar synchronous quasi-recurrent satellite. This paper describes the control of the injection of the MOS-1 into the specified orbit and the control of the orbit in order to retain local hours at descending nodes.

2. Control of WRS Injection

The MOS-1 circles the earth 237 times in 17 days, observing the entire surface, and returns to its starting point. At this time, a ground track, which will become a standard, is established by fixing one of the 237 descending nodes at 130.8 degrees East longitude. This ground track is the world reference system [WRS] of the MOS-1, and the injection of this WRS is controlled so that the MOS-1 is injected into an orbit satisfying the WRS.

Recurrent conditions of the MOS-1 are formed by long radius a (a is approximately equal to 7,287 km) of the specified orbit and eccentricity e (e is approximately equal to 1 x 10^{-3}). Whether or not these conditions satisfy the WRS depends on the position of the satellite in orbit. As shown in Figure 1, in the case of the MOS-1, 17 specified positions exist in orbit. Therefore, the injection of the WRS into orbit is attained by repeating the acceleration and
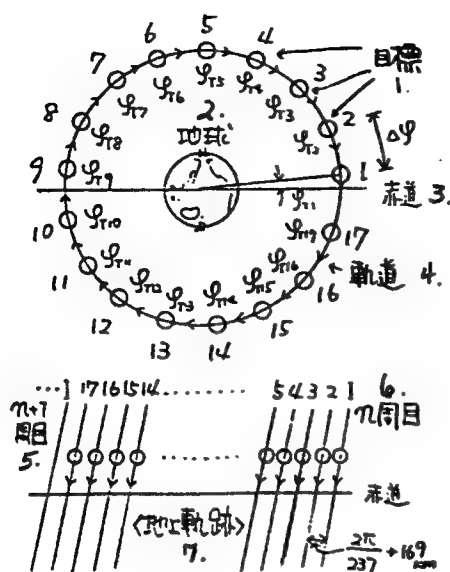
Figure 1. WRS Injection Target

Key:
1. Target
2. Earth
3. Equator
4. Orbit
5. n + 7th time
6. nth time
7. Ground track

deceleration in the tangential directions ($\rightarrow$ in Figure 2) of the orbit and by setting the satellite to one of the targets while controlling a and e.

Figure 3 shows the WRS injection of the MOS-1 launched into orbit. In this figure, the up arrow expresses the change of the orbit according to the control. The lower direction indicates the control of acceleration, while the upper direction indicates the control of deceleration. Also, the slotted arrow shows that the orbit has been changed by the acceleration effect caused by injection from a thruster in order to retain the attitude of the MOS-1 in the FYCM (mode which retains the three axis attitude of the MOS-1 by means of a thruster). Following the confirmation of functions (injection for 60 seconds and the $_\Delta V_{+x}$ and $_\Delta V_{-x}$ test shown in the figure) of the thruster, the WRS was injected into orbit three times (deceleration once and acceleration twice). Table 1 outlines the control of the WRS injection into orbit.
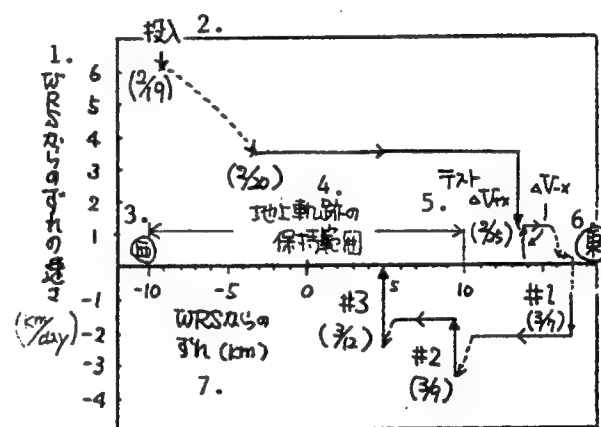
Figure 3. Change of Deviation from WRS

Figure 2. Control of Acceleration and Deceleration

Key:
1. Control of acceleration (increase in a)
2. Control of deceleration (decrease in a)
3. Earth
4. Orbit

Key:
1. Speed of deviation from WRS (km/day)
2. Injection
3. West
4. Retaining range of ground track
5. Test
6. East
7. Deviation from WRS (km)

Table 1.
Outline of WRS Injection Control

	Control time (uT)	Control amount (m/s)	Thruster injection time (sec)	Deviation from WRS* (km)	Speed of deviation from WRS* (km/day)	Consumed propellant amount (kg)
No 1	87-03-07; 00:07:14	0.084 (acceleration)	34	17	-2.3	0.054
No 2	87-03-09; 23:58:44	-0.112 (deceleration)	88	10	-1.7	0.065
No 3	87-03-12; 10:47:15	-0.167 (deceleration)	136	5	0.0	0.079 * East is taken to be positive

Also, even after the above injection, ground tracks of the MOS-1 deviate gradually from the WRS due to the decrease in a according to atmospheric resistance, but the ground tracks are retained to within +/-10 km from the WRS at all times by controlling the increase (acceleration) of a, as necessary.

3. Retention of Local Hours at Descending Nodes

Another feature of the MOS-1 orbit is that the local hour Ts is in the vicinity of 10 o'clock at all times when the MOS-1 passes through descending nodes. This is because, as shown in Figure 4, when the earth is thought to be central, the orbital plane of the MOS-1 is rotated by synchronizing it with the fact that the sun rotates approximately 7 degrees a day, and because the angle formed by the solar direction and the orbital plane is constant at all times. The rotational speed of this orbital plane depends mainly on the inclination (i is approximately equal to 99 degrees) of the orbit, and this inclination depends on the right ascending node Ω.

It was not necessary to control the i and Ω because the MOS-1 was launched and injected into orbit with almost the specified i and Ω. However, the Ts subsequently became increasingly faster because the i gradually decreased due to the influence of the attractions of the moon and sun and and the rotational speed of the orbital plane became low. Since the Ts retaining range has been determined to be 10 to 11 o'clock, before Ts could surpass 10 o'clock, in April 1988 the

correction of the rotational speed of the orbital plane was controlled by increasing i. (This control has been carried out by taking synchronous operation with the MOS-1 into consideration.)

One-time control is insufficient because, as shown in Figure 5, the amount of i to be controlled is large, the control position is limited to an ascending node, and the allowable range of continuous injection of the MOS-1 thruster is 510 seconds. Therefore, the control was broadly carried out three times at several stages (one stage is within 510 seconds) in April. Figure 6 and Table 2 outline the Ts retaining control.
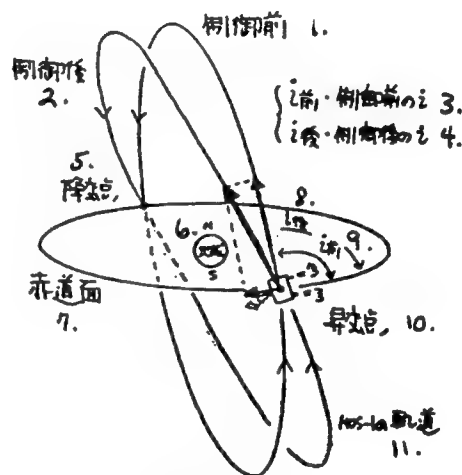
Figure 5. Control of i

Key:
1. Before control
2. After control
3. Before i: i before control
4. After i: i after control
5. Descending node
6. Earth
7. Equatorial face
8. After i
9. Before i
10. Ascending node
11. Orbit of MOS-1
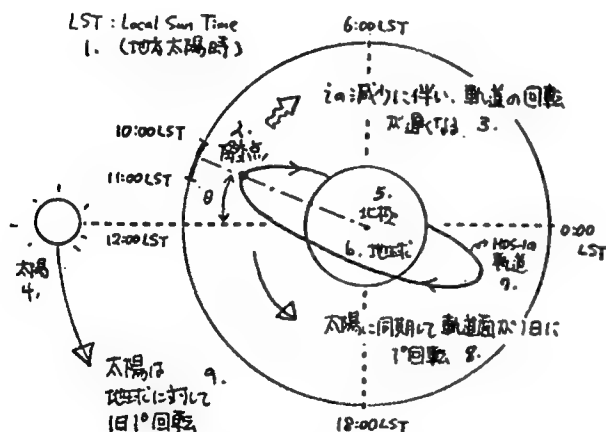
Figure 4. Rotation of Orbital Face

Key:
1. LST: Local Sun Time
2. Descending node
3. Rotation of orbit becomes slow in accordance with decrease in i
4. Sun
5. North Pole
6. Earth
7. MOS-1a orbit
8. Orbital face rotates 1° per day while synchronizing with the sun
9. Sun goes around the earth 1° a day
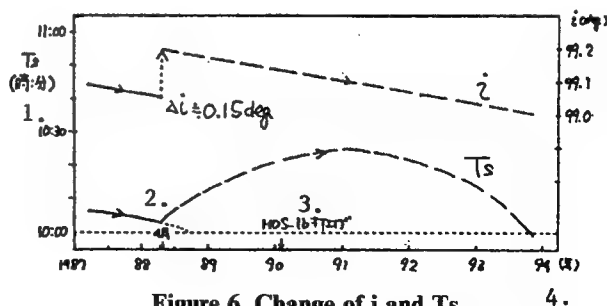
Figure 6. Change of i and Ts

Key:
1. Ts (hour and minutes)
2. April
3. Launching of MOS-1
4. (Year)

Table 2.
Outline of Ts Retaining Control

	Control starting time (uT)	Control amount		Injection time/ stage (sec)	Number of stages	Amount of propel-lant consumed (kg)
		Δi (°)	ΔV (m/s)			
1	88-04-03; 19:37:32	0.024	3.16	510	3	1.1
2	88-04-06; 18:12:44	0.065	8.44	510	9	2.9
3	88-04-13; 06:52:34	0.061	7.91	500	10	2.7
Total		0.153	19.51		22	6.7

4. Postface

As previously mentioned, the MOS-1 is a solar synchronous quasi-recurrent satellite launched for the first in Japan. For this reason, unlike the geostationary satellites launched previously, we have no accumulated data or experience in orbit control. However, we can obtain knowledge concerning future solar synchronous quasi-recurrent satellites by gradually accumulating experience. We consider this to be one of the missions of the MOS-1.

Research on High Performance IRCCD, Study of Radiometer Concept

43065012f Tokyo PROCEEDINGS OF THE 32ND SPACE SCIENCES & TECHNOLOGY CONFERENCE in Japanese 26-28 Oct 88, No 2D7, pp 400-401

[Article by Masakatsu Nakajima, Takashi Moriyama and Masao Furukawa of the National Space Development Agency of Japan]

[Text] 1. Preface

A point sensor is currently used to observe thermal infrared rays with a band of 10 micrometers. However, the point sensor has low reliability because it is of the scanning type and depends on the spin of satellites and mechanical driving. It also requires much time for the imaging. Therefore, an infrared charge coupled device [IRCCD] in thermal infrared areas is being developed since the application of a charge coupled device [CCD] to an imaging element will be able to solve the above problem, and a rise in sensitivity can be expected as an integral effect of such a CCD. Also, the concept of an electronic scanning-type thermal infrared radiometer was studied based on the target performance of this IRCCD.

2. Development of IRCCD

Investigations were carried out toturn a thermal infrared imaging element into a CCD. As a result, it was discovered that it would be difficult to do so using conventional materials. However, research on a new infrared light receiving material (crystal growth process) was conducted during fiscal 1985 to 1987. In this research, the growth of light receiving materials was promoted on a single crystal substrate by using molecular beam epitaxy

[MBE], and light receiving films were made. Such a light receiving film is used as a basic element of an infrared detector. Metal/Si Schottky barrier-type light receiving films have been used in the past in IRCCDs in short-wave infrared areas. It was discovered that the cut-off wavelength could be extended to the long wavelength side by using mixed crystals of Si and Ge ($pSi_{1-x}Ge_x$) instead of Si in such light receiving films. In addition, not only Schottky barrier-type light receiving films, but also light receiving films using heterojunction barriers of pSi and pSi_{1-x} were devised as thermal infrared light receiving films. Light receiving films using $Hg_xCd_{1-x}Te$ were made, but a barrier was generated by the difference in grating constants. The difficulty of converting such light receiving films into devices was confirmed.

Figure 1 shows the principle of operation of a heterojunction barrier-type device.

The following items were investigated or measured to evaluate light receiving films as light receiving materials: 1) film thickness, 2) crystallinity, 3) carrier density, 4) mobility, 5) infrared absorption, 6) current-voltage characteristics, 7) capacity voltage and 8) photoelectric effect.

As a result of the investigation and measurement, promising results of heterojunction barrier-type $pSi/pSi_{1-x}Ge_x$ and Schottky barrier-type $Pt/pSi_{1-x}Ge_x$ were obtained.
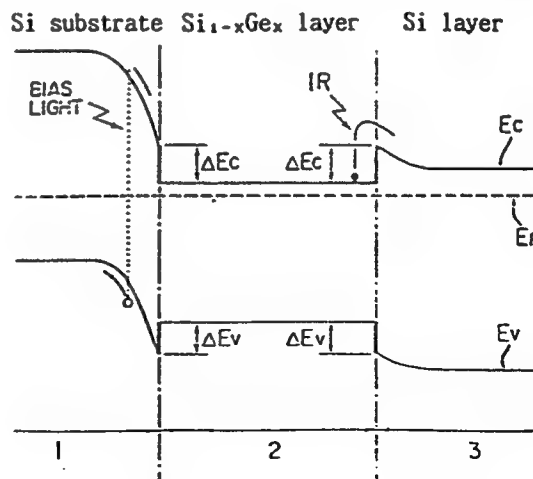
Figure 1. Principle of Operation of Hetero-type Device
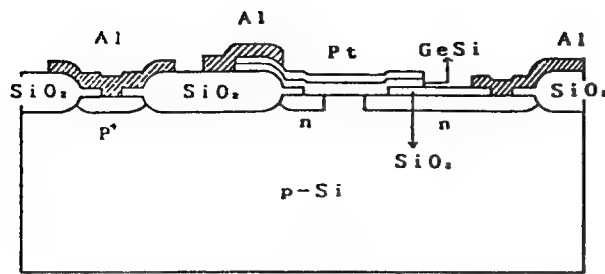
Figure 2. Cross-sectional Drawing of Element

Research on fine elements was initiated in fiscal 1988. The fine element forms the foundation of the IRCCD. One of the purposes of this research is to select one of the above two as promising and preferable through the study of these elements. Figure 2 shows a cross section of a Schottky-type element.

3. Radiometer Using IRCCD

If an electronic scanning observation sensor is used to observe from geostationary orbit, it will be possible to raise the reliability due to the lack of a mechanical driving section, to raise the sensitivity due to the integral effect of the CCDs, and to carry out imaging in a moment because each element simultaneously watches all sites. Also, even when such a sensor is mount on a circumterrestrial satellite, rises in reliability and sensitivity can be expected in the same way.

Table 1 shows the main target performance of a thermal infrared radiometer mounted on a middle and high altitude circumterrestrial satellite in which IRCCDs currently being developed are used.

Table 1.
Data on Target Performance

Observation wavelengths	1:6.0 - 7.0
	2:10.5 - 11.5
	3:11.5 - 12.5
NEΔT	0.1 K
Scanning width	50 km
IFOV	50 m
Number of picture elements	1,000

In addition, pointing and zooming, as well as electronic scanning, can be regarded as functions of this radiometer.

The use of the pointing function will bring about mobile observations with high frequency, while that of the zooming function will bring about observations with high resolving power in specific ranges.

In addition, it is generally necessary to cool an infrared detector because, in the case of a quantum-type detector, the number of electron excited thermally must be reduced and the degree of thermal noise must be lowered. Therefore, it is necessary to develop a cooler with a long life.

The use of a thermal infrared radiometer with high sensitivity and high resolving power will bring about global observations of vegetation, farm produce, forests, atmospheric phenomena and resources. It is also expected that the stationary observation from geostationary orbit will be useful in examining disasters.

4. Postface

If observations are carried out from a three-axis attitude stabilization satellite in geostationary orbit, the IRCCD must be two-dimensional. However, if they are carried out from a circumterrestrial satellite, the IRCCD can be one-dimensional. We plan to develop a thermal infrared radiometer to be mounted on the JPOP, which will be launched around 1998, in order to observe the earth in infrared areas at middle and high altitudes and to check orbital system functions and performances as the first stage of the development of an IRCCD and a radiometer which will be used to carry out observations from geostationary orbit.

Development of Bubble Memory Recorder for Mounting on Earth Resources Observation Satellite

43065012g Tokyo PROCEEDINGS OF THE 32ND SPACE SCIENCES & TECHNOLOGY CONFERENCE in Japanese 26-28 Oct 88 No 2E2 pp 402-403

[Article by Tsunehiko Araki, Mitsuru Takei and Naoto Matsuura of the National Space Development Agency of Japan; Kazuo Nomura and Kiyoshi Ochiai of Mitsubishi Electric Corporation; Tatsuhiro Nozue and Kyozo Tachibana of Hitachi, Ltd.]

[Text] 1. Preface

The bubble memory recorder [BMR] will be mounted on the earth resources observation satellite-I. It is a data recorder with a recording capacity of 16 megabits, and employs magnetic bubble memory elements.[1] The mission of this recorder is to record and reproduce telemetry data.

We have developed an engineering model of this BMR and, in this paper, will describe this engineering model.

2. Features of BMR

The BMR is a solid-data recorder which uses bubble memory elements as the recording media. Similar to the tape recorders previously adopted, it possesses the following features: 1) non-volatility, 2) random access is possible, 3) no frictional section and 4) no movable section.

3. Examples of Use of BMR

The recording area of the BMR is divided into two sections, i.e., an endless recording section with a

recording capacity of 4 megabits and a block-specified-recording section with a recording capacity of 12 megabits. The former section generally keeps endless records in order to record telemetry data before and after the detection of abnormalities which occur suddenly, while the latter section records telemetry data as necessary before and after changes of attitude and orbit. Examples of the use of the BMR are shown below.

(1) Placing into Orbit by Launching

When the BMR receives the "Satellite Separation Signal" when the power is turned off, it will automatically begin to retain block specified records at 12 megabits per minute. When the satellite returns to the vicinity of a ground station, the BMR will discontinue record retention and will reproduce them in accordance with commands.

(2) Telemetry Monitor of Changes of Attitude and Orbit

The BMR can freely divide data into some sections of units of 64 seconds (= 128 kilobits), up to a maximum of 102 minutes and 24 seconds (= 12 megabits), and can record them in the block specified recording section in accordance with commands. When the satellite returns to the vicinity of the ground station, the BMR will reproduce recorded sections according to these commands.

(3) Usual Operation

(a) When the BMR receives an "Abnormal Detection Signal" during the endless recording, it will continue recording in the endless recording section for another 17 minutes (= 2 megabits), and then will stop automatically. With this function, the BMR can record telemetry data before and after the detection of abnormalities for 17 minutes each. The BMR makes this possible for the first time.

(b) When the BMR receives the "Abnormal Detection Signal" during the block specified recording, after the this work is completed, it will continue to record in the endless recording section for another 17 minutes and then will stop automatically. With this function, the BMR can record telemetry data for 17 minutes after the detection of abnormalities, even during the block specified recording.

4. Main Specifications of BMR

(1) Full capacity: 16 megabits (nominal) (endless recording capacity, 4 megabits; block specified recording capacity, 12 megabits) (2) Input and output signal type: Biφ-L (3) Record data rate: 2,048 bits/second (4) Maximum recording time at specified block: 102 minutes 24 seconds (5) Reproduction data rate: 32.768×10^3 bits/second (6) Maximum reproduction time: 8 minutes 32 seconds (7) Bit error: 10^{-7} or less (8) Power consumption: When input voltage on the primary side is within the range of 20 to 35 volts direct current, and when each piece of equipment is under the specified temperature conditions, the power consumption is less than the

following values: Stand-by, 6.1 watts; Record, 8.0 watts (average), 16.0 watts (peak); Reproduction, 10.3 watts (average), 16.7 watts (peak) (9) Command item: Discrete 2 and magnitude 1 (10) Telemetry item: Active analog 1, passive analog 1, and serial digital (6 words) (11) Weight: 5.40 kg +/- 0.27 kg (12) Dimensions: 295 (width) x 249 (depth) x 129 (height) mm or less

References

1. Koizumi, et al., "Bubble Memory Recorder for Circumterrestrial Satellite," Proceedings of the 29th Space Sciences and Technology Conference, 3C167, 1985.

Actual Operational Results of Bubble Data Recorder Mounted on Scientific Satellite

[Article by Tomonao Hayashi and Fumiaki Makino of the Institute of Space and Astronautical Science; Masahiko Ikeda, Tatsuhiro Seki, Kazuhisa Ogawa and Kazutoshi Yoshida of Hitachi, Ltd.]

[Text] Preface

The bubble data recorder [BDR] for scientific satellites was announced at the 28th Space Sciences and Technology Conference.[1] The first BDR has operated smoothly since it was mounted on the scientific satellite "Ginga," and was placed into orbit on 5 February 1987. The following is a report of the actual results of the operation of the first BDR during its first 18 months, ending 4 August 1988.

1. Outline of First BDR

Details are given in the references,[2] while main specifications are as follows:

Recording capacity: 40 megabits

Recording speed: 0.5, 2 and 16 kbps

Reproducing speed: 64 and 128 kbps

2. Actual Results of Operation for First 18 Months

(1) Number of Reproductions

The number of reproductions totaled 1987, accounting for 86 percent of the entire visible circumterrestrial amount.

(2) Recording Time

Data were recorded for a total of 8638.25 hours, and, of that time, 1016.38 hours represented the skies of the South Atlantic Anomaly [SAA] which has an extremely large number of trapped proton beams. In addition, one recording period was approximately 4 hours, and data were recorded at a rate of about 15 hours/day.

(3) Total Operating Time

The total operating time, including the reproducing time, was 8814.87 hours.

(4) Operation of BDR

1) Operation of Bubble Memory The bubble memory experienced no problems or temporary malfunctions.

2) Bit Error Rate of Bubble Memory The BDR possesses an error correcting function, and no error bits were observed in the data output to the bubble memory. Therefore, judging from the number of reproductions mentioned in item (1), the bit error rate of the bubble memory was 1.2×10^{-11} or less.

3) Operation of BDR Every 2 megabits, an address is given to the BDR memory, and this address information is transmitted as telemetry.

As a result of analyzing the status during recording and reproducing, it has been confirmed that access was performed in normal sequence at all times and the BDR operated normally.

4) Latch-up A power current limiting circuit is installed as a measure for latching up single events to all large-scale integrated circuits [LSI]s used in the BDR. The status of this circuit during operation is transmitted as telemetry data.

It can be appreciated that neither the status output nor the latch-up phenomenon occurred during the first 18 months.

3. Analysis of Software Errors

(1) Software Error Extraction Method

All reproduction data were processed in accordance with the following extraction flow in order to detect the software errors caused by trapped-proton beams in the SAA skies. Step 1: Detection of bit errors—Detection of bit errors (1 bit error) of SYNC CODE in reproduction data Step 2: Discrimination of SIRIUS status—Deletion of bit errors in which frame contents were abnormal in the SIRIUS status Step 3: Discrimination of factors— Deletion of bit errors which accorded in time with the switching of the antenna from the command history Step 4: Discrimination of SAA—Discrimination of whether recording time was in SAA

(2) Results of Analysis

As a result of processing the reproduction data collected during the first 18 months, nine phenomena corresponded to Steps 1 or 2 above. Details of these nine phenomena are shown in Table 1.

Table 1.
Phenomena Corresponding to Steps 1 and 2

Item No	Path No	Time	Antenna Switching Time	SAA	Sync Code
1	8705120514	07:45:04.504	Accordance	Non	BAF320
2	8705260148	01:03:06.909	Discordance	Non	BAF320
3	8707191544	23:12:54.639	Discordance	Non	DAF320
4	8708051028	14:57:21.807	Accordance	Non	7AF320
5	8708110822	11:22:37.981	Discordance	Non	7AF320
6	8801060633	07:59:29.978	Accordance	Non	FAF324
7	8801090927	13:21:38.811	Accordance	Non	7AF320
8	8804140821	11:28:04.254	Discordance	Non	7AF320
9	8808050219	17:42:35.728	Discordance	Non	7AF320

No software errors were detected because four of the nine phenomena accorded with the antenna switching time, and the remaining five phenomena occurred outside the SAA.

According to the recording time shown in 2(2), the bit error rate in the SAA is 0 +/- 1.0 bit/day, while that outside the SAA is 0.7 +/- 0.3 bit/day. Therefore, the ceiling value of software errors in the SAA is 0.9 bit/day.

In addition, software errors are caused by the trapped protons involving the entire BDR. The ceiling value of the cross section of these software errors is 3×10^{-8} sq cm, because the number of protons with 100 MeV or more in the SAA is 7×10^6 per (cm^2 x day).

4. Summary

The status of the first BDR mounted on the Ginga was analyzed for the first 18 months, from 5 February 1987 to 4 August 1988. As a result, the following matters were observed: 1) The total operation time of the BDR was 8,814 hours, and 1,987 recording and reproducing cycles were repeated. During this period, the operation of the BDR experienced no abnormalities. 2) The bit error rate of the bubble memory in orbit is 1.2×10^{-11} or less. 3) No latching up phenomena occurred. 4) It was impossible to detect software errors of the BDR, even by using an extraction method in which features of burst errors and software errors of the communications systems were taken into consideration. Softward errors are caused by

trapped protons involving the entire BDR. The ceiling value of the cross section of these software errors is 3 x 10^{-8} sq cm or less.

This analysis proves that the BDR is an excellent data recorder with respect to environmental resistance. BDRs with the above features should be mounted on scientific satellites in the future.

References

1. Hayashi, et al., "Bubble Data Recorder for Scientific Satellites," the 28th Space Sciences and Technology Conference, No 2D11, 1984

2. Hayashi, et al., "Development of Bubble Data Recorder for Scientific Satellites," Communication Society and Space Navigation Electronics Research Meeting, 1985

Research, Development of TEDA Installed in ETS-VI

[Article by Tetsuya Ouchi, Takeo Goya and Tamisuke Koizumi of the National Space Development Agency of Japan; Tsuyoshi Kono, Takashi Imai, Masaru Matsuoka, Etsuya Chiba and Hiroshi Kato of the Institute of Physical and Chemical Research]

[Text] 1. Preface

Environmental conditions in space are severe, and many unknowns are involved. In order to ensure the normal functioning of equipment installed in artificial satellites and operated over a long period of time in space, it is necessary to be informed about the space environment and to acquire technical data on the degradation characteristics, etc., of the electronic parts and materials used in these space environments.

The ETS-VI is scheduled to be launched in the summer of 1992, which will be the most active solar flare period. Technical data acquisition equipment [TEDA] will be mounted on the ETS-VI to measure the intensity and kinds of particles incident in space radiation, the degradation characteristics of electronic parts and materials, and the influence of space radiation on these electronic parts and materials, and to investigate the correlation among them.

2. Outline of Research and Development of TEDA

The TEDA is composed of monitors possessing the following component functions: A) Monitors which acquire data on the degradation of parts and materials 1) Integrated Circuit Monitor [ICM] The ICM is used to investigate the degradation of the complementary metal oxide semiconductor integrated circuit [CMOS-IC] caused by the absorbed radiation dose. 2) Single Event

Upset Monitor [SUM] The SUM is used to measure the frequency of software error generation, etc., caused by single events involving semiconductor memory elements and arithmetic elements. 3) Solar Cell Monitor [SCM] The SCM is used to change the V-I characteristics of solar cells into the load and to measure the load. 4) Contamination Monitor [COM] The COM is used to measure the degree of contamination of satellite thermal control materials by AKE/RCS plumes. B) Monitors which acquire data involving space environments 1) Heavy Ion Telescope [HIT] The direction of distribution, the intensity, nuclear mass, energy and the kinds of heavy ion particles, from Li to Fe, are measured using a semiconductor sensor with an angle of visibility of 90 degrees. 2) Dose Meter [DOM] Electrons, protons, α particles and heavy ions are measured with a silicon semiconductor detector with an angle of visibility of 20 degrees. 3) Potential Monitor [POM] The electrification of satellite surface materials caused by the inflow of plasma is detected using a microfork chopper, and the degree of electrification is measured with it. The range of measurement is from +1 kilovolt to -10 kilovolts. 4) Magnetic Monitor [MAM] The intensity (three components) of magnetic fields in geostationary orbit is measured using a flux gate-type detector.

The above-mentioned monitors have been classified into two units, i.e., the Parts and Materials Degradation Measurement Unit [DMU] and Space Radiation Measurement Unit [SRU], and have been integrated in the units, respectively (see Figure 1).
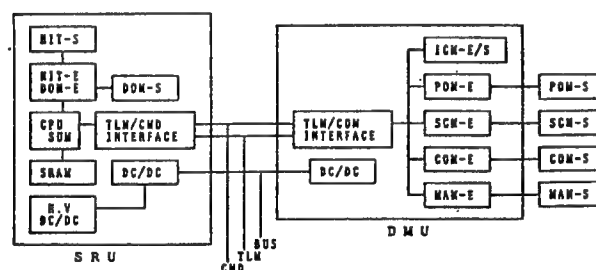
Figure 1. TEDA Functional Block Diagram

As shown in the functional block diagram, the DMU and SRU consist of a sensor, signal processing section, power source section, and I/F circuit, respectively. The primary power source is supplied from the bus system of the satellite system to the power source section common to each monitor. The I/F circuit is interfaced with the RIU of the system, and each monitor of the TEDA is controlled with discrete and magnitude commands. Data obtained from each monitor is transmitted using digital and analog telemetry.

The TEDA is currently being designed and manufactured, and it is characterized by being composed of the HIT, DOM, POM, COM, specimen-solar cell (GaAs),

radiation-resistant CMOS-IC, static random access memory [SRAM], microprocessor unit [MPU], thermal control material and MAM. The HIT and DOM are improved versions of those used by the Institute of Physical and Chemical Research [IPCR] to observe space radiation. The POM and COM are improved versions of those used in the ETS-V. The specimen-solar cell (GaAs), radiation-resistant CMOS-IC, SRAM, MPU and thermal control materials are newly developed. The MAM will be mounted for the first time on the ETS-VI.

3. Postface

These monitors will be reflected in the development of highly reliable equipment following evaluations, analyses and research on the degradation of parts and materials used in space, and will be used to acquire detailed data on space radiation and space environments as well.

Development of Radiation-Resistant 16-Bit Microprocessor LSI

43065012j Tokyo PROCEEDINGS OF THE 32ND SPACE SCIENCES & TECHNOLOGY CONFERENCE in Japanese 26-28 Oct 88 No 2E7 pp 410-411

[Article by Takeo Goya, Satoshi Kuboyama and Yukio Ito of the National Space Development Agency of Japan; Seki Kojima, Yoshihiko Kameda and Yasuo Ishige of Toshiba Corporation]

[Text] 1. Preface

The National Space Development Agency of Japan [NASDA] has developed a radiation-resistant 16-bit microprocessor LSI [16-bit MPU] using a 10 K gate array as a common part (see Photograph 1 [not reproduced]). The following is a report of the configuration and features of the 16-bit MPU and test results of single event software errors.

2. Basic Functions and Performance

Table 1 shows the basic functions and performance of the 16-bit MPU. The 16-bit MPU is of a microprogram system, and has 13 floating point instructions as well as 101 basic instructions.

**Table 1.
Basic Function and Performance of 16-Bit MPU**

Processing word length	16 bits
Element	Radiation-resistant CMOS gate array
Package	124-pin ceramic flat package
Operation frequency	dc-5 MHz
Operation speed	16-bit fixed point
	Addition and subtraction: 0.2 µs
	Multiplication: 5.8 µs
	Division: 8.0 µs
	32-bit floating point

**Table 1.
Basic Function and Performance of 16-Bit MPU (Continued)**

	Addition and subtraction: 12.0 µs
	Multiplication: 24.8 µs
	Division: 64.0 µs

3. Countermeasures Against Radiation

Figure 1 shows a cross section of a pellet of the 16-bit MPU. A total dose of 10^5 RAD (Si) was realized to reinforce the radiation resistance by adopting the following methods in the MPU:

* Low temperatures and low damage processes
* Thin film gate oxide film
* Edgeless transistor
* Guard band

4. Configuration

Figure 2 shows a functional block diagram of the 16-bit MPU. A microprogram read only program [ROM] is installed on the exterior of the 16-bit MPU. The arithmetic
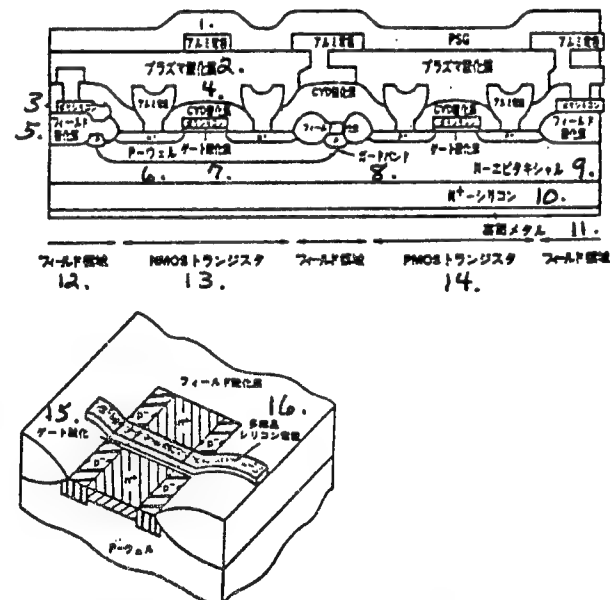
Figure 1. Cross-Sectional Drawing of 16-Bit MPU Pellet

Key:
1. Aluminum electrode
2. Plasma oxide film
3. Poly-silicon
4. CVD oxide film
5. Field oxide film
6. P-well
7. Gate oxide film
8. Guard band
9. N-epitaxial
10. N^+-silicon
11. Backside metal
12. Field area
13. NMOS transistor
14. PMOS transistor
15. Gate oxidation
16. Polycrystalline silicon electrode
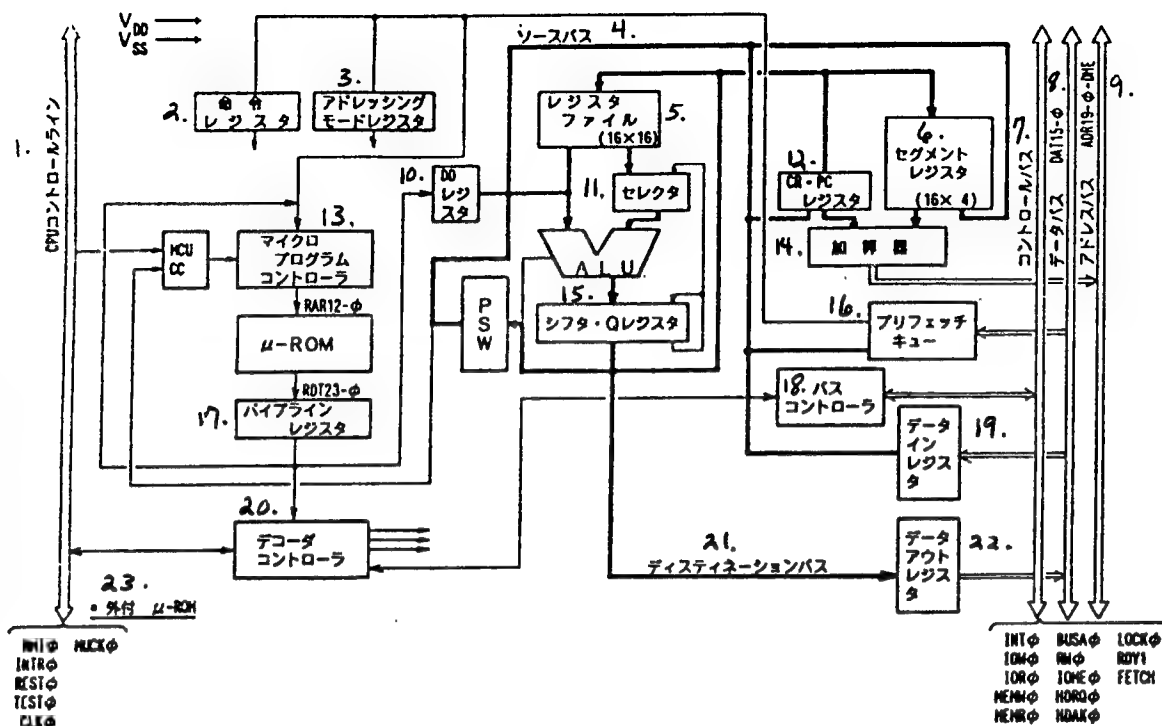
Figure 2. 16-Bit MPU Functional Block Diagram

Key:
1. CPU control line
2. Command register
3. Addressing mode register
4. Source bus
5. Register file (16 x 16)
6. Segment register
7. Control bus
8. Data bus
9. Address bus
10. DD register 11. Selector
12. CR/PC register
13. Microprogram controller
14. Adder 15. Shifter/Q register
16. Pre-fetch queue
17. Pipeline register
18. Bus controller
19. Data in register
20. Decoder controller
21. Destination bus
22. Data out register
23. External installation of μ-ROM

and logical unit [ALU], shifter and Q-register have special-purpose hardwares to increase the speed of the multiplication and division and 6-byte-prefetch queues due to the increase in speed. Basic multiplication of 16 x 16 bits or basic division of 32[1]6 bits is executed with 16 clocks. A 1-mega-byte address area is controlled using a segment register.

5. Development System

When the system includes a 16-bit MPU, an in-circuit emulator, cross assembler and cross C compiler are developed so that the hardware and software can be developed readily. The BITX-2000 (only for 16-bit MPUs) made by Bitran Co., Ltd., is used as an in-circuit emulator. The software is developed on the VAX series made by DEC Co., Ltd., in accordance with the procedure shown in Figure 3.

6. Test of Single Event Software Error

Tests of single event software errors were conducted at the Tsukuba Space Center by irradiating the software with californium (Cf_{252}) shown in Figure 4. The results did not indicate any generation of latch-up or software errors.

7. Future Schedule

The development evaluation test of the 16-bit MPU was completed in September 1988, and the 16-bit MPU will now enter the manufacturing stage. Such 16-bit MPUs are currently scheduled to be used in the attitude control electronic circuit and antenna direction control electronic circuit of the engineering test satellite type VI. It is anticipated that such 16-bit MPUs will be used in the intelligent direct memory access [DMA] controller, digital signal processor [DSP], etc., in the future since microprograms will be installed on the exteriors of these MPUs.
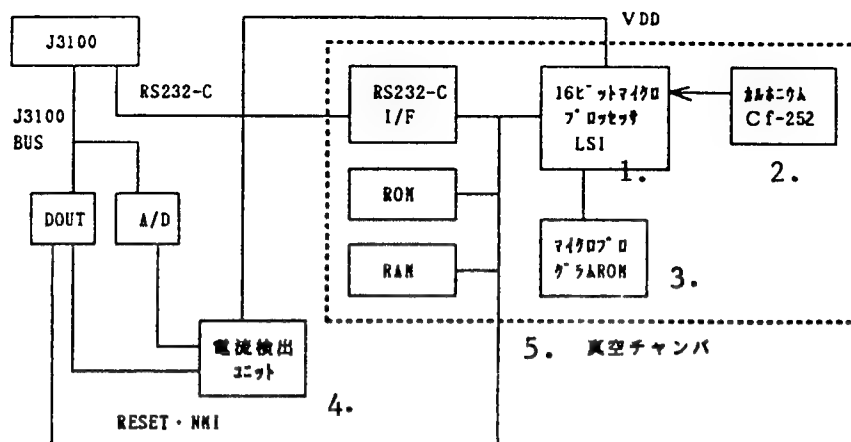
Figure 4. Single Event Software Error Test Block Diagram

Key:
1. 16-bit microprocessor LSI
2. Californium Cf-252
3. Microprogram ROM
4. Current detecting unit
5. Vacuum chamber
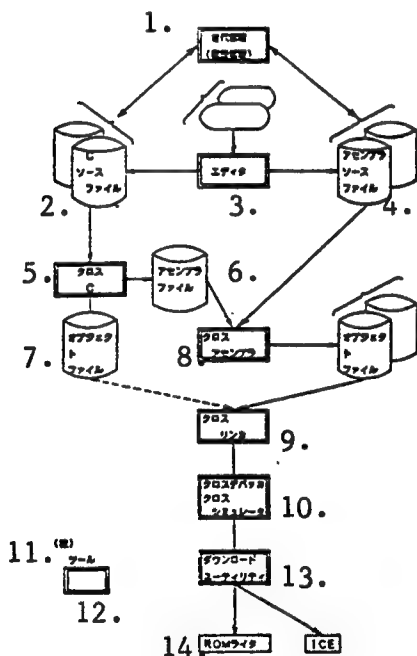
Figure 3. Software Development Procedure

Key:
1. [illegible]
2. Source file
3. Editor
4. Assembler source file
5. Cross
6. Assembler file
7. Object file
8. Cross assembler
9. Cross linker
10. Cross debugger, cross simulator
11. [illegible]
12. Tool
13. Down-load utility
14. ROM writer

References

1. "ETS-VI—Development of Attitude Control Electronic Circuit," The Proceedings of the 32nd Space Sciences and Technology Conference.

2. "ETS-VI—KS Antenna Direction Control Electronic Circuit to be Mounted," The Proceedings of the 32nd Space Sciences and Technology Conference.

RF Sensor for KSA Antenna Mounted on ETS-VI

[Article by Mitsuaki Ogasa and Senshu Ueno of Toshiba Corporation; Yasumasa Hisada and Yuuichi Murakoshi of the National Space Development Agency of Japan]

[Text] 1. Preface

Experimental K-band inter-satellite communications equipment will be mounted on the EST-VI scheduled to be launched in fiscal 1992. Various experiments involving inter-satellite communications are planned for this equipment. One important item is a capture and tracking experiment intended to communicate with a moving spacecraft. The RF sensor is the main piece of equipment constituting the antenna direction control system necessary for the capture and tracking process. This report outlines the trial manufacture of the RF sensor.

2. Configuration of RF Sensor

The RF sensor receives beacon waves emitted from a satellite, and detects the incoming direction of electric

waves. Table 1 shows the RF sensor system that was trial manufactured. As shown in Figure 1, the RF sensor consists of a horn (antenna section), comparator, phase adjuster and tracking receiver. The comparator can synthesize the electric waves input by the horn, generating sum and difference signals. The phase adjuster adjusts the phase relationship among the respective difference signals against the sum signals, and sends signals to the tracking receiver. The tracking receiver receives and processes the signals, and outputs an angular error signal as dc voltage. This output signal is sent to the antenna direction control electronic circuit, and is used as a sensor signal.

Table 1.
RF Sensor System

System	Multi-horn
Number of horns	5 (central horn is for communications)
Tracking receiver	Channel 1
Frequency	32.99 GHz
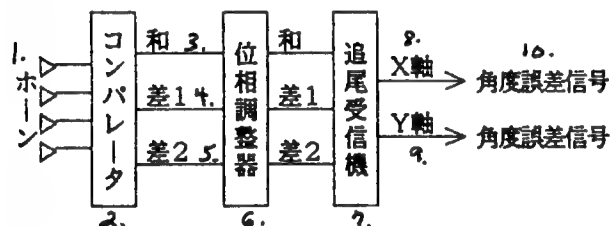
Figure 1. RF Sensor System

Key:
1. Horn
2. Comparator
3. Sum
4. Difference 1
5. Difference 2
6. Phase adjuster
7. Tracking receiver
8. Axis X
9. Axis Y
10. Angular error signal

3. Test Results

The RF sensor with the above configuration was tested with the measuring system shown in Figure 2. Figures 3 and 4 show the antenna pattern of the RF sensor and the output characteristics of the tracking receiver, respectively. The antenna pattern rotates the shaft of the positioner and records sum and difference signals from the phase adjuster output to the pattern recorder.

As shown in Figure 3, the difference signal demonstrates a pattern that generates a null in the bore site direction. The phase reverses by 180 degrees at the bore site between the + and - sides.

By using the signal, the tracking receiver detects this signal as an angular error because the output is proportional to the angle in the vicinity of the bore site. The null depth is 40 decibels or more and, as shown in the following equation, the error caused by the deterioration of the null
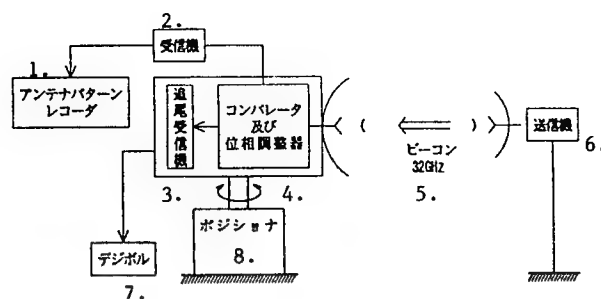
Figure 2. Measurement Configuration

Key:
1. Antenna pattern recorder
2. Receiver
3. Tracking receiver
4. Comparator and phase adjuster
5. Beacon 32 GHz
6. Transmitter
7. Digital voltmeter
8. Positioner
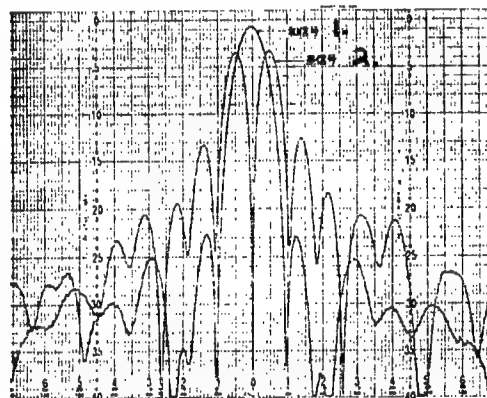
Figure 3. Antenna Pattern

Key: 1. Sum signal   2. Difference signal
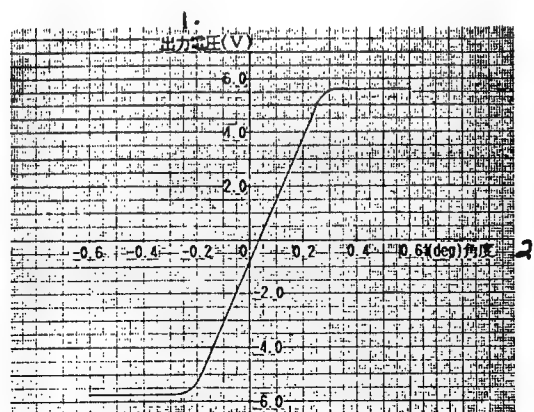
Figure 4. Output of Tracking Receiver

Key: 1. Output voltage (volts)   2. Angle (°)

depth is 0.004 degree or less. If α is the error sensitivity, θ_E = $1/\alpha$ (difference signal gain - sum signal gain) = -7.2 - 40 = -47.2 decibels x degrees 0.0040° (bore site)

The output of the tracking receiver monitors and records the dc output of the tracking receiver by using its digital voltmeter. The output characteristics of the tracking receiver shown in Figure 4 are saturated in the vicinity of 5.6 volts. However, no problems occur when drawing the antenna into the bore site since the polarity is retained. Table 2 shows the characteristics of the RF sensor.

Table 2.
Characteristics of RF Sensor
(Normal Temperatures)

	Item	Test results	Target value
Antenna system	Antenna gain (including loss of piping waveguide)	34.7 dB	34.5 dB
	Axial rato	0.83 dB	2.0 dB
	Error sensitivity	2.3 V/°	1.9 V/° or more
	Null depth	40 dB or more	40 dB or more
Tracking receiver	Output error sensitivity	22 V/°	1.5 V/°
	Linera range	0.25°	0.35°
	dc offset	-39 mV	+/-250 mV or less
	Lock time	1.5 sec or less	1.5 sec or less
	Receiver noise	20 mVrms or less	1 Vrms or less

This trial manufacturing process indicates that the linear range is 0.25 degree, but this is due to the output sensitivity being 22 volts/degree. Therefore, if the output sensitivity is at the preferred value, 15 volts/degree, it will be possible to expand the linear range.

4. Summary

The RF sensor is the main element constituting the antenna direction control system, and has been manufactured on a trial basis. As a result of testing it at normal temperatures, the selected value was almost satisfactory. It will be necessary to study temperature characteristics in detail, taking the space environment into consideration. In the future, we plan to manufacture products by studying systems that include these temperature characteristics and by establishing specifications so that these products can be mounted on satellites.

References

1. Hisada, et al., "Outline of KSA Antenna System Mounted on ETS-VI," Proceedings of the 31st Space Sciences and Technology Conference.

2. Hisada, et al., "Study of KSA Antenna System Tracking System Mounted on ETS-VI," Proceedings of the 31st Space Sciences and Technology Conference.

KSA Antenna Direction Control System Mounted on ETS-VI

[Article by Keiichi Hirako and Masaki Tanaka of Komukai Works, Toshiba Corporation; Yasumasa Hisada and Yuuichi Murakoshi of the National Space Development Agency of Japan]

[Text] 1. Preface

Japan is planning to perform experiments involving inter-satellite communications by using its engineering test satellite [ETS]-VI, and is developing a KSA antenna system to be mounted on the ETS-VI so that a data relay satellite can be put to practical use.

In this paper, the function of the subsystem, mainly the control mode, and items involving the antenna direction control system (APS), which controls the driving of the KSA antenna, required by the subsystem, are outlined. In addition, results of a test on a static closed loop which was conducted by using a trial-manufactured and experimental model of an antenna direction control electric circuit (APE) are reported.

2. Antenna Direction Control System

The following is an outline of the characteristics of the subsystem, which is a baseline for the APS design, and describes the items required by the subsystem.

(1) Requirements of subsystem

The tracking accuracy can be regarded as a basic requirement for capturing and tracking a user's satellite, while other requirements are taken into consideration as well. (a) It shall be possible to capture and track the user's satellite. Open loop tracking accuracy: 0.60 degree Closed loop tracking accuracy: 0.15 degree (b) Even if the main system malfunctions, it should basically be possible to drive the antenna. (c) Information on the driving of the antenna will be given to the attitude control system in order to restrain the satellite's attitude disturbance. (d) The subsystem should not resonate with the flexible modes of the solar cell paddle and antenna boom.

(2) Subsystem configuration

Figure 1 shows the configuration of the APS that will satisfy the above requirements.

The antenna driving mechanism (APM) is composed of a stepper motor, and is equipped with a potentiometer. It is possible to control angles by using the output angular signals.

Lock-on and error signals output from the RF sensor (RFS), consisting of a tracking receiver and feeding
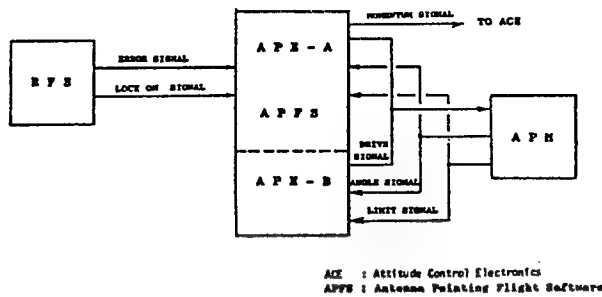
Figure 1. Subsystem Configuration

section, are used to capture the user's satellite during the initial stage and to track the closed loop, respectively.

(3) Outline of Functions

The APS has a number of control modes for providing the capture and tracking functions. The operation is carried out efficiently by combining these functions. Table 1 outlines the operation of each control mode.

**Table 1.
Outline of Operation of Control Mode**

Control mode	Outline of operation
Through mode	It is driven by controlling angles up to the APM target angle given by the ground command
Open loop tracking mode	Angular control for APM target angle obtained by calculating the orbit of user satellite and that of host satellite
Scan search mode	Capture operation which carried out conical scan around the nominal direction together with open loop tracking in the nominal direction
Closed loop tracking mode	Feedback control based on tracking error signals sent from RF sensor
Stop mode	It drives and stops the APM when the APE power is on
Manual mode	It drives the APM by using driving pulse numbers given by the ground command
Automatic capture tracking	It automates a series of operations involving open loop tracking, scanning and closed loop tracking

In the case of the initial capture, a scan search is carried out by the KSA antenna due to the relationship between the open loop tracking accuracy and the visual field of the RF sensor. Modes are transferred using the lock-on signals output by the RFS.

An automatic mode is used to automatically conduct the capturing and tracking operations, and has been established to lighten the burden of the operation and to increase the tracking performance.

3. Static Closed Loop Test

The following is a report of a static closed loop test [SCLT] conducted by using a trial-manufactured APE. Figure 2 [not reproduced] shows the system configuration of the SCLT. The control logic for directing and controlling the antenna is executed by incorporating a 16-bit MPU in the APE, and dynamic characteristics, such as antenna dynamics, orbit movements, etc., are solved by an outside computer.

Figure 3 shows the results of the SCLT. As can be seen from this figure, the scan search enables the phase to be transferred stably from the open loop tracking to the closed loop tracking.
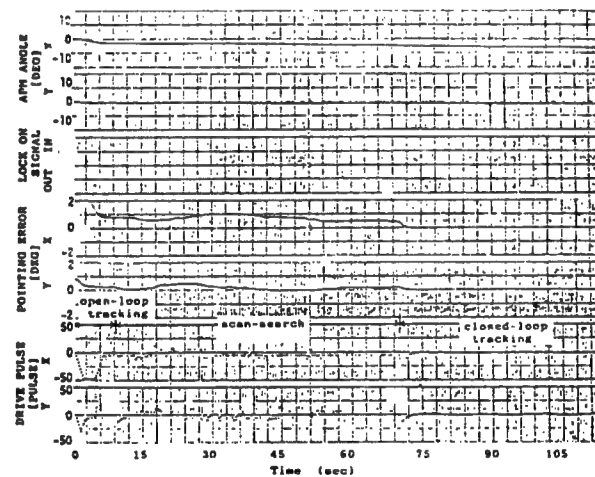
Figure 3. SCLT Test Results

4. Field Tracking Test

The following is a description of an outdoor tracking test involving the use of the trial-manufactured APE, APM and RFS. Figure 4 [not reproduced] shows a trial-manufactured model of the KSA antenna used in this test. The antenna simulates the user's satellite on the transmitting side, and the location is fixed. The APM is operated only with a shaft. An interface of the actual hardware has been confirmed by conducting a test involving the capturing and tracking operations.

5. Postface

We have presented the subsystem requirements for the direction control system of the KSA antenna mounted on the ETS-VI, and have outlined the characteristics of the designed subsystem.

We have also outlined a closed loop test conducted by using a trial-manufactured APE.

In the future, we plan to fully utilize the above results in designing a model to be mounted on the satellite.

Development of Rendezvous Radar Capture Tracking Mechanism System. I. Basic Test of Mechanism System

[Article by Hiroshi Anegawa of the National Space Development Agency of Japan; Hiroshi Takahashi, Toshikatsu Akiba, Kenichi Takahara, Shichita Aramiya and Yoshiharu Shimamoto of Toshiba Corporation]

[Text] 1. Preface

We have obtained basic data on the mirror driving mechanism system used to conduct capture and tracking from the rendezvous radar which will be mounted on a spacecraft in the future and will be used to guide and control the spacecraft. A two-axial mirror driving mechanism controls two degrees of freedom of rotation, consists of two pairs of moving coils and non-contacting angle sensors, and drives two gimbals supported by elastic pivots. Such a mirror mechanism is highly reliable and durable as a space equipment item because it does not require lubrication. This report describes the basic data obtained by Toshiba Corporation in connection with the design and research of a rendezvous radar system which is being conducted by the National Space Development Agency of Japan [NASDA].

2. Configuration of Capture and Tracking System

Figure 1 shows the configuration of the capture and tracking system. This system consists of a two-axial mirror driving mechanism equipped with a scanning mirror, control system and optical system. The control system consists of a linear riser, mirror driving mechanism control circuit (PD circuit), power amplifier and tracking control circuit (PID circuit). The linear riser corrects data on the signals output from an angle sensor set in the mirror driving mechanism. The optical system consists of the laser oscillator required for the capture and tracking, a two-dimensional spot position sensor and other optical parts. The capture and tracking method is as follows: laser beams are scanned by a scanning mirror based on the information obtained outside on the position of a spacecraft, are reflected in a corner cubic reflector [CCR] installed in the spacecraft, and are detected and captured by a two-dimensional spot position sensor. In addition, the movement of the spacecraft subsequent to the detection and capture is tracked, and the azimuth angle and angle of attack are measured.

3. Outline of Structure of Mirror Driving Mechanism

The mirror driving has a comparatively large trackable range (+/-15 degrees), and can become stationary at an arbitrary angle within the range. It requires high driving
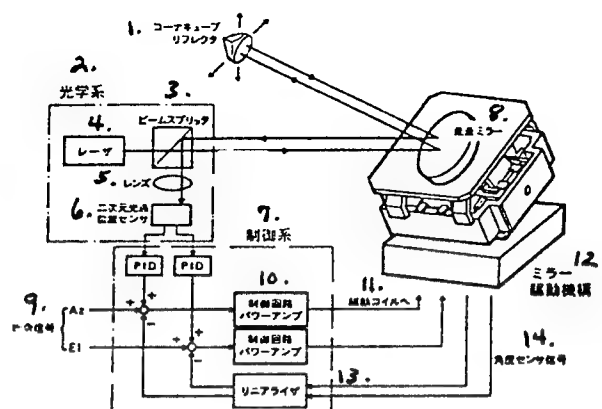
Figure 1. Configuration of Capture Tracking System

Key:
1. Corner cube reflector
2. Optical system
3. Beam splitter
4. Laser
5. Lens
6. Two-dimensional node position sensor
7. Control system
8. Scanning mirror
9. Command signal
10. Control circuit power amplifier
11. To driving coil
12. Mirror driving mechanism
13. Linear riser
14. Angular sensor signal

resolution capability and angular accuracy. Figure 2 shows the configuration of the mirror driving mechanism. Interior and exterior gimbals are supported with two elastic pivots, respectively. A moving coil wound circularly has been adopted to drive the mirror. The angular sensor consists of a non-contacting displacement sensor (overcurrent type) and a sensor target with a
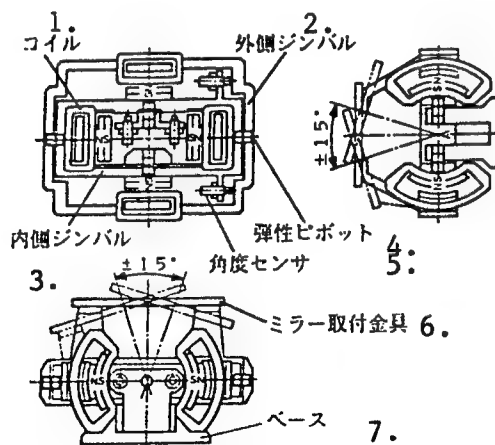
Figure 2. Outline of Mirror Driving Mechanism Structure

Key:
1. Coil
2. Exterior gimbals
3. Interior gimbals
4. Elastic pivot
5. Angle sensor
6. Mirror fitting
7. Base

taper, and it detects gaps in its axial direction and changes them into angular signals. Errors caused by eccentricity are removed by taking the differential output by means of two non-contacting displacement sensors. One pair is fixed on the base and detects angles of rotation of the interior gimbal, while the other pair is fixed on the interior gimbal and detects angles of rotation of the exterior gimbal.

4. Results of Basic Test

4-1. Performance of Single Structure of Mirror Driving Mechanism When this mechanism, equipped with a mirror, is driven by sweeping sine waves within a capture range (corresponding to the capture range of +/-1.5° of the laser beams) of +/-0.75°, the driving band width for both the interior and exterior gimbals is 20 hertz. It has been confirmed that when the response to fine rectangular wave command signals was measured, the driving resolution capability for both the interior and exterior gimbals was 0.002° or less.

4-2. Capture and Tracking Function According to Laser Beams A capture test was performed when the CCR was stationary in order to obtain the basic characteristics of this system. Figure 3 shows a time history of angular sensor signals and one of two-dimensional spot position sensor signals during the capture and tracking. The two-dimensional spot position sensor signals following the capture are converged into a constant value set at the origin. Also, when the CCR was moved following the capture, the maximum tracking angular velocity was 5°/second. Table 1 summarizes the data obtained after checking the test results.
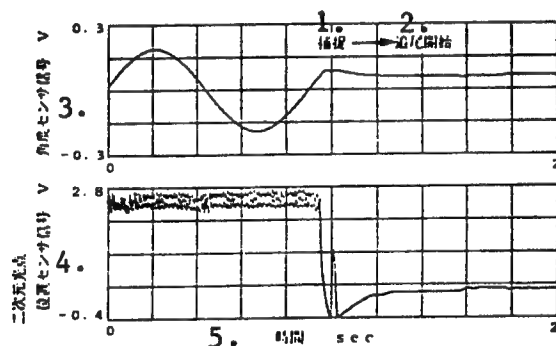
Figure 3. Time History of Capture Tracking

Key:
1. Capture
2. Tracking
3. Angle sensor signal V
4. Two-dimensional node position sensor signal V
5. Time (seconds)

**Table 1.
Capture Tracking System Data**

Item	Characteristic Value
Search angle range	+/-30°
Scanning angle speed at search	20°/sec

**Table 1.
Capture Tracking System Data (Continued)**

Item	Characteristic Value
Tracking angle speed	5°/sec
Measurement angle accuracy	+/-0.025°
Mirror driving mechanism	
Degree of freedom	2
Driving range	+/-15°
Driving resolution capability	0.002°
Angular sensor accuracy	+/-0.025°
Weight (except for that of mirror)	3.3 kg

5. Summary

We have performed the basic test involving the capture and tracking mirror driving mechanism for rendezvous radar equipment, have confirmed the capture and tracking functions according to laserbeams, and have basically seen our way clear to putting this mechanism to practical use. This report also describes the results of a trial-manufactured product being used in basic tests at Toshiba Corporation in connection with the research involving rendezvous radar equipment that is being conducted by NASDA. In the future, we intend to fully utilize this basic data in the design of a functional test model.

References

1. Ito, et al., "Study of Concept of Rendezvous Radar Equipment," Proceedings of the 30th Space Sciences and Technology Conference, 1986, pp 272-273

2. Anegawa, et al., "Optical Technology Application System in Space Development," JAPAN AEROSPACE JOURNAL, Vol 36, No 408, 1988

Development of Capture, Tracking Mechanism for Optical Communications

[Article by Kenichi Takahara, Shichita Aramiya and Hiroshi Takahashi of the General Research Institute, Toshiba Corporation; Yoshiharu Shimamoto of Komukai Works, Toshiba Corporation]

[Text] 1. Preface

The research and development of optical communications are being carried out enthusiastically so that various optical systems[1] and mirror driving mechanisms[2] can be put to practical use based on the increase in capacity of future communications, the transmission of a large amount of data from various kinds of observation equipment, etc. Optical communications requires a highly accurate optical driving system that can capture a satellite receiving communications and track the movement of the satellite through the sharp directivity of laser beams.

This report describes an experimental unit in which receiving laser beams are tracked roughly and accurately by using a CCD and a four quarter photo diode [4QD] as optical detectors, as well as results of characteristic tests of a tracking system and characteristics of a mirror driving mechanism.

2. System Configuration

Figure 1 shows the system configuration of a tracking system experimental unit manufactured on a trial basis. This unit consists of two mirror driving mechanisms, a CCD (for rough tracking), a 4QD (for accurate tracking), three control circuits and a changeover circuit. The mirror driving mechanism controls the directivity of the laser beams, the CCD and 4QD, as optical detectors, detect the spot position of these laser beams, and the three control circuits are used to drive the mirror and to roughly and accurately track a satellite. The changeover circuit switches their control systems. In this unit, first laser beams are put in the CCD by driving the mirror driving mechanism and are then placed in an accurate tracking area within the visual field of the CCD by using the rough tracking control circuit. When these laser beams are placed in the visual field of the 4QD, accurate tracking will be carried out through the driving of the accurate tracking control circuit because the accurate tracking area of the CCD corresponds to the visual field of the 4QD.

3. Mirror Driving Mechanism

Figure 2 shows the mirror driving mechanism incorporated in the tracking system experimental unit. This mechanism is designed so that it can drive the mirror with high accuracy and without incurring any friction

Figure 2. Mirror Driving Mechanism

Key:
1. Elastic pivot
2. Mirror
3. Permanent magnet
4. Angle sensor
5. Coil

or wear, since elastic pivots are used for support bearings, and moving coils are used as the rotation driving systems in the mechanism.

4. Test of Characteristics

4.1 Frequency Response Characteristics of Mirror Driving Mechanism

Figure 3 shows the frequency response characteristics of the mirror driving mechanism in which sine waves equivalent to a target value of +/-0.12° are input. As can be seen from this figure, the response frequency of this mechanism exceeds 100 hertz, and possesses sufficient response properties.

4.2 Response from Rough Tracking to Accurate Tracking

Figure 4 shows the time history of the CCD output and that of the 4QD for the case in which the rough tracking control system is changed to an accurate one. As can be seen from this figure, this change is normal. The deflection following the accurate tracking process was within +/-3.3 x 10^{-5} degrees (+/-0.58 microrad).

Figure 1. System Configuration of Tracking System Experimental Unit

Key:
1. Accurate tracking control circuit
2. Coarse tracking control circuit
3. Switching circuit
4. Mirror driving control circuit
5. Signal processing
6. Angle sensor signal processing
7. Driver
8. Mirror driving mechanism
9. Laser beam
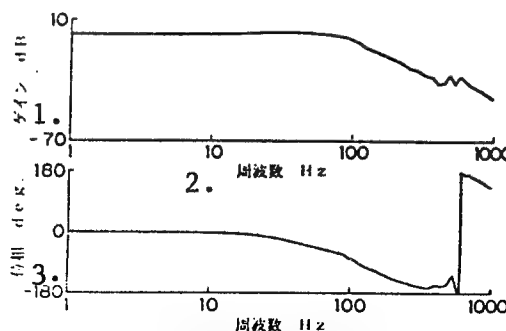
Figure 3. Frequency Response of Mirror Driving Mechanism

Key: 1.Gain (dB)   2. Frequency (Hz)   3. Phase (°)
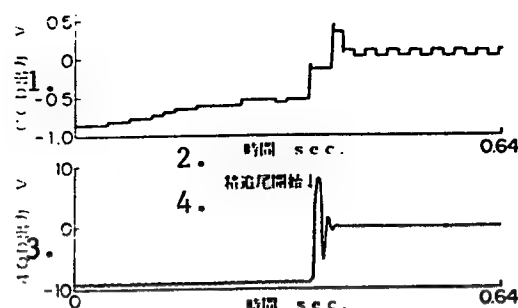
Figure 4. Response from Coarse Tracking to Accurate Tracking

Key:
1. CCD output (V)   3. 4QD output (V)
2. Time (seconds)   4. Start of accurate tracking

4.3 Response to Disturbance

Figure 5 shows mirror angles for the case in which the disturbance is equivalent to +/-0.0037°, with 0.6 hertz given to the mirror driving mechanism through the operation of the accurate tracking system. As can be seen from this figure, the amplitude of the response to the disturbance is +/-5.0 x 10^{-5} degrees (+/-0.87 microrad). If the value of +/-0.03 degree is considered when studying the fluctuation of attitudes of a satellite as a disturbance, it is anticipated that this response amplitude will be +/-4.2 x 10^{-4} degrees (+/-7.3 microrads).
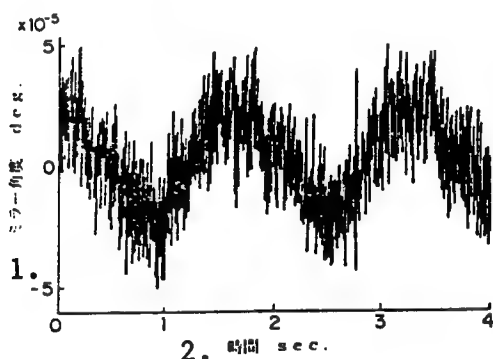
Figure 5. Response to Disturbance of Accurate Tracking System

Key: 1. Mirror angle (°)   2. Time (seconds)

Table 1. Mirror Driving Mechanism Data

Item	Characteristic Value
Degree of freedom	1
Driving range	+/-1.0°
Driving frequency	100 Hz
Angle sensor resolution capability	4 μrad
Maximum power consumption	1 W

5. Conclusion

An experimental tracking system unit for laser communications was manufactured on a trial basis and, as a result of a test of its characteristics, it was confirmed that the accuracy of its mirror driving mechanism was satisfactory and that it could be applied to the tracking system. In this system, elastic pivots are used for support bearings, and moving coils are used as the rotation driving systems. In the future, we plan to increase the tracking accuracy 10-fold by adjusting the control systems, and will carry out development so that new equipment can be put to practical use.

References

1. Hisada, et al., "Study of Inter-Satellite Laser Communications System," Proceedings of the 31st Space Sciences and Technology Conference, 1987

2. Shimamoto, et al., "Development of Capture and Tracking Mechanism for Optical Communications," Proceedings of the 31st Space Sciences and Technology Conference, 1987

Study of Capture, Tracking System for User's Spacecraft

[Article by Eiichi Hashimoto of the National Space Development Agency of Japan; Yoshiharu Shimamoto, Seiichi Motohashi and Tsuyoshi Kosugi of Toshiba Corporation]

[Text] 1. Preface

Spacecraft are operated in orbits at low, intermediate and high altitudes, and are used to transmit observed and image data to operation centers on the ground. It is necessary to establish a systen that can continuously exchange communications between these spacecraft and operations centers at high speeds. The data relay tracking satellite [DRTS] system is being planned as a means of realizing the above system.

In this plan, it is necessary to develop the DRTS system proper as well as a spacecraft anti-DRTS antenna system of earth observation platforms, etc., which are DRTS users. In order for communications exchange to be enabled at all times, it is very important to develop capture and tracking technologies.

This resport describes theresults of establishing the target specifications for the capture and tracking system of an antenna with a diameter of 2 meters. This system must survive the most severe conditions as a user spacecraft capture and tracking system.

2. Flowchart

Figure 1 presents a flowchart of the capture and tracking system study.
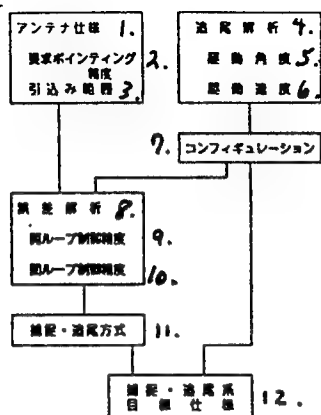
Figure 1. Flowchart of Capture Tracking System

Key:
1. Antenna specifications
2. Required pointing accuracy
3. Retracting range
4. Tracking analysis
5. Driving angle
6. Driving speed
7. Configuration
8. Error analysis
9. Open loop control accuracy
10. Closed loop control accuracy
11. Capture tracking system
12. Target specifications of capture tracking system

3. Antenna Specifications

It is preferable that the user space antennas fit the respective spacecraft, and that the optimum design process be carried out on an individual basis. However, it is necessary to develop common equipment, systematized according to use, for the following reasons: 1) lightening the burden on the user, 2) simplifying the structure and operation, and 3) reducing the cost.

Table 1 shows common user antenna specifications established taking the above-mentioned items into consideration.

**Table 1.
Specifications of Common User Antenna
(Provisional Values)**

Antenna Diameter Specifications of User Antenna	2 mφ	1.4 mφ	1 mφ	0.8 mφ	0.5 mφ
Required pointing accuracy: 32 GHz	+/- 0.055	+/- 0.078	+/- 0.12	+/- 0.14	+/- 0.22
Retracting range: 23 GHz	+/- 0.27	+/- 0.38	+/- 0.54	+/- 0.67	+/- 1.08
Transmission amount (MBPS) (output 10 W)	302	125.9	79.4	50.1	20.4

4. Tracking and Analysis

A circumterrestrial satellite with three kinds of orbits and directivities was tracked and analyzed, and the capture and tracking range and tracking speed shown in Table 2 were obtained.

**Table 2.
DRTS Tracking Analysis Results**

	Sun synchronous, quasi-recurrent orbit, earth-directional satellite	Common driving sun-directional satellite	Common driving earth-directional satellite
Tracking requirement range	Azimuth angle: +/-180°	Azimuth angle: +/- 180°	Azimuth angle: +/-180°
	Angle of attack:+/-120°	Angle of attack: 85-95°	Angle of attack:+/-120°
Angular velocity (except for vicinity of zenith)	Azimuth angle: 3.0°/sec or less	Azimuth angle: 0.009°/sec or less	Azimuth angle: 3.0°/sec or less
	Angle of attack:0.073°/sec or less	Angle of attack: 0.006°/sec or less	Angle of attack: 0.073°/sec or less

5. Configuration

The antenna driving system was configured based on the capture and tracking range and the tracking speed obtained from the above tracking and analysis. This concept is shown in Figure 2.

6. Error Analysis

Two control systems can be regarded as the capture and tracking systems: (1) Open loop control: Based on user
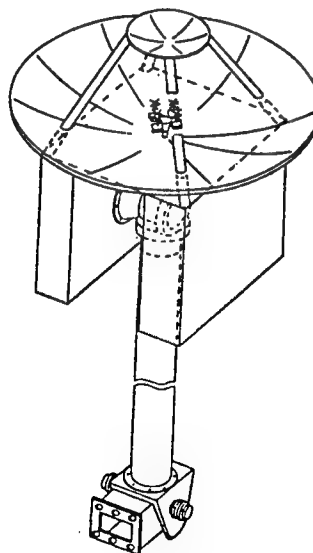
Figure 2. Antenna Driving System Configuration

spacecraft, information on attitude and position of DRTS (2) Closed loop control: Zero control by using an RF sensor

The errors found in the two systems were analyzed based on the configuration shown in Figure 2. As a result, the following accuracy levels were obtained: Open loop control accuracy: +/-0.207° Closed loop control accuracy: +/-0.048°

7. Capture and Tracking System

The capture and tracking system has been adopted since it is possible to change a system from open loop control to closed loop control, and to adjust the accuracy to within the RF sensor pulling range (+/-0.27°) due to the open loop control.

In this system, it is possible to adjust the accuracy to within the required pointing range (+/-0.055°) due to the closed loop control. Figure 3 demonstrates the capture and tracking system concept.
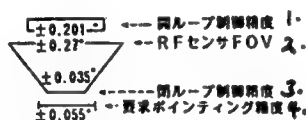
Figure 3. Capture Tracking System

Key:
1. Open loop control accuracy
2. RF sensor FOV
3. Closed loop control accuracy
4. Required pointing accuracy

8. Summary

We have established the target specifications (shown in Table 3) of the capture and tracking system necessary for the development of the elemental technologies required by user spacecraft antenna systems.

Table 3.
Capture Tracking System Specifications

Item	Value
Antenna diameter	2 mφ
Open loop control accuracy	+/-0.27°
Closed loop control accuracy	+/-0.055°
Driving range	
Azimuth angle	+/-180°
Angle of attack	+/-120°
Driving angular velocity	
Azimuth angle	3.0°/sec
Angle of attack	3.0°/sec

We are currently manufacturing, on a trial basis, an antenna driving system based on the above results.

Development of KSA Antenna Pointing Mechanism for ETS-VI

[Article by Eiichi Hashimoto, Yasumasa Hisada and Yuuichi Murakoshi of the National Space Development Agency of Japan; Takahiro Amano, Toshiro Ohashi and Yoshiharu Shimamoto of Toshiba Corporation]

[Text] 1. Preface

A K-band single access [KSA] antenna system will be mounted on an engineering test satellite type VI (ETS-VI) in order to establish the technology to capture and track a user satellite from a geostationary satellite. The ETS-VI is scheduled to be launched in the early 1990s. The antenna pointing mechanism [APM] is a constituent of the KSA antenna system, and represents a key component for capturing and tracking satellites. An engineering model [EM-1], representing only one axis of the APM, has been designed and manufactured to make an early check of its function and performance as well as to be fully utilized in flight products. The EM-1 is currently being tested. This report describes the results of designing the APM's EM-1.

2. Required Performances

Table 1 shows the performance specifications required in this EM-1. The maximum driving rate has been established by taking the capture of user satellites into consideration, and a driving range has been established so that these user satellites can be tracked at all times. The driving resolution capability has been determined from the standpoint of requirements of the antenna system's pointing accuracy. Also, a retaining torque is required so that the antenna is not rotated by the disturbance caused by the unfolding of the KSA antenna or that caused by the injection of the thruster when controlling the attitude of the satellite proper or correcting the orbit.

Table 1.
Performance Required for APM's EM-1

Item	Required Performance
Weight	5 kg or less
Power consumption	19.5 W or less (during small mode)
	2.25 W or less (during stationary tracking)
Maximum driving rate	0.3°/sec
Driving range	+/-10° or more
Driving resolution capability	0.005° or less
Retaining torque	2.5 Nm or more
Maximum inertial load	12 kg/m^2
Working life	3 years

3. Design

3.1 Driving System Trade-Off

Table 2 shows three kinds of trade-offs involving APM constituents. A step motor/speed reducer system has been selected for the following reasons: 1) angles can be controlled in accordance with the number of motor driving pulses, 2) speeds can be controlled in accordance with the pulse rate, 3) the open loop can be controlled, 4) a highly accurate angular sensor and brake are not necessary, 5) the driving circuit is simple, and 6) the EM-1 is comparatively lightweight. It has been decided that a zero sensor will be developed as a position sensor and an absolute angular signal will be added to the redundant constitution. The zero sensor is an improved version of a lightweight potentiometer with a simple processing circuit. Such potentiometers have actually been used in space development. Design, manufacturing and vacuum-lubricating technologies, etc., have been obtained from the development of a paddle driving mechanism over the past five years. By utilizing these technologies in the APM, it will be possible to shorten the development period if the above-mentioned system is selected.

Figure 1. Sketch of APM's EM-1

Key:
1. Mechanical stopper
2. Potentiometer
3. Bearing
4. Electric limit switch
5. Housing
6. Harmonic drive
7. Step motor

Table 2.
Trade-off of Driving System

	Step Motor/ Speed Reducer	DC Motor/ Speed Reducer	DD Motor
Loop control	Possible when open	Closed	Closed
Position sensor	Highly accurate zero point sensor	Highly accurate angle sensor	Highly accurate angle sensor
Angular velocity sensor	Unnecessary	Necessary	Necessary
Rotational speed	Low	High	Low
Self-holding capacity	Exists	Brake is necessary	Brake is necessary
Torque	Large	Large	Small
Weight form	Small	Small	Large
Electronics	Simple	Complex	Complex
Actual development results (for space use)	Developing with paddle driving mechanism	Developing with space station program	New development is not necessary
Ranking	1	2	3

3.2 Design Results

Figure 1 and Table 3 show design results of the APM's EM-1. The EM-1 is driven by a step motor with a step angle of 0.45° and a harmonic drive with a reduction ratio of 1/157, and is equipped with a potentiometer offering a zero accuracy of +/-0.016° and an angular accuracy of +/-0.08°. It satisfies each required performance specification.

Table 3.
Design Results of APM's EM-1

Item	Design results
Weight	4.9 kg
Power consumption	19.5 W or less
	2.25 W or less
Maximum driving rate	0.31°/sec
Driving range	+/-13°+/-0.5° (mechanical stopper)
	+/-11°+/-0.5° (electrical limit switch)
Driving resolution capability	0.0029° (nominal)
Holding torque	2.51 Nm or more
Maximum inertial load	12 kg/m^2
Working life	5.3 x 10^5 rev (equivalent to 3 years in terms of motor shaft)

In order to carry out highly accurate pointing, it is important to study the alignment errors of the mechanism system as well as the driving resolution capability. Alignment errors are generated in a clearance between the outer ring and housing, and are dependent on temperature. For example, the EM-1 was designed taking alignment errors, the coefficient of thermal expansion, strength, etc., into consideration. Figure 2 [not reproduced] shows the EM-1 of the APM we manufactured.

4. Summary

We have designed the EM-1 of the KAS APM for the ETS-VI. We plan to confirm each design result by means of performance tests, environmental tests and duration tests, and to fully utilize the data obtained from these tests in the development of a two-axial antenna driving system, the EM-2, which will be a flight product.

References

1. Amano, T., et al., "Antenna Pointing Mechanism for ETS-VI K-Band Single Access (KSA) Antenna," 16th ISTS.

Study of Navigation System for Future Spacecraft

43065012q Tokyo PROCEEDINGS OF THE 32ND SPACE SCIENCES & TECHNOLOGY CONFERENCE in Japanese 26-28 Oct 88 No 2F15 pp 460-461

[Article by Noboru Muranaka and Tadashi Uo of NEC Corporation]

[Text] 1. Outline

It is expected that future spacecraft, such as the space plane [SP], orbital transfer vehicle [OTV], OSV and PF, will be realized. Some reports on the navigation systems of such spacecraft have already been made, as have many reports on accuracy evaluation. This paper briefly presents results of studies of the operations and selections of an algorithm for use in realizing this navigation system. Figure 1 shows a block diagram of the navigation system which is taken as a premise. The navigation system mainly consists of an inertial measuring unit [IMU], star sensor [ST], and global positioning system receiver [GPSR]. Rendezvous radar [RVR] and a proximity sensor [PRS] will be added when the mission involves rendezvous docking. These sensors are connected to computers through interface electronics.

2. Acquisition of Initial Attitude

Generally, the step from the acquisition of the sun to that of the earth has been taken in previous earth pointing satellites, but this method is disadvantageous in that the acquisition must be carried out in a specific orbit position. For
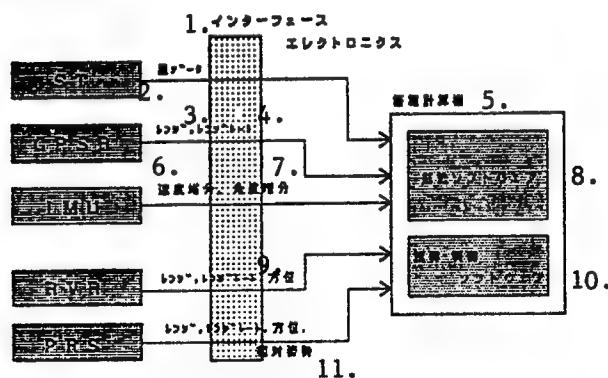
Figure 1. Configuration of Navigation System

Key:
1. Interface electronics
2. Data on quantity
3. Range
4. Range rate
5. Computer mounted on satellite
6. Increase in speed
7. Increase in angle
8. [illegible] software
9. Azimuth
10. [illegible] software
11. [illegible] attitude

future spacecraft, the following acquisition methods are being studied in order to obviate this disadvantage.

1) Determination of attitude according to ST stand alone: Stars detected with an ST are identified by matching patterns and, after the attitude is determined, an IMU will be utilized for acquisition. With this method, substantial software and a star catalog are required for the pattern matching, and a trade-off with computer performance is also necessary.

2) IMU integral system: The attitude and orbit are propagated by mounting the IMU on the spacecraft after launch. It is believed that information on the spacecraft navigation can be supplied to a craft to be launched, or that the guidance of the craft itself can be carried out by its computers. Although this system has the advantage that it does not require any sensors other than the IMU, it does involve the following problems: 1) the dynamic ranges of the gyroscope and accelerometer must be wide, and 2) the burden on navigation software increases.

3) Terrestrial magnetism sensor-using system: If the orbit of a spacecraft has been acquired, the direction of the magnetic fields can be calculated using a model of these magnetic fields. Therefore, the attitude can be determined by using a terrestrial magnetism sensor and a sun sensor. Either the propagation of the attitude after the craft has been launched or the initial acquisition according to the GPSR are needed for this determination. This can be regarded as a method. The attitude determination accuracy according to the terrestrial magnetism sensor is not very high, but the ST star acquisition according to direct matching can offer sufficient accuracy.

3. Filter

The UD resolution filter is frequently used as an attitude and orbit filter to ensure numerical stability. In addition, a fading factor is introduced to prevent divergence. Filter divergence is caused by bias correction errors, etc., of the IMU. The fading factor restrains such divergence in the stationary pointing mission, but it is necessary to take a part of the bias (e.g., a gyroscope filter) in the filter since the effect of the restraint is not sufficient for a mission requiring high speed maneuvering.

4. Detection of Problems

Methods of detecting problems involving sensory and actuators are as follows: 1) a direct method in which the status of each component is monitored, and 2) a method in which the deviation is monitored through the nominal value of the attitude and the orbit determining value. When a deviation is detected, the malfunctioning components are identified and separated from the value, and the configuration of a new control system is indicated to the guidance and control system. An interface is necessary between the navigation and control system to prevent errant operations from being caused by the transitional dynamics of the spacecraft during the reconfiguration.
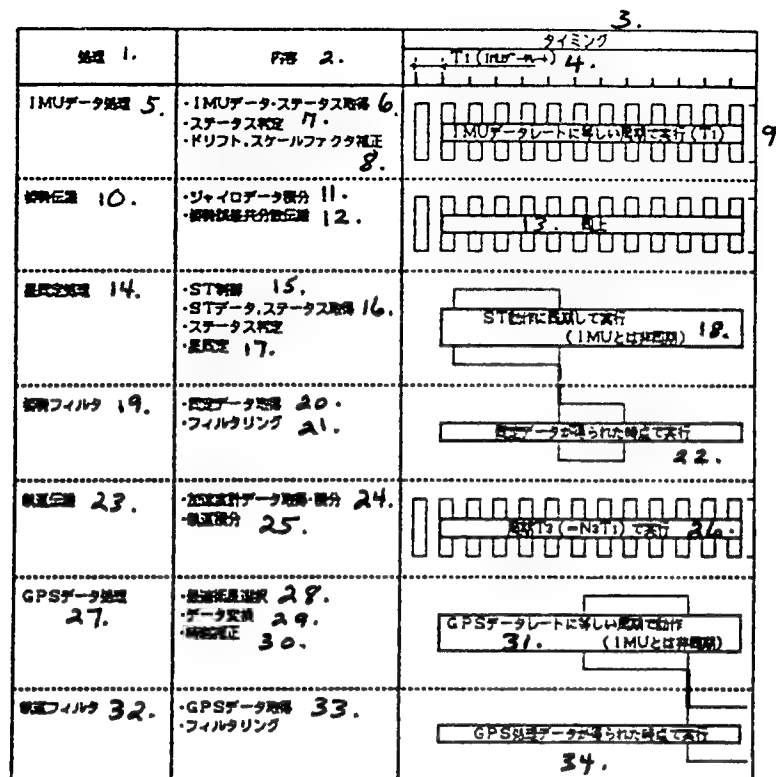
Figure 2. Navigation Software Contents

Key:
1. Processing
2. Contents
3. Timing
4. T_1 (IMU data rate) 5. IMU data processing
6. Obtaining IMU data status
7. Judgment of status 8. Correction of drift and scale factor
9. Execution during cycle equivalent to IMU data rate (T_1)
10. Attitude propagation
11. Integration of data on gyroscope
12. Attitude error covariance propagation
13. Same as above
14. Quantity identification processing
15. ST control
16. Obtaining of ST data and status
17. Identification of quantity
18. Execution of synchronization with ST operation (asynchronous with IMU)
19. Attitude filter
20. Obtaining of fixed data
21. Filtering 22. Execution when fixed data obtained
23. Orbit propagation
24. Obtaining and integrating data on accelerometer
25. Orbit integration
26. Execution during T_3 cycle ($-N_3T_1$)
27. GPS data processing
28. Selection of optimum satellite
29. Data conversion
30. Time correction
31. Operation during cycle equivalent to GPS data rate (asynchronous with IMU)
32. Orbit filter
33. Obtaining GPS data
34. Execution when GPS processing data obtained

5. Software

It is necessary to divide navigation system software into tasks according to function, and to control the system operation by the real time OS since the software has so many functions. Figure 2 shows an example of the task division and operation timing of this software. Attitude integration, requiring rapid responses, operates according to the IMU data period and has low frequency, but the selection of the optimum satellite for the GPS with a long processing time and the establishment of a star-identifying initial stage are executed during this period.

6. Summary

We have summarized the topics to be studied to realize the navigation systems of future spacecraft. In the future, we plan to study and demonstrate practical systems, taking these study topics into consideration.

References

1. Uyeminami, R.T., "Navigation Filter Mechanization for a Space-borne GPS User," IEEE, 1976.

Accessories for Future Spacecraft Control

*43065012r Tokyo PROCEEDINGS OF THE 32ND
SPACE SCIENCES & TECHNOLOGY CONFERENCE
in Japanese 26-28 Oct 88 No 2F17 pp 464-465*

[Article by Yukiharu Shimizu and Haruki Ayata of NEC
Corporation]

[Text] 1. Preface

Future spacecraft (ADEOS, OTV, STEP, etc.) will be
equipped with accessories such as antennas, solar cell pad-
dles and manipulators. It is expected that these accessories
will become more complex and larger and will have a large
influence on the attitude control system. This paper presents
technical topics involved in the development of control
systems for future spacecraft and results of identifying the
vibration parameters of particularly flexible accessories.

2. Technical Topics for Development of Control Systems
for Future Spacecraft

(1) Identification of Vibration Parameters of Flexible Struc-
tures

Generally, the vibration parameters of flexible structures
are estimated by analyzing vibration by means of com-
puters, but it is difficult to obtain these parameters precisely
by conducting ground experiments as the means of verifi-
cation. It is not necessary to adjust the values of such
vibration parameters obtained in advance since the possi-
bility exists of the vibration parameters being changed
slowly with time. Accordingly, it is preferable that such
vibration parameters be identified in orbit.

(2) Variability of Control System Parameters

When solar cell paddles are folded or unfolded and when
manipulator arms are expanded or contracted frequently, it
will be difficult for fixed control systems determined on the
ground to cope with these paddles and arms since the
characteristics of the control objects will be changing.
Accordingly, future control systems must be able to adjust
the control parameters based on the commands sent from
the ground in accordance with the changes in vibration
parameters.

(3) Control of Change of Shape of Large Accessories
Caused by Thermal Strain

When large accessories are changed sharply and thermally in
the boundary between sunshine and shade, the possibility
exists of thermal strain being generated or flexible vibration
being excited in them. Accordingly, it is necessary to control
the shape of these large accessories so that the thermal strain
and excitation can be restrained.

(4) Environmental Resistance Disturbance

The solar radiation pressure torque, gravity inclination
torque and aerodynamic torque will become larger than
those of conventional satellites in proportion to the increase

in size of the spacecraft. Accordingly, it is necessary to study
control system structures, taking these torques into consid-
eration.

3. Identification of Vibration Parameters of Flexible
Structures

The following is a study of methods for identifying the
vibration parameters of the particularly flexible structures
mentioned in the technical topics above. A displacement
gage is installed on flexible accessories, and vibration
parameters are identified based on the signals emitted from
the displacement gage. However, this method is disadvan-
tageous when noise is involved since the calculation of
acceleration signals will require differential operations.
Therefore, acceleration is detected by an accelerometer
mounted on a flexible accessory, and vibration parameters
are identified by integrating the acceleration and by finding
the displacement of the modes. The identification process is
outlined below.

(1) Dynamics

As shown in Figure 1, the object of control is regarded as a
model combined with a satellite proper, a flexible accessory
and a solar cell paddle sheet. An accelerometer is regarded
as being installed on the top of the solar cell paddle. Taking
flexible modes of up to three dimensions into consideration,
an equation of motion can be expressed:

$$\ddot{\eta}_1 + 2\zeta_1\omega_1\dot{\eta}_1 + \omega_1{}^2\eta_1 + \delta_1\dot{\omega}x\sin\theta - \delta_1\dot{\omega}z\cos\theta = 0$$

$$\ddot{\eta}_2 + 2\zeta_2\omega_2\dot{\eta}_2 + \omega_2{}^2\eta_2 + \delta_2\dot{\omega}x\sin\theta + \delta_2\dot{\omega}z\cos\theta = 0$$

$$\ddot{\eta}_3 + 2\zeta_3\omega_3\dot{\eta}_3 + \omega_3{}^2\eta_3 + \delta_{e3}\ddot{\theta} - \delta_{e3}\dot{\omega}y = 0$$

where, η_i is the displacement mode, ζ_i is the attenuation
coefficient, ω_i is the natural frequency, ωx, ωy, ωz represent
each acceleration of the satellite proper, θ is the angle of
rotation of the paddle, and δ_* is the coupling coefficient.

In addition, the output of the accelerometer is shown by
the following equation:

$$\ddot{u} = \sum_{i=1}^{\infty} \phi_i \ddot{\eta}_i$$
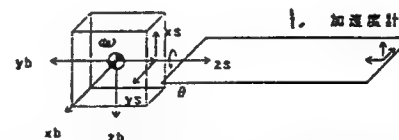
Figure 1. Definition of Coordinate System
Key: 1. Accelerometer

where, φ is the mode shape.

(2) Method of Identifying Vibration Parameters

Signals sent from the accelerometer are combined with
each mode acceleration, so they can be separated from

each other with the addition of a filter. Parameters a_{1i}, a_{2i}, b_{0i}, b_{1i} and b_{2i} are estimated by using a successive method of least squares, under the assumption that a mode dynamic model can be expressed by the following equation and that vibration parameters can be obtained by transforming these parameters. In this case, input signals of dynamics are regarded as angular accelerations of the satellite proper.

$$D_i = (b_{0i} + b_{1i}z^{-1} + b_{2i}z^{-2})/(1 - a_{1i}z^{-1} - a_{2i}z^{-2})$$

(3) Problems in Identifying Vibration Parameters of Flexible Structures

It is necessary to plan sensors so that only a certain mode is emphasized since a number of mode accelerations are included in the signals sent from the accelerometer. It is also necessary to study the following topics: 1) the necessity of readily detecting the acceleration by exciting the vibration of flexible structurres by means of a thruster, etc., and 2) the possibility of estimating vibration parameters by means of free responses.

4. Postface

We have presented technical topics for the development of control systems of future spacecraft and have studied problems with and methods for identifying the vibration parameters of flexible structures. In the future, we plan to use computer simulations to confirm the validity of vibration parameter identification methods, to clarify the limits of the identifications, and to study control systems.

Development of Ion Engine System To Be Mounted on ETS-VI

43065012s Tokyo PROCEEDINGS OF THE 32ND SPACE SCIENCES & TECHNOLOGY CONFERENCE in Japanese 26-28 Oct 88 No 2G9 pp 484-485

[Article by Kenichi Kajiwara of the National Space Development Agency of Japan; Haruki Takegawara, Sadanori Shimada, Kazuo Sato and Shoji Goto of Mitsubishi Electric Corporation]

[Text] 1. Preface

Ion engines will be mounted for the first time ever as propulsion systems for controlling north and south orbits on the engineering test satellite ETS-VI, which will be launched in 1992. The ion engine is an electrostatic acceleration-type electric propulsion system characterized by high specific impulse. An ion engine with a 20 mN-class thrust is being developed so that it can be mounted on the ETS-VI. Xenon is used as the propellant in the ion engine. This paper outlines the project, describes the contents of component combination tests,

and presents the status of the development of the ion engine system [IES].

2. Function

Figure 1 shows a system block diagram of the IES, and Table 1 illustrates its comprehensive performance. The IES executes the following functions: 1) It receives the electric power supply from electric source systems, produces ions, and generates thrust by accelerating and injecting the ions. 2) It generates and stops thrust through the TTC system in accordance with the commands sent from the ground. 3) It outputs the data necessary for monitoring and diagnosing the operational status to the TTC system and instrumentation systems. 4) It controls the north and south orbits of satellites by means of the composite thrust generated by simultaneously operating two properly-positioned TRSs. 5) It can store the propellant necessary for controlling the north and south orbits. 6) It receives the electric power from the thermal control systems and controls the temperature of the respective components. It also outputs the temperature-related data necessary for this control.
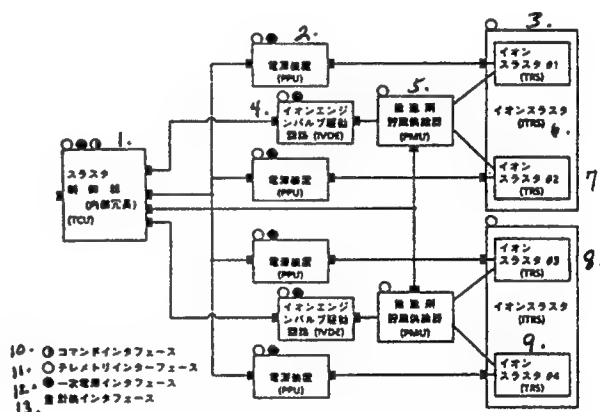
Figure 1. System Block Diagram

Key:
1. Thruster control unit (inside redundancy) (TCU)
2. Power source unit (PPU)
3. Ion thruster No 1 (TRS)
4. Ion engine valve driving circuit (IVDE)
5. Propellant storing and supplying unit (PMU)
6. Ion thruster (ITRS)
7. Ion thruster No 2 (TRS)
8. Ion thruster No 3 (TRS)
9. Ion thruster No 4 (TRS) 10. Command interface
11. Telemetry interface
12. Primary power source interface
13. Instrumentation interface

Table 1. Overall Performance

Item	Performance						
Thrust	(1) Ideal capability						
	(a) Nominal ideal thrust: 25mN (TRS simple substance)						
	(b) Ideal thrust variable range: 20 to 30 mN (TRS simple substance)						
	(2) Actual thrust: 93 percent or more of ideal thrust						
	(3) Thrust generating time: 3^{+2}_0 from start command						
	(4) Thrust (cant angle: 30°) for controlling north and south orbits: 25 mN, operation effect thrust: 40.3 mN						
Specific impulse	(1) Ideal thrust						
	(a) Ideal thrust: 20 mN or more and 23 mN or less: 2,640 sec or more (TRS substance)						
	(b) Ideal thrust: 23mN or more and 30 mN or less: 3,125 sec or more (TRS simple substance)						
)impulse							
)2,640 sec or more: 23 mN or more: 2,516 sec or more							
Simultaneous injection performance	IES possesses the following injection performances when two TRSs are injected simultaneously						
	(1) Time difference between two TRSs in respect to thrust generation: 2 sec or less						
	(2) Time difference between two TRSs in respect to stop of thrust: 2 sec or less						
Propellant storing capability	(1) Maximum storing capacity: 41.0 kg (stored separately in two PMU tanks)						
	(2) Mass of remaining propellant: 0.25 kg (two PMUs total)						
Weight	91.558 kg (current value)	Contents	ITRS	PMU	IVDE	PPU	TCU	
			11.332 x 2	9.795 x 2	1.562 x 2	9.74 x 4	7.22 x 1	
			22.664 kg	19.59 kg	3.124 kg	38.96 kg	7.22 kg	
Power consumption	1503.4 W current value (nominal value at 25 mN operation)	Contents	ITRS	PMU	IVDE	PPU	TCU	ITRS replacement heater
			624.5 W^{x2}	6 W^{x1}	2 W^{x2}	111.2 W^{x2}	8.0 W	(7+20) W^{x4}
			1249 W	6 W	4 W	222.4 W	8.0 W	14 W

3. Combination Test of Thruster, Electric Power Unit and Thruster Control Unit

A combination test was performed to confirm the conformity of an interface among such components as the thruster (TRS), electric power unit (PPU) and thruster control unit (TCU).

Transitional Performance

Figure 2 shows the telemetry data waveform of the transitional characterics from the input of the command "IES START" to the "Generation (Bon) of Thrust." As can be seen from this waveform, it has been confirmed that the PPU and TRS are controlled by a control logic incorporated in the TCU.

Stationary Performance

Table 2 shows comprehensive performances of the IES at its five kinds of operating modes.

Table 2. Overall Stationary Performance

Operation mode	Beam	Beam	Beam	Beam	Beam	Beam	Beam	Beam	IDLG	ACTV	NEUT	DISC
Thrust (mN)	25.4	25.3	30.2	30.1	23.2	23.3	20.2	20.2	N/A	N/A	N/A	N/A
VBUS (V)	50	47	50	47	50	47	50	47	47	47	31	47
Propellant-using effect (%)	80.6	80.4	80.6	80.4	80.9	81.1	70.6	70.5	N/A	N/A	N/A	N/A
Ion production cost (ev/ion)	258.9	258.2	241.0	241.8	271.7	270.5	236.6	237.3	N/A	N/A	N/A	N/A
Specific impulse (sec)	3156.0	3148.2	3229.2	3221.2	3172.5	3180.3	2768.5	2764.7	N/A	N/A	N/A	N/A
TRS power consumption (W)	624.4	621.7	741.6	740.5	578.8	579.5	492.0	494.0	9.2	48.5	11.4	109.4
TRS electric power effect (%)	77.9	78.0	79.9	79.9	77.1	77.2	78.9	78.5	N/A	N/A	N/A	N/A
TRS propulsion efficiency (W)	62.8	62.7	64.4	64.2	62.4	62.6	55.7	55.3	N/A	N/A	N/A	N/A
PPU power consumption (W)	723.5	720.3	839.6	864.3	668.2	670.2	564.9	568.7	25.9	88.9	25.6	149.7
PPU efficiency (%)	86.3	86.3	88.3	85.7	86.6	86.5	87.1	86.9	35.5	54.6	44.5	73.1

* The propellant-using efficiency, specific impulse and TRS propulsion efficiency include the flow rate of the neutralizer.

Vb

Ib

Ia

Vd

Id

Vck

Ick

Vch

Vnk

Ink

Vnh

Ippu

△ IES START △ Non △ Bon

△ CKon

△ Don

1 min
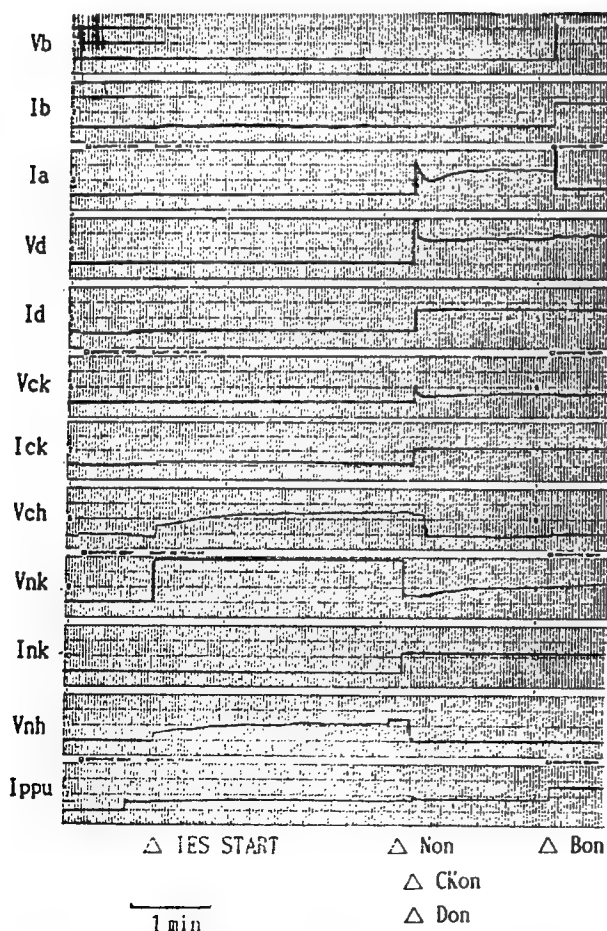
Figure 2. Transitional Characteristics

4. Conclusion

As a result of administering the combined test of the TRS, PPU and TCU, the conformity of the interface was confirmed. It has also been confirmed that both the transitional and stationary performances satisfied the IES specifications.

We have performed a solar cell and satellite thermal control material contamination test, in accordance with the thruster electrical discharge chamber wear materials, and are currently evaluating the results.

We plan to evaluate the following items by using an EM manufactured this fiscal year: I. Confirm all IES components (including PMU andIVDE) II. Prepare a detailed evaluation of electromagnetic adaptability.

References

1. Sato, et al., "Proceedings of the 31st Space Sciences and Technology Conference," No 3F11, 1987.

Development of Ion Thruster To Be Mounted on ETS-VI

[Article by Kenichi Kajiwara of the National Space Development Agency of Japan; Sadanori Shimada, Haruki Takegawara, Satoshi Ota and Shoji Goto of Mitsubishi Electric Corporation]

[Text] 1. Preface

The development of an ion thruster is currently being carried out. This ion thruster will be mounted on an

engineering test satellite, the ETS-VI, scheduled to be launched in 1992. Two prototype thrusters have been subjected to various tests since they were completed in November 1987, and are currently undergoing a long-term test. This report describes the results of various tests of the thruster.

2. Test Flow and Configuration

Figure 1 shows a flowchart of the tests administered to the two prototype thrusters, while Figure 2 shows the basic configuration for the testing.

3. Thermal Vacuum and Propulsion Performance Test

A thermal vacuum and propulsion performance test was conducted in a space chamber made by simulating space. The contents of this test involve low temperature/normal temperature ignition performance test, rated operation test and parameter changing test. It was confirmed in the ignition performance test that the thruster would satisfy the specification for injecting beams within 5 minutes of the start at both low temperatures (base plate temperature of -30 degrees C) and normal temperatures (20 degrees C). The rated operation test was conducted for the respective operating points of 25, 20, 23, and 30 mN. Table 1 shows the results of this test for an operating point of 25 mN. The parameter changing test extended
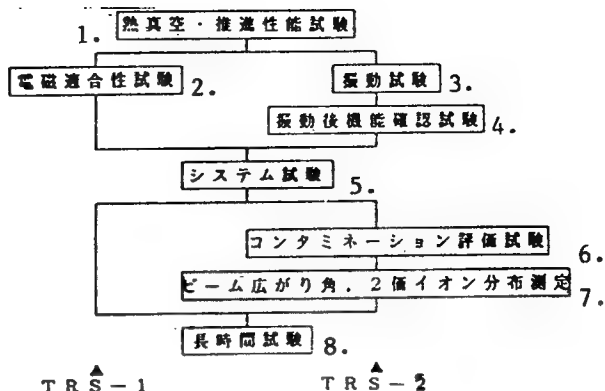
Figure 1. Test Flow

Key:
1. Thermal vacuum and propulsion performance test
2. Electromagnetic adaptability test
3. Vibration test
4. Function confirming test after vibration
5. System test 6. Contamination evaluation
7. Angle of divergence of beam, bivalent ion distribution and measurement
8. Long-term test
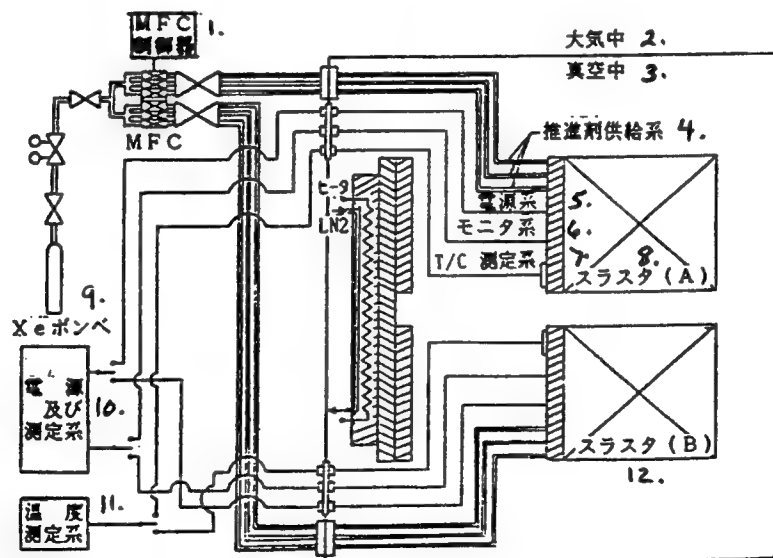
Figure 2. Test Configuration

Key:
1. MFC control unit
2. In atmosphere
3. In vacuum
4. Propellant supply system
5. Power source system
6. Monitor system
7. T/C measuring system
8. Thruster (A)
9. Xe cylinder
10. Power source and measuring system
11. Temperature measuring system
12. Thruster (B)

the propulsion characteristic data discharge current, beam voltage and flow rate over a wide range.

Table 1.
Result of Thermal Vacuum and Propulsion Performance Test

	TRS-1	TRS-2
Thrust (mN)	25.7	25.0
Propellant using efficiency*, %	82.6	80.6
Ion production cost, ev per ion	261.2	253.3
Specific impulse*, S	3231	3152
Power consumption, W	631.0	616.7
* Includes the flow rate of the neutralizer		

4. Electromagnetic Adaptability Test

The electric field radiation noises and magnetic field radiation noises emitted from the thruster proper were measured in the electromagnetic adaptability test. Figure 3 shows a test configuration. Electric field radiation noises outside those mentioned in the specifications were measured at 100 to 300 megahertz. This is caused by the switching noises of the power source and the motion of electronic cyclotrons in the thruster electric discharge chamber. However, it has been confirmed that these outside noises do not affect any satellite systems since different frequencies are used.
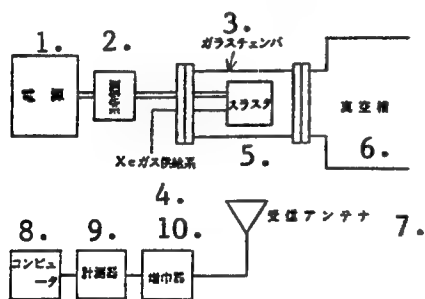
Figure 3. Electromagnetic Adaptability Test Configuration

Key:
1. Power source
2. Measuring system
3. Glass chamber
4. Xe gas supply system
5. Thruster
6. Vacuum tank
7. Receiving antenna
8. Computer
9. Measuring instrument
10. Amplifier

5. Vibration Test

A vibration test (vibration of sine waves and random vibrations) was conducted at the thruster simple substance level, but no problems were generated. Following this test, a thruster function confirmation test was performed, confirming that the thruster was operating normally.

6. Measurement of Beam Spread Angle and Distribution of Bivalent Ions

The beam spread angle and the distribution of bivalent ions were measured in cooperation with the NAL [National Aerospace Laboratory]. Figures 4 and 5 show the respective measurement results. The beam spread angle is about 10 degrees (95 percent of the total current) at an operating point of 25 mN, and the bivalent ion current is less than approximately 10 percent of the monovalent ion current.

7. Summary

(1) It was confirmed that the specified performance was satisfied at the thruster simple substance level. (2) Subjects for future study are as follows:

- Obtaining performance transition by conducting long-term test
- Measuring actual thrust.
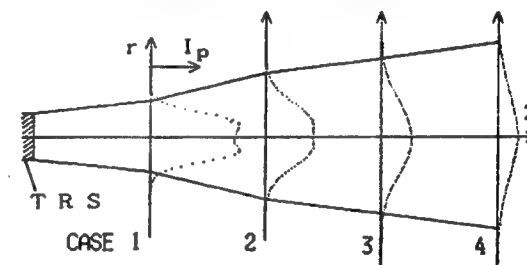
Figure 4. Results of Measuring Angle of Beam Divergence
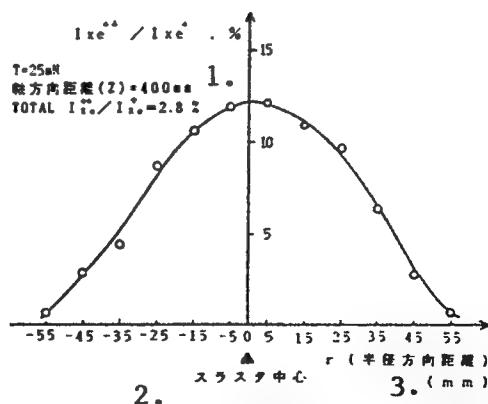
Figure 5. Results of Distributing and Measuring Bivalent Ions

Key:
1. Distance in axial direction (Z) = 400 mm
2. Center of thruster
3. r (distance in radial direction) (mm)

References

1. Kajiwara, et al., "Development of Ion Engine System Mounted on ETS-VI," Pre-proceedings of the 32nd Space Sciences and Technology Conference, 1988.

Trial Manufacturing, Testing of Electric Power Unit for Ion Engine Mounted on ETS-VI

[Article by Kenichi Kajiwara of the National Space Development Agency of Japan; Ryoji Osakabe, Norikazu Kitagawa, Yasuhiko Onuma, Aritsune Yamamoto, Yoshiaki Takeshita, and Fumihiro Ito of Komukai Works, Toshiba Corporation]

[Text] 1. Preface

An ion engine with 20 m-class thrust will be mounted on the engineering test satellite ETS-VI, and will be used to control the north and south orbits. The electric power unit (PPU) for this ion engine has a maximum total output of 787 watts and high voltage output of 1,200 volts. It is also a multi-output power unit with eight systems, and is the largest of the Japanese electric power units mounted on satellites. A model of this PPU has been manufactured on a trial basis, and subjected to electric performance and environmental tests, as well as to a combination test with the ion engine. This report describes the structure of this model and the contents of these tests.

2. Structure and Appearance

The PPU is one of the components constituting an ion engine system, is operated in accordance with the signals output from the thruster control unit [TCU], and supplies the necessary electric power to the thruster.

The power source output to the thruster consists of seven power source sections of eight systems. Figure 1 shows a block diagram of the PPU, and Photograph 1 [not reproduced] shows its exterior.

3. Design

(1) PS1/2 Section: The increase in efficiency of the PPU depends on the increase in efficiency of the beam/acceleration grid power source (PS1/2), which accounts for approximately 80 percent of the total output. The PPU can continuously input the current, and consists of a current resonance inverter and a boosting chopper
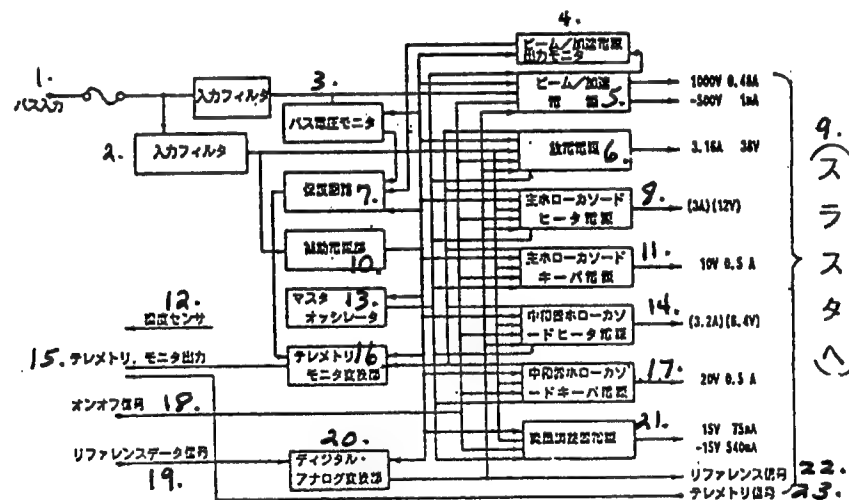
Figure 1. Block Diagram of Power Source Unit

Key:
1. Bus input
2. Input filter
3. Bus voltage monitor
4. Beam/acceleration power source output monitor
5. Beam/acceleration power source
6. Discharge power source
7. Protective circuit
8. Main hollow cathode heater power source
9. (To thruster)
10. Auxiliary power source section
11. Main hollow cathode key bar power source
12. Temperature sensor
13. Master oscillator
14. Neutralizer hollow cathode heater power source
15. Telemetry monitor output
16. Telemetry monitor conversion section
17. Neutralizer hollow cathode key bar power source
18. On-off signal
19. Reference data signal
20. Digital analog conversion section
21. Flow rate adjuster power source
22. Reference signal
23. Telemetry signal

regulator whose efficiency is essentially higher than that of other regulators. The PPU is also designed so that the transformer boosting ratio is lowered by a doubling rectification circuit, and factors generating corona discharge are reduced since the corona discharge shortens the life of the PPU. The inverter is designed so that high efficiency and high frequency can be obtained by eliminating the switching loss of the elements and by resonating the current with the doubling rectification section capacity by means of the transformer primary center and inductor, inserted into the direct current line. Also, the drive electric power is eliminated by adopting a current feedback drive according to the current transformer in the drive circuit.

(2) Control Section: A regulator IC (UC1525) possessing the following features is adopted in the control section, making the control section compact and lightweight. (a) It facilitates the stable driving of equipment, such as the PPU, with a wide load range since the output stage is shaped like a totem pole, i.e., it can carry out sink/source driving tasks. (b) It facilitates the synchronous operation

Table 1. Main Performance Specifications

1. 項 目	2. 比 元	3. ※ レベル	4. タイプ	5. 電 圧	6. 電 流
7. ビーム電源	PS1	N. L	DC	1000(V) 1200(Vmax)	0.6(A) 0.6(Amax)
9. 加速グリット電源	PS2	N. L	.DC	-500(V) -600(Vmax)	-5(mA) 5(mAmax)
4. 放電電源	PS3	N. L S. L	DC	45(V) 80(V)	4(A) 0.1(Amax)
10. 主ホローカソード ヒータ電源	PS4	L. L N. L S. L	DC	2.8(V) 12(V) 15(V)	1.4(A) 3(A) 3.5(A)
11. 主ホローカソード キーバ電源	PS5	N. L S. L	DC	15(V) 150(V)	0.5(A) 10(mA)
12. 中和器ホロー カソードヒータ電源	PS6	L. L N. L S. L	DC	2(V) 6.4(V) 10(V)	2(A) 3.2(A) 4.3(A)
13. 中和器ホロー カソードキーバ電源	PS7	N. L S. L	DC	30(V) 150(V)	0.5(A) 10(mA)
14. 流量調節器電源 (±15(V))	PS8	N. L	DC	15(V) -15(V)	0.2(A) 0.6(A)

Telemetry: Temperature 1, analog 12

Monitor signal: 5

Reference signal: Digital 8 bit

Dimension: 282 x 332 x 130 millimeters

Weight: 8.84 kilograms

Efficiency: 85 percent at the rated value, 25 mN

Key:
1. Item
2. Data
3. Level
4. Type
5. Voltage
6. Current
7. Beam power source
8. Acceleration grid power source
9. Discharge power source
10. Main hollow cathode heater power source
11. Main hollow cathode key bar power source
12. Neutralizer hollow cathode heater power source
13. Neutralizer hollow cathode key bar power source
14. Flow rate adjuster power source (+/-15 V)

of a number of power sources. The output varies from analog interfaces from a conventional TCU to digital interfaces. A hybrid IC has been adopted in the D/A converting circuit compactness and light weight. Table 1 shows the main performance specifications.

4. Trial Manufacturing and Testing

As a result of conducting the following electric performance tests and environmental tests, the adequacy of the electric and mounting designs has been confirmed. (1) Electric Performance Test: Problems with the efficiency of the PS1/2 were determined. The electric performances of the other power sources almost reached the target performances. (2) Thermal Vacuum Test: This was performed within the temperature range of from -20 to +55 degrees C. (3) Electromagnetic Adaptability Test: It was subjected to the PPU simple substance and the PPU-TRS, and data involving the evaluation of the electromagnetic adaptability was obtained. (4) Vibration Test: Sine wave vibration and random vibration tests were conducted when the low voltage section was turned on with an electric current. It had been judged, from the anticipated values, possible to actually mount the PPU on the ETS-VI, and it was confirmed that the volume ratio decreased by about 90 percent and the weight was reduced by approximately 0.5 kg from those of a model previously manufactured on a trial basis. (5) Combination Test: This was conducted for the TCU-PPU-dummy thruster, PPU-TRS, TCU-PPU and TCU-PPU-TRS. The functioning and performance were confirmed, as was the adaptability of the interface with the thruster. (6) Impact Test: Component dropping tests have been conducted in the past, but an impact test according to the dripping weight system shown in Figure 2 was conducted

Figure 2. Impact Test

Key:
1. Drop weight
2. Test piece
3. Impact test jig
4. MOS-1 vibration test jig
5. Vibration test jig (stand)

for partially trial-manufactured sections, including a converter-transformer of the PS1/2, which will be most critical against impact environments in the PPU.

5. Summary

As a result of conducting the combination test with the PPU simple substance, the adaptability of the interface with the TCU and the TRS was confirmed. We are currently manufacturing an engineering model based on the evaluation of the model manufactured on a trial basis.

Thermal Design of Two-Liquid-Type Apogee Propulsion System (LAPS)

143065012v Tokyo PROCEEDINGS OF THE 32ND SPACE SCIENCES & TECHNOLOGY CONFERENCE in Japanese 26-28 Oct 88 No 2H6 pp 512-513

[Article by Yoshihiro Hashimoto and Masumi Miyata of Ishikawajima-Harima Heavy Industries Co., Ltd.]

[Text] 1. Preface

The LAPS is being developed as an apogee propulsion system for the engineering test satellite ETS-VI, and is a subsystem consisting of an engine, a 50N-thruster, propellant tank, LAPS supporting body structure, etc. Each piece of LAPS equipment is subjected to very severe thermal environmental conditions, such as apogee engine combustion, solar beam irradiation, and heat sinking to space. For this reason, thermal control of the LAPS in environments with high and low temperatures is an important system theme. This report first confirms the conditions required for the thermal control of the LAPS, and then outlines the results of thermal analysis and describes thermal control methods satisfying these conditions.

2. Thermal Design Conditions

Figure 1 and Table 1 show the LAPS structure and indicate environments affecting the design conditions of the thermal control systems, respectively.
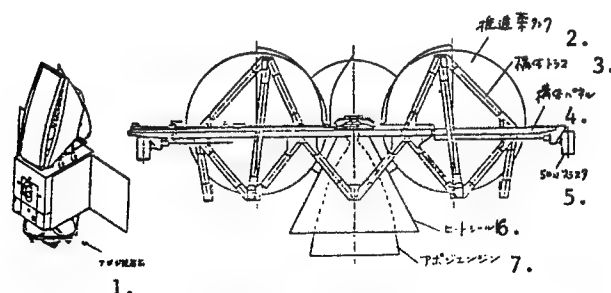
Figure 1. Sketch of Two-Liquid-Type Apogee Propulsion System

Key:
1. Apogee propulsion system
2. Propellant tank
3. Body structure truss
4. Body structure panel
5. 50N thruster
6. Heat shield
7. Apogeen engine

Table 1. Environmental Conditions in LAPS Operation Orbit

Item	Condition
Solar irradiation intensity (Is)	1,353 +/- 21 (w/m^2)
	Seasonal fluctuation: -3.25 to +3.4
Sink temperature (Ts)	0 (K)
Solar light irradiation angle	While coasting: 0°
	Before and after AEF: 32°

It is permissible to ignore the heat input from the albedo and earth infrared radiation during the LAPS operation (transfer) orbit since the solid angle of the earth, as viewed from the LAPS, is small.

3. Thermal Design

Thermal design according to the thermal control shown in Table 2 was carried out to maintain the respective component parts of the LAPS within their allowable temperature ranges. Tanks, pipes and valves are protected independently from heat with thermal brackets, and are equipped with heaters since they have narrow allowable temperature ranges and are used under thermally severe conditions. Carbon fiber-glass reinforced plastics [CRRP] are used in the body structure panel and truss to lighten them, and they are thermally controlled with thermal brackets and low-ε tapes in accordance with their allowable temperature ranges. Engine heat shields are used to restrain the heat input generated from the engines to the propellant tanks, body structures, etc. It is necessary to carry out the optimum design for the LAPS by taking the shape and characteristics into consideration because, when the thermal control effect of such engine heat shields is increased excessively, the amount of heat reflected to the engine proper will increase.

Table 2. Thermal Control Method

Equipment	Dominant Thermal Factor		Thermal Control Method
Propellant tank	High temperature side	Engine, thermal radiation of 50N thruster, solar light irradiation	Thermal blanket, Heat shield
	Low temperature side	Heat dissipation to space	Thermal blanket, heater (thermostat control)
Propellant piping	High temperature side	Engine, thermal radiation of 50N thruster, solar light irradiation	Thermal blanket, heat shield
	Low temperature side	Heat dissipation to space	Thermal blanket, heater (thermostat control)
Apogee engine, injector	High temperature side	Heat transfer from combustion gas	Cooling of film according to propellant, cooling according to propellant, Heat dissipation to space

Table 2.
Thermal Control Method (Continued)

Equipment	Dominant Thermal Factor		Thermal Control Method
	Low temperature side	Heat dissipation to space	Heater
Propellant valve	High temperature side	Heat conduction from engine	Cooling according to propellant during AEF, heat dissipation to space upon heat soak back
	Low temperature side	Heat dissipation to space	Heater (thermostat control)
Body structure panel (including engine support bracket)	High temperature side	Engine, thermal radiation and heat conduction of 50N thruster, solar light irradiation	Thermal blanket, heat shield, heat resistant blanket, thermal barrier
	Low temperature side	Heat dissipation to space	Thermal blanket
Body structure truss	High temperature side	Solar light irradiation	Low-ε tape

Table 2.
Thermal Control Method (Continued)

Equipment	Dominant Thermal Factor		Thermal Control Method
	Low temperature side	Heat dissipation to space	Low-ε tape

4. Thermal Analysis

(1) Thermo-Mathematical Model A thermo-mathematical model (278 node) was constructed subsequent to the interface between the satellite body structure and the LAPS body structure.
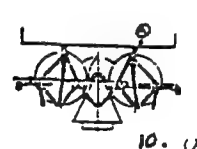
(2) Analytical Conditions The worst high temperature case and the worst low temperature case were analyzed thermally under the following conditions. Table 3 shows the analytical results. a. Worst high temperature case Under the conditions in which solar beams are incided from the direction of axis +X,

- Engine and thruster operation mode (stationary)
- Heat soak back after cessation of combustion (non-stationary)

b. Worst low temperature case

- Non-operation mode without any input of external heat (stationary and non-stationary)

Table 3. Analyzing Conditions

Key:
1. Item
2. Worst high temperature conditions
3. Worst low temperature conditions
4. Temperature in space
5. Temperature of satellite body structure
6. LAPS separation point A
7. Plume
8. Amount of heat input from outside
9. Solar light
10. (Incident angle: 0°)
11. (Solar eclipse)
12. Amount of propellant (N₂H₄NTO)
13. Electric power for heaters providing insulation (tank heater, valve heater, etc.)
14. (ON and OFF are controlled by thermostat
15. Injector, tank, propellant valve and piping temperature
16. Tank: 20°C or more (heater controlled)
17. 50N thruster
18. Blanket surface
19. Panel
20. Catalytic heater electric power

(3) Analytical Results Figure 2 shows an example of temperature changes in the injectors and propellant valves during the heat soak back. Figure 3 shows the amount of heat input from the LAPS to the satellite.

It has been confirmed through thermal analyses that the temperature of each LAPS equipment item remains within its allowable temperature range.

5. Summary

It has been confirmed that all the equipment constituting the LAPS, such as the apogee engine proper, etc., have been designed to satisfy thermally-required functions. In the future, we plan to improve the thermal design in the following ways: 1) lightening the thermal control parts, 2) decreasing the electric power of the heaters, 3) making an up-to-date model, 4) obtaining test data on a LAPS thermal development model, and 5) confirming thermal characteristic values.
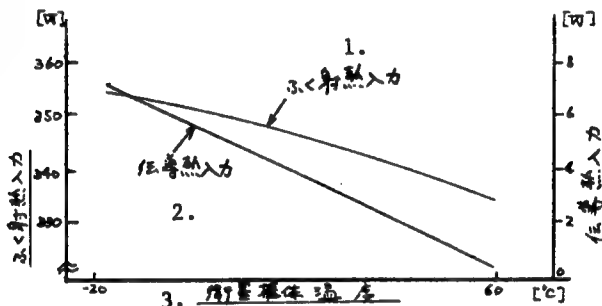
Figure 2. Amount of Thermal Input from LAPS to Satellite

Key:
1. Radiation heat input
2. Conducting thermal input
3. Temperature of body structure of satellite
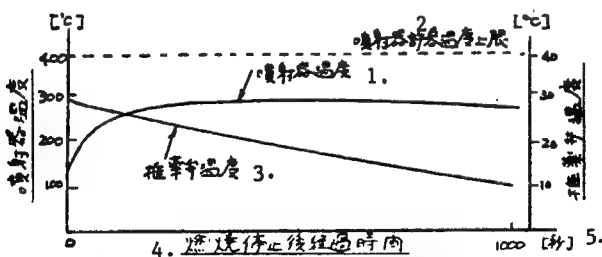
Figure 3. Change of Temperatures During Heat Soak Back

Key:
1. Temperature of injector
2. Upper limit of allowable temperature of injector
3. Temperature of propellant valve
4. Elapsing time after stop of combustion
5. Seconds

Outline of Engineering Test Satellite (ETS-V)

[Special Lecture by Hidetoshi Murayama of the National Space Development Agency of Japan]

[Text] 1. Preface

The ETS-V was launched by the three-stage H-I test rocket from the National Space Development Agency of Japan [NASDA]'s Tanegashima Space Center on 27 August 1987, and was released into geostationary orbit at the 150th degree of East longitude on 17 September. Subsequently, the satellite's initial stage functioning was confirmed, and it entered the stationary operation stage on 26 November. Data on the satellite bus was obtained, and an experiment involving mobile radio communications was conducted.

This lecture outlines the operational status and development of the ETS-V.

2. Development of the ETS-V

2.1 Purposes of Development

The ETS-V is a satellite developed to confirm the performance of the H-I test rocket (three-stage-type), establish the fundamental technology for three-axis satellite buses, accumulate the independent technologies necessary for next-generation application satellites, and to conduct experiments involving mobile radio communications for controlling aircraft on the sea, communicating with ships, providing navigation suppport, and for search and rescue purposes. In order to attain these goals, the main data shown in Table 1 was established, both the satellite bus and the experimental equipmented on the satellite were developed by using domestic technologies (although a portion of the components and parts was imported), the foundation of the technologies for designing and manufacturing the system and subsystem of geostationary three-axis satellite buses was formed, new technologies for data bus equipment, a non-stable power source bus, lightweight solar cell paddle, lightweight thrust cylinder, heat pipe, surface tension-type gas jet propulsion tank, solid apogee motor, etc., were developed in preparation for the development of a future satellite bus, and, in addition, the launching environmental measuring unit (LEM), technical data obtaining unit (TEDA) and thermal control demonstration equipment (CVT) were mounted on the ETS-V to obtain bus technology-related data.

**Table 1.
Data on Main System of ETS-V**

Item	Function and Performance
Shape, Dimensions	Rectangular prism: 1.4 x 1.7 x 1.7 (m) (body structure of satellite)
	Height, including antenna: 3.5 m

**Table 1.
Data on Main System of ETS-V (Continued)**

Item	Function and Performance
	Overall length in paddle direction after unfolding of paddle: 9.7 m
Weight	1,096 kg at satellite launching
	BOL: approx. 550 kg
Attitude retaining accuracy	Roll/pitch: within +/-0.072°
	Yaw: within +/- 0.40°
Orbit	Geostationary satellite orbit: 150°E
Orbit retaining accuracy	Within +/-0.1° in both east/west and north/south
Mission period	1.5 years
Reliability	0.953 (after 1.5 years, except for TEDA, LEM and AMEX)
Generation of electric power	Summer solstice after 1 year: 820 W
	EOL vernal equinox: 900 W

The experimental mobile radio communications equipment (AMEX) was mounted on the ETS-V to conduct experiments involving mobile radio communications. This is a newly-developed product.

2.2 Satellite System

As shown in Figure 1, the ETS-V proper has the shape of a box and its sides are equipped with solar cell paddles. When the satellite is launched, these solar cell paddles are folded and, after it is released into drift orbit, they are unfolded.

After the satellite becomes geostationary, it retains its attitude while turning the face (+ yaw axis) on which the antennas, earth sensor, etc., are installed in the direction of the earth, and that (pitch axis) on which the solar cell paddles are installed in the north and south directions.

Each equipment item is mounted on the platform in the center of the satellite, northern face panel, southern face panel, and antenna panel. Both the northern and southern panels are divided into mission panels and bus panels.

The ETS-V consists of a power source paddle system (EPS), attitude orbit control system (ACS), telemetry tracking and command system (TTC), gas jet system (RCS), body structure system (STR), thermal control system (TCS), apogee motor (ABM), instrumentation system (INT), and experimental equipment (AMEX, LEM, TEDA and CVT). Each system is outlined below.

2.2.1 Satellite Bus

(1) EPS The solar cell paddle is a semi-rigid-type light-weight structure in which a panel is made by attaching solar cells to the CFRP thin films, approximately 0.1 mm in thickness.
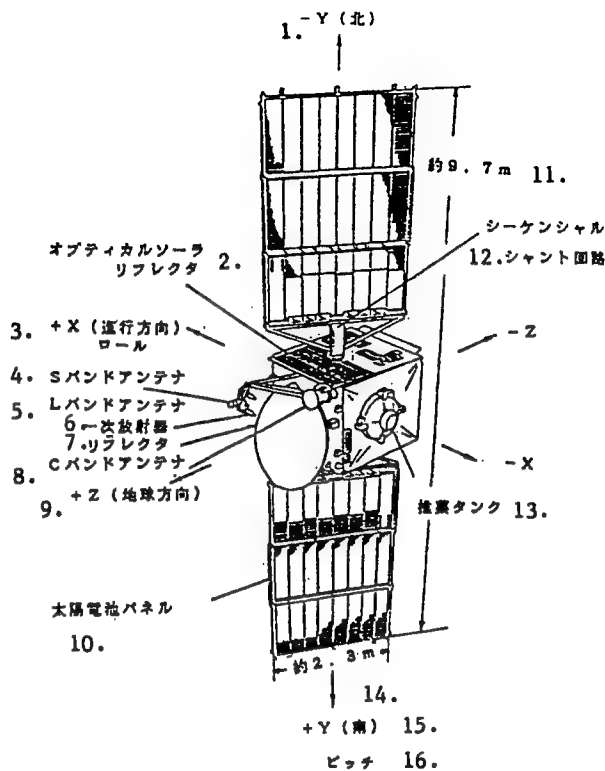
Figure 1. View of ETS-V

Key:
1. -Y (north)
2. Optical solar reflector
3. +X (progressive direction) roll
4. S-band antenna
5. L-band antenna
6. Primary radiator
7. Reflector
8. C-band antenna
9. +Z (earth direction)
10. Solar cell panel
11. Approx. 9.7 meters
12. Sequential shunt circuit
13. Propellant tank
14. Approx. 2.3 meters
15. +Y (south)
16. Pitch

Similarly to the MOS-1, two 13.5 AHs serve as batteries on the satellite.

The bus power source is a single bus, with the bus voltage in sunshine stabilized by means of a digital shunt system with small heating value. A non-stable power source bus system is adopted in large satellites because it is advantageous to lighten these satellites and to reduce the electric power loss in shade.

(2) ACS The attitude control electronic circuit (ACE), which serves as the pivot of the ACS, is an analog system.

The wheel consists of the main system and the sub-system. The main system is formed by combining a small momentum wheel (SMW), whose rotation axis is a + yaw axis, and a momentum (MW-A) whose rotation axis is inclined by +6.32 degrees from the - pitch axis in the pitch/yaw face. The subsystem is formed by MW-B, whose rotation axis is a - pitch axis.

An earth sensor is used to detect the roll and pitch attitudes and, when the orbit is controlled, a sun sensor, as well as the earth sensor, is used to detect yaw attitudes.

The satellite is stable in respect to spin during the transfer orbit. When the orbit is controlled, or during the period from the despin to the establishment of a three-axis attitude, the actuator operates with the ACS. The flywheel is used for stationary control. The pre-session control and orbit control are also carried out through the ACS. The ACS possesses a safety mode function.

(3) TTC The S-band (2.3/2.1 gigahertz) is used as the frequency between the satellite and NASDA tracking control site, while the C-band (5/6 gigahertz) is used as the frequency between the seashore of the organ in use and the aeronautic earth station. A data bus is adopted to process telemetry commands since it has general purpose properties and flexibility and can contribute to reducing the weight of the wires in large satellites. This data bus consists of a central unit and a remote-interface unit.

(4) RCS The thrust of the thruster for controlling the pre-session is 20 N, while that for controlling the three-axis attitudes and orbit is 1 N.

The tank storing hydrazine as a propellant is a surface-tension-type one. Unlike the bladder-type or diaphragm-type tanks, it has no movable sections (rubber-based film) and is appropriate for use in larger RCSs with long life.

(5) STR A thrust cylinder is installed on the center of the STR because a solid ABM is used in the STR. Therefore, the STR is structured like a box. Various equipment items are mounted on the antenna panels, north/south panels and platforms. These panels and platforms are sandwich-structured, with an Al skin and Al core, after taking thermal conductivity, etc., into consideration. The thrust cylinder, east/west access panel skin, panel supporting structure, RCS tank supporting structure, antenna tower, etc., are all made of CFRP to lighten them.

(6) TCS The TCS employs an active control system, using a heater and a heat pipe, together with a passive control system using an optical solar reflector (OSR), an insulator, a heat sink, etc.

The north/south panels to which the OSRs are attached are taken as the main heat exhausting faces, and other faces are covered with multi-layer insulators. The AMEX's high heat generator is mounted on the north panel, and heat is controlled efficiently with a heat pipe incorporated in the honeycomb panel.

(7) ABM The combustion speed is lowered by adding a high melting point explosive compound (HMX) to the terminal hydroxyl group polybutadiene (HTBM). This raises the specific impulse and lightens the insulation. Three-dimensional carbon/carbon materials are used in the nozzles to lighten them.

The specific impulse is 292.6 seconds, the total combustion time is approximately 57 secones and the maximum thrust is 4,000 kg-force or less.

(8) INT Wire harness, bracket, etc.

2.2.2 Experimental Equipment Mounted on ETS-V

(1) AMEX The frequency used among satellites, seashores and aeronautical earth stations is the C-band (5/6 gigahertz), while that used among moving objects, such as ships and aircraft, is the L-band (1.5/1.6 gigahertz).

The L-band is available in two kinds of beams. One is the north beam (beam center: 37 degrees N/161 degrees E), which irradiates the north Pacific area, including all of Japan, and the other is the south beam (beam center: 5 degrees N/137 degrees E), which irradiates the southwest Pacific area.

(2) LEM Six accelerometers are installed on a satellite, and the vibration, etc., generated from rockets is measured with the LEM.

(3) TEDA The TEDA consists of a solar cell paddle vibration monitor(PVM), radiation absorbed dose monitor (DOM), electrified potential monitor (POM), electrified discharge monitor (DIM), integrated circuit monitor (ICM), solar cell monitor (SCM), thermal control material deterioration monitor (TDM), and RAM software error measuring unit (RSM).

(4) CVT The CVT is used to obtain data on the thermal control capabilities of the panelsin which fixed/variable conductance heat pipes are incorporated, by using about half the area of the north mission panel.

2.3 Development Method and Schedule

The development of conventional satellites consists of three sequential steps, from EM to PM to FM, but that of the ETS-V consists of two steps, from EM to PFM. Prior to the development of the EM, the ACS, STR and TCS were manufactured on a trial basis and were tested. Technically uncertain matters were clarified during the development of the EM, and an efficient development method was adopted so that the schedule could be adopted smoothly and the cost reduced. In addition, the EM was subjected to a qualification level test and the PFM to a test of flight worthiness.

With regard to the development of the AMEX, the Electronic Navigation Research Institute [ENRI], Ministry of Transport, the Central Research Laboratory [CRL], Ministry of Posts and Telecommunications, and NASDA were in charge of the C-band equipment, L-band equipment and antenna equipment, overall assembly and installation of the AMEX on the satellite, respectively.

Table 2 shows the schedule followed for the above-mentioned development.

2.4 Problems Occurring During Development Process

Table 2. Development Schedule

Key:
1. Item	13. Mobile object communications experiment equipment
2. Fiscal year	14. Examination of basic design
3. 1982	15. Examination of detailed design
4. 1983	16. Examination before shipping, launching
5. 1984	17. Research and development
6. 1985	18. Basic design
7. 1986	19. Detailed design
8. 1987	20. Design
9. Milestone	21. Assembly proto-flight test
10. System design	22. Range completion work
11. Engineering model	23. Proto-flight model
12. Proto-flight model	24. For engineering and proto-flight models
	25. Transportation

The ETS-V is a 550-kg-class geostationary satellite produced for the first time in Japan. Certain problems, including some never before experienced, occurred during the design, manufacturing and test processes. Of these problems, we will describe the main ones which occurred subsequent to the system design and PFM system integration.

2.4.1 Main Problems in System Design

(1) Ensuring Stable Attitude of Satellite During ABM Operation

With the first design, it was impossible to ensure the stability of the satellite spin during ABM operation due to the small moment ratio of inertia and the influence of the sloshing of the RCS propellant.

The first design was modified to correct this problem. This involved 1) reducing the height of the body structure to 26 cm, 2) increasing the spin rate from 50 to 90 rpm, 3) moving the center of the RCS propellant tank closer to the satellite's center of gravity, and 4) changing the battery from 19 to 13.5 AH.

Also, the sloshing was analyzed by developing a pendulum model, and the stability was evaluated as a part of these measures.

(2) Response Acceleration in Excess of Design Specifications During Acoustic Test of Thermal Structure Model

The response acceleration of some of components exceeded the component design specifications (19.5 Grms) during an acoustic test of a thermal structure model.

It was confirmed that there were no problems with the bus equipment when random vibrations, exceeding the response acceleration, were applied to EM components. The vibration-proof mounting system and vibration-proof rubber mounted system were exchanged for AMEX components, while the vibration-proof rubber system was adopted for the PFM since this system experiences little change in resonance frequency.

(3) Analysis of ABM Plume

The following information was obtained during the detailed design state: The shape of the plume of the ABM used in foreign satellites is quite different from that used

as an interface condition for the ETS-V's ABM. In addition, it seems that the amount of heat rendered to a satellite by the STAR30B is considerably larger than the figure used in the ETS-V. (The size of the STAR30B is equivalent to that of the ABM mounted on the ETS-V.) After investigating and studying the plume analysis, it was determined that the plume circulation in the bottom of the satellite is given a low estimate and the convection heat is low because the boundary layer is not taken into consideration when analyzing the flowing area of the ABM nozzle in respect to plume characteristics, which have, in the past, been interface conditions.

This problem was clarified, but there was no room in the schedule for analysis preparation, waiting for the analysis, or moving toward determining a plume shield design, etc. Accordingly, it was decided that sufficient margin had been allowed in the design.

The preparation of a new method for analysis was abandoned and an existing foreign program was purchased since, eventually, both time and technical background would have proven to be insufficient.

However, there is no data that is backed by actual measurements of such parameters as thickness of the boundary layer in the nozzle, alumina particle size distribution, etc. Accordingly, when this program was used for the analysis, it was confirmed through changing the respective values of some of these parameters, combining them, analyzing the combined value and using the satellite heating volume covering each case that the design of the plume shields, etc., would not experience any problems.

2.4.2 Main Problems Subsequent to PFM System Integration

The main problems occurring subsequent to the PFM system integration are as follows: (1) Short in power transistor for remote interface unit (2) Inability to start momentum wheel (3) Breakage of wire-wound resistor for battery heater, replacement of same kind of wire-wound resistor with new one (4) Abnormal output of LEM sensor (5) Replacement of same kind of power source section's power transistor, which had experienced short in CS-3 (6) Frequency shift of L-band beacon (7) Decrease in gain of L-band high electric power amplifying section

As a result of these problems, all components were removed from the satellite, repaired and tested.

However, problems (2) to (6) were generated at almost the same intervals during the latter half of the system's proto-flight test, and large-scale work was carried out to cope with them, i.e., 13 components were removed from the ETS-V. Therefore, the satellite launching data was unavoidably postponed for 20 days.

3. Operation of ETS-V

3.1 Operation at Launching and During Initial Stage

The ETS-V (Kiku-5) was launched by a test rocket, the H-I (three-stage) from Tanegashima Space Center at 18:20:0, 27 August 1987, was separated from the third stage rocket at 18:47:34 of the same day, and was released into the transfer orbit.

Subsequently, the attitude was changed in preparation for the operation of the ABM, and the ABM began operating upon reaching the seventh apogee at 14:50:02, 30 August. The combustion in the ABM was normal, and the ETS-V was injected into almost the perfectly specified drift orbit.

However, the temperature was lowered by despinning the satellite, unfolding the paddle and acquiring the solar rays earlier than expected, due to an increase in the temperature inside the satellite which was caused by the generation of a phenomenon whereby the ABM case temperature exceeded the temperature of the interface with the satellite proper and, in addition, the cooling speed was slower than expected. After the satellite passed through a radio interference area with the broadcasting satellite BS-2b, the acquisition of the three-axis attitude was initiated at the point where the sun was acquired (the negative roll axis points in the direction of the sun), and the three-axis attitude was established at 5:59, 3 September. Subsequently, geostationary orbit was controlled and the ETS-V was injected into this orbit at the 150th degree of east longitude on 17 September.

For reference, Figure 2 shows the sequence of events of the satellite, from its launch until it reaches geostationary status.

Bus equipment of the ETS-V was subjected to initial function confirmation tests during two periods—from 3 September to 4 October and from 28 October to 11 November. The AMEX and C-band TTC of the ETS-V were also subjected to such tests from 5 October to 27 October. The ETS-V was moved to stationary status on 26 November because the tests had confirmed that the bus equipment, AMEX and C-band TTC were all operating normally.

The ENRI and CRL operated the AMEX on a trial basis at this stage in order to obtain data on the inspections that had been conducted by a radio station in advance and to check the overall experiment system.

Also, after the satellite was launched, an ecliptic period passed for the first time for 47 days, from 31 August to 16 October, but the satellite was maintained normally during the period by charging and discharging its batteries.

The orbit was retained and controlled during this period five times east and west and once north and south.

It was also confirmed from data obtained by using the LEM that the acceleration (static state + vibration) imposed on the satellite launched at the center was within the range of design conditions of the body structure, and the data on paddle vibration was almost as
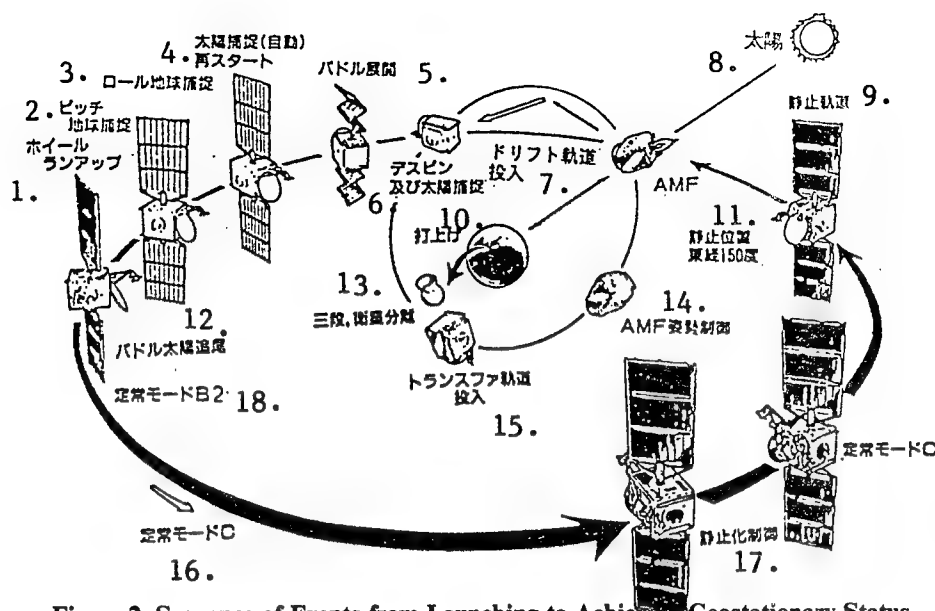
Figure 2. Sequence of Events from Launching to Achieving Geostationary Status

Key:
1. Wheel run-up
2. Pitch earth acquisition
3. Roll earth acquisition
4. Re-start of automatic solar acquisition
5. Unfolding of paddle
6. Despin and solar acquisition
7. Injection into drift orbit
8. Sun
9. Geostationary orbit
10. Launching
11. Geostationary position, 150°E longitude
12. Paddle solar tracking
13. Three-stage, separation of satellite
14. AMF attitude control
15. Injection into transfer orbit
16. Stationary mode C
17. Geostationary control
18. Stationary mode B2

expected. This paddle vibration was measured when the paddle was unfolded with the TEDA-PVM and when the orbit was controlled.

3.2 Operation During Stationary Stage

The following operations were carried out during the stationary stage moved to on 26 November 1987.

Problems with the command decoding and output control section of the RIU-1's A system occurred on 1 December of the same year, but since then, the ETS-V has operated continuously without any problems by switching the RIU-1's A system to its B system.

3.2.1 Maintenance of Satellite Status, and Control and Operation of Satellite

The status of the satellite was monitored at all times, distance measurement data was obtained once a week, and the orbit was controlled (15 times east and west and 6 times north and south during the period subsequent to movement to the stationary stage, up to 23 August).

Prior to the ecliptic periods of the vernal and autumnal equinoxes, batteries were conditioned, so the satellite

was operated during those periods. In addition, immediately following the operation of the ABM, the battery temperature increased critically. However, a deterioration of the battery characteristics was not confirmed.

3.2.2 Operation for Obtaining Data on Future Development of Satellite Bus Equipment

(1) Bus Equipment Subsystem Data is necessary in order for the trends of the TTC, EPS, etc., characteristics to be evaluated, and it is obtained approximately twice a year.

(2) ACS Data necessary for designing and evaluating the ACS is obtained by conducting experiments to estimate the natural disturbance and changes in control system parameters.

(3) CVT/TCS Data on the temperatures of each section of the satellite are obtained by each operational mode of the heater constituting the CVT at the vernal/autumnal equinoxes and the summer/winter solstices in order to evaluate the performance of the thermal control system using heat pipes.

(4) TEDA Data on DOM, POM, DIM, and RSM are obtained constantly, those on SCM and ICM are

obtained once a week, and those on TDM are obtained at the vernal/autumnal equinoxes and summer/winter solstices, respectively.

(5) Experiment on Communications of Mobile Objects
An experiment on the communications of mobile objects is being conducted for the first time in Japan by using the satellite.

This is being conducted mainly the the ENRI and CRL, and Nippon Telegraph and Telephone Corporation [NTT] and Kokusai Denshin Denwa Co., Ltd. [KDD] participated in the experiment.

The mobile objects are as follows: 1) a Japan Air Lines Co., Ltd. [JAL] B-747 (ENRI/CRL), 2) ENRI B-99, 3) Hokkaido University's training ship, the "Oshoro-Maru," (CRL), 4) NTT's cable ship, the "Tsugaru-Maru," 5) Tokai University's training ship, the "Tokaidai-Maru II Generation," (KDD), 6) various vehicle mounting stations (CRL/NTT), 7) portable message communications equipment, etc.

The CRL Kashima Station, in which ENRI and KDD terminal station equipment is also installed, and NTT's Nobi Station are used as coast/aeronautical earth stations.

In addition, AUSSAT Co., Ltd. in Australia is conducting an experiment in collaboration with the CRL.

4. Postface

Judging from the operational results from the launching to the current status, it is believed that the developmental purpose of the ETS-V has almost been attained by establishing the basic technologies for a geostationary three-axis satellite bus, and technical results have been obtained from experiments involving the communications of mobile objects.

From now on, we intend to continue to collect data involving the development of future satellite buses and to cooperatively carry out operations and experiments involving the communications of mobile objects.

References

1. Anzai and Yamada, "Status of Operation and Development of ETS-V," Fourth NASDA Technical Result Study Meeting Pre-Journal, 9 June 1988.

Development of ETS-V Body Structure System, Evaluation of Flight Data

[Article by Hidehiko Mitsuma and Hidehiko Katagi of the National Space Development Agency of Japan; Koitaro Kasai and Kazumi Hirose of Mitsubishi Electric Corporation]

[Text] 1. Preface

The structural system of the body of the ETS-V was developed as a 550-kg-class three-axis satellite bus body structure by using independent technologies. This development was carried out in the following three stages: 1) trial manufacturing and testing model, 2) static load model [SLM] and thermal structural model [STM], and 3) proto-flight modle [PFM]. Finally, the environment of acceleration during flight was monitored. This paper presents the development of the structural system of the body and the results of data evaluating the acceleration obtained during the flight.

2. Development of Body Structural System

(1) Trial-Manufactured Test Model The specified environmental tests, such as the static load test and sine wave vibration test, were conducted in order to collect the basic data necessary for the design work. The results obtained from these tests were fully utilized to determine the design conditions for each section of the body structure.

(2) SLM and STM The main design conditions are shown in Table 1.

Table 1. Design Conditions

Key:
1. Name of member
2. Design conditions
3. Upper cylinder
4. Lower cone
5. The following items are quasi-static acceleration conditions (limit load conditions) stipulated by rocket interface conditions. Materials shall not be yielded. The ultimate loading condition is found by multiplying the safety factor, 1.5, by the above conditions. Also, the materials should neither break nor buckle.
6. Axis (G)
7. Axis verticality (G)
8. Panel assembly
9. Panel supporting member
10. RCS supporting structure
11. Materials should neither break nor buckle against any 20G axis.

It has been confirmed that the SLM has the specified strength against the quasi-static accleration load conditions stipulated by rocket interface conditions. Sine wave vibration tests were conducted with the STM based on the rocket interface conditions. The results confirmed that the STM had the specified strength in vibration environments.

(3) PFM The design and workmanship have been confirmed by a proto-flight test [PFT], with no problems verified during the flight.

3. Data on Flight Acceleration Environments

The ETS-V is equipped with six launching environment measuring units [LEM]s, and flight data was evaluated in accordance with the analysis flow shown in Figure 1 based on the data obtained from the six LEMs.

Results are as follows:

(1) Acceleration Environment Conditions of Each Section of ETS-V Table 2 shows the flight response data generated during the main flight events. It has been confirmed that the data values were smaller than those of the design conditions for each section of the body structure shown in Table 1.
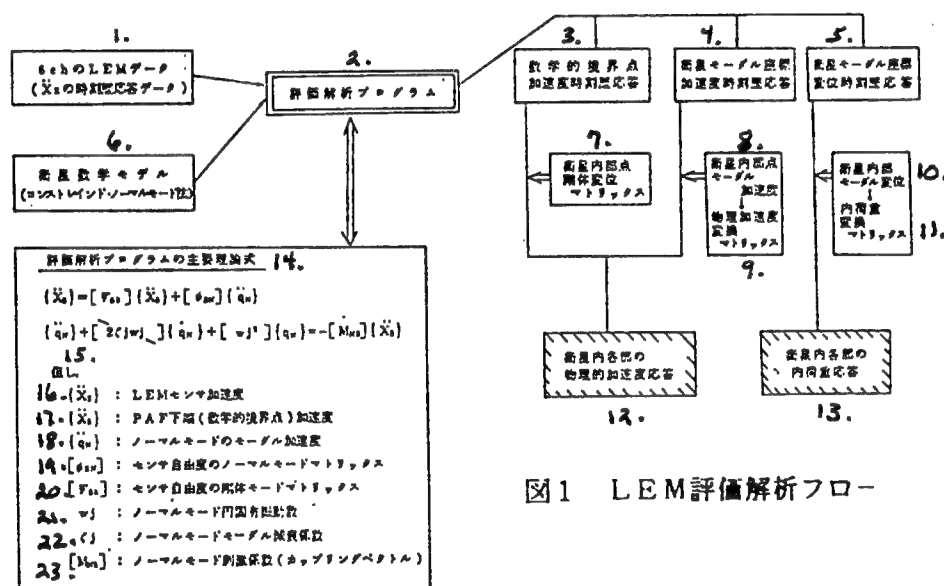
Figure 1. LEM Evaluation and Analysis Flow

Key:
1. Data on 6 ch LEM (data on time history response of Xs)
2. Evaluation and analysis program
3. Mathematical boundary point acceleration time history response
4. Satellite modal coordinate system acceleration time history response
5. Satellite modal coordinate system displacement time history response
6. Satellite mathematical model (constrained normal mode method)
7. Satellite internal point rigid body displacement matrix
8. Satellite internal point modal acceleration
9. Physical acceleration transformation matrix
10. Satellite internal modal displacement
11. Internal load displacement matrix
12. Physical acceleration response of each section in satellite
13. Internal load response of each section in satellite
14. Main theoretical formula for evaluation and analysis program
15. Where, 16. LEM sensor acceleration
17. PAF lower end (mathematical boundary point) acceleration
18. Modal acceleration of normal mode
19. Normal mode matrix of sensor degree of freedom
20. Rigid mode matrix of sensor degree of freedom
21. Normal mode circle characteristic frequency
22. Normal mode modal attenuation coefficient
23. Normal mode stimulation coefficient (coupling vector)

Table 2.
Environment Conditions at Main Points During Flight Acceleration

Main point of satellite	Lift-off		MECO/POGO	
	Axial Direction	Axial vertical direction	Axial direction	Axial vertical direction
Upper end of upper cylinder	1.98G	0.82G	5.47G	0.52G
Center of ABM	2.00G	0.38G	5.49G	0.30G
Center of separation face	1.98G	0.42G	5.49G	0.27G

However, the static acceleration compounds 1.06G and 4.01 G are included in the lift-off and MECO/POGO.

(2) Evaluation of Sine Wave Vibration Test The acceleration time history responses of the excitation control position during the sine wave vibration test were found from the data on the LEM. The SRS was analyzed on the basis of the acceleration time history response values, and the maximum response was found by adding the transient vibration to be evaluated to a spring with a degree of freedom system and an arbitrary resonant frequency. Figure 2 and Table 3 show the results of finding a sine wave vibration level (equivalent sine wave vibration conditions) that gives a resonant response equal to the maximum response obtained to the spring with a degree of freedom system. Table 4 shows the sine
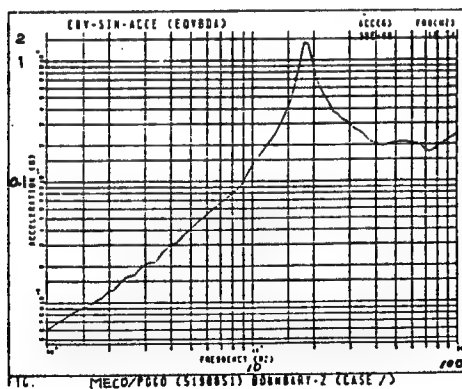
Figure 2. Axial Direction (Z Direction) at MECO/POGO. PAF lower end equivalent sine wave vibration conditions.

wave vibration conditions stipulated by the rocket interface conditions. It has been confirmed that the sine wave vibration conditions were lower than the rocket interface conditions. However, factor Q is supposed to be 10.

Table 3.
Maximum Value of Equivalent Sine Wave Vibration Conditions

Axis/Flight Event	At launching (lift-off)	Pre-MECO/POGO	At POGO
Axial vertical direction (X-direction)—Maximum value of PAF lower end equivalent sine wave vibration	0.33G (14.2 Hz)	0.06G (23.7 Hz)	0.23G (17.9 Hz)
Axial direction (Z-direction)—Maximum value of PAF lower end equivalent sine wve vibration	0.38G (22.6 Hz)	0.70G (23.7 Hz)	1.38G (18.7 Hz)

Table 4.
Rocket Interface Sine Wave Vibration Test Conditions (AT)

Axis	Frequency (Hz)	Level (Go-p)	Sweep rate (Oct/min)
Axial vertical direction	5-100	0.7	4
Axial direction	5-6.2	12.7 mmDA	4
	6.2-15	1.0	
	15-21	4.0	
	21-100	1.0	

(PFT level is AT level x 1.5)

(3) Comparison and Evaluation of Satellite/Rocket Flexible Combination Analysis Results Flexible combination analyses were carried out for the main flight events on the rocket side based on the 2σ high level forcing fucntion during flight. Taking this fact into consideration, it appears that the results of evaluating and analyzing the LEM are comparable to those of flexibly combining and analyzing the LEM. Table 5 shows the results of comparing the vibration components at the MECO/POGO.

Table 5 (1/2).
Comparison of Axial Directions

Main point of satellite	LEM Evaluation Analysis	Flexible Combination Analysis
	Z-direction	Z-direction
Upper end of upper cylinder	1.46G	3.78G
Center of ABM	1.48G	3.99G
Center of separation face	1.48G	3.68G

Table 5 (2/2).
Comparison of Axial Vertical Directions

Main point of satellite	LEM Evaluation Analysis		Flexible Combination Analysis	
	X-direction	Y-direction	X-direction	Y-direction
Upper end of upper cylinder	0.49G	0.52G	1.62G	1.58G
Center of ABM	0.24G	0.30G	0.95G	0.90G
Center of separation face	0.27G	0.07G	0.18G	0.15G

4. Postface

The values mentioned in the flight data obtained were lower than those stipulated by the design conditions, and the validity of the design conditions has been confirmed.

Operation, Development of Apogee Motor for ETS-V

43065012y Tokyo PROCEEDINGS OF THE 32ND SPACE SCIENCES & TECHNOLOGY CONFERENCE in Japanese 26-28 Oct 88 No 3A11 pp 562-563

[Article by Teruo Yofue, Yukio Hyodo and Hidehiko Katagi of the National Space Development Agency of Japan; Junichi Oda and Satoshi Hirano of Nissan Motor Co., Ltd.]

[Text] 1. Preface

The research and development of an apogee motor was started in fiscal 1979, the operation of the apogee motor for the ETS-V was begun on 30 August 1987, and the satellite was injected into the specified orbit. The following is an outline of the results of the operation and development of the apogee motor developed domestically for the first time.

2. Main Data

Table 1 shows the main data for the ETS-V apogee motor, and Figure 1 shows an outline of this motor.

Table 1. Main Data

Gross mass (full load)	544.4 kg
Mass of propellant	504.3 kg
Mass ratio	0.926
Maximum anticipated working pressure	46.5 kgf/cm^{2}a
Maximum thrust (20°C)	3060 kgf
Maximum pressure (20°C)	41.6 kgf/cm^{2}a
Total combustion time (20°C)	54 sec
Specific impulse (20°C)	293.6 kgf.s/kg

3. Outline of Development

The apogee motor was first developed for a 350-kg-class geostationary satellite, but the satellite was changed to the 550-kg-class ETS-V in fiscal 1983. Accordingly, the apogee motor became larger, and its performance was increased by changing its system from a conventional forward ignition system to a backward ignition system. The following new technologies were adopted in the apogee motor in accordance with this change: 1) head-end-wave-type grain design, 2) propellant pressurizing

Figure 1. Sketch of Apogee Motor for ETS-V

Key:
1. Motor case (Ti-6Al-4V)
2. HTPB propellant with HMX (head end wave grain design)
3. EPDM insulation backward igniter
4. Sphere φ745
5. C/C nozzle for backward ignition

Figure 2. Development Schedule

Key:
1. Development phase
2. Fiscal year
3. 1979
4. 1980
5. 1981
6. 1982 7. 1983
8. 1984
9. 1985
10. 1986
11. 1987
12. Milestone
13. Launching of ETS-V
14. Development of 350-kg-class apogee motor (component equipment); development of apogee motor for ETS-V (up to PM); qualification test of apogee motor for ETS-V
15. Thick-walled motor

Table 2.
High Air Combustion Test Results and Flight Results

Item/Motor	PM#1	PM#2	QM#1	QM#2	QM#3 (LAT)	Flight Motor	
						Actual Measurement	Anticipated
Test Date	86/6/19	86/7/30	86/10/30	86/11/26	86/12/18	87/8/30	
Mass of propellant (kg)	454.6	504.3	454.2	504.5	504.8	504.9	
Temperature of propellant (°C)	38.0	2.5	38.0	3.5	22.0	26.0	
Maximum thrust (kgf)	3187	3041	3134	2943	3016	3020	2980
Maximum internal pressure (kgf/cm^{2}a)	44.5	41.0	44.1	40.4	41.0	42.3	40.3
Total combustion time (s)	46.8	55.5	46.9	56.2	55.7	55.2	55.8
Specific impulse (kgf.s/kg)	294.2	293.0	293.4	292.0	292.2	293.7	292.8
Ignition delay time (ms)	65	42	64	42	46	-	-
Environmental test*	H	C, VS	H, C	C, VS	-	-	-

* H: high temperature test; C: Temperature cycle test; VS: Nozzle vibration and impact test

and hardening method, and 3) backward igniter. The development of a propellant with HMX was initiated in fiscal 1984, and the propellant was adopted in a proto-type motor [PM]. On the other hand, the reliability was increased and a CT inspection unit was introduced into a C/C nozzle. During this period, we conducted research on the following items in collaboration with the NAL [National Aerospace Laboratory], and have carried out the development of the backward ignition system, etc., smoothly with the NAL's technical support: 1) experimental research on the standard, as well as an evaluation of the reliability of, the upper stage solid rocket motor, and 2) research on the rise in performance of the apogee motor. Figure 2 shows a development schedule, and Table 2 shows results of combustion tests conducted subsequent to those of the PM.

4. Results of Operation

After the separation from the satellite, the apogee motor flew in a transfer orbit for approximately 68 hours, beginning 14:50:02 on 30 August 1987 (JST), its ignition was started upon reaching the seventh apogee, and its combustion was carried out normally, on schedule, for about 55 seconds. We successfully injected the satellite into the specified drift orbit. The increase in speed of the apogee motor was 1,793 meters/second, which was an increase of approximately 7.3 meters/second over that expected before the satellite was launched. The specific impulse of the propellant was 293.7 kg-force second/kg. Table 2 shows the combustion performance of the apogee motor.

The combustion in the apogee motor was normal. With regard to the temperature following combustion, 1) the

motor case surface temperature reached 385 degrees C, which exceeded the specified temperature of 300 degrees C, 2) the cooling speed was lower than expected, and 3) the rise in temperature of the nozzle was delayed, and the maximum temperature of the nozzle was lower than expected. Figure 3 shows this status. As a result of studying this phenomenon, it was clarified that it was caused by the following: (1) The convection cooling amount had been estimated based on the gas flow in the low pressure chamber during a high air combustion test. The radiant cooling amount from the nozzle was overestimated because the convection cooling amount was smaller than the actual one. As a result, the difference between the rise in temperature of the motor case up to the highest temperature and the cooling speed was generated by this overestimate. (2) A value was estimated based on the data obtained under a low pressure state because no value had been measured with respect to the thermal conductivity in the vacuum of the carbon felt used in the nozzle. This value was smaller than the actual one, and caused the delay in the rise of the nozzle temperature and the lowness of the highest temperature.

5. Summary

Although problems occurred in estimating temperatures, the apogee motor, produced domestically for the first time, displayed the specified performance and we were able to obtain actual flight results. Such an apogee motor will be used in our third broadcasting satellite, and we will make efforts to further increase the degree of completion based on the results obtained from the development of the apogee motor for the ETS-V.
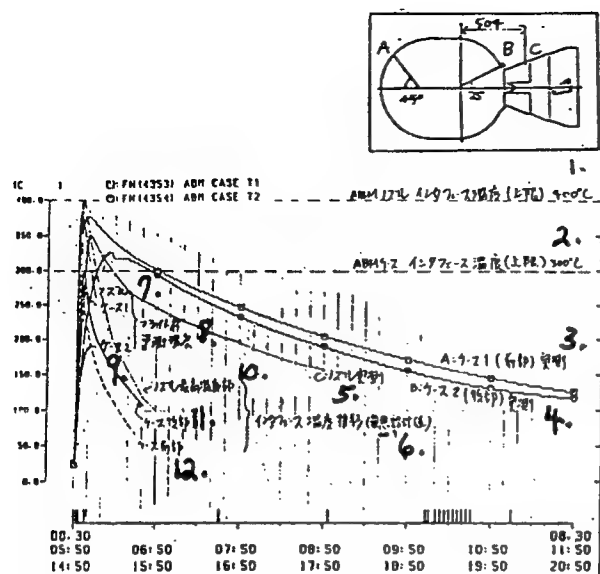
Figure 3. Temperature of Surface of Apogee Motor
Key:
1. ABM nozzle interface temperature
   (upper limit) 400°C
2. ABM case interface temperature (upper limit) 300°C
3. A case 1 (front section) actual measurement
4. B case 2 (rear section) actual measurement
5. C nozzle actual measurement
6. Transfer of interface temperatures
   (worst design values)
7. Nozzle case 1
8. Anticipated temperature before flight
9. Case 2
10. Nozzle highest temperature
11. Rear section of case
12. Front section of case

Tracking Control Operation of ETS-V

43065012z Tokyo PROCEEDINGS OF THE 32ND SPACE SCIENCES & TECHNOLOGY CONFERENCE in Japanese 26-28 Oct 88 No 3A14 pp 568-569

[Article by Takao Anzai, Ranpo Sato, Susumu Wakaba-yashi, Hirohiko Dojyo and Shoji Tsunematsu of the National Space Development Agency of Japan]

[Text] 1. Preface

The ETS-V has been used to conduct experiments on mobile radio communications, etc., since it was launched on 27 August 1987, its initial functioning was confirmed and it was moved to the stationary stage on 26 November 1987. The tracking control and operation of satellite have been carried out smoothly, and the status of these satellites is fairly good, except for some of the equipment of the telemetry tracking and command [TTC] system.

2. Tracking Control System

Figure 1 shows the tracking control system of the ETS-V at the stationary stage.

In general, the Tracking and Control Center of the National Space Development Agency of Japan [NASDA] operates, maintains and controls the satellites, retains and controls their orbits, and conducts experiments on the bus systems in order to evaluate and analyze the performance, etc., of the ETS-V. In the same way, the Kashima Earth Station of the Communications Research Laboratory [CRL], Ministry of Posts and Telecommunications, carried out most of the operations related to the experiments involving mobile radio communications. Both come into close contact during their respective operational plan stages, and carry out their operations in cooperation with each other.

3. Tracking Control Operation

The following operations are carried out to obtain the status of the satellites and to maintain the functions and performance of these satellites: (1) Stationary monitoring of the satellite status, 2) Obtaining data on ranges, (3) Retaining and controlling orbit, (4) Correcting pointing direction of solar cell paddles, (5) Reconditioning batteries, (6) Eclipse operation and (7) Others.

The satellite has been retained within a range of 150 +/- 0.1°E in the east-west direction and 0 +/- 0.1° in the north-south direction since it became geostationary on 17 September 1987. The east-west and north-south directions are controlled at a cycle of once approximately every three weeks and once approximately seven days, on the average, respectively. Table 1 shows some of the results obtained involving orbit control. The amount of fuel remaining, as of 15 August 1988, was approximately 51 kg, and it is anticipated that it will be possible to retain the orbit for another three years, even if the past orbital control is continued.

Table 1.
Summary of Results of Controlling Orbit of ETS-V

Control No	Execution Date	Increase in Speed	Injection Time	Anticipated Fuel Consumption	Residual Fuel (Tank Pressure Method)	Remarks
Geostationary	17 Sep 1987	0.11 m/s	173 pulses*	0.036 kg	66.891 kg	* Injection of 0.2 seconds during 4-second cycle
No 18EW	21 Jun 1988	-0.04 m/s	60 pulses*	0.014 kg	54.780 kg	
No 7NS	15 Aug 1988	-8.58 m/s	3,328 sec	2.241 kg	51.270 kg	Continuous injection
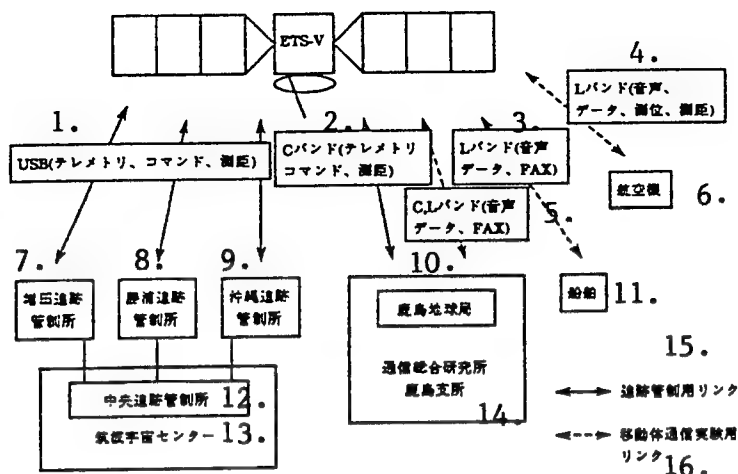
Figure 1. Tracking Control System of ETS-V

Key:
1. USB (telemetry, command and measurement of range)
2. C-band (telemetry, command and measurement of range)
3. L-band (voice, data and FAX)
4. L-band (voice, data, measurement of position and measurement of range)
5. C- and L-bands (voice, data and FAX)
6. Aircraft
7. Masuda Tracking Control Center
8. Katsuura Tracking Control Center

9. Okinawa Tracking Control Center
10. Kashima Earth Station
11. Ship
12. Central Tracking Control Center
13. Tsukuba Space Center
14. CRL's Kashima Branch 15. Tracking control link
16. Link for experiments involving mobile radio communications
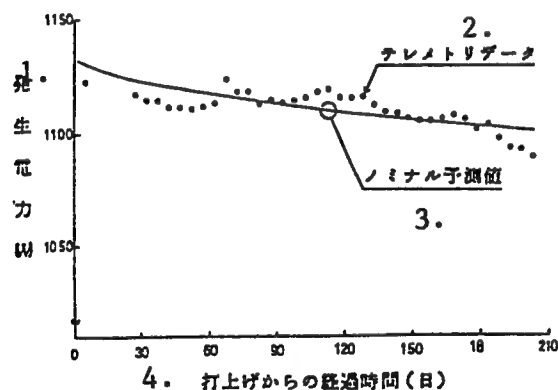
Figure 2. Electric Power Generated from Solar Cell Paddle

Key:
1. Generated electric power (W)
2. Telemetry data
3. Nominally anticipated value
4. Elapsed time from launch (days)

Figure 2 shows the telemetry data and anticipated values of the electric power generated from the solar cell paddles for approximately seven months following the launching of the

satellite. The rate of decrease in the electric power generated during this period is about 3 percent (30 watts).

Battery conditioning and eclipse operations have been carried out normally, and it has been confirmed that there were no problems with the performance of the batteries exposed to high temperatures immediately following the AMF.

4. Other Operations

In addition to the maintenance and control operations of the satellites, the following operations are carried out: (1) Operation of experiment involving bus system: This is carried out approximately twice a year in order to obtain data for evaluating orbital functions and performances of the ETS-V and for using in the development of future satellites. (2) Operation of experiment involving thermal control demonstration equipment (CVT): This is carried out during the period including the vernal and autumnal equinoxes and the winter and summer solstices in order to evaluate the design of a heat pipe waste heat system and to obtain data on the operating characteristics in space. (3) Obtaining data from a technical data obtaining device [TEDA]: Data on the space environment, characteristics of elements mounted on satellites in space, etc., are obtained periodically or constantly from eight kinds of devices.

5. Problems

The TTC's RIU-1A malfunctioned on 1 December 1987 and was not able to receive specific commands. Therefore, it was converted to the RIU-1B of the redundancy system. After collecting sufficient data on satellite buses and mobile radio communications, we plan to restart the RIU-1A in order to determine the cause of the problem.

6. Summary

The status of the ETS-V has been fairly good and its operation has also been smooth up to now. In the future, we want to maintain and control the satellite in order to complete missions, to obtain various data and to cooperatively conduct experiments on mobile radio communications.

Evaluation of Performance of L-Band Antenna Mounted on ETS-V

43065013a Tokyo PROCEEDINGS OF THE 32ND SPACE SCIENCES & TECHNOLOGY CONFERENCE in Japanese 26-28 Oct 88 No 3A15 pp 570-571

[Article by Shigeo Yamada of the National Space Development Agency of Japan; Yasuo Tamai of Mitsubishi Electric Corporation]

[Text] 1. Preface

An L-band antenna is mounted on the ETS-V in order to conduct experiments on mobile radio communications. It is an offset system dual beam antenna and irradiates the earth, beam-focused with respect to specified points on the northern and southern hemispheres. The following is a description of the results of the unit test using a prototype flight model [PFM] of the L-band antenna, and performances obtained from check-out after the launching of the satellite.

2. Structure

As shown in Figure 1, the L-band antenna consists of a reflecting mirror and a primary radiator corresponding to the beams. Figure 2 [not reproduced] shows the exterior of the PFM of the L-band antenna. In order to lighten the mirror, it has been given a sandwich structure made by putting aluminum honeycomb cores between meshes made of carbon fiber reinforced plastics [CFRP]. As a result, the weight of the mirror system, including a support, is 2.7 kg, while that of the primary radiator system, including a primary radiator support, is 3.3 kg. The mirror accuracy is 0.5 mm RMS. The primary radiator is equipped with a helical antenna which can be located in the vicinity of this radiator is order to maintain the antenna's high efficiency and to increase the cross-over level of two beams. The specified temperature conditions are satisfied by simple thermal control, i.e., by installing multilayer insulation [MLI] on the satellite body structure installation section of the supports of both the mirror system and the primary radiator system. Temperature monitoring sensors are installed in the vicinity of the helical antenna installation
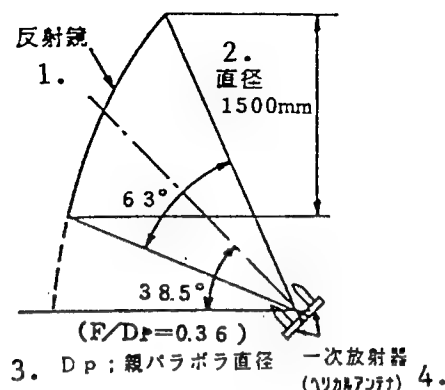
Figure 1. Configuration of Antenna

Key:
1. Reflecting mirror
2. Diameter
3. Dp; diameter of master parabolic antenna
4. Primary radiator (helical antenna)

support of the primary radiator system and at the rear of the mirror center in the mirror system in order to verify the thermal control.

3. Results of Unit Test

The performance of the L-band antenna was confirmed by subjecting the PFM to environmental resistance tests, such as a thermal vacuum test and sine wave vibration test, in addition to an electric test, as unit tests. Table 1 and Figure 3 show the main electric performances and two-dimensional radiation patterns (transmission), respectively. The aperture efficiency of the transmission bands is 59 percent (N-beam), and the cross-over level of the N/S beams is approximately 3 decibels.

**Table 1.
Main Electric Performances
(Actual Measurement of Simple PFM Substance)**

Item	N-Beam	S-Beam
1. Frequency (MHz)		
(1) Transmitting	1540.5-1548.0	1540.5-1548.0
(2) Receiving	1642.5-1650.0	1642.5-1650.0
2. Polarized wave	LHCP	LHCP
3. Beam center position (°)	37N, 161E	5S, 137E
4. Gain (dBi)		
(1) Transmitting		
a. Beam center	>/= 25.4	>/= 25.0
b. 2.8 (°) coverage	>/= 23.8	-
c. 5 (°) coverage	>/= 20.0	>/= 19.5
(2) Receiving		
a. Beam center	>/= 26.2	>/= 25.7
b. 5 (°) coverage	>/= 20.4	>/= 19.9

Table 1.
Main Electric Performances
(Actual Measurement of Simple PFM Substance)
(Continued)

Item	N-Beam	S-Beam
5. Axial ratio (dB)	</= 1.7	</= 2.5
6. VSWR	</= 1.18	</= 1.13
7. Electric power resistance (W)	>/= 60	>/= 60

this figure, the measured temperature leaves a sufficient margin for the allowable temperature.

Table 2.
Results of Checking Out AMEX L-Band System

Line		Data (dBm, antenna end electric power value of diplexer)	
		In orbit (at check out)	Ground test (after transportation to range)
Beacon* (L-band transmission)	N-beam	32.6	33.1
	S-beam	33.3	33.2
Between L and LL** (L-band transmit-ting-receiving)	N-beam	31.2	31.9
	S-beam	30.6	31.2

* Between ETS-V and Kashima Earth Station

** Between Kashima Earth Station, ETS-V and back to Kashima Earth Station

Figure 3. Secondary Radiation Pattern
(Actual Measurement of Simple PFM Substance)

Key:
1. KSM: Kashima
2. N-beam
3. S-beam
4. Transmission
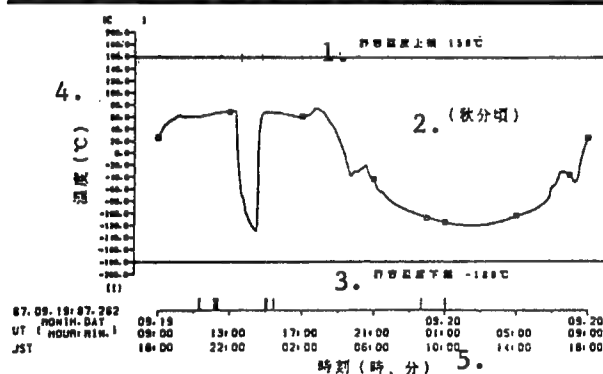
Figure 4. Actual Temperatures of Reflecting Mirror Measured at Check-Out

Key:
1. Allowable upper temperature limit: 150°C
2. (Around autumnal equinox)
3. Allowable lower temperature limit: -180°C
4. Temperature (°C)
5. Time (hour and minute)

4. Orbital Check-out Results

The orbital performance of the L-band antenna was confirmed by measuring the system check-out, including the ground facilities, of all mobile radio communications experimental equipment [AMEX]. Table 2 shows the check-out results of the AMEX L-band. In this table, the results are converted into the transmission electric power value at the end of the antenna of the diplexer in order to compare them with the ground test data. In addition, the orbital data in the table agree with the ground test data within the range of measurement error. This means that the gain of the antenna is the same as that of the ground test. Figure 4 shows the orbital temperature measured value of the reflecting mirror. In

5. Conclusion

In order to lighten the L-band antenna, it is equipped with a mesh mirror. Unit tests of the PFM have confirmed that the specified electric and mechanical performances have been obtained. In addition, as a result of check-out following the launching of the satellite, it was confirmed that the L-band antenna possesses the PFM unit performance, even while orbiting.

Development of ETS-V AMEX, Orbital Check

*43065013b Tokyo PROCEEDINGS OF THE 32ND
SPACE SCIENCES & TECHNOLOGY
CONFERENCE in Japanese 26-28 Oct 88 No 3A16
pp 572-573*

[Article by Kimio Kondo and Naokazu Hamamoto of
the Communications Research Laboratory, Ministry of
Posts and Communications; Akira Ishide of the Elec-
tronic Navigation Research Institute; Shigeo Yamada of
the National Space Development Agency of Japan;
Norio Nikawa of NEC Corporation; and Keiichiro
Nagashima of Mitsubishi Electric Corporation]

[Text] Preface

The ETS-V was launched by the H-I rocket on 27 August
1987, and the Communications Research Laboratory
[CRL], Electronic Navigation Research Institute
[ENRI], the NTT Radio System Research Institute and
KDD Meguro Research Institute are currently con-
ducting experiments involving mobile radio communi-
cations by using this satellite.

This report describes the results of developing the
AMEX, which is a relay of the ETS-V, as well as those of
checking orbital characteristics.

1. Development of AMEX

The CRL, ENRI and NASDA started developing the
AMEX in 1983, had manufactured, design and evalu-
ated an AMEX model for mounting on the ETS-V EM by
December 1984, mounted the model on the ETS-V EM,
and checked its adaptability. A model for mounting on
the PFM was manufactured and mounted on the satellite
in November 1985. As a result of ETS-V proto-flight
tests conducted from February 1986 to April 1987, it was
judged that the model's functioning and performance
were satisfactory and that it possessed flight qualities.
After the model was transported to the range in May
1987 and was inspected, it was launched on 27 August
1987.

2. Functions and Characteristics of AMEX

The AMEX is a double conversion-type relay in which
140 megahertz is the IF frequency, and it consists of an
antenna, and L-band, C-band and IF sections. Figure 1
shows a block diagram of the AMEX. The L-band and
C-band are used for vehicles and feeder links, respec-
tively.

The L-band antenna is an offset parabolic one with an
aperture diameter of 1.5 meters, and is composed of
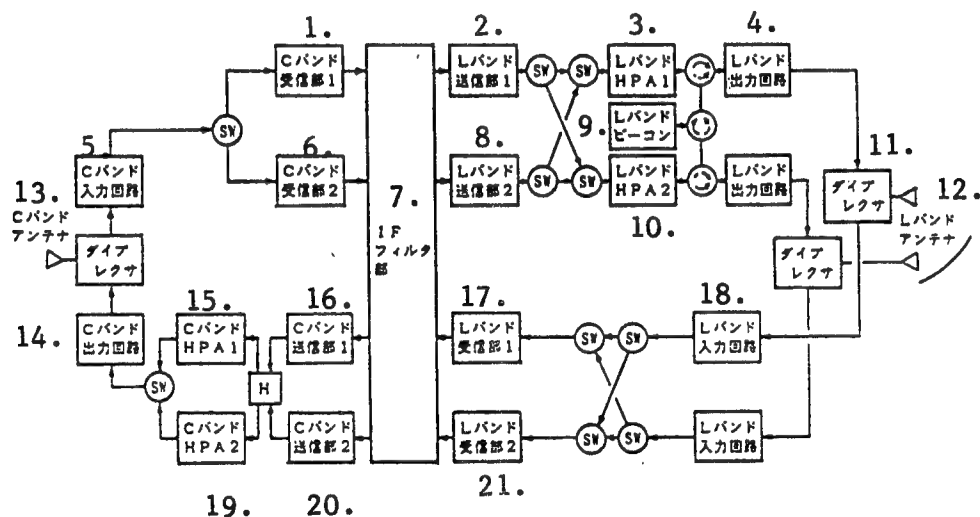
Figure 1. Block Diagram of AMEX

Key:
1. C-band receiving section 1
2. L-band transmitting section 1
3. L-band HPA 1
4. L-band output circuit
5. C-band input circuit
6. C-band receiving section 2
7. IF filtering section
8. L-band transmitting section 2
9. L-band beacon
10. L-band HPA 2
11. Diplexer
12. L-band antenna
13. C-band antenna
14. C-band output circuit
15. C-band HPA 1
16. C-band transmitting section 1
17. L-band receiving section 1
18. L-band input circuit
19. C-band HPA 2
20. C-band transmitting section 2
21. L-band receiving section 2

multi-beams consisting of two north and south beams. In order to lighten the reflector, a CFRP mesh honeycomb structure has been adopted.

The C-band is a completely redundant system for current and spare uses, while the L-band consists of two systems for current use, corresponding to two beams. They constitute mutual function redundant systems by means of switches. It is also possible to output L-band beacons from an arbitrary beam.

The IF section consists of a filter group using surface acoustic wave [SAW] filters, and it is possible to generate C/L, L/C, C/C and L/L circuits, depending on the frequency selection.

The AMEX requires linearity in consideration of the operation of the SCPC of each mobile station. The HPAs of the L-band and C-band employ 25 watt-A class gallium arsenide field effect transistors [GaAs FET]s and 8 watt-A class GaAs FETs, respectively. In the case of C/L and L/C, the total gain between AMEX diplexers is 123 decibels, for C/C it is 106.5 decibels and for L/L 139.5 decibels. The total gain can be changed by 5 or 10 decibels.

GaAs FET is also used in a low noise amplifier [LNA] to lower the noise. The noise figure of the L-band LNA is realized at 1.7 decibels in order to receive the low level signals output by vehicles in particular.

Table 1. Data on AMEX

			1. Lバンド		2. Cバンド
周波数 4.送信		MHz	1542±1.5	1546.5±1.5	5230±11.25
3. 5.受信		MHz	1644±1.5	1648.5±1.5	5960±11.25
アンテナ 6.			オフセットパラボラ 7.		ホーン 8.
開口径 9.			1.5mφ		0.22mφ
偏波 10.			LHCP		LHCP
11.利得 *			(Nビーム) 14.	(Sビーム) 15.	
	送信	dBi	25.4	25.0	19.5
12.	受信	dBi	26.2	25.7	21.6
給電損失		dB	1.2	1.1	0.6
軸比 13.		dB	1.8	2.5	2.8
LNA NF		dB	1.7	1.6	2.1
G/T *		dB/K	-3	-4	-8
HPA 出力 16.		dBW	13.7	14.5	8.5
EIRP *		dBW	35.5	35	25
中継器利得** 17.		dB	C/L 123 (0、+5、+10)/3MHz		
/帯域幅 18.		MHz	L/C 123 (0、+5、-5) /3MHz		
			L/L 139.5(0、+5、-5)/0.3MHz		
19.			C/C 106.5(0、+5、+10)/3MHz		
スプリアス D/U		dB	40以上 20.		
C/IM3		dB	30以上 21.		
ビーコン 22.			1545MHz 5.6dBw		
重量 23.		Kg	64 (アンテナ7.4Kg含む) 25.		
消費電力 24.		W	300 (L2系統運用、RF出力時) 26.		

* ビーム中心 27. ** ダイプレクサ間の利得 28.

Key:
1. L-band
2. C-band
3. Frequency
4. Transmitting MHz
5. Receiving MHz
6. Antenna
7. Off-set parabolic antenna
8. Horn
9. Aperture
10. Polarized wave 11. Gain*
12. Feed loss
13. Axial ratio
14. (N-beam)
15. (S-beam)
16. HPA output
17. Repeater gain**
18. band width
19. Spurious D/U dB 20. 40 or more
21. 30 or more
22. Beacon
23. Weight (kg)
24. Power Consumption (W)
25. 64 kg (including weight of antenna - 7.4 kg)
26. 300 W (operation of L2 system, at RF output)
27. * Beam center
28. ** Gain between diplexers

Table 2. Results of Checking Characteristics of AMEX

		中継器 1. 最終電気性能		衛星搭載 2. 最終電気性能		打上後 3. チェックアウト		第1回 4. 定期チェック	
		M	A	M	A	M	A	M	A
標準出力レベル (dBm)									
	C/L M1/A1	30.9 /	31.58	31.13/	31.79	29.5 /	30.5	30.5 /	31.2
入力	M1'/	30.42/	–	30.61/	–	29.4 /	–	– /	–
-91.5	M2/A2	31.07/	30.68	31.39/	31.25	30.8 /	30.7	31.7 /	31.9
6.	C/C M/A	14.8 /	15.59	15.72/	16.52	14.5 /	15.4	14.4 /	14.5
	L/C M1/A1	15.41/	15.49	16.26/	16.18	15.1 /	16.0	15.7 /	16.1
-108	/A1'	– /	15.71	– /	16.10	– /	16.3	– /	–
	M2/A2	14.98/	14.95	15.80/	15.66	14.7 /	14.9	14.4 /	14.0
7.	L/L M1/A2	31.40/	30.88	31.74/	31.42	31.3 /	30.6	31.6 /	31.7
飽和出力レベル *									
	C/L M1/A1	40.44/	–	40.7 /	–	40.5 /	–	40.4 /	40.5
	M1'/	40.46/	–	40.8 /	–	40.6 /	–	– /	–
	M2/A2	41.55/	–	41.9 /	–	42.1 /	–	42.3 /	42.3
	L/L M1/	40.41/	–	40.8 /	–	40.4 /	–	40.7 /	–

* 2dB圧縮点出力レベル

Key:
1. Final electric performance of repeater
2. Final electric performance of AMEX mounted on satellite
3. Check out after launching of satellite
4. First periodic check
5. Standard output level (dBm)
6. Input
7. Saturation power level*
8. * 2 dB compression point output level

In order to develop the AMEX, the EMC was carefully controlled, taking the following matters into consideration: (1) The AMEX antenna shall be used to both transmit and receive signals. (2) The difference between the output electric power and receiving electric power of the L-band shall be as large as approximately 150 decibels. (3) The frequency difference of the L-band shall be as small as approximately 100 megahertz.

Main data on the AMEX are shown in Table 1.

3. Orbital Check of AMEX

(1) Initial Check The ETS-V was launched on 27 August 1987, and became geostationary on 17 September. During 5 to 27 October, the AMEX and the C-band TTC were checked out at the Kashima Branch of the CRL in parallel with the evaluation of the satellite proper. The following characteristics of the AMEX were confirmed: (1) input/output characteristics, (2) amplitude frequency characteristics, (3) frequency conversion characteristics, (4) spurious characteristics, (5) gain switching function, (6) delay frequency characteristics, and (7) overall transmission characteristics.

With regard to (1), the difference of the obtained value from the final electric performance test conducted on the ground was within 1 decibel in most circuits. Other items sufficiently satisfied the specification as well,

and it was confirmed that after the satellite was launched, the AMEX was operated without the occurrence of any problems.

(2) The First Periodic Check The AMEX was given its first periodic check in April 1988. As shown in Table 2, compared with its status at the initial check, there were no significant differences.

Postface

The AMEX has demonstrated satisfactory characteristics in orbit since being developed as a relay used to conduct Japan's first experiments involving mobile radio communications. Valuable data to be used in studying future mobile radio satellite communications systems are being collected from experiments being actively conducted by the respective bodies using the ETS-V/AMEX.

References

1. Kosaka, et al., "Plan for Experiment Involving Mobile Radio Communications by Using ETS-V," COMMUNICATION ASSOCIATION JOURNAL, Vol 69 No 8, August 1986.

2. Kondo, K., et al., "Aeronautical Maritime Experimental Transponder on Engineering Test Satellite-V," 19th European Microwave, Stockholm, 12-15 September 1988.

Experiment of Mobile Radio Satellite Communications by Using ETS-V—Results of Experiment Conducted by Ministry of Posts and Telecommunications

[Article by Hiromichi Wakana, Naokazu Hamamoto, Yoshihiro Hase, Shingo Ohmori and Kimio Kondo of the Communications Research Laboratory, Ministry of Posts and Communications]

[Text] The ETS-V was launched with the H-I rocket from a site at NASDA [National Space Development Agency of Japan]'s Tanegashima Space Center on 27 August 1987, and was injected into the specified geostationary orbit position at 150 degree E longitude on 17 September 1987. This manuscript outlines the results of an experiment involving mobile radio satellite communications using the ETS-V as conducted by the CRL. Table 1 outlines the mobile earth stations used in this experiment.

Table 1.
Outline of Various Mobile Earth Stations

Moving object	Antenna type (gain)	Homing system, mechanism	Modulation system
Ship	40-cm short back fire (15 dBi)	Program, machine	SCPC/MSK, BPSK, NBFM, TDM/TDMA/BPSK
Aircraft	16-element circular patch phased array (14 dBi)	Step, electron	SCPC/MSK, BPSK, NBFM
Movement on ground	Circular patch (7 dBi)	Non-homing/ manual	SCPC/MSK, QPSK, digital FM, ACSSB
	8-element spiral (15 dBi)	Automatic homing, machine	SS/BPSK
	4 winding helical (4 dBi)	Non-homing	

Ship Experiment

An earth station is located on a training ship, the "Oshyoro-Maru," of the Department of Fisheries, Hokkaido University. The first and second ship experiments were conducted in the south and north sea routes from 20 October to 24 December 1987 and from 6 June to 17 August 1988, respectively. Figure 1 maps these routes.

In order to check the basic signal transmitting function of the ship-based earth station as a telecommunications system, a voice speech test was conducted using the minimum shift keying [MSK] and frequency modulation [FM] systems, and mainly the single channel per carrier
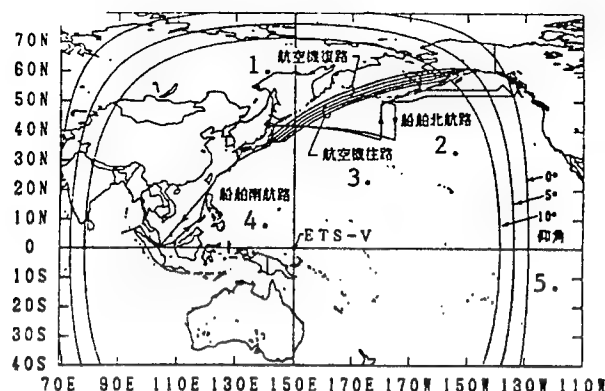

Figure 1. Sea Route of CRL's Ship Experiment and Air Route of CRL's Aircraft Experiment

Key:
1. Air return route of aircraft
2. Northern sea route of ship
3. Outbound air route of aircraft
4. Southern sea route of ship
5. Elevation angle

[SCPC] system, and a data transmitting test was conducted by using personal computers and facsimile machines basedon the BPSK and FM analog systems in the first ship experiment. Characteristics of the bit error rate to C/No or the S/N to C/No were also measured. As a result of these tests and the measurement, it was confirmed that the ship-based earth station was operating satisfactorily.

Figure 2 shows the relationship between the average value of the elevation angle, the azimuth angle of the antenna, and the root mean square [RMS] value of the amount of electric power received and fluctuated for a total of 826 measurements (each lasting 3 minutes) during the first ship experiment. Large areas of fluctuation of the received electric power are affected by a block system according to the hull construction, such as the mast around the antenna, etc. The influence of the block system is currently being studied theoretically.

The generation of phasing phenomena caused by sea clutters could not be observed in the first ship experiment on the south sea route because the elevation angle for observing the satellite from the ship was high. Data obtained from the second ship experiment is currently being analyzed.

Aircraft Experiment

An aircraft-based earth station is mounted on an international cargo transport Boeing 747 owned by Japan Air Lines Co., Ltd. [JAL]. As shown in Figure 1, the air route is between Narita and Anchorage, and the time allowed for conducting an experiment one way is 5 to 6 hours. The earth stations are outlined in Table 1. The configuration of an aircraft-based earth station is the same as that of the ship-based earth station except for the following points: 1) neither a time division multiplexing
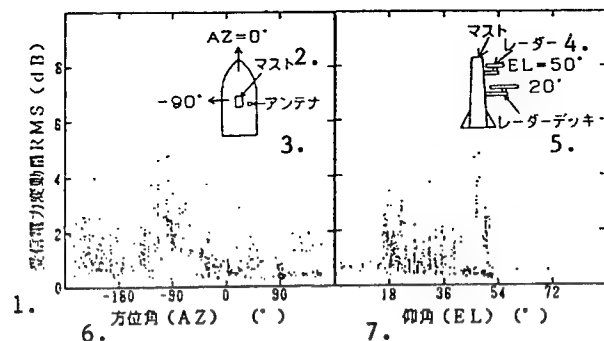
Figure 2. Dependence of Fluctuation of Electric Power Received on Azimuth Angle and Elevation Angle

Key:
1. Amount of received electric power RMS (dB)
2. Mast
3. Antenna
4. Radar equipment
5. Radar deck
6. Azimuth angle
7. Elevation angle

Figure 3. Standard Deviation of Electric Power Received by Aircraft Earth Station

Key:
1. Standard deviation (dB)
2. Anchorage to Narita
3. Az: Azimuth angle
4. El: Elevation angle
5. Singapore to Narita
6. Narita to Singapore
7. Narita to Anchorage
8. Azimuth angle of antenna

[TDM] device nor a time division multiplex access [TDMA] device is mounted on the communications end station system, and 2) the aircraft-based earth station has an automatic frequency control [AFC] function compensating for the Doppler shift.

The antenna employs a circular patch-phased array system consisting of 16 elements, is constructed with two faces, and is used by switching it during the round-trip routes. The direction of the azimuth angles is controlled with eight phase converters to carry out the automatic tracking based on a step system. The elevation angle direction is not tracked, but is fixed at an angle of 25 degrees. The width of 3-decibel beams is 60 degrees in the direction of the elevation angle.

Figure 3 shows the dependence of the antenna on the azimuth angle. This antenna also shows the amount of received and fluctuated electric power (standard deviation). The azimuth angle from 127.4 to 150.6 degrees corresponds to the departing route from Narita to Anchorage, while that from 290.4 to 330.6 degrees corresponds to the return route from Anchorage to Narita. This figure indicates that the fluctuation of the electric power signal received by an aircraft is very small. However, the fluctuation of the receiving level during the departing route is slightly larger than that during the return route. It is believed that this is caused by the following two matters: 1) antenna beams point in the direction of the main wings of the aircraft, and 2) phasing phenomena are generated, with waves reflected on the main wings. Similarly to the ship-based experiment, basic signal transmission characteristics were measured, and good results were obtained.

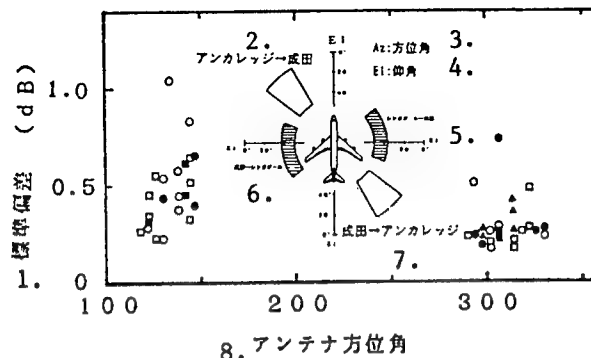Experiment Involving Ground-Based Mobile Radio Communications

The basic transmission characteristics of message communications and ACSSB voice communications were measured as an experiment involving ground-based mobile radio communications.

Measurement of Propagation Characteristics

Non-modulating waves of 1.5 gigahertz were sent by the ETS-V to cities and quasi-open areas, and phasing phenomena were measured to fully utilize the measurement results in designing the circuits of ground-based mobile radio communications.

Experiment on Message Communications Equipment

This system is used to exchange character messages between the base station and portable mobile stations by means of packet communications based on an aloha system, and the transmission speed is 100 bps. Figure 4 shows the results of measuring the bit error rate. It seems that this system will be put to practical use because an error of approximately one character is attained with a transmission of three packets (120 characters) and with a C/No of about 34 decibel-hertz.

Experiment Involving ACSSB Communications

The ACSSB communications system differs from the conventional SSB one with respect to the following points: 1) voice signals are compressed and expanded at the respective transmitting and receiving sides, and 2) pilot signals are added and transmitted to such voice signals in order to synchronize and demodulate them. These two points modify the demodulation characteristics and the S/N for the auditory sensation of voices. Figure 5 shows the results of measuring C/No in comparison to S/N by placing a device on a carriage while moving the carriage. It can be appreciated that the measured S/N has an almost linear relationship to C/No.
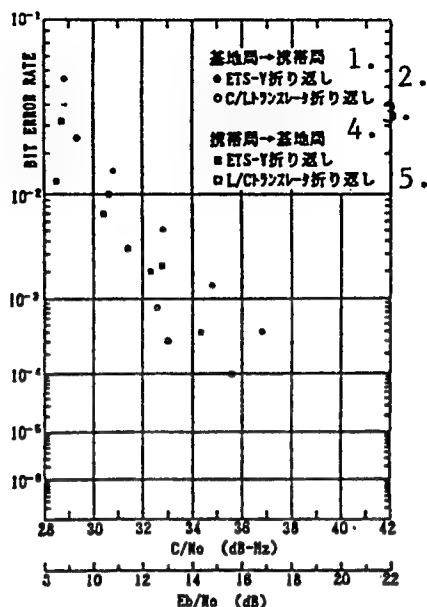
Figure 4. BER of Message Communications System
Key:
1. Base station to portable mobile station
2. Turn of ETS-V
3. Turn of C/L translator
4. Portable mobile station to base station
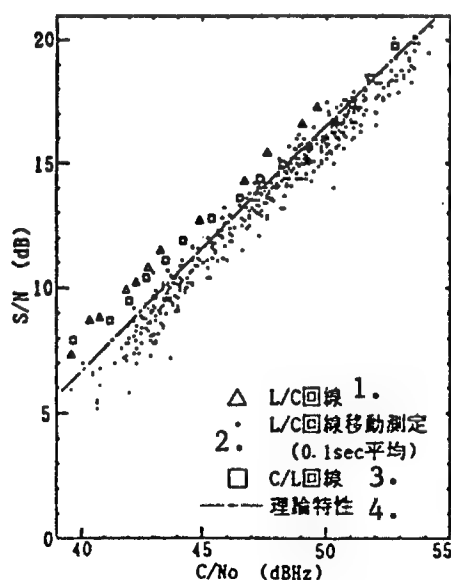5. Turn of L/C translator

Figure 5. ACSSBC/No to S/N Characteristics
Key:
1. L/C line
2. Measurement of movement of L/C line (0.1 sec on average)
3. C/L line
4. Theoretical characteristics

According to the evaluation of the this system's auditory sensation of voices, the limit of speech intelligibility at C/No is 45 decibel-hertz, while that at practical use is 48 decibel-hertz.

Experiment Involving Navigation Aid Utilizing ETS-V—Outline of Aircraft Experiment

43065013d Tokyo PROCEEDINGS OF THE 32ND SPACE SCIENCES AND TECHNOLOGY CONFERENCE in Japanese 26-28 Oct 88 No 3A18 pp 576-577

[Article by Kazuaki Hoshinobi, Akira Ishide, Michihiko Mitsugaki, Mitsuhiro Fujita, Ken Ito, Minoru Ito, Kenji Niimi, Hideomi Nasu and Shuuji Nishi of the Electronic Navigation Research Institute, Ministry of Transport]

[Text] 1. Preface

The Electronic Navigation Research Institute [ENRI], Ministry of Transport, is currently conducting experiments involving navigation aids using the ETS-V, a Beechcraft B99 (ENRI's aircraft for these experiments), and a JAL Boeing 747 cargo transport in order to develop the position measuring technology, satellite communications, etc., necessary as navigation aids for ships on the sea and air traffic control conducted on the sea.

This report outlines the experiments we conducted in Japan using the B99 as well as the results of our experiments employing the Boeing 747 on the North-Pacific Air Route.

2. Outline of Experiments

Experiments have been conducted by using repeaters, the AMEX mounted on the ETS-V, aircraft, and aeronautical and coastal earth stations installed in the CRL's [Communications Research Laboratory, Ministry of Posts and Telecommunications] Kashima Branch.[1][2][3][4]

These experiments are conducted by using the Boeing 747 on the North-Pacific Air Route between Narita and Anchorage. The elevation angle of the satellite has a range of approximately 10 to 45 degrees.

Figure 1 shows the flight courses of the B99 used when the experiment was conducted in Japan. The elevation angle of the satellite is 40 to 50 degrees. An experiment involving the measurement of position is conducted by using a pseudo satellite in an air area adjacent to the Boso Peninsula.

The experimental objects included data transmission, the measurement of range and position, voice transmission and radio wave propagation.

3. Results of Experiments

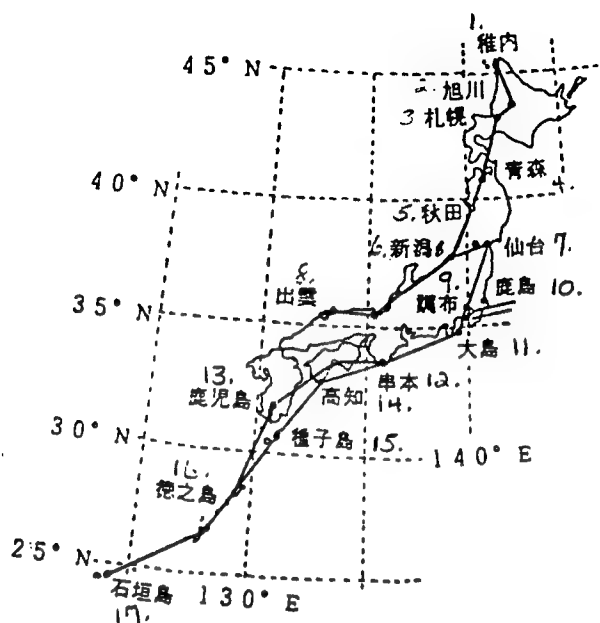3.1 Change in Frequency and Receiving Level

Figure 1. Flight Course of B99

Key:
1. Wakkanai	9. Chofu
2. Asahikawa	10. Kashima
3. Sapporo	11. Oshima
4. Aomori	12. Kushimoto
5. Akita	13. Kagoshima
6. Niigata	14. Kochi
7. Sendai	15. Tanegashima
8. Izumo	16. Tokunoshima
	17. Ishigakijima

Figure 2. Change of Signal Level and Frequency (Boeing 747)

Key:
1. Frequency deviation (Hz)
2. Level (dBm)
3. Time (min)
4. Elevation angle of satellite
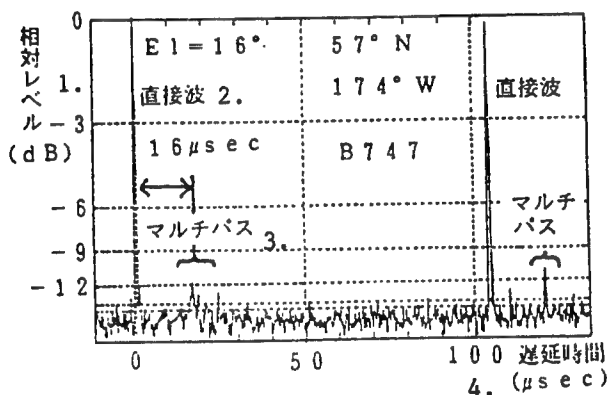
Figure 3. Example of Measurement of Multi-Pulse Electric Power Against Delay Time

Key:
1. Relative level (dB)
2. Direct wave
3. Multi-pulse
4. Delay time (microseconds)

The basic data relate to the fluctuation of frequency and that of the receiving level during flight. Figure 2 shows the results of measuring the frequency and the level of the signals transmitted from an aircraft flying on the North-Pacific Air Route to the IF bands of the aeronautical and coastal earth stations. The sampling interval is 1.7 seconds, and the elevation angle of the satellite is within the range of 12 to 36 degrees. The maximum fluctuation of the signal level in a short time is approximately 3 decibels, and the signal level is changed by 5 to 6 decibels during the overall route. When using the Boeing 747, the maximum change in frequency according to the Doppler effect is approximately 1.3 kilohertz.

The existence or nonexistence of sea clutters has been confirmed by using a multipath measuring device employing spread spectrum signals. Figure 3 shows an example of measuring the multipath relative electric power against the delay time. This measurement was carried out in the vicinity of an elevation angle of 16 degrees when flying from Anchorage to Tokyo. This example indicates that the power ratio between direct waves and sea clutters is approximately 12 decibels. The amount of delay from the direct waves is about 16

microseconds, which is in good agreement with the delay calculated from the elevation angle and altitude of the aircraft.

Figure 4 shows an example of the change in frequency and signal levels received at the aeronautical and coastal earth stations when experiments were conducted using the B99. This example was obtained from measuring the frequency and level on a flight from Sendai to Niigata, Aomori, Sapporo, Asahikawa and Wakkanai. A portion of the example shows the frequency and level changing sharply and stepwise. This portion refers to a point at which the flight direction was changed by switching the antenna. The change level, as a whole, is 7 to 8 decibels.
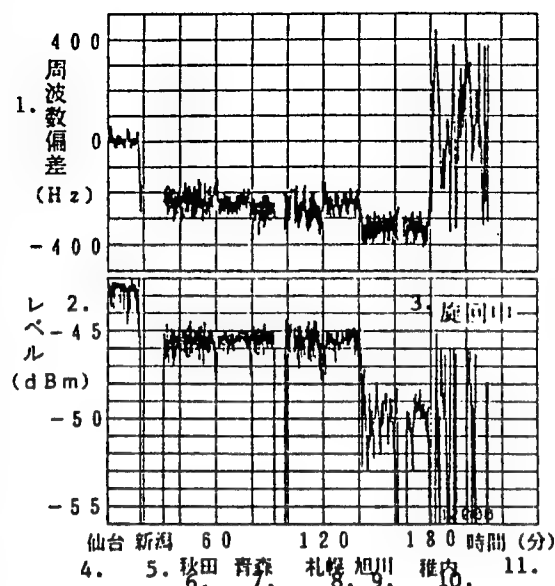
Figure 4. Change in Signal Level and Frequency (B99)

Key:
1. Frequency deviation (Hz)
2. Level (dBm)
3. Turning
4. Sendai
5. Niigata
6. Akita
7. Aomori
8. Sapporo
9. Asahikawa
10. Wakkanai
11. Time (minutes)

The Doppler effect is a maximum of approximately 350 hertz, because the speed is about one-fourth that of the Boeing 747.

3.2 Range and Position Measuring Characteristics

An experiment involving position measurements was carried out by using pseudo satellites and the B99 within a range that could be seen from the aeronautical and coastal earth stations in which these pseudo satellites were set.

Figure 5 shows the difference between the position obtained from an experiment on the relative measuring position and that obtained from the global positioning system [GPS]. This difference is 800 meters or less.

3.3 Data Transmitting Characteristics

The BPSK and bit error rate [BER], according to the PM system, are measured as data transmitting characteristics.

Figure 6 shows the BER characteristics during flight as obtained by the aeronautical and coastal earth stations. The reason for the more serious deterioration of the B99 in comparison to the Boeing 747 in regard to the BPSK is that the influence of HPA on the B99 seems to be greater than that on the 747.
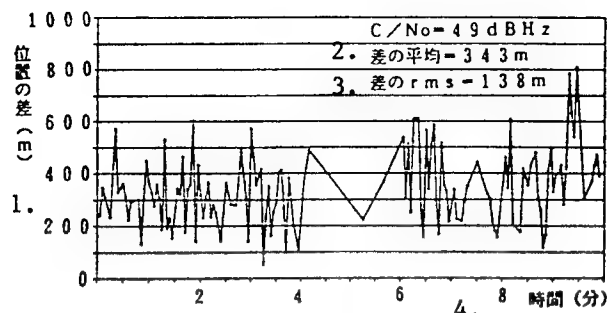
Figure 5. Difference Between Results of Experiment on Measurement of Relative Position and Value of Measurement of GPS Position

Key:
1. Difference in position (m)
2. Average difference = 343 m
3. rms of difference = 138 m
4. Time (minutes)
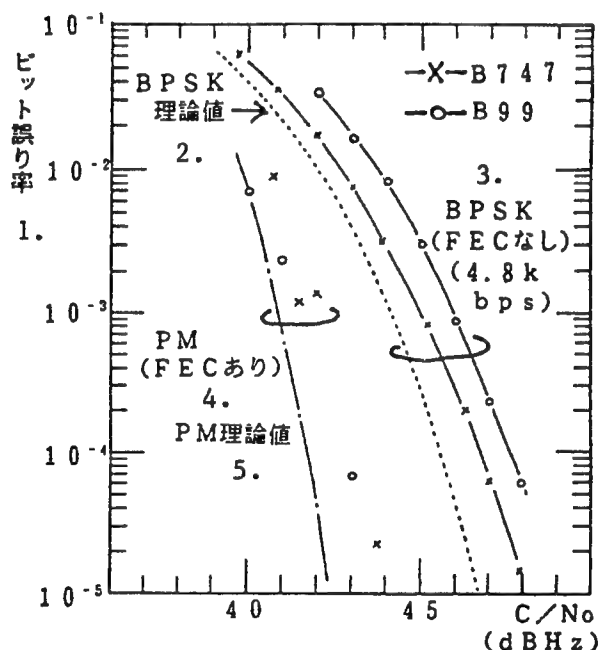
Figure 6. BER Characteristics

Key:
1. Bit error rate
2. BPSK theoretical value
3. BPSK (no FEC)
4. PM (existence of FEC)
5. PM theoretical value

3.4 Voice Transmitting Characteristics

An experiment involving voice transmissions has been conducted by using articulation test tapes, narrow band

frequency modulation [NBFM] and linear predictive coding [LPC] methods of 4.8 and 2.4 kilobits/second [kbps].

4. Postface

We have outlined the results obtained from experiments on navigation aids conducted by using the ETS-V and aircraft. We acknowledge our appreciation to concerned persons at the CRL, NASDA and JAL. We would also like to express our gratitude for the cooperation extended relevant to the operation of the B99.

References

1. Ito, et al., "Plan for Experiment on Navigation Aids by Using the ETS-V," Electronic Information Communication Association Technical Research Report, SANE 86-48, January 1987.

2. Niimi, et al., "Device Mounted on Aircraft for Experiment on Navigation Aids by Using the ETS-V," Electronic Information Communication Association Technical Research Report, SANE 87-12, July 1987.

3. Hoshinobi, et al., "Terrestrial Station End Office Device for Experiment on Navigation Aids by Using ETS-V," Electronic Information Communication Association Technical Research Report, SANE 87-13, July 1987.

4. Fujita, et al., "Prompt Report of Experiment on Navigation Aids by Using ETS-V," Electronic Information Communication Association Technical Research Report, SANE 88- , August 1988.

Experiment on Mobile Radio Satellite Communications, Conducted by KDD Using ETS-V—Outline of Results of Experiments Involving Communications Between Ships and Aircraft

43065013e Tokyo PROCEEDINGS OF THE 32ND SPACE SCIENCES AND TECHNOLOGY CONFERENCE in Japanese 26-28 Oct 88 No 3A19 pp 578-579

[Article by Yutaka Yasuda and Yoshio Karasawa of Meguro Research Institute, Kokusai Densin Denwa Co., Ltd.]

[Text] 1. Preface

Kokusai Densin Denwa Co., Ltd. [KDD] is conducting an experiment on communications between ships and aircraft as a part of the experiments on mobile radio satellite communications [EMSS] currently being conducted utilizing Japan's ETS-V and being promoted by the Ministry of Posts and Telecommunications. This paper outlines this experiment.

2. Basic Configuration of Experimental System

A ship-based earth station and an aircraft-based earth station are prepared for vehicles, the four kinds of digital communications devices shown in Table 1 are connected to these stations, and experiments involving communications

related to voice, images, facsimile machines, personal computers, etc., are conducted at the stations. As shown in Table 2, a circular batch antenna for receiving only, as well as two kinds of ship antennas (parabolic and short backfire antennas) and an aircraft phased array antenna consisting of nine elements, is used for the vehicles. The Communications Research Laboratory [CRL]'s Kashima coast, an aeronautical earth station's antenna and RF-based facilities are for common use on the ground side (C-band system), and the digital communications devices shown in Table 1 are connected with the IF band.

Table 1. Basic Parameters of Communications Equipment

Type	Type I	Type II	Type III	Type IV
Information transmission speed	64kbit/s	16kbit/s	16/9.6 kbit/s	4.8kbit/s
FEC	Rate 1/2	Rate 1/2	Rate 1/2, 3/4	Rate 1/2
	Viterbi	Viterbi	Viterbi	Viterbi
Modulation system	QPSK	QPSK	QPSK/OQPSK	QPSK
Communications speed	128kbit/s	36kbit/s	24kbit/s	13.2kbit/s
Voice coding system	-	APC	APC-MLQ	RELP
Terminal connection	INVITE64 (visual telephone set)	Voice telephone set, facsimile machine, personal computer	Voice telephone set, facsimile machine, personal computer	Voice telephone set, facsimile machine, personal computer
Connecting RF device (name of antenna)	85-cm parabolic antenna	85-cm parabolic antenna	85-cm parabolic antenna	85-cm parabolic antenna
	40-cm SBF	40-cm SBF	40-cm SBF	40-cm SBF
	9-element patch array	9-element patch array	9-element patch array	9-element patch array

Note) OQPSK: Offset QPSK; SBF: Short backfire

Table 2. Data on Mobile Earth Station/RF-Type Facility

Item	Ship-based earth station		Aircraft-based earth station	Mobile receiving station
	High gain antenna	Intermediate gain antenna	Intermediate gain antenna	Low gain antenna
Antenna type	85-cm parabolic antenna	40-cm SBF	9-element patch array	Circular patch
Antenna gain	21 dBi	15 dBi	11.5 (transmitting)/13 (receiving) dBi	7 dBi

Table 2.
Data on Mobile Earth Station/RF-Type Facility
(Continued)

Item	Ship-based earth station		Aircraft-based earth station	Mobile receiving station
G/T	-4 dBK	-10 dBK	-13 dBK	-19 dBK
e.i.r.p.	32 (31) dBW	27 dBW	25 dBW	—
Homing system	4-axial control	2-axial Az-El system	Beam scanning	Nil
	Step tracking	Program tracking	Program tracking	

Note) Class-C during use of HPA, 32 dBW; Class-A during use of HPA, 31 dBW

3. Outline of Experimental Results

Experiment Involving Ship Communications

An experiment involving ship communications was conducted by using a small ship with a gross tonnage of 700 tons (shown in Photograph 1 [not reproduced]) on a round-trip course between Shimizu, Shizuoka Prefecture, and Ogasawara, Tokyo, from 3 to 9 July 1988. In this experiment, the ship's antenna was only slightly affected by phasing phenomena, satellite link characteristics were obtained as almost circuit-designed, and stable telecommunications lines were set because the elevation angle of the ship's antenna was 50 to 60 degrees. The experiment was conducted by using all the communication devices shown in Table 1. Visual telephone communications were carried out by using an image transmitting system (INVITE 64) of 64 kilobits/second at between the Kashima Ground Station and a ship at sea, and satisfactory results were obtained. Table 3 shows an example of the circuit design of this experimental system, and Figure 1 shows an example of measuring the BER characteristics of the communications device (Type I).

Table 3.
Example of Design of Ship Communications System Line
(Standard Value for No Phasing Phenomenon)
(Note: Earth station setting position: Tokyo; GES: Coast aeronautical earth station; SES: Ship earth station (intermediate gain); C/L repeater: Low gain mode (satellite gain 166.2 dB); L/C repeater: Intermediate gain mode (satellite gain 165.1 dB))

	GES to SES	SES to GES
Up link		
Earth station e.i.r.p. (dBW)	63.0	27.2
Propagation loss (dB)	199.4	188.2
Absorption loss, etc. (dB)	0.2	0.2
Satellite G/T (dBK)	-8.0	-4.9
Up link C/No (dBHz)	84.0	62.5
Down link		
Satellite e.i.r.p. (dBW)	32.6	3.9

Table 3. (Continued)

Propagation loss (dB)	187.6	198.2
Absorption loss, etc. (dB)	0.2	0.2
Earth station G/T (dBK)	-10.0	33.7
Down link C/No (dBHz)	60.4	67.8
Comprehensive C/No (dBHz)	60.4	61.4
Required C/No* (dBHz)	54.1	54.1
Margin (dB)	6.3	7.3

* 64 Kbit/s at transmission of information (target, BER = 10^{-6})
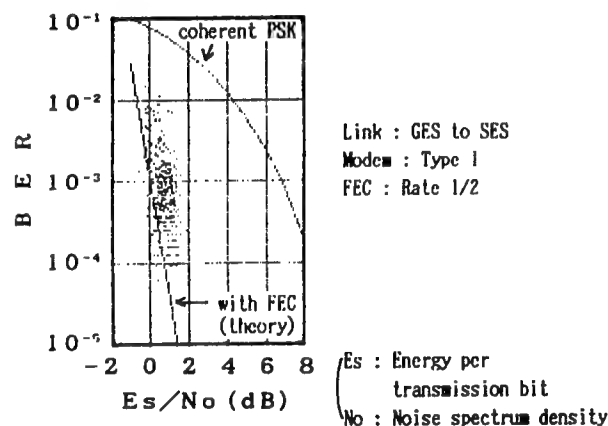
Figure 1. Example of Error Rate Characteristics of Communications Equipment with 64 Kbit/s (Ship Experiment)

In this experiment, data on propagation characteristics was obtained by using a circular batch antenna for receiving signals only. Figure 2 shows the status of the receiving level fluctuations of the intermediate gain antenna (40 cm SBF) and the batch antenna. A sea clutter phasing phenomenon of 4 decibels (value of 50 to 99 percent) was observed from the wide-beamed batch antenna.
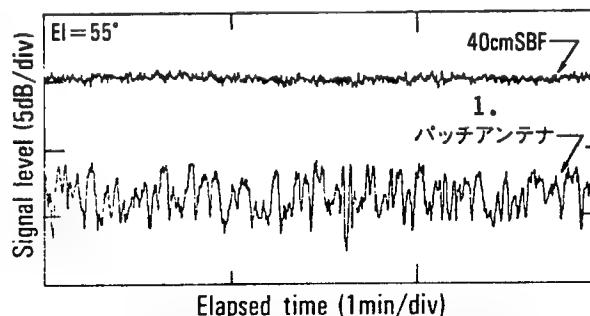
Figure 2. Example of Propagation Characteristics Obtained from Use of Circular Patch Antenna (Ship Experiment)

Key: 1. Patch antenna

Experiment Involving Aircraft Communications

Since late August, an experiment on aircraft communications (voice, facsimile machine, personal computer, etc.) has been conducted using the ETS-V's L/L repeater (receiving capacity: 1.6 gigahertz, transmitting capacity: 1.5 gigahertz), a communications device (Type III), and a light plane (Cessna). (See Photograph 2 [not reproduced].) The contents of this experiment involved the Cessna (landing and take off at Chofu Airfield) and a ship's intermediate gain antenna being directed toward each other. This antenna is installed at KDD's Meguro Research Laboratory. Table 4 shows an example of the design of an experimental communications circuit.

Table 4.
Example of Design for Line Involving Experiment on L/L Communications
(Standard Value with No Phasing Phenomenon)
(Note: Earth station setting position: Tokyo; AES: Aircraft earth station; SES: Ship earth station (intermediate gain); L/L repeater: High gain mode (satellite gain 198.8 dB))

	AES to SES	SES to AES
Up link		
Earth station e.i.r.p (dBW)	25.0	27.2
Propagation loss (dB)	188.2	188.2
Absorption loss, etc. (dB)	0.2	0.2
Satellite G/T (dBK)	-4.9	-4.9
Up link C/No (dBHz)	60.3	62.5
Down link		
Satellite e.i.r.p. (dBW)	26.4	28.6
Propagation loss (dB)	187.6	187.6
Absorption loss, etc. (dB)	0.2	0.2
Earth station G/T (dBK)	-10.0	-13.0
Down link C/No (dBHz)	57.2	56.4
Comprehensive C/No (dBHz)	55.5	55.4
Required C/No* (dBHz)	47.5	47.5
Margin (dB)	8.0	7.9

* 16 Kbit/s upon transmission of information (target, BER = 10^{-3})

4. Postface

We have outlined KDD's ship and aircraft communications experiments utilizing the ETS-V. From the experiments, it has been confirmed that various communications systems employing voices, images, facsimile machines and personal computers function almost as planned and have been offered to users satisfactorily. Finally, we acknowledge our appreciation to the relevant personnel at the Ministry of Posts and Telecommunications for their promotion and arranging of the EMSS experiment.

Scenario of Space Station Construction

[Article by Tsutomu Iwata of the National Space Development Agency of Japan; Masaya Yamamoto, Shunsuke Tanaka, Toshihide Maeda and Suguru Nakajima of Hitachi, Ltd.]

[Text] 1. Preface

The advancement and development of mankind regarding space will change greatly toward the 21st century. According to the space infrastructure concept, mankind is attempting to send such spacecraft as orbital working vehicles, inter-orbital transports and polar orbit platforms to space by considering the space station as the key, and to use space in a manner that differs from the conventional one. Objects used by mankind in space are not only the peripheries of the earth, but also the moon, Mars, and small planets. The following is a scenario of the construction of a future space station that will become a mainstay of the space infrastructure.

2. Functions of Future Space Station

The space station of the future is defined by the following items as premises for studying its construction. In other words, this space station must be capable of the following functions: (1) It will be possible for humans to stay there at all times. (2) It will be possible to conduct scientific and engineering experiments there. (3) It will be possible to assemble large structures there. (4) The space station will have a hangar for OTVs and a port for OSVs. (5) It will be possible to supply, store and keep materials, fuel, etc., there. (6) It will be possible for humans to escape from it in an emergency. (7) It will be possible to carry out such services as repair, supply and replacement of spacecraft in it.

3. Study of Construction of Future Space Station

3.1 Study of Cost Factors

Generally, it is believed that the costs shown in Table 1 are required for the development and operation of future spacecraft. In order to assemble new and large space structures or spacecraft, it will be necessary to minimize the costs related to the realization of orbital assembling processes.

Table 1.
Cost of Development and Operation of Spacecraft

Development cost		Development cost of spacecraft and operation support system
Integration cost		Cost of integration with rocket, etc.
Cost of assembly in orbit		Operation cost of space robot, etc.

Table 1.
Cost of Development and Operation of Spacecraft
(Continued)

Launching cost		Cost of launching means
Maintenance cost		Inspection, replacement of parts, supply of consumables, etc.
Operation cost	Variable cost	Cost of communications link, tracking control, etc.
	Cost of installation	Cost of ground facilities, depreciation, etc.
	Orbital services cost	Cost to replace ORU, supply propellant, etc.
Recovery cost		Cost of recovery, transportation, ground support, etc.
Management cost		Management cost of launching means, operation means, etc.
Risk cost		Cost of launching, operation, recovery, etc., risk
Others	Others	

The following are required if spacecraft are to be assembled in orbit at a low cost: (1) Clarification of mission The addition of unnecessary functions to the space station will increase the cost related to its development, launching and assembly.

(2) Increase in efficiency of mounting work for launching means Orbital assembly will sharply increase the degree of freedom of the system configuration. In order to realize low cost, it will be necessary to highly efficiently store spacecraft, that has been divided into sections, in the cargo bay and fairing, which is a launching means, and to fully utilize the launching capacity (weight on board) of the launching means. The storage and full utilization will decreasing the number of launching means and will lower the cost.

A matter more important in its relation to mounting work involves studying assembly in orbit because, even if a spacecraft can be stored with high efficiency, if many processes are required to conduct the assembly in orbit, the cost will increase, and this increase will become negligible.

(3) Optimization of Division

When a spacecraft divided into two or more sections is launched, it will become necessary to adjust the interface, and the number of tests conducted during the development will increase. Therefore, it will be necessary to divide such spacecraft into an optimal number of sections. It will also be necessary to take the assembly sequence in orbit into consideration.

(4) Precise Scheduling

It will be necessary to devise the best schedule, extending from the launch to the assembly in orbit, by taking into consideration the processing capacity of the robots which will be conducting the assembly work in orbit, the processing ability of the humans who will be operating and monitoring the robots, the shade, link with the ground, etc.

(5) Ground Test/Simulation Technology

Tests and simulations of large space structures will be conducted by using their miniaturized models because it is important to actually use large space structures on the ground when conducting tests. In the same manner, it is necessary that testing methods and the simulation of assembling technologies be studied on the ground.

3.2 Elements Constituting Future Space Station

Elements which will constitute the space station of the future are shown below based on the previously-mentioned premises:

(1) Pressurized Modules

Living module, experimental module, supply section, escape capsule, and module to serve as the connection between modules

(2) Large Folding Structures

Solar thermal electric conversion facility, solar cell paddle, radiator and various antennas with large apertures

(3) Structural Materials

Truss (structural member and contact point); folding and fixed types

(4) Space Robots

Truss-moving-type and space-moving-type robots for assembling work

(5) Fuel Supply Tank for OTV and OSV

(6) Warehouse for ORU Used in Space Factories and Platforms

3.3 Study of Assembly Method in Orbit

Assuming that the operation of the future space station will be initiated around 2005, it is thought that JEM will be an appropriate base for the assembling conducted in orbit.

It is expected that the following technologies will be used to carry out the assembly work conducted in space: (1) Tele-operation (2) Tele-presence (3) Automatization/autonomous proper

Even if the robots employing these technologies can be adapted for various tasks, if the time required for the assembly work is long, the cost of operating these robots will increase. Accordingly, the simpler the work given to them, the better it will be. Also, it will be necessary that the robots carrying out the assembly work in orbit possess the following: (1) High-function manipulator (2)

A number of working arms that can be controlled harmoniously (3) Advanced sensors (force, torque, visual sensation, and tactile sensation) (4) Advanced image processing capability (5) Problem solving and self-diagnosing abilities (6) End effectors for use in assembling, welding and cutting

4. Postface

We have studied the construction of the future space station peculiar to Japan mainly from the standpoint of reducing the construction costs. It is expected that the operation of this space station will begin around the beginning of the 21st Century.

In the future, we plan to study the working contents of robots, their frequency of use, and partial modification of missions for humans and robots, as well as further studying technology development methods.

Study of Space Factories

43065013g Tokyo PROCEEDINGS OF THE 32ND SPACE SCIENCES & TECHNOLOGY CONFERENCE in Japanese 26-28 Oct 88, No 3B2 pp 582-583

[Article by Tsutomu Iwata of the National Space Development Agency of Japan; Toshihide Maeda, Shunsuke Tanaka, Masaya Yamamoto and Suguru Nakajima of Hitachi, Ltd.]

[Text] 1. Preface

There is an increasing demand for the use of conditions found in space, such as high vacuums and microgravity, in addition to its use for such things as broadcasting, communications and meteorology. Japan is also planning to conduct experiments by using spacecraft and rockets, such as a space flyer unit [SFU], space station and advanced technology platform, as well as a first material processing test [FMPT] utilizing the space shuttle.

The following is a discussion of a space factory from the standpoint of its functions and structure assuming that this space factory will be developed from its experimental stage and that the mass production of products in space will be started around 2005 to 2010.

2. Outline of Space Factory

2.1 Purpose of Space Factory

(1) Some materials and products cannot be produced on the ground, but are commercially profitable. Such materials and products will be manufactured in a space factory utilizing conditions found in space, such a microgravity and a high vacuum. The demand for these materials and products has been anticipated, to some extent, and their unit prices per unit weight are expected to be high. When products are manufactured in space, their process costs can be reduced. Therefore, the manufacturing of such products must be considered.

(2) It is preferable to process and manufacture some of the materials for constructing the future space station, etc., some of those supplied during the construction work, and some of those collected from the lunar surface in space since the costs will be lower.

2.2 Scale

The Japanese platform-type spacecraft planned to be used in science and engineering experiments is available in two types: One is a 4-ton-class SFU, while the other is an 8-ton-class advanced technology platform.

In order to carry out large-scale manufacturing in space, it will be necessary to connect platforms with each other based on the technologies obtained from the platform-type spacecraft and to provide larger-scale platforms. The establishment of assembly technologies in orbit will not pose any problems in the construction of large platform-type spacecraft.

Therefore, we will assume the scale of the space factory to be approximately 16 to 50 tons.

2.3 Operation

First, the space factory must be an unmanned platform in order for microgravity to be satisfactorily maintained over a long period of time. Therefore, it will be necessary to completely and autonomously automate production systems and bus-based equipment by adopting artificial intelligence. When a malfunction occurs in a space factory system and the system cannot be recovered, the overall space factory or a portion of the space factory (module, orbital replacement unit [ORU], etc.) will be towed to a manned platform (space station, etc.) for repair or will be repaired by using an orbital service vehicle [OSV] and a manned space plane.

All materials, products, etc., to be mass produced will be stored in space factory warehouses, and will periodically be dispensed by an automated inventory management system. In the same manner, consumables, such as secondary batteries and fuel, will be dispensed in orbit.

2.4 Orbit

Assuming that services will be carried out in orbit, a common orbit, serving as the base for the OSV, etc., is desired, and space stations will become the bases for various services.

3. Study of Space Factory Systems

The following two items have been set as mission models, and systems have been studied as to profitability, etc.: (1) The manufacturing of bio-materials according to cell culture and segregating formation (2) The manufacturing of single crystals of compound semiconductors

It is believed that, as shown in Figure 1, the space factory can be divided into three modules by taking expansibility and common use for initial-type platforms into consideration. The mission module consists of a mission
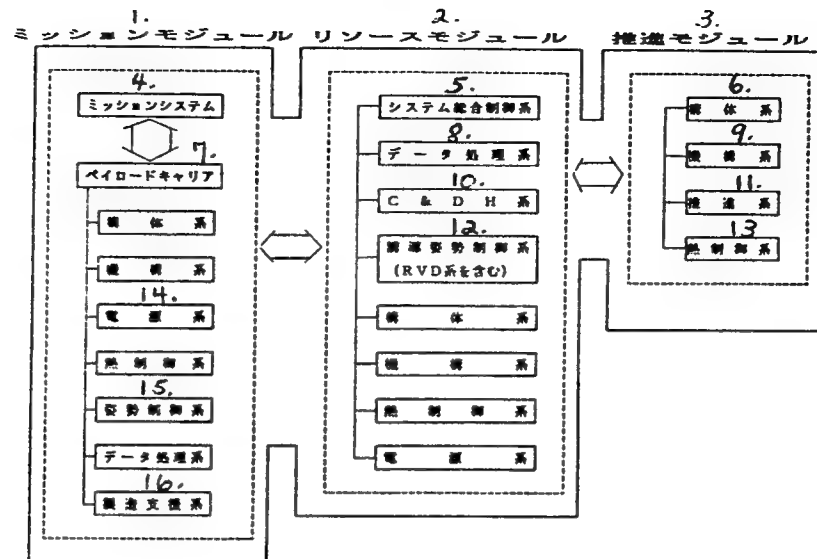
Figure 1. System Configuration of Space Factory

Key:

1. Mission module
2. Resource module
3. Propulsion module
4. Mission system
5. System comprehensive control system
6. Structure system
7. Payload carrier
8. Data processing system
9. Mechanism system
10. C & DH system
11. Propulsion system
12. Guidance attitude control system (including RVD system)
13. Thermal control system
14. Power source system
15. Attitude control system
16. Manufacturing support system
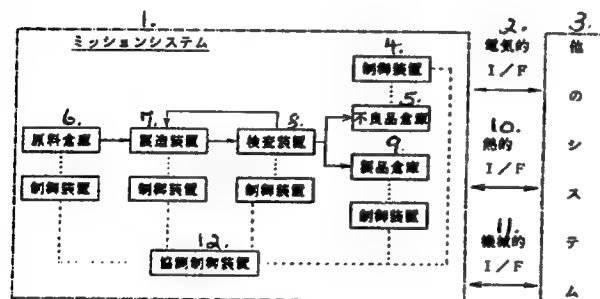
Figure 2. Mission System Configuration

Key:

1. Mission system
2. Electric I/F
3. Other systems
4. Control unit
5. Warehouse for defective goods
6. Warehouse for raw materials
7. Manufacturing unit
8. Inspection unit
9. Warehouse for products
10. Thermal I/F
11. Mechanical I/F
12. Cooperative control unit
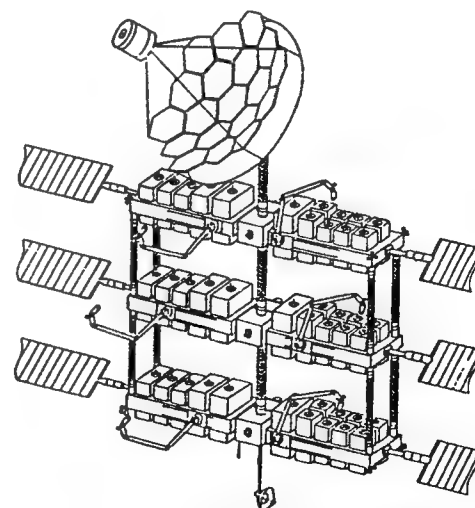
Figure 3. Sketch of Space Factory

system, which carries out missions, and a payload carrier for mounting the mission system. Figure 2 shows a mission system configuration.

The mission system will be equipped with ORUs and will be located on the payload carrier. Before positioning this mission system, it will be necessary to study the configuration so that materials can be readily transferred between the ORUs. The main subsystems are equipped

with ORUs. As has been studied for use in JEM, we have adopted a method involving the direct transferral of materials among the ORUs, not one in which small ORUs are stored in large ORUs. Figure 3 shows a sketch of the space factory.

4. Outline of Operation

The operation profile of the space factory is outlined as follows: (1) Range maintenance (2) Launching and injecting into orbit (3) Establishment of attitude, unfolding a portion of the solar cell paddle, establishing line with data relay satellite, and determining autonomous orbit according to global positioning system [GPS] (4) Assembly in orbit and testing of functions (5) Complete unfolding of solar cell paddle and radiator (6) Establishment of microgravity (7) Start of manufacturing (8) Holding (9) Orbital service (10) Repetition of items (6) to (9) (11) Periodic maintenance

5. Postface

We have described the results of studying the main functions and configuration of the 50-ton-class space factory expected to be realized early in the 21st century. In the future, we plan to further study technical development methods in particular, with the aim of realizing the space factory.

Design of Jupiter Probe System Using Space Station

43065013h Tokyo PROCEEDINGS OF THE 32ND SPACE SCIENCES & TECHNOLOGY CONFERENCE in Japanese 26-28 Oct 88, No 3B3 pp 584-585

[Article by Tatsuaki Takai, Eiji Nakagawa and Toru Nakano of NEC Corporation]

[Text] 1. Preface

Various spacecraft based on a space station project have been proposed in accordance with its anticipated characteristics (e.g., co-orbital platform). We have studied a planet probe system based on a space station so that experiments can be conducted using this spacecraft concept, and the following is a report of the planet probe system. The Jupiter probe has been regarded as a target since Voyager and Galileo exist as actual models, facilitating the carrying out of studies and making of comparisons. Other planet probe missions can be studied in the same way.

2. Merits of Space Station Base

The following are advantages gained by regarding this kind of probe system as a space station base:

a) The loosening of restrictions on payload weight according to the performance of the probes to be launched

In the planet probe system, it is necessary to obtain a certain speed in order to separate from the gravisphere,

which includes the weight range of the probes to be launched, and to distribute the weight of the propellant required by these probes to reach the intended planet orbit. Therefore, when the performance of the rocket to be launched is determined, the absolute upper limit of the weight of the probe will also be determined. Shortening the arrival period or increasing the ΔV capability will bring about an increase in the amount of propellant required, and will require the weight of the probe to be reduced. The ΔV capability enables humans to diversify the observation.

If it is possible to individually launch a probe proper and a booster for separating from the gravisphere and for operating the Jupiter sphere maneuver, and to assemble them in orbit, the payload will be increased by making the booster a multistage one. Figure 1 shows the relationship between the payload weight and the amount of propellant in the following two cases by means of a simple comparison. One case involves the H-II rocket being launched and injected once into a mission orbit based on the fact that an 8,000 kg (= weight of probe proper + that of booster) space station would be possible to inject into orbit, while the other case involves a probe proper, launched separately, being installed on a booster weighing 8,000 kg.
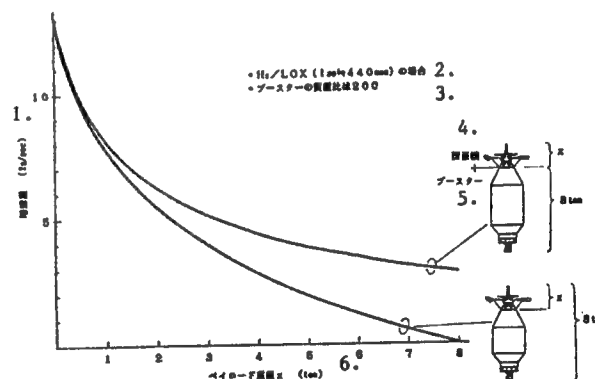
Figure 1. Relationship Between Speed Increase and Weight of Probe According to Launch System

Key:
1. Amount of speed increase (km/sec)
2. In the case of H_2/LOX (I_{sp} is approx. equal to 440 sec)
3. Mass ratio of booster is 200
4. Probe
5. Booster
6. Payload weight x (ton)

b) Flexibility of configuration

The aperture of the Voyager antenna shown in Figure 2 is restricted by the fairing, and is approximately 3.7 meters. This fact restricts the performance of the telecommunications lines. The folding-type mesh antenna shown in Figure 3 is used in the Galileo, and the aperture

of the antenna is 4.8 meters. If it becomes possible to transport antennas divided into sections and to assemble them on a space station, large, highly-accurate dishes can be used. The observation platform and supporting boom of the radioisotope thermoelectric generator [RTG] have, so far, been folding types, but if they can be assembled instead, their shapes will be advantageous in terms of rigidity, strength, etc., and the folding mechanism will not be necessary.

Figure 2. Voyager Spacecraft from NASA SP-420
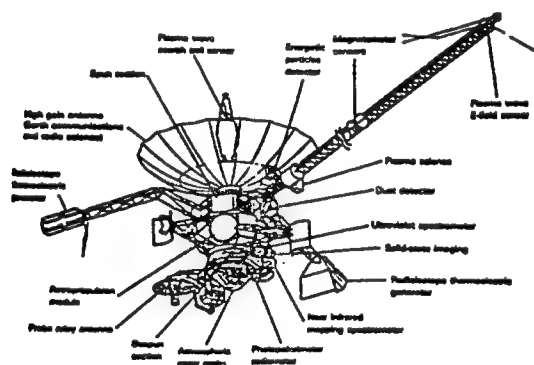
Figure 3. Galileo Spacecraft from NASA SP-479

c) Rise in reliability

It is possible for humans to conduct the final inspection, in orbit, of a probe which has been assembled in a station and to keep it linked with the space station at all times. Therefore, compared with the conventional orbital inspection, it will be possible to check such probes more flexibly and effectively.

d) Flexibility of operation of injection into mission orbit

Conventional probes have had low flexibility of the SOE, from launching to injection into mission orbit, due to the ground station visibility characteristics, etc., of the parking orbit. This lowness restricts the launch window

for the parking orbit separation to one which satisfies the relationship between the positions of Jupiter, the Earth and the required probe. However, when the space station base is used, the visible range restriction on the earth station can be ignored by giving the injection and operation control to the space station. Also, only conditions needed to rendezvous with the space station will be required in the case in which the rocket is launched from the ground. Accordingly, if it is possible to ensure assembly in orbit and the time margin for the final inspection, the period for launching from the ground can be determined on a relative and flexible basis.
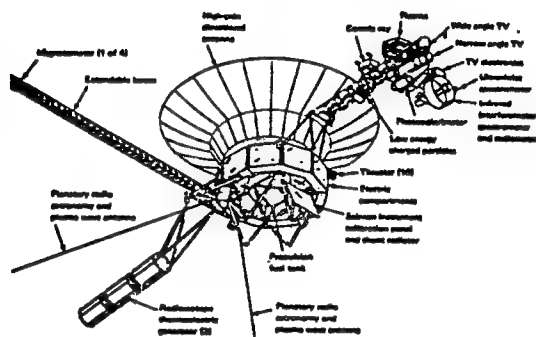
3. Conclusion

The above-mentioned concept presents a technical possibility that can be studied now, but involves many items that should be investigated in order to evaluate the merits and feasibility of this concept. However, when a sample return and a manned mission are assumed, significant advantages can be realized by constructing a system employing a space station.

Extravehicular Activity Discussed

[Article by Noriyoshi Arai and Kazuhiko Kamezaki of the National Space Development Agency of Japan; Kazuhiro Aizawa and Katsumi Fushiki of Ishikawajima-Harima Heavy Industries Co., Ltd.]

[Text] 1. Preface

Extravehicular activities [EVAs] inside and outside the living area of the space station are required for the construction, operation and maintenance of the space station [S/S] and the Japanese experimental module [JEM].

Such EVAs are indispensable for the operation and maintenance of the JEM's exposed facility [EF] since missions under exposed environmental conditions are being considered for the EF. This paper reports the EVA concept and results of preliminary designs corresponding to EVA to be used in the development of EFs.

2. Outline of EVA

2.1 Development of EVA System

Leonov was the first ever to participate in EVAs when the Soviet Union launched Vostok-2 in 1965. This was a demonstration, with the United States beginning full-scale EVAs during Project Gemini. Subsequently, lunar activities, lasting for 12 hours, were undertaken by Project Apollo, orbital experiments for full-scale EVAs were conducted repeatedly by Project Skylab, and an EVA system was put to practical use in the space shuttle project.

The main elements comprising the development of the EVA system are the space suit, extravehicular mobility unit [EMU], extravehicular excursion unit [EEU], etc., and in the S/S, their operational costs must be low, their activities high and their maintenance and inspection in orbit simple. The EVA system for the shuttle [STS] is

Table 1. Comparison of Conditions Required in Design of STS EMU and Those Required for Design of S/S EMU

	STS EMU	S/S EMU	
軌道上滞在期間 /.	3～7日 7.	90日～1年 14.	
EVA作業回数 2.	0～3	3/週 15.	
		39/90日～ 156/1年	16.
EVA時間 (hr) 3.	0～21	250～1000	
チェックアウト 4.	マニアル 8.	自 動 17.	
5. EMUへの補給手段	マニアル補給 9.	自 助 補 給 18.	
6. EMU/MMUの	10. 非常に限定された内容のみ	モジュール化がなされモジ	19.
軌道上の保守/保全	11.・ベアリングの潤滑	ュール毎に交換	
	12.・故障品の削除	・定期交換 20.	
	13.・故障品の目視検査	・不定期交換 21.	
		・サイズ調整 22.	
		・故障品の自動検知と表	23.
		示	

24. 軽量化
25. 長寿命化
26. 機動性向上
27. 装着の迅速化
28. 圧力洩れの低減化
29. 耐デブリス性向上
30. 自動チェックシステム化
31. 低開発コスト化

Key:
1. Orbiting period
2. EVA frequency
3. EVA time (hours)
4. Check-out
5. Means of supplying EMU
6. Orbital maintenance of EMU/MMU
7. 3 to 7 days
8. Manual
9. Manual supply
10. Very limited contents only
11. Bearing lubrication
12. Removal of malfunctioning products
13. Visual inspection of malfunctioning products
14. 90 days to 1 year
15. 3 times/week
16. 39 times/90 days to 156 times/year
17. Automatic
18. Automatic supply
19. Modularization and replacement of every module
20. Regular replacement
21. Irregular replacement
22. Adjustment of size
23. Automatic detection and indications of problems
24. Lightening
25. Lengthening of working life
26. Increase in maneuverability
27. Increase in mounting speed
28. Decreasing pressure
29. Raising resistance to debris
30. Automatic checking of systematization
31. Reduction in developmental cost

going to be modified. Table 1 compares the EMU functions of the STS and those of the S/S which are based on the STS EMU functions.

2.2 EVA Required in S/S

Many EVAs are required in the S/S, as is the construction and operation of the ground-based experimental facilities from the standpoint of space experimental facilities. Compared with the contents of EVAs in the STS, many of those of the [S/S] EVAs are varied and complex. In addition, the EVAs in the S/S require long working times. In order to satisfy these requirements, the following has been planned: the pressure in the space suit must be 57.3 KN or more per square meter so that the EVAs can be started promptly, within 30 minutes, by using the EMU in the S/S, in addition to the functions shown in Table 1. Also, with regard to the EVA contents, construction support of the S/S, maintenance (240 man-hours/year), experimental support (280 man-hours/year), and emergency measures for the S/S (104 man-hours/year) are planned for the initial phase of the S/S.

3. S/S EVA System and JEM's EVA

Table 2 shows the configuration of the EVA system in the S/S and the developmental allotments of the JEM being planned. It is necessary to design and study a portion of the EVA system since the JEM will receive EVA services. Specifically, it will be necessary to carry out the design for the transfer of EVA crewmen and support equipment and materials, as well as the design to ensure the safety of those EVA crewmen while at work. A test of these EVA systems is scheduled to be conducted in a Japanese water tank, and the performance of the EVA systems is scheduled to be verified. In addition, EVAs will be undertaken by Japanese crewmen to be launched in a satellite in the future.

Table 2. Partial Allotments for Development of JEM in S/S EVA System

Contents of S/S EVA System Configuration	Partial Allotments for Development of JEM
1. EMU/MMU/supporting unit	Nil
2. Maintenance and inspection system of EMU/MMU/supporting unit	Nil
3. Supply system	Nil
4. Communications system with crewmen	Nil
5. Crewman tracking system	Nil
6. Offering of services	*
7. Crewman rescue system	Nil
8. Environment monitoring system	Nil
9. Air lock system	Nil
10. Transfer/movement system	*
11. Illumination	*
12. Arresting tools	*
13. Tools and support equipment	*

* shows the existence of partial allotments for the development

4. Design Corresponding to EVA of JEM's EF

4.1 Contents of JEM's EF EVA Task

The following items can be cited as EVAs in the EF: 1) the initial assembly of the EF and pressure module [PM], 2) replacement of orbital replacing unit [ORU] when orbital manipulator is malfunctioning, and 3) removal of failures from extravehicular excursion unit [EEU]. Figure 1 shows an example of this EVA concept.
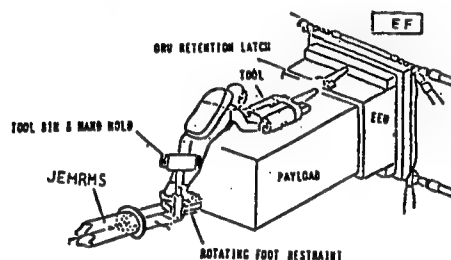

Figure 1. Removal of Problems Involving EEU and EVA

4-2 Design Items for JEM's EF

The design items corresponding to EVAs can be broadly classified into two categories: one is the design and study involving the receiving of EVA services, and the other is the design of facilities necessary for the above design and study. Table 3 shows the contents of these items.

Table 3.
Design Items Corresponding to JEM's EVA

Study of Design	EVA access route	Access route and route safety
	Adaptability of working environment and its verification	Working space, illumination, etc.
	Adaptability of contents of work and its verification	Weight to be used and capacity
		Working time, support equipment, etc.
	EVA working procedure manual and its verification	
Hardware design	Installation of arresting tools for portable foot restraints	
	Hand rail/hand-held tools/ (drill adapter, etc.)	
	Tether fixture	

For example, when EVA crewmen use screwdrivers to remove payloads under null gravity environmental conditions, they will be rotated along with the payloads unless they are able to fix their feet. Accordingly, foot fixings, etc., are very important for the EVA work.

5. Postface

The JEM represents the first EVA in Japanese space development. It is necessary to study the following items further, including verifying the EVAs in the JEM, before asking NASA for EVA services since NASA is quite experienced in such EVAs. (1) Analysis of contents (including analysis of resources) of EVA task (2) Method and contents of verifying EVA task in JEM (3) Adjustment of interface with NASA

Geostationary Earth Orbit Orbital Service Vehicle

[Article by Tetsuo Yasaka of NTT Radio System Research Institute]

[Text] 1. Preface

It has been recognized that the orbital service vehicle [OSV] is a part of the infrastructure that will inevitably be introduced to space activities in the near future. OSVs are currently being studied in Japan and in other countries since they will be used to join humans in carrying out work in orbit and are limited to those for low earth orbit [LEO], i.e., personnel, for the time being, will remain near the space station.[1, 3] The precedence of OSVs for geostationary earth orbit [GEO] is limited, because there is no plan to branch out human activities into the GEO. However, the majority of the current space market is for geostationary orbit missions, and the importance of GEO missions will not change in the future. The importance of OSVs is similar to that of LEOs, i.e., these OSVs are urgently required. It is believed that the study of the geostationary earth orbital service vehicle [GEO-SV] should be initiated with an approach differing from that taken toward the OSV.

2. Scenario of OSV Operation

OSV operation can be considered to take the following three forms: (1) Ground based: After completion of the specified work, return to the earth (2) Station based: Start from and return to space station (3) Independent: Basically, neither supply nor modification is premised. No recovery theoretically

Very specialized missions (maintenance of space telescope, etc.) would be based on item (1), because they are accompanied by complex ground preparations. Item (2) is effective for the work around the space station, coming and going between co-orbital platforms, etc. Item (3) is for missions that do not require many consumables, and is effective only when there are many customers that can rendezvous with only small increases in speed. Special-purpose OTVs are required for geostationary satellites since an increase in speed of 4 km/second is required for the coming and going of space planes corresponding to items (1) and (2). It is technically possible to increase the speed, but is quite difficult to do so economically. Currently, 200 customers occupy geostationary orbits. The geostationary orbit is the only operation area suitable for item (3), and this item is the only method of operation that will be economically possible in the near future. However, when a geostationary platform is studied further in the future, it can be expected that this

method will develop to the unmanned form (second generation) mentioned in item (2). Figure 1 shows the relationship among the amount of propellant, the increase in speed required for rendezvous, and the number of services which can be executed in one year.[2] The annual increase in speed of the GEO-SV is 100 meters/second, which is about twice that required for retaining normal orbits. The GEO-SV can rendezvous 15 satellites, and can supply actual work services for a week to respective satellites. It is possible to operate the GEO-SV continuously, without replenishment, for 3 or 4 years, because the propellant load is small. The GEO-SV can execute approximately 50 services during its working life.
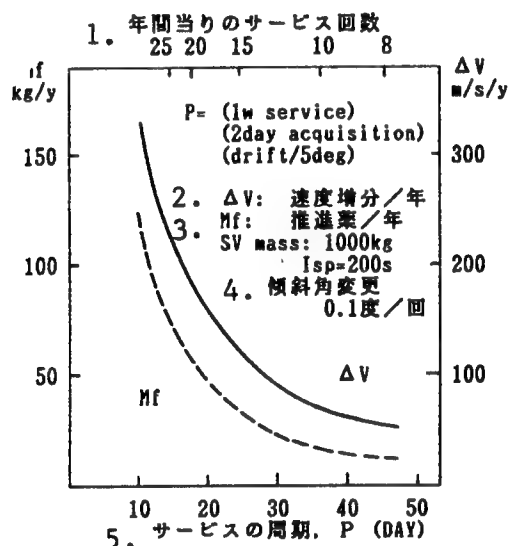

Figure 1. GEO-SV Service Capabilities
Key:
1. Number of services per year
2. ΔV: Increase in speed per year
3. Mf: Propellant per year
4. Change in inclination: 0.1°/number
5. Service cycle

3. Orbital Work Team

The main missions of the GEO-SV have been assumed based on NASA's OMV Reference Mission.[3] (See Table 1.) The first generation GEO-SV is for single function satellites with weights from 0.5 to 2 tons. The second generation is classified into two kinds—one is the satellite premised on the GEO-SV, and the other is one at the advent of GEO platforms. The first generation-GEO-SV is limited to visual inspection, changing position and orbit, and handling very simple tasks. The contents of GEO-SV services have been further studied for every relationship between the position of the GEO-SV and that of the satellites with respect to a) docking, b) rendezvous and c) acquisition, which is midway between items a) and b). (See Table 2.) Precise work, such as

Table 1. Orbital Task Items

OMV Reference Mission	GEO-SV I	GEO-SV II
LARGE OBSERVATORY SERVICING	—	—
PAYLOAD DELIVERY	—	—
PAYLOAD RETRIEVAL	—	○
PAYLOAD REBOOST	○	○
DEBOOST REENTRY	—	○
PAYLOAD VIEWING	◎	◎
SUBSATELLITE	—	—
MULTIPLE PAYLOAD	○	○
REMOTE SERVICING	○	◎
MODULE CHANGE	—	○
BASE SUPPORT	—	○
OTV/PAYLOAD TRANSFER	—	○

replacing modules, replenishing propellant, etc., is limited to objects with special-purpose docking ports. Accordingly, it is believed that the tasks mentioned in item a) will be subsequent to the second generation. The tasks mentioned in b) and c) do not require the replenishment of a large number of consumables or materials, but demonstrate the possibility of a GEO-SV accessing a very large number of geostationary satellites and offering services to them.

**Table 2.
GEO-SV Services**

a) Docking mission	
Module Exchange	Cooperative target only
Repair	
Refuel	
Satellite retrieval	
b) Rendezvous mission	
Visual monitor	2D, 3D; Fine, coarse
Temperature monitor	IR scan
Dynamics observation	approx. 100 Hz, Point trace
RF reception, mapping	approx. 50 GHz
c) Grapple mission	
Deployment assist/repair	Pull, shake, unscrew, screw
Deorbit	Tumble deorbit,+500 km
Minor repairs	Exterior only

4. Problematical Points and Subjects

The GEO-SV involves many systematic and legal problems rather than technical ones, i.e., international agreements are required for all of the following matters: indemnities for customers and non-customers, guarantees and persuasion for satellite holders who do not like proximity observation, operating the main body and earth station network, service frequency, etc. The level of difficulty of the technical subjects is lower than that of the OSV subjects currently being studied, i.e., the second generation will gradually require most of the robot

technologies that will be developed enthusiastically in the future. It is believed that the first generation will require only elementary remote-control equipment.

5. Conclusion and Effectiveness of GEO-SV

Most of the previous orbital and initial problems experienced by satellites can be remedied with the first generation GEO-SV outlined in this paper. When the satellites being used are deorbited with this GEO-SV, their working lives can be increased by approximately half a year, and the satellites used and thoughtlessly abandoned in the past can finally be removed from their orbits. The orbital and visual inspection will facilitate satellite housekeeping and the correct derivation of an operational plan, as well as the auxiliary and critical command operations. The most important point of geostationary satellites is their economic efficiency, and the economic efficiency of the GEO-SV can be enhanced by reducing the risk and lengthening its working life. It is thought important to affix the first generation GEO-SV by tackling a small number of technical subjects through international agreements.

References

1. Iwata, Honma, "OSV," Proceedings of the 31st Space Sciences and Technology Conference, October 1987.

2. Nakaya, "Development of Space Robot—Proposal of Unmanned Space Station," Proceedings of 4th Space Station Conference, April 1988.

3. Huber, W.G., "Orbital Maneuvering Vehicle: A New Capability," ACTA ASTRONAUTICA, Vol 18, 1988 pp 13-23.

Developmental Concept of Spacecraft for Technical Experiment

43065013k Tokyo PROCEEDINGS OF THE 32ND SPACE SCIENCES & TECHNOLOGY CONFERENCE in Japanese 26-28 Oct 88, No 3B9 pp 596-597

[Article by Takao Anzai, Mitsushige Oda, Rhoichi Imai and Kazuo Ota of the National Space Development Agency of Japan]

[Text] 1. Preface

The platform [P/F] type spacecraft will occupy a very important position in future space activities in order for orbital missions to be conducted.

This paper mentions the developmental concept of the technical experiment spacecraft [STEP], which is an experimental aircraft of the P/F-type spacecraft, and the advanced concept subsequent to COP [co-orbital P/F], POP [polar orbital P/F], OSV [orbital service vehicle], OCM [orbital change module], etc.

2. Purpose and Location of STEP

Since fiscal 1986, the National Space Development Agency of Japan [NASDA] has established basic technologies for the P/F-type spacecraft, conducted scientific and engineering experiments, and has studied the concept of applied technology P/F [ATP] for use in carrying out environmental-use-related missions in space.

However, it is recognized that it is necessary to conduct orbital experiments on important basic technologies prior to their practical use in order the review the system and to reduce the developmental risks resulting from the delay of the station plan because the ATP has been premised on receiving services from the space station.

The purpose of the STEP as an experimental aircraft of the P/F-type spacecraft is to conduct such orbital experiments, and problems involve the selection of mission contents and establishing STEP as a system.

On the other hand, it will be absolutely necessary that Japan attain the technologies for launching satellites, executing orbital missions and recovering these satellites in the future in order to freely participate in space activities to some extent.

Of these technologies, it will first be necessary to conduct orbital experiments on rendezvous docking [RVD] technologies and orbital service technologies as basic P/F technologies. The first mission of STEP will be to establish these technologies.

3. System Configuration of STEP and Developmental Concept

Figure 1 shows the system configuration of the STEP consisting of a core (resource + experiment) module, propulsion module and EX module (sub-satellite), which is a target of RVD experiments, etc. The core module and sub-satellite are linked to a docking mechanism, making it possible for them to be removed and installed in orbit.

Technical and orbital experiments for various services are scheduled to be conducted between the STEP proper and the sub-satellite based on ground commands directing the use of a remote-control-type manipulator mounted on the core module of the STEP.

Additional experiments on the following elemental technologies common to the P/F have also been studied as missions: (1) Two-phase fluid loop-type thermal control and exhaust heat technology (2) Data processing/handling technology according to optical data bus system (3) Very low gravity maintaining control technology (4) Others

Figure 2 shows a developmental concept involving the COP, POP, OSV and OCM technologies developed for the STEP.

4. Postface

The STEP is quite significant as an experimental aircraft for the future P/F-type spacecraft and as a testing basis for the development of elemental technologies which will form the foundation of such future space activities as the RVD, orbital services, etc. This fiscal year, we intend to carry out more detailed studies of the work described.
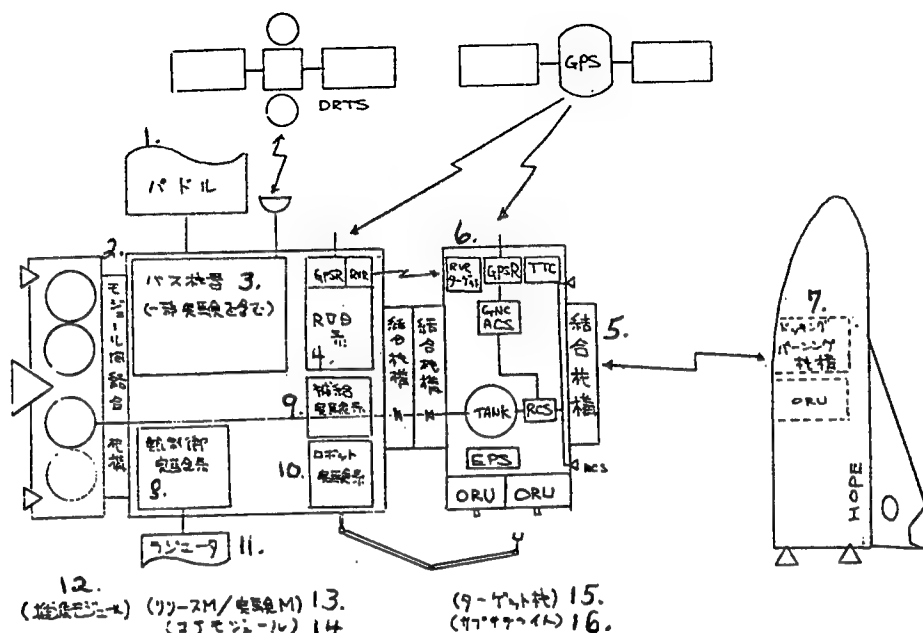
Figure 1. System Block Diagram of STEP

Key:
1. Paddle
2. Combination mechanism between modules
3. Bus equipment (including experiments)
4. RVD system
5. Combination mechanism
6. RVR target
7. Docking and berthing mechanism
8. Experimental thermal control system
9. Experimental supply system
10. Experimental robot system
11. Radiator
12. (Propulsion module)
13. (Resource M/experiment M)
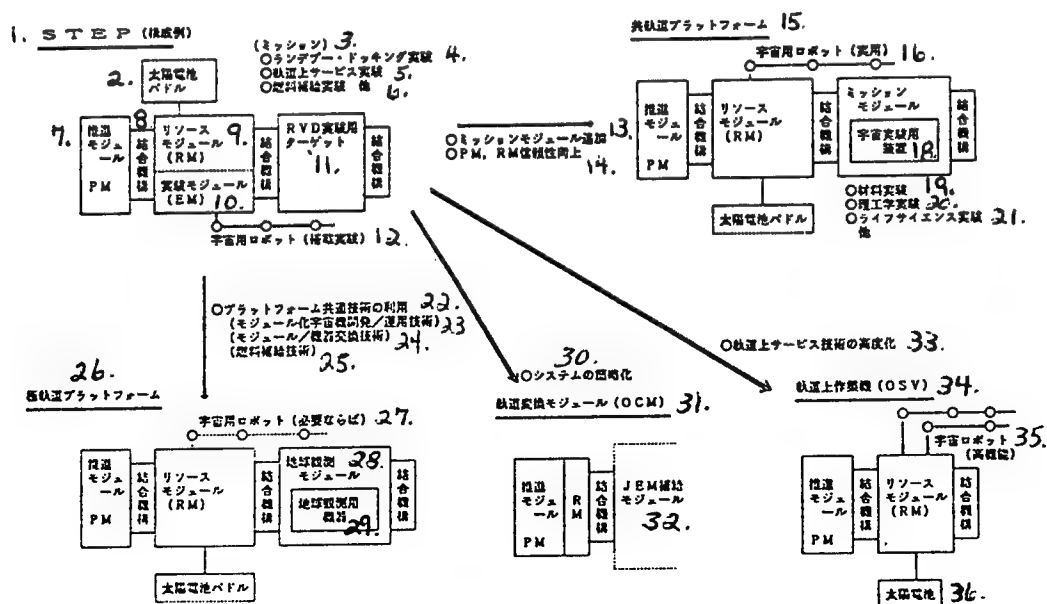14. (Core module)
15. (Target plane)
16. (Sub-satellite)

Figure 2 continued on next page.

Figure 2. Conceptual Drawing of Development of STEP Technology

Key:
1. STEP (example of contents)
2. Solar cell paddle
3. (Mission)
4. Experiment on rendezvous and docking
5. Experiment on orbital services
6. Experiment on supplying fuel, etc.
7. Propulsion module (PM)
8. Combination mechanism
9. Resource module (RM)
10. Experimental module (EM)
11. Target for experiment on RVD
12. Space robot (to be mounted for experiment)
13. Addition of mission module
14. Increase in reliability of PM and RM
15. Co-orbital platform
16. Space robot (for practical use)
17. Mission module
18. Space experimental unit
19. Experiment on materials
20. Engineering experiment
21. Life sciences experiment, etc.
22. Use of platform for common technologies
23. (Development of modularized spacecraft/operation technology)
24. (Module/equipment replacement technology)
25. (Fuel supply technology)
26. Polar orbit platform
27. Space robot (if necessary)
28. Earth observation module
29. Earth observation equipment
30. Simplification of system
31. Orbit changing module (OCM)
32. JEM supply module
33. Advancement of orbital service technology
34. Orbital service vehicle (OSV)
35. Space robot (high functioning)
36. Solar cell

Conceptual Design of Multipurpose OSV

430650131 Tokyo PROCEEDINGS OF THE 32ND SPACE SCIENCES & TECHNOLOGY CONFERENCE in Japanese 26-28 Oct 88, No 3B10 pp 598-599

[Article by Hiroaki Obara, Naoki Tsuya and Toru Takagi of Mitsubishi Electric Corporation]

[Text] 1. Preface

The OSV is a spacecraft used to carry out such services as the replacement and recovery of samples and equipment from platforms, the supply of consumables, such as propellant, etc., towing to recover and unfold platforms, and the orbital inspection of platforms. It will discharge its important duties through the effective and efficient operation of space infrastructures around the end of the 1990s. This paper introduces an example of the conceptual design of the OSV, specifically the mission requirements, a system outline and key technologies.

2. Analysis of Mission

The following items can be thought of as main missions (service-related items) of the OSV: (1) The unfolding and recovery of co-orbital platforms in orbit (the space station would serve as the base). (2) The recovery of a logistic module, etc., launched and injected in the vicinity of the space station, and returning it to the base. (3) The replacement of a mission payload with a new one on a platform. (4) The inspection and repair (replacement of equipment) of platforms. (5) Supplying samples to the platform and recovering products. (6) Supplying consumables, such as liquids, gas, etc., to the platform. (7) Recovering debris and satellites. (8) The orbital assembly and support of large space structures. Of the above items, (1) to (6) refer to the platform premised on OSV services, while (7) and (8) do not always involve

sufficient interface with the OSV in regard to services. For this reason, in order to execute the latter services, more advanced technologies are required for the OSV. The following system was studied taking into consideration the possibility of extending the development of the first generation OSV to that of the the next generation. This OSV will carry out the basic services mentioned in (1) to (6) with respect to the platform.

3. First Generation OSV

3.1 Premise

The first generation OSV is based on the following system design contents: (1) The OSV's operation is based on the space station. (2) All service-related factors are planned in advance, and, theoretically, are executed automatically. The introduction of operations to the OSV is permissible, however. (3) The platform is designed so that it can satisfy the interface conditions necessary for the RVD, taking into consideration the use of the ORU in the mission payload and the OSV interface involving the modularization of basic equipment, etc.

3.2 Outline of System

An example of the system design is shown below. Table 1 shows the main performances of the first generation OSV. Figure 1 is a block diagram showing the system configuration. The OSV is divided into three modules, i.e., the interface module [IM], bus module [BM], and propulsion module [PM]. The IM carries out direct services for the spacecraft, the BM autonomously controls the OSV, particularly its system, and the PM offers propulsion functions. The respective modules are interconnected through a standardized interface. Accordingly, it is possible to unfold and expand the OSV system by replacing modular units.
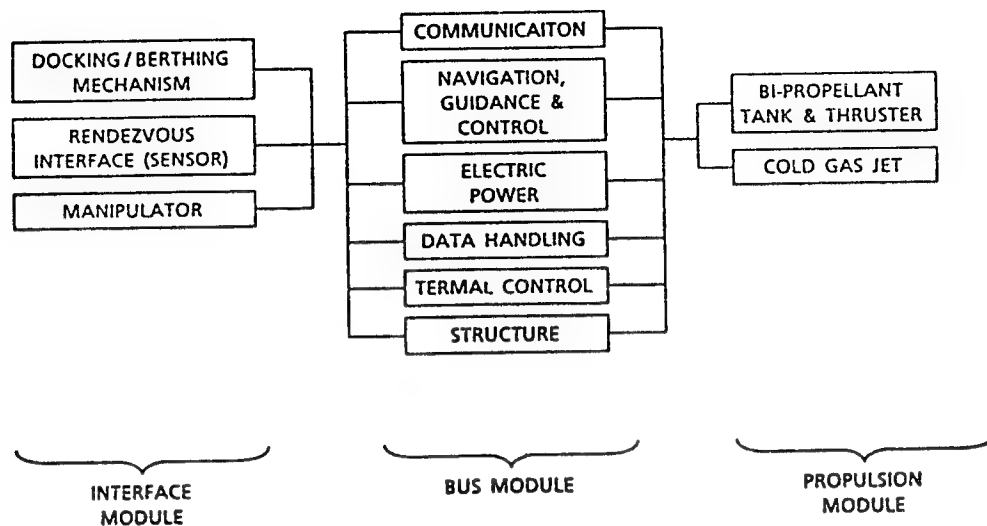
Figure 1. Block Diagram of the Initial OSV

Table 1. Summary of OSV Characteristics

Base	Space based: Japanese Experiment Module Space Station, Coorbital platform, Space Station
Operation orbit	inclination: 28.5°; altitude: 400-700 km
Dimensions	φ4.6 x 3.8 m
Weight	4 tons (including payload)
Payload	1 ton (max)
Working life	10 years

3.3 Key Technologies

Of the key technologies necessary for future development, the particularly important key technologies for realizing the first generation OSV are as follows: 1) autonomous operating technology, including sensor system, 2) service factor planning technology and its tools, 3) RVD technology, and 4) manipulator technology. Items 1) and 2) are included in the BM, while 3) and 4) are included in the IM. With regard to 1), it is necessary to study and consider the autonomous operating technology in regard to every subsystem at the module and system levels so that missions can be executed efficiently. It is necessary to include the ground system when studying 2), and to include the sensor system, navigation and guidance system and attitude control system when studying 3). Also, with regard to 4), it is necessary to develop an actuator, which constitutes a manipulator, and to develop a technology for automatically and autonomously controlling the movement of the manipulator.

4. Developmental Concept for Next Generation

It is possible to carry out cooperative work by using a manipulator system with a number of arms as part of the development of autonomous technologies, and it is also

possible to execute the more advanced services mentioned in items (7) and (8) of section 2. In such a case, the next generation OSV system would be formed by combining more advanced IMs and PMs.

Operational Concept of Platform

[Article by Hiroaki Obara, Naoki Tsuya and Toru Takagi of Mitsubishi Electric Corporation]

[Text] 1. Preface

Preparations for space infrastructures, specifically a space station, will be started in the late 1990s, and various platforms, such as coorbital platforms, geostationary platforms and polar orbital platforms, are scheduled for launching. The kinds of orbits vary, and when these platforms are classified according to purpose, the number of platforms will become very large. However, common characteristics have been narrowed down to the following: 1) the platform will be a spacecraft that is operated efficiently by means of orbital services, 2) numerous mission payloads will be mounted on the platform, and 3) it will be possible to replace these payloads with others (whether or not this replacement is carried out in orbit depends on the platform purpose). This paper describes the system design and developmental concept, and specifically the basic technologies for the platforms, taking these common characteristics into consideration.

2. Basic Technologies for Platforms

2.1 RVD Technology

RVD technology is one of the most basic technologies for platforms premised on orbital services, and can be broadly classified into two kinds, i.e., RVD technology for multiple spacecraft and that for spacecraft connected to a space station. In addition, RVD technology can be classified by docking system, i.e., docking technology and berthing technology. However, it is necessary to design equipment that can be used for any case since it is expected that the equipment wil be used in common for both rendezvous and docking purposes. Also, it will be necessary to operate the platform autonomously, including the attitude control, because a GPS will be used to guide the platform. In addition, it is expected to be necessary to establish an automated RVD technology for the platform, including the sensor and actuator, and to standardize the RVD interface.

2.2 Orbital Service Technologies

The main orbital service technologies are as follows: 1) orbital service technology using a manipulator, 2) technology for supplying consumables, such as the propellant, etc., 3) the design technology for modularization or technology for using the ORU in orbital work. The main contents of 1) include operation by means of a data relay satellite, autonomous technology which supports this operation, and image processing technology. The standardization of platform design and a standard interface are important for 2) and 3).

2.3 Platform Bus Control Technologies

Of the platform bus control technologies, the following three have entered the limelight: 1) autonomous control technology, including self-diagnosis, 2) data handling technology using an optical data bus, and 3) reconfiguration technology. Item 1) includes the autonomous operating control, up to the system level, of every sub-system, and must be considered together with partial charges involving the ground system. With regard to 2), it is necessary to define partial charges together with conventional electric signals, and to design a standardized interface. Item 3) includes a) technology for a navigation guidance system (including an actuator), b) electric power controlling technology, and c) large capacity thermal control technology using a two-phase liquid. Item a) must be able to cope with the fluctuation of mass characteristics caused by reconfiguration, and b) must be able to cope with fluctuation caused by the distribution of resources.

3. System Design

The system design of platforms is realized with the above-mentioned basic technologies. On the other hand, the bus section has many sub-systems that can either be used as is in any platform or can cope with relatively small design changes. The capability required for the propulsion section depends on the orbit in which it will be operated, but it is possible to make standard preparations for this section or to carry out a standard design. Therefore, in order to increase the efficiency of the
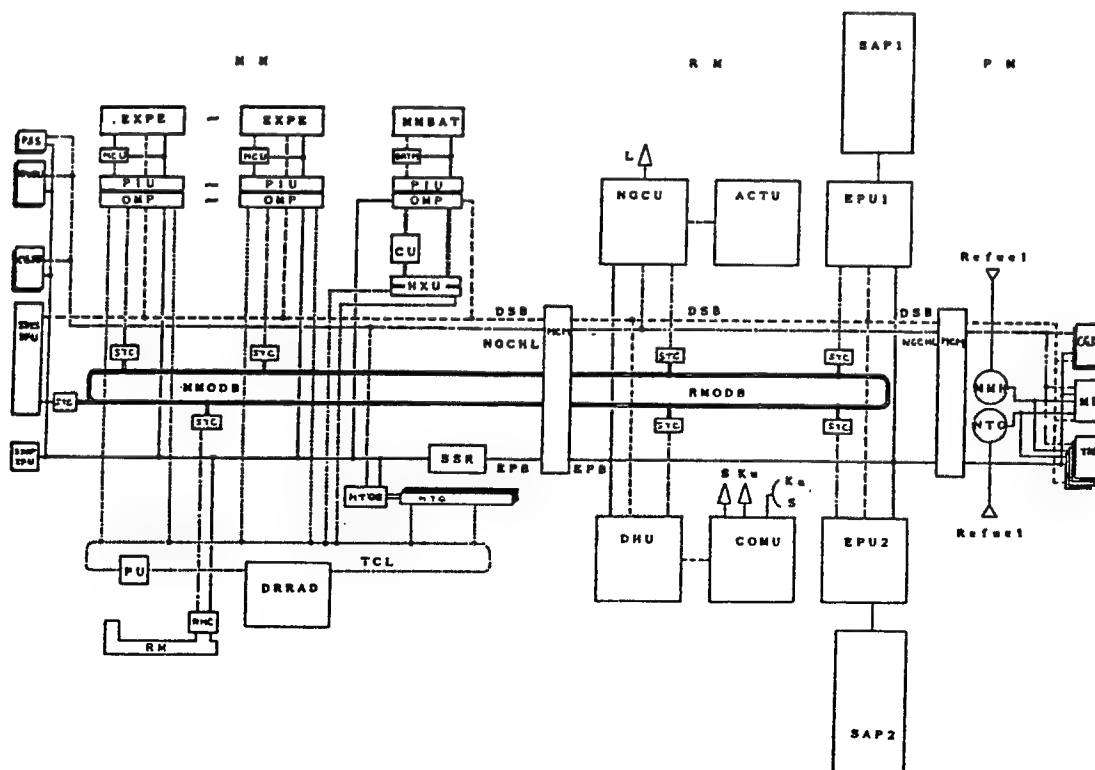

Figure 1. Example of Platform Contents

design work and to reduce the cost, it is preferable that the platform-like propulsion module [PM], bus module [BM] and mission module [MM] actually be modularized. In addition, when the sub-system is mini-modularized, it is possible to widen various platforms by combining modules. Figure 1 shows an example of the contents of a modularized platform.

4. Developmental Concept

The development of platforms is accompanied by the many technical subjects mentioned above, and most of the subjects, as basic technologies, affect the realization of these platforms. For this reason, it is critical that a basic platform technology be established and verified as the first step of the development work, and it is thought to be necessary to develop a platform for use in engineering tests prior to developing a practical platform.

Guidance, Analysis of Rendezvous With Space Station

43065013n Tokyo PROCEEDINGS OF THE 32ND SPACE SCIENCES & TECHNOLOGY CONFERENCE in Japanese 26-28 Oct 88, No 3B12 pp 602-603

[Article by Isao Kono, Yasushi Wakabayashi and Hiroyuki Nakamura of the National Space Development Agency of Japan]

[Text] 1. Preface

The National Space Development Agency of Japan [NASDA] is currently developing the Japanese Experimental Module [JEM] for a space station [S/S], and is developing and studying such spacecraft as a space plane, the HOPE, COP, etc., which will for the foundation for the construction of future space infrastructures. The HOPE will be used to supply materials to the S/S and recover them, and the COP will be operated closely with the S/S.

The RVD technology for the S/S is an important orbital technology from the standpoint of international cooperation, as well as from the standpoint of Japan's ensuring her independence in space activities.

This paper reports the main subjects that should be studied in the future, and results of rendezvous analyses, based on the approach to the S/S that is currently being taken.

2. Features of RVD to S/S

Currently assumed as spacecraft that will carry out RVD to the S/S are: 1) a vehicle related to the ELM, 2) HOPE and 3) COP/OSV. The RVD to the S/S will possess the following characteristics: (1) An operating control zone will be defined around the S/S's orbit. (2) The RVD sequence will be determined before launching the spacecraft since the approach to the S/S has time restrictions from the standpoint of the S/S crewmen's work schedule. It will be necessary to assume that a sequence will not be changed following the launch. (3) It is anticipated that the RV orbit transfer will be carried out at an altitude of 250 to 370 km so that it does not interfere with the S/S's CVZ, since the lowest of the S/S's orbit will be 407 km. (4) It will be necessary for the OSC to have checked, in advance, the safety of the spacecraft which enter the CCZ. (5) Spacecraft in the CCZ must conform to the S/S control, and the OSC must make efforts to prevent emergencies while constantly monitoring the spacecraft. (6) The navigation of the spacecraft in the CCZ will be carried out based on the GPS, with data on the GPS transmitted to the S/S and data on targeting and relative navigation released from the S/S. (7) Unmanned spacecraft in the CCZ will be controlled by commands from the S/S, and will be brought closer to the S/S. Spacecraft unable to receive commands from the S/S will be towed with an OMV, etc., and brought closer to the S/S. (8) Spacecraft in the POZ will be brought closer to the S/S by remote control directed by the S/S crewmen, and will be berthed by an SSRMS operated by these crewmen. (9) Even when a rendezvous support system malfunctions, the spacecraft must be brought closer to the S/S and must be separated from it by means of a method that will not endanger either one, contaminate the S/S, or require any S/S elusion maneuvering. The constitution of a system for carrying out RVD to the S/S must be considered on the basis of the 1FO/2FS.

3. Analysis of Guidance and Control System for RVD to S/S

With regard to the guidance and control system of the HOPE as an example of a spacecraft that can carry out RVD to the S/S, an outline of the research involving the guidance and analysis of the contents, from launching to docking/berthing, is shown below each phase.

(1) Launching Phase There is one launch window in Japan each day, and it is currently considered to last about 10 minutes. The following items employing upper-stage spacecraft are being studied to lighten the burden of mating orbital planes: 1) the transfer and guidance of the H-II's orbital plane, and 2) fixing, as much as possible, the RVD sequence following launching.

(2) RV Orbital Transfer (Coarse Injection) Phase After the separation, the orbital altitude, phase and orbital plane will be adjusted and the RV orbit will be transferred so that the satellite can enter the RVZ at the specified time. In this phase, the inertial navigation system and the GPS-ST-IMU composite navigation system will be used during thrust flight and inertial flight, respectively. As a result of analyzing the navigation systems, it has been clarified that the orbit determining accuracy at a position of approximately 100 meters -3σ and a speed of about 10 cm/sec -3σ can be obtained in the GPS-R by using the C/A code + Doppler effect, and the attitude determining accuracy of $0.2°$ -3σ can be obtained in the attitude system by making gyro-alignments according to the ST approximately every 10 hours. It has also been confirmed that the satellite can be guided with the necessary accuracy in initial phase

mating maneuvers by means of targeting using conic propagation and the VIC guidance law, which is excellent at controlling the orbital form, and that it can be guided at the necessary accuracy in terms of altitude and final adjustment maneuvers of the orbital plane by means of targeting using precision propagation and the LRDV guidance law, which is excellent in terms of controlling the time of arrival. With regard to the sequence of orbit transfer maneuvers, the following is being studied, i.e., a method to determine the necessity of orbit transfer maneuvers at certain intervals.

(3) RVZ Injection Approach (Accurate Injection) Phase (Up to 45 km Point Shown in Figure 1) The satellite enters the RVZ from the TPI, conducts a rendezvous with others in the RVZ, and makes a relative stop at a point 45 km behind the S/S. The navigation system is the same as that of the RV orbit transfer phase. As a result of analyzing the navigation system, it has been confirmed that mid-course maneuvers are required once or twice because the accuracy of the absolute navigation is not sufficient.

(4) CCZ Injection Approach (Relative Approach) Phase (Up to 300 Meter Point Shown in Figure 1) A communications channel with the S/S is established, and the use of relative navigation is initiated by means of the GPS difference mode and rendezvous radar [RVR] equipment. In the case of the GPS difference mode, the status amount calculated at HOPE and the pseudo-range obtained from HOPE are transmitted to the S/S. In the S/S, the relative navigation is calculated, targeting is carried out, and the results are transmitted to HOPE. This method can realize highly accurate relative navigation that is not influenced by ionospheric delay, etc., as well as approach guidance controlled by the S/S. The

approaching flight path is based on the multi-path approach method from the standpoint of relative navigation accuracy and collision avoidance (even when maneuvers are not carried out, satellites do not enter the collision course). It has been determined that it is better to carry out mid-course maneuvers because higher navigation accuracy is required. The following matter is being studied, i.e., the target pointing attitude is controlled to within several km in order to ensure the visual field of the RVR equipment. It will be necessary to control the automatic flight to avoid collisions subsequent to leaving the CCZ. This matter is scheduled to be studied in the future.

(5) S/S (Final Approach/Berthing) Phase (Subsequent to 300 Meter Point Shown in Figure 1) In the S/S phase, it will be necessary to carry out research involving the following points. In order to cope with the S/S's remote control within approximately 300 meters, it will be necessary for the satellite to be capable of the appropriate acceleration (rotation and translation) and to have an automatic pilot mode corresponding to the S/S control panel. The NAL and NASDA are carrying out joint research on maneuverability, etc., because the details have not yet been determined. Automatic flight control technologies for attaining the 2FS are very important in the POZ, and details will be studied in the future.

4. Subjects Which Should Be Studied in the Future

We have outlined the S/S rendezvous-related research conducted up to now. The basic design of the S/S has not yet been finished, and certain matters are pending. In the future, we hope to study the following points further and to clarify the S/S rendezvous guidance and control system. (1) Launching phase: Launch window, method of
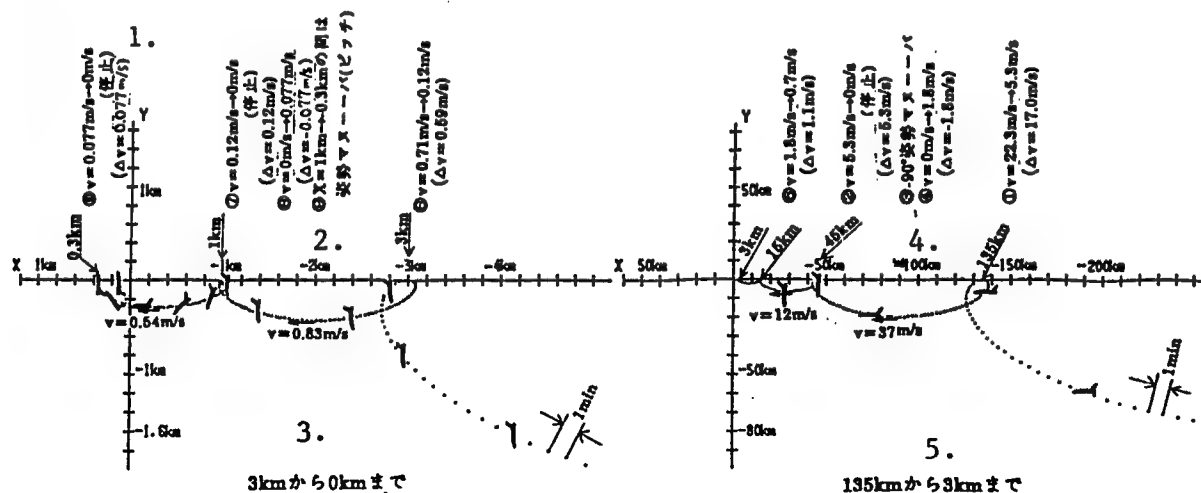

Figure 1. Rendezvous Profile to S/S (Subsequent to 135 and 3 km)

Key:
1. (Stop)
2. Interval between X = 1 to 0.3 km:
   Attitude maneuver (pitch)
3. 3 to 0 km
4. -90°-attitude maneuver
5. 135 to 3 km

mating and launching the orbital plane, and simultaneous orbital injection accuracy (2) RV orbit transfer phase: Method for setting rendezvous time, targeting method and navigation accuracy requirements (3) RVZ injection approach phase: RVD sequence in which recovery is taken into consideration, and navigation accuracy requirements upon approaching (4) CCZ injection approach phase: Automatic flight control, automatic flight path design and judgment criteria for CCZ injection (5) S/S phase: Collision avoidance system, remote-control performance and automatic pilot mode.

References

1. JSC-30000 rev. D, "Space Station System Requirements," January 1987.

2. JSC-30201, "Space Station Operation Plan," September 1986.

3. Letters, "NASA/NASDA H-II/ELM Supply Rendezvous Study (Plan)," July 1987 and May 1988.

Laser, Radar Equipment for Rendezvous

[Article by Hiroshi Anegawa, Yasushi Wakabayashi and Yasumasa Hisada of the National Space Development Agency of Japan; Ken Nagai and Norio Shimizu of NEC Corporation]

[Text] 1. Preface

Rendezvous docking is a basic technology, indispensable in the orbital infrastructure age. In order to promote this technology, it is absolutely necessary to use radar equipment to measure the relative distance, relative speed, line of sight [LOS] angle, relative attitude angle, etc., between spacecraft. Particularly, in order to carry out automatic rendezvous docking, it is necessary to measure short-distance areas by using radar equipment with much higher accuracy than that of the RF (microwave) radar equipment which has been used in the past by the United States, etc.

From this standpoint, the National Space Development Agency of Japan [NASDA] is conducting the research and development of rendezvous docking laser and radar equipment referred to as "rendezvous radar equipment." This paper outlines the research involving the design of the rendezvous radar equipment, the configuration of the equipment, etc.

2. Configuration of Laser and Radar Equipment

This is tracking-type laser and radar equipment with acquisition and tracking functions. Figures 1 and 2 show the configuration block diagram and a conceptual drawing of the equipment, respectively. The acquisition is carried out based on the information on the LOS angles of the target spacecraft transmitted from the navigation system by pointing semiconductor laser beams with a beam angle of
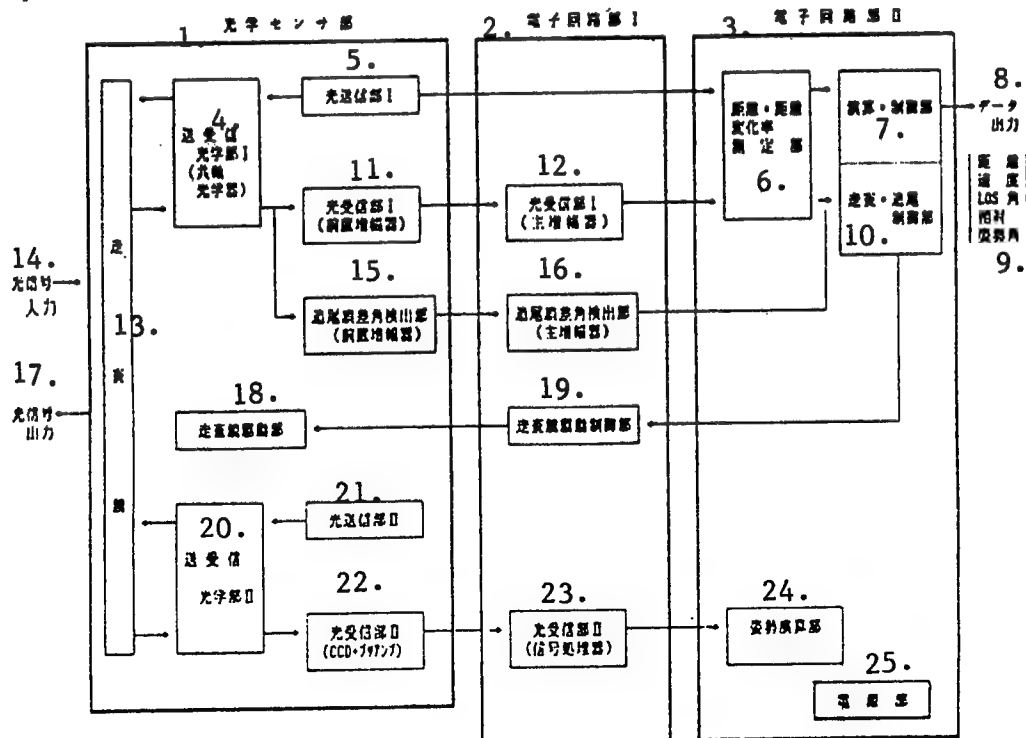
Figure 1. Block Diagram of Contents of Laser and Radar Equipment

Key:
1. Optical sensor section
2. Electronic circuit section I
3. Electronic circuit section II
4. Transmitting and receiving optical section I (coaxial optical equipment)
5. Optical transmitting section I
6. Distance and distance change rate measuring section
7. Arithmetic and control section
8. Data output
9. Distance, speed, LOS angle and relative attitude angle
10. Scanning and tracking control section
11. Optical receiving section I (preamplifier)
12. Optical receiving section I (main amplifier)
13. Scanning
14. Optical signal input
15. Tracking error angle detection section (preamplifier)
16. Tracking error angle detection section (main amplifier)
17. Optical signal output
18. Scanning driving section
19. Scanning driving control section
20. Transmitting and receiving optical section II
21. Optical transmission section II
22. Optical receiving section II (CCD + preamplifier)
23. Optical receiving section II(signal processor)
24. Attitude arithmetic section
25. Power source section
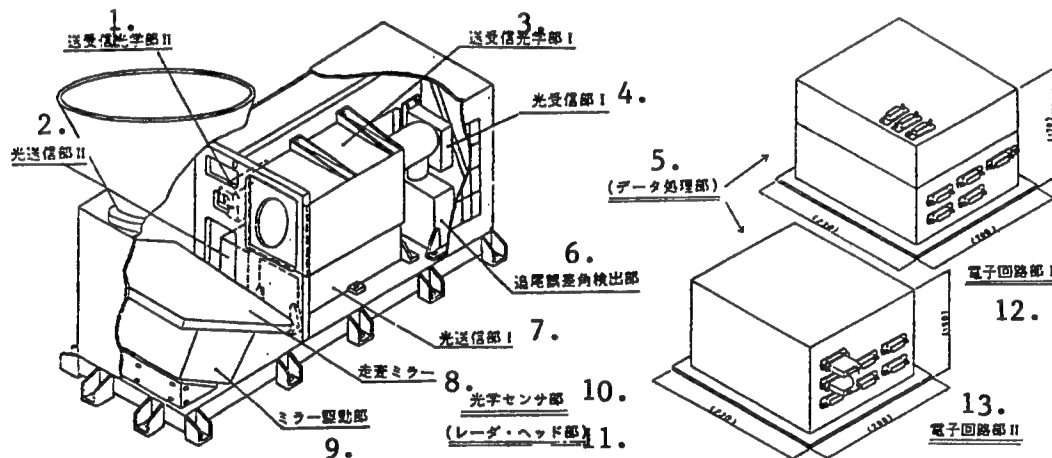
Figure 2. Conceptual Drawing of Laser and Radar Equipment

Key:
1. Transmitting and receiving optical section II
2. Optical transmitting section II
3. Transmitting and receiving optical section I
4. Optical receiving section I
5. (Data processing section)
6. Tracking error angle detection section
7. Optical transmitting section I
8. Scanning mirror
9. Mirror driving section
10. Optical sensor section
11. (Radar head section)
12. Electronic circuit section I
13. Electronic circuit section II

divergence of 0.05°, a wavelength of 0.8 micrometer-band, and an output of 10 mW, and by scanning an angle range of approximately 3° x 3° by means of a two-axis gimbal mirror. A corner cube reflector [CCR] is installed on the target spacecraft, and light reflected by the CCR is introduced into the Si-APD of optical receiving section I and the four-quadrant detector [QD] of the tracking error angle detection section, respectively, through the transmitting and receiving coaxial optical system. After the target spacecraft is acquired, it will be tracked while driving and controlling the two-axis gimbal mirror so that the angle error signal generated from the QD will be zero.

The distance is measured by amplifying and modulating the laser beams by means of tone frequency and by measuring the phase difference between the signals transmitted and received. Measurements with a distance ranging from 20 to 1 km are carried out at a

direct range rate based on a sub-carrier Doppler system using tone modulation signals of approximately 100 mHz. With regard to the detection of relative attitudes, the following method is being studied: the CCD detects two-dimensional patterns of the CCR installed on the target spacecraft within a relatively short distance area (approximately 200 meters or less). Table 1 shows the main specifications of the targeted laser and radar equipment.

Table 1.
Main Target Specifications

Item			Target Specification
Acquisition tracking performance/ measuring range	Acquisition tracking range		50 km to 2 m
	Acquisition tracking range rate		+/- 100 m/s or more
	Acquisition tracking LOS angle		Az +/- 15° or more
			El +/- 30° or more
	Maximum acquisition time		Within 20 s
Instrumentation performance	Range	20 km or more	Random (3σ): 2%
			Bias (o-p): 100 m
		20 to 1 km	Random (3σ): 0.5 m
			Bias (o-p): 10 m
		1 km to 2 m	Random (3σ): 2 cm
			Bias (o-p): 10 cm
	Range rate	20 to 1 km	Random (3σ): 0.4 m/s
			Bias (o-p): 0.2 cm/s
		1 km to 2 m	Random (3σ): 1 cm/s
			Bias (o-p): to 0 cm/s
	LOS angle	Az	Random (3σ): 0.1°
			Bias (o-p): 0.1°
		El	Random (3σ): 0.1°
			Bias (o-p): 0.1°
	LOS angle rate	Az/El	0.05° or less
Data renewal time			0.1 to 1 sec

3. Study of Maximum Measuring Range System

This radar equipment involves the cooperative passive method, and it is necessary to study the overall radar
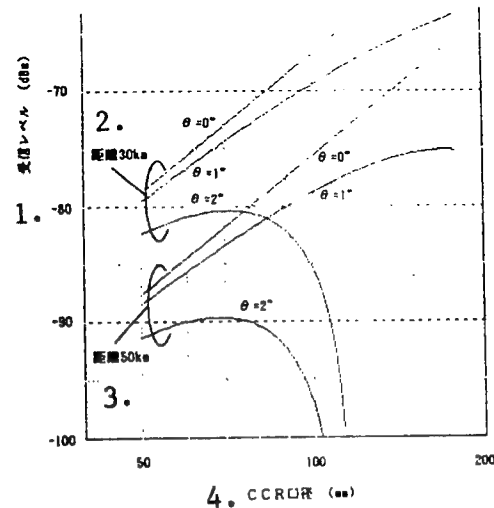

Figure 3. Optical Characteristics and Receiving Level of CCR

Key:
1. Receiving level (dB)
2. Distance of 30 km
3. Distance of 50 km
4. CCR Aperture (mm)

equipment system, including the optical characteristics of the CCR installed on the target spacecraft. Figure 3 shows the results of analyzing the relationship among the aperture of the CCR, the θ parallel deflection angle of beams, and the receiving level when there is one CCR. In the future, it will be necessary to carry out a further overall study of the maximum measuring range, the optical performance of the CCR, the number of CCRs, the laser output, etc., and to determine the optimum system arrangements based on these results.

4. Postface

We have outlined our study of the high performance rendezvous laser and radar equipment. In the future, we plan to further study the design of this equipment, to make a research model on a trial basis, and to conduct a test of this model.

Development of ORU Combination Mechanism

43065013P Tokyo PROCEEDINGS OF THE 32ND SPACE SCIENCES & TECHNOLOGY CONFERENCE in Japanese 26-28 Oct 88, No 3B16 pp 610-611

[Article by Eiichi Michioka, Ken Kishimoto and Akio Koyama of Mitsubishi Electric Corporation]

[Text] 1. Preface

One of the main missions of a platform-type spacecraft is to conduct an experiment utilizing the space environment in orbit, and it will be absolutely necessary to replace experimental units in orbit.

The replacement must be carried out promptly, and safety must be given sufficient consideration since the work will be carried out, unmanned, in orbit.

The following items can be considered as systems satisfying these requirements: (1) The experimental unit is integrated in a standard module structure termed an "orbital replacement unit" [ORU]. (2) The ORU is fixed on a spacecraft while transmitting and receiving the electric power, signals, heat, etc., required by this experimental unit through a standard interface termed an "ORU combination mechanism."

The following is a report on the functional model of the ORU combination mechanism manufactured on a trial basis.

2. Configuration and Specifications

The ORU combination mechanism serves as an electrical, thermal and mechanical interface between the ORU and the spacecraft, and consists of an ORU mechanism and a spacecraft mechanism.

This unit's system is simplified through the adoption of a method for installing and removing these interface elements simultaneously. With regard to the electrical combination, the electric power and signals are supplied by a general-purpose cylindrical connector. With regard to the thermal combination, the independent localizing function is increased through the adoption of a dry contact-type expansion-type heat exchanger that expands with the working fluid pressure. As for the mechanical combination, the weight is reduced by using a method in which a handle is installed on the side of the ORU, and is gripped and pulled by two gripping levers installed on the side of the spacecraft.

Table 1 shows the specifications of the ORU combination mechanism.

Table 1.
Specifications of ORU Combination Mechanism

Item	Specifications
System	Interface batch installation and removal
Electric combination system	Cylindrical connector
Electric power supply capability	dc 100 V x 20 A; 2 systems
Signal transmitting capability	13 circuits; 2 systems
Thermal combination system	Expansion-type heat exchanger
Heat exchange amount	0.3 kW
Mechanical combination system	
Guide system	Guide pin/cone
Positioning system	Guide pin/hole
Latch system	Handle/lever
Pull-in system	Screw/nut
Combination power	2,000 N
Holding power	20,000 N
Guide function	+/- 10 mm

Table 1.
Specifications of ORU Combination Mechanism (Continued)

Item	Specifications
Position accuracy	+/- 0.2 mm
Installation and removal stroke	100 mm
Power consumption (during operation)	20 W
Outside dimensions (in combination)	700 mm x 700 mm x 300 mm
Mass (pair)	45 kg

3. Outline of Trial Manufacturing

This unit has vacuum specifications and was made to a scale that is 70 percent of its actual size.

Figure 1 [not reproduced], and Figures 2 and 3 show photograph, an interface and the cross-sectional structure of the unit, respectively.
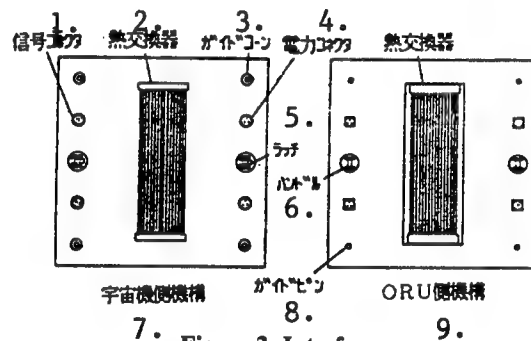

Figure 3. Interface

Key:
1. Signal connector
2. Heat exchanger
3. Guide cone
4. Electric power connector
5. Latch
6. Handle
7. Mechanism at side of spacecraft
8. Guide pin
9. Mechanism at side of ORU
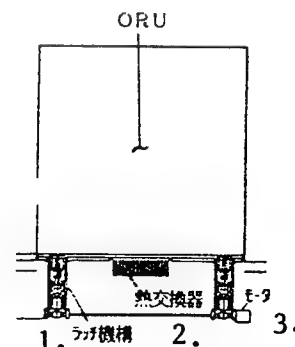
Figure 3. Cross-sectional Structure

Key:
1. Latch mechanism
2. Heat exchanger
3. Motor
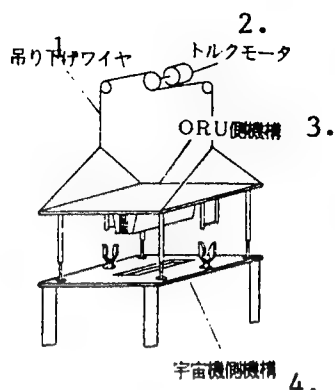
Figure 4. Test Configuration

Key:
1. Suspending wire
2. Torque motor
3. Mechanism at side of ORU
4. Mechanism at side of spacecraft

This unit requires a linear mechanism with a large stroke because it employs the expansion-type heat exchanger. The handle on the side of the ORU is gripped and pulled only with the driving motor installed on the side of the spacecraft in order to realize this linear mechanism.

4. Test

Figure 4 shows a test configuration. As shown in this figure, the ORU side mechanism is suspended by four wires from above, and gravity is cancelled with a torque motor.

Tests were originally conducted using manipulators, but the combination and separation were carried out by bringing the mechanisms closer to each other while finely adjusting the output of the above-mentioned motor.

The installation and removal properties, as well as the allowable misalignments, were checked simultaneously as items to be evaluated, resulting in all specifications being satisfied.

5. Summary

It has been confirmed that it is possible to install and remove various interface elements simultaneously by using this unit. In the future, we plan to collect data on the testing and operation of the expansion-type heat exchanger under a vacuum, and to evaluate the installation and removal by using a manipulator.

Synthetic Aperture Radar Antenna Mounted on ERS-1

[Article by Hideo Hino, Ryoichi Kuramasu and Yukiaki Nemoto of Resource Remote Sensing System Technical Research Association; Yoshiteru Ogata, Noriko Kanai, Nobuyuki Tajika, Kazuo Yazawa and Yamato Aizawa of Mitsubishi Electric Corporation]

[Text] 1. Preface

The synthetic aperture radar [SAR] antenna mounted on the earth resource satellite-1 [ERS-1] is a large folding-screen-type structure. A test of its unfolding was conducted by using an engineering model [EM] with electrical, mechanical and thermal performances almost equal to those of the actual structure. The following is an outline of this test.

2. Folding Screen Operation of SAR Antenna and Technical Background

This antenna is the largest in Japan, is unfolded to about 12 meters in the specified orbit, and is mounted on a satellite. Its unfolding mechanism and operation represent an extension of the conventional folding-type solar cell paddle technology, but differ greatly from conventional ones in respect to the following items: 1) a unique three-stage unfolding and operation sequence has been adopted in this antenna (see Figure 1 and Table 1), and 2) the paddle does not pose any problems, but latch-up accuracy and determent of thermal deformation are required in the antenna. In addition, unlike usual aperture antennas, it is an array antenna equipped with a feed circuit. Therefore, this antenna possesses the following characteristics: 3) the moment of inertia of the antenna panel is large for the area, and 4) flexibility regarding the unfolding movement is required for a portion of the feed circuit. It can be said to be quite difficult to realize a folding efficiency equivalent to that of paddles and to simultaneously meet all the requirements. It can also be said that devising a method for conducting ground-based unfolding tests of such a large and complex folding structure represents a substantial developmental subject.

**Table 1.
Unfolding Operation and Corresponding Mechanism**

Unfolding Operation	Holding/ Releasing	Unfolding/ Latch	Synchronous Control
90°-rotation	Holding and releasing mechanism	Center hinge	
Elongation of both wings	Folding prevention mechanism	Double hinge/ panel hinge	Unfolding synchronous cable
Off-nadir inclincation	Center hinge	Center hinge	

3. Outline of EM Unfolding Test

Unfolding tests were conducted to ensure that the EM possessed the specified unfolding capabilities and to obtain data on the unfolding characteristics. The test method is as follows: the empty weight is cancelled by suspending a specimen on the folding test jigs, the unfolding rotation axes are set perpendicularly and,
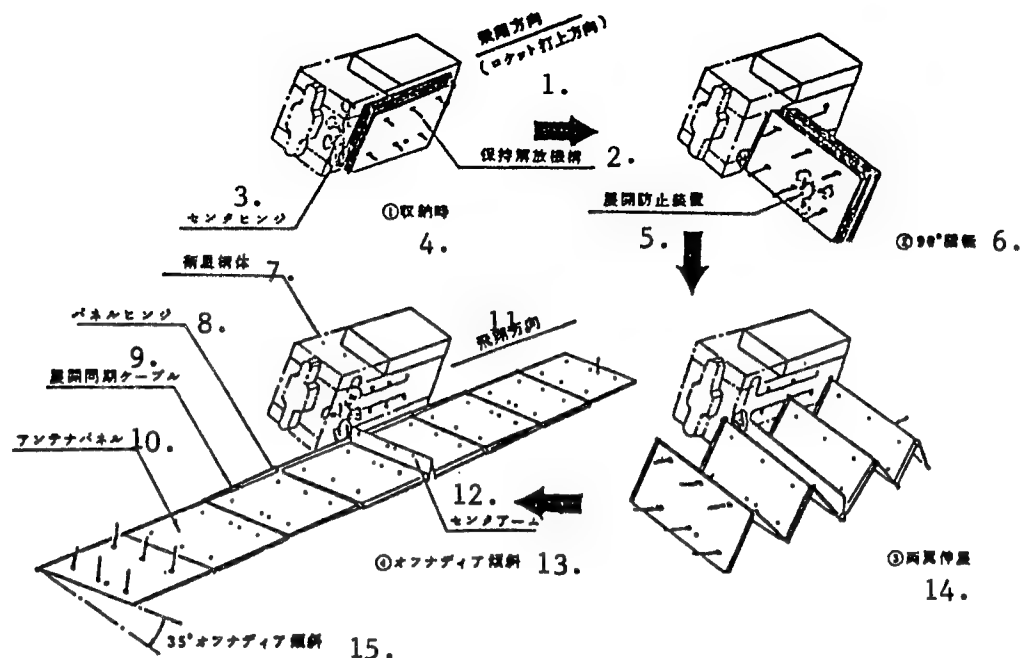
Figure 1. Unfolding Operation Sequence

Key:
1. Flying direction (rocket launching direction)
2. Holding and releasing mechanism
3. Center pin
4. In storage
5. Unfolding inhibitor
6. 90°-rotation
7. Body structure of satellite
8. Panel hinge
9. Unfolding synchronous cable
10. Antenna panel
11. Flying direction
12. Center arm
13. Off-nadir inclination
14. Elongation of both wings
15. 35°-off-nadir inclination

when the specimen moves horizontally, the hoisting accessories will move in accordance with the specimen's movement. Respective tests were conducted independently because the direction of the unfolding rotation axes varied depending on the unfolding operation. Figures 2 and 3 [not reproduced] show 90° rotation and the extension of both wings. After the antenna panel was folded and the unfolding rotation axes were set perpendicularly, a test of off-nadir inclination was conducted. Data on the time history of the unfolding angles, latch-up impact strain, etc., were obtained by conducting the respective unfolding tests.

4. Results of Tests

It was confirmed that the unfolding time was as analyzed and expected (for ground test time), and neither the final unfolding angular velocity nor the latch-up impact strain experienced problems in terms of strength when unfolding tests corresponding to the respective stages of the three-stage unfolding operation sequence were conducted. Table 2 compares the analyzed values and test values for unfolding. The test values vary widely because synchronization was affected and disturbed by jig resistance during the test involving the unfolding of both

wings. However, the reproducibility of the other test values was very good.

**Table 2.
Comparison Between Analyzed Values and Test Values During Unfolding**

Unfolding Operation	Test Value (sec)	Analyzed Value (sec)
90° operation	19.6 to 20.0	16.6 to 22.0
Elongation of both wings	11.8 to 16.7	11.5 to 26.5
Off-nadir inclination	21.6 to 22.3	19.0 to 32.9

5. Summary

We were able to confirm characteristics of the specimen and to clarify which jig times should be re-studied by conducting unfolding tests of the EM of the SAR antenna. We plan to conduct another unfolding test by using an explosive device.

(Note) This research was carried out as a part of the large project "Research and Development of Observation System for Resource Investigation" promoted by the Agency of Industrial Science Technology [AIST], MITI.

Vibration Test of SAR Antenna Mounted on ERS-1

[Article by Hideo Hino, Ryoichi Kuramasu and Yukiaki Nemoto of Resource Investigating Observation System Research and Development Organization; Toshio Inoue, Yoshiteru Ogata, Noriko Kaneko, Masatoshi Toyosawa and Yoshiyasu Kosaka of Kamakura Works, Mitsubishi Electric Corporation]

[Text] 1. Preface

The SAR [synthetic aperture radar] antenna mounted on the ERS-1 [earth resource satellite-1] is a large, folding-screen-type structure. We have conducted a vibration test on the EM [engineering model], which has electrical, mechanical and thermal characteristics equivalent to those of the actual equipment, and the following is a report of the test results.

2. Outline of Test

The purpose of the test is to ensure that the SAR antenna has the specified strength and rigidity, and to improve the mathematical model based on the analyzed results.

Figure 1 shows the test configuration. Boat-form jigs were used, and a specimen was installed on an excitation table through a satellite simulation side wall because the area of the specimen was larger than that of the excitation table. The contents of the test were as follows: the respective models were surveyed in three axis directions of the specimen, and sine waves were excited at the AT and QT levels. The exciting level is shown in Table 1. Measurements were carried out using an accelerometer with 68 channels and a strain gage with 20 channels, and the exciting force was controlled with a 4-channel accelerometer installed on the satellite simulation side wall.

Table 1.
QT Level Sine Wave Sweeping Environmental Test

X-axis direction			
	5 to 9.4 Hz	12.7 mm D.A.	
	9.4 to 15 Hz	2.25 Go-p	2 Oct/min
	15 to 21 Hz	6.0 Go-p	UP/DOWN
	21 to 30 Hz	2.25 Go-p	SWEEP
	30 to 100 Hz	6.0 Go-p	
Y- and Z-axis directions			
	5 to 15.3 Hz	12.7 mm D.A.	2 Oct/min
	15.3 to 35 Hz	6.0 Go-p	UP/DOWN
	35 to 100 Hz	3.0 Go-p	SWEEP

Note) The AT level is 1/1.5 that shown in this table.

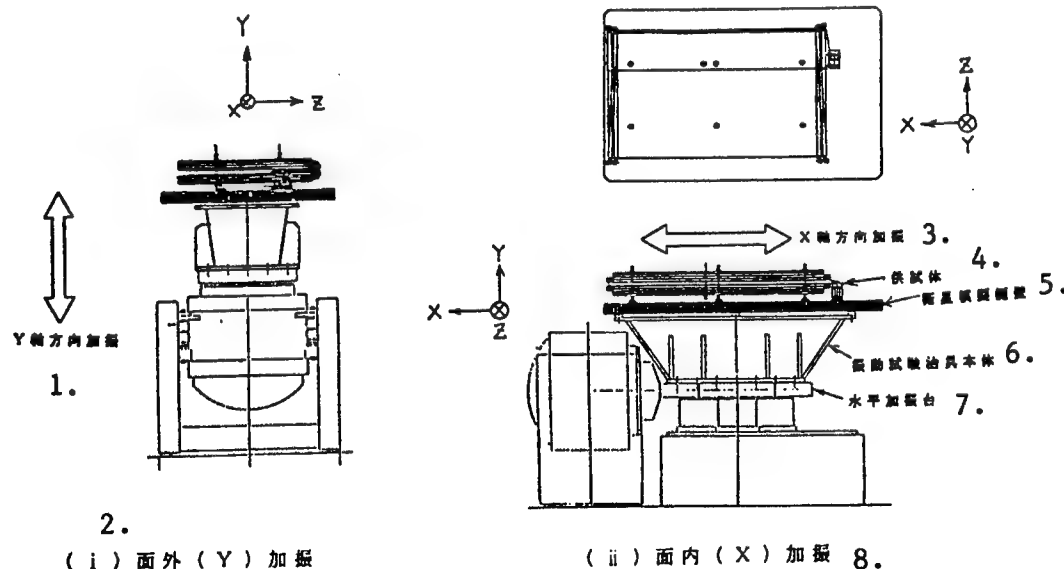
(i) 面外 (Y) 加振   (ii) 面内 (X) 加振

Figure 1. Vibration Test Configuration

Key:
1. Excitation in Y-axis direction
2. (i) Out-of-plane (Y) excitation
3. Excitation in X-axis direction
4. Specimen
5. Satellite simulation side wall
6. Vibration test jig proper
7. Horizontal exciting table
8. (ii) In-plane (X) excitation

3. Test Results

The test was finished safely, without any specimen breakage generated in any of the three axis directions. It was clarified that the resonance points in the X, Y and Z directions were 57, 61 and 44 hertz, respectively, satisfying the specification values (35 hertz or more). This fact demonstrates that both the design strength and rigidity of the SAR antenna are appropriate. Figure 2 shows data on the measurements of typical points (Z direction on the outermost layer). The intensity of the response acceleration was not proportional to the excitation level, and the response magnification was lowered in accordance with the rise in the excitation level, i.e., nonlinearity was recognized. In addition, close couplings among the respective directions were observed.

4. Comparison with Analyzed Values

Table 2 compares the test values with the analyzed ones of basic natural frequencies. Before making a model for analysis, the rigidity of the bush-superposed section of the hold-down section was simulated with a beam on the assumption that the cross-section of the beam had an equivalent geometric moment of inertia in which the contribution of the panel rigidity was taken into consideration. In addition, although the panel is asymmetric and has a honeycomb sandwich structure doubled with an antenna radiative section and a support structural section, only the support structural section was modeled since it is dominant for rigidity. As can be seen from Table 2, it was confirmed that the rigidity in the cross section was good, and the method of modeling the bush was correct.
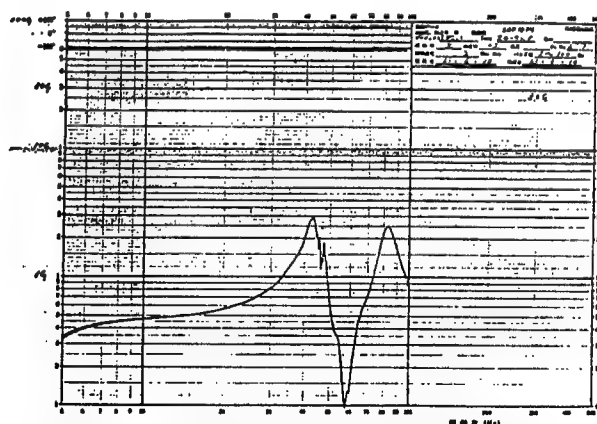

Figure 2. Z-Direction Response Acceleration (Outer-most Layer Panel) at Excitation in Z-direction

Key: 1. Vibration frequency (Hz)

Table 2.
Comparison Between Analyzed Values and Test Values of Basic Natural Frequency

Exciting Direction	Test Value (Hz)	Analyzed Value (Hz)
X	57	59.7
Y	61	52.1
Z	44	40.9

(Note) This research was carried out as part of the large project "Research and Development of Resource Investigating Observation System" promoted by the Agency of Industrial Science and Technology [AIST], MITI.

References

1. Yasumasa Hisada, et al., "Results of Environmental Test of SAR Antenna," Proceedings of the 29th Space Sciences and Technology Conference, No 1D2.

2. Hideo Hino, et al., "Results of Acoustic Test of EM of SAR Antenna Mounted on ERS-1," Proceedings of the 32nd Space Sciences and Technology Conference.

Acoustic Test of SAR Antenna Mounted on ERS-1

43065013S Tokyo PROCEEDINGS OF THE 32ND SPACE SCIENCES & TECHNOLOGY CONFERENCE in Japanese 26-28 Oct 88, No 3C1 pp 614-615

[Article by Hideo Hino, Ryoichi Kuramasu and Yukiaki Nemoto of Resource Investigating Observation System Research and Development Organization; Noriko Kanai, Yoshiteru Ogata, Hiroyuki Naruki and Nobuyoshi Imura of Kamakura Works, Mitsubishi Electric Corporation]

[Text] 1. Preface

The SAR [synthetic aperture radar] antenna mounted on the ERS-1 [earth resource satellite-1] is a large folding-screen-type structure. An EM [engineering model] of the SAR antenna was made so that its electrical, mechanical and thermal functions were equivalent to those of the actual equipment, and was subjected to a series of development tests in order to obtain an overall evaluation of the SAR antenna. An acoustic test, which is one of the development tests, has been finished. The following is a report of the results of the acoustic test.

2. Test Specimen and Outline

The purpose of the test was to ensure that (1) the SAR antenna could withstand the high-frequency acoustic vibrational environments generated with the ERS-1 is launched, and (2) the random vibration environmental conditions of the respective components (feeder circuit, cables, etc.) of the SAR antenna are appropriate.

Figure 1 shows an outline of the specimen. When the ERS-1 is launched, eight SAR antenna panels with divided apertures will be folded and retained, with thepanel faces parallel to the side wall of the satellite. The panels are numbered from (1) to (8), in sequence, from the face closest to the side wall of the satellite. A center arm is put between panels (4) and (5). The clearance between the panels. As can be seen from the detailed section shown in Figure 1, the antenna panel is based on a double honeycomb sandwich structure, the antenna radiating section and supporting structural section are integrated, and a feeder circuit is incorporated in the supporting structural section. Each panel is covered with beta cloth and MLI thermal control material.
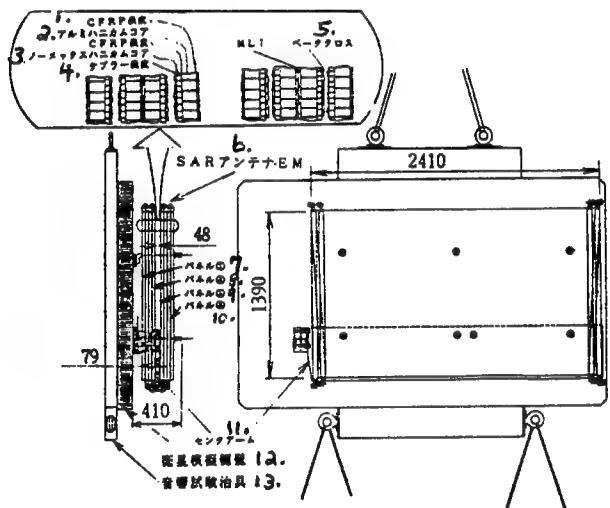
Figure 1. Specimen

Key:
1. CFRP skin
2. Aluminum honeycomb core
3. Nomex honeycomb core
4. Kevlar skin
5. Beta cloth
6. SAR antenna EM
7. Panel (1)
8. Panel (4)
9. Panel (5)
10. Panel (8)
11. Center arm
12. Satellite simulation side wall
13. Acoustic test jig

Figure 2 [not reproduced] shows the test configuration. The test levels are shown in Table 1. The test was conducted for the sound pressure load at both the pretest and full test levels.

Table 1.
Acoustic Test Level

1/1 Octave Center Frequency (Hz)	Pretest Sound Pressure Level (dB) (0 dB = 20 micropascals)	Full Test Sound Pressure Level (dB) (0 dB = 20 micropascals)
31.5	122	126
63	125	129
125	129	133
250	134	138
500	138	142
1000	132	136
2000	129	133
4000	125	129
8000	122	126
Overall	141	145
Test time	60 (sec)	120 (sec)

3. Test Results

The response ratio of the response acceleration to the load sound pressure at the pretest level and that at the full test level were almost linear. The maximum value of the response acceleration was seen at panel (8), and was 36.8 [Grms] at the full test level. Figure 3 shows the results of analyzing the 1/1 octave at this value. Figures 4 through 6 shows results of analyzing the 1/1 octave of the response acceleration of panels (1), (4) and (5) in the vicinity of the above value at the full test level. Following the sound pressure load, no abnormalities were generated from the specimen.
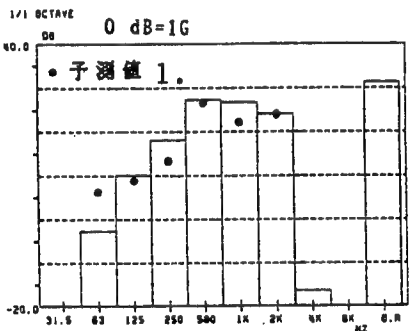

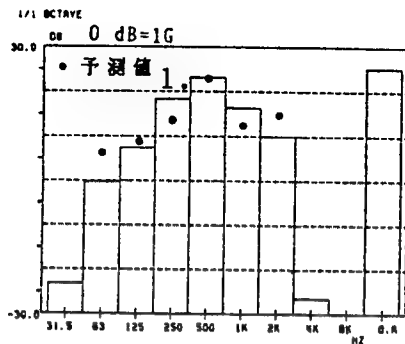**Figure 3. Panel (8) Response Acceleration**
Key: 1. Predictor

Figure 4. Panel (1) Response Acceleration
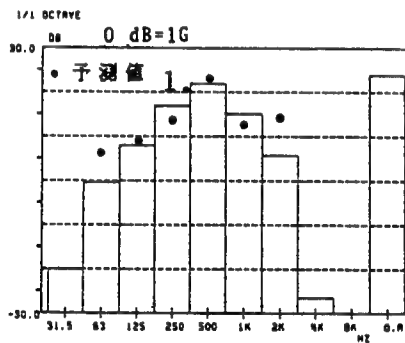
Key: 1. Predictor

Figure 5. Panel (4) Response Acceleration
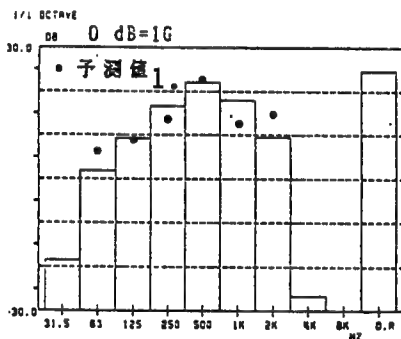
Key: 1. Predictor

Figure 6. Panel (5) Response Acceleration

Key: 1.Predictor

4. Summary

The EM of the SAR antenna was subjected to an acoustic test. As a result, it was confirmed that the specimen could withstand high frequency vibration environments assuming that the H-I two-stage rocket would be used for the launch. Random vibration environmental conditions have been loaded in each component of the SAR antenna. These conditions have been recognized as being appropriate.

(Note) This research was carried out as part of the large project "Research and Development of Resource Investigating Observation System" promoted by the Agency of Industrial Science and Technology [AIST], MITI.

References

1. JOURNAL OF SOUND AND VIBRATION, Vol 91 No 1, 1983 pp 103-118.

2. Lyon, R.H., "Statistical Energy Analysis of Dynamical Systems," 1975, pp 232-234.

Study of Operation Performance of Space Manipulator

[Article by Ryo Okamura and Hajime Sudo of Toshiba Corporation]

[Text] 1. Preface

Conducting an assembly operation in space requires the performance of various tasks, extending from precise engagement using a remote-controlled manipulator to the transportation of large payloads. These tasks are scheduled to be carried out by a main arm, with a length of approximately 10 meters, and subarms installed on top of the main arm (as of July 1988). These subarms will be approximately 1.5 meters long. The reliability of work conducted in extreme environments greatly depends on the operation performances of manipulators. Of the factors related to the operation performance, this report describes the results of studying the work difficulty, visual devices and arm oscillation by means of simulations.

2. Simulations

A maximum displacement of 50 mm is formed on the top of the long and large main arm by the arm deflection and the loosness of the joints in the arm, depending on the attitude and operation statuses. It is anticipated that when the work is carried out with such subarms, oscillations having this value as the maximum amplitude will remain in the installation base. The device shown in Photograph 1 [not reproduced] was fabricated in a research laboratory to simulate this oscillation. The shoulder of the slave arm, with three joints, moves on an air surface plate. The above device has been designed so that this shoulder can be installed on the linear guide and transferred freely between stoppers set at certain distances, imitating the looseness of the joints of the main arm. Also, springs, imitating the rigidity of the main arm, are incorporated in these stoppers, with the combined looseness and spring displacement set at +/- 50 mm. A television camera is set 500 mm above the shoulder of the slave arm, and the operator handling the

master arm executes tasks while watching a TV monitor showing a site that he cannot observe directly.

Simulations were carried out at the two phases shown in Table 1. This report indicates that experiment (I) is the main one, and another report will present the details of experiment (II). Figure 1 shows the transfer path of the arm set for a task contained in experiment (I). In the case of the multi-point transfer task, arm wrist pointers must be stopped for one second or longer in the sequence (1)→(2)→(3)→(4)→(5)→(4)→(3)→(2)→(1) in a 20-mm-diameter marker on the air surface plate. For a two-point reciprocating task, the operation must be carried out in the following sequence: [1]→[2]→[3]→[4]→[5]→[4]→[3]→[2]→[1]. The arm transfer distance, in both cases, totals 4 meters, but when .the arm transfers among adjacent points, the former case requires only one-joint-operation while the latter requires three-joint-operation. This subject isa 25-year-old male familiar with this arm operation.

図1 設定タスク

Figure 1. Set Task

Key:
1. Pointer
2. Wrist
3. Elbow
4. Surface table
5. Shoulder
6. The operator carries out the positioning work with the pointer, in sequence, from (1) → (2) → (3) → (4) → (5) → (4) → (3) → (2) → (1) or [1] → [2] → [3] → [4] → [5] → [4] → [3] → [2] → [1].

Table 1.
Simulation Contents

I. Positioning (unload, +/- 10 mm)		II. Engagement of parallel pin with a diameter of 8 mm (setting interval: 345 mm; engagement accuracy: +/- 50 m; load: 10 kg, 100 kg)	
Experimental factor	**Level**	**Experimental factor**	**Level**
Shoulder oscillation	* 0.5 Hz, +/- 50 mm	Shoulder oscillation	* 0.5 Hz, +/- 50 mm
	Nil		0.25 Hz, +/- 50 mm
TV camera	* Monocular (FOV: 45°)		* Nil
	* Stereoscopic (FOV: 45°)	TV camera	* Monocular (FOV: 45°)
Set Task	* Multipoint movement		* Monocular (FOV: 10°)
	* Two-point reciprocation		* Stereoscopic (FOV: 45°)

3. Test Results

After the subject was sufficiently trained, an experiment was conducted by executing five sets of tasks, each consisting of eight trials. The execution time of each trial was measured, and the three intermediate sets were extracted and analyzed. The order of trial executing in a set was determined at random. Table 2 shows the work execution time, and Table 3 shows the upper probability value obtained from the above extraction and analysis. These results indicate the following: (1) When the positioning is executed by approximately +/- 10 mm during unloading, the shoulder oscillation will steadily increase the execution time of the manipulator's task. The value is approximately 12 percent. (2) When the arm is oscillated and when it is necessary for a number of the manipulator's joints to be operated in a cooperative manner, there is a strong possibility that the working
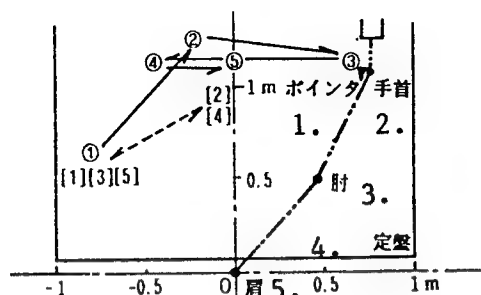
time will increase. This suggests that the degree of influence of the arm's oscillation on the manipulator varies with every task. According to this experiment, easy work refers to work that is carried out through the operation of a single joint rather than work involving the execution of a small number of tasks. (3) When the arm is oscillated, and when the observation means is a monocular camera, there is a strong possibility that the working time will increase. According to the second phase test results mentioned in another report, it has been observed that the workability is enhanced, in sequence, from a standard lens monocular camera to zoom lens monocular camera to stereo camera, in accordance with the decrease in the oscillation cycle (identical amplitude).

Table 2.
Work Execution Time

Trial	Shoulder Oscillation	TV Camera	Set Task	Work Execution Time (seconds)
(1)	Exists	Monocular	Multipoint	116+/-2.6
(2)	Exists	Monocular	Two-point	117+/-4.9
(3)	Exists	Stereoscopic	Multipoint	114+/-1.7
(4)	Exists	Stereoscopic	Two-point	110+/-5.9
(5)	Nil	Monocular	Two-point	89+/-6.3
(6)	Nil	Monocular	Two-point	101+/-7.8
(7)	Nil	Stereoscopic	Multipoint	94+/-5.4
(8)	Nil	Stereoscopic	Two-point	95+/-7.1

Table 3.
Results of Dispersion and Analysis

Oscillation of Shoulder	TV Camera	Set Task	Upper Side Probability (percent)
*			47
	*		51
		*	4.4E-4
*	*		23
*		*	57
	*	*	15
*	*	*	52

(* denotes factors of upper side probabilistic values)

The upper side probability values do not confirm that items (2) and (3) above are significant, but there is a strong possibility that these items are significant. Therefore, their significance must be examined through detailed tests to be conducted in the future.

4. Postface

As a result of observing the workability of subarms under the oscillation of the main arm through simulations employing two-dimensional arms, it has been confirmed that it is possible to execute the positioning task by approximately +/- 10 mm, but this execution causes the working time to increase. It has also been suggested that when the means of operation and observation of the manipulators are properly selected, it is possible for this working time to be shortened.

According to computer simulations, the degree of oscillation obtained from this experiment is equivalent to that of the worst case scenario. Actually, this oscillation is not constant, but instead decreases along with the frequency and amplitude. In the future, we plan to continue studying this operation taking arm dynamics into consideration.

Teleoperation Using Skill Superposition

43065013u Tokyo PROCEEDINGS OF THE 32ND SPACE SCIENCES & TECHNOLOGY CONFERENCE in Japanese 26-28 Oct 88, No 3F2 pp 716-717

[Article by Narutomo Hirai and Tomomasa Sato of the Electrotechnical Laboratory; Hironobu Urabe and Masaaki Uenishi of Kawasaki Heavy Industries, Ltd.]

[Text] 1. Preface

The master slave manipulator is effective as a means of intuitively carrying out teleoperating tasks in space. However, skill is indispensable when carrying out skillful work. In order to facilitate the carrying out of skillful work without involving training, it is important that the skillfulness of robots and human operation be superposed. This paper describes the control method constituting the skillfulness used in teleoperating work, and demonstrates a method of conducting skillful teleoperation by superposing human operation and the above skillfulness.

2. Analysis of Skillfulness

In order to realize the above-mentioned matter, it is necessary to clarify the human operation and the skillfulness which should be handled by a slave manipulator in respect to basic operations.[1] Operations which cannot be carried out by robots should be selected as human operations when taking the purpose of the task into consideration. In the case of such an operation, human judgment is taken as feedback. On the other hand, static and dynamic restrictive operations, compliant operations, etc., can be cited as operations in which the local interaction with the environment represents a problem. These operations are equivalent to the operation in which robots autonomously carry out and compensate for the human operation. Generally speaking, such operations are those for which feedback information can be obtained only locally and those for which the control processing speed is high. Table 1 shows an example of analysis of an operation summarized in the above manner. For example, humans bend and extend their fingers when gripping an object, while robots are controlled compliantly and are adapted to the shape and attitude of such an object.

Table 1.
Skillfulness Knowledge Base

Name of task	Coordinate system	Human operation	Robot operation
Grip	Finger coordinate	Width of grip	Compliant control
Release	Finger coordinate	Width of grip	Compliant control
Lift	Table operation coordinate	Height	No operation involving the lower side
Place	Table operation coordinate	Height	Absorption of impact force
Put on	Table operation coordinate	Height	Absorption of impact force
Turn	Coordinate axis of rotation	Angle of rotation	Compliant control
Fit	Surface operational coordinate	Pushing operation	RCC operation
Insert	Coordinate hole task	Height	RCC operation

3. Skillfulness Superposing Mechanism

Figure 1 outlines the skillfulness superposing mechanism consisting of a master slave manipulator, skillfulness
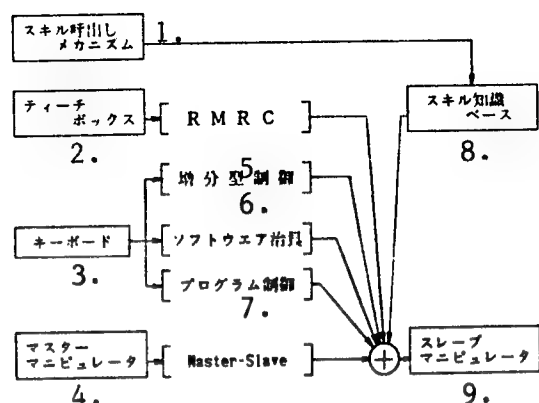
Figure 1. Skillfulness Superposition Mechanism

Key:
1. Skillfulness calling mechanism
2. Teaching box
3. Keyboard
4. Master manipulator
5. Incremental control
6. Software jig
7. Program control
8. Skillfulness knowledge base
9. Slave manipulator

knowledge base, and skillfulness calling mechanism. The master slave manipulator superposes various control methods, the skillfulness knowledge base accumulates the skillfullness analyzed in 2, and the skillfulness calling mechanism uses the accumulated skillfulness. In order to carry out the task, first the system must recognize the name of the task through the automatic detection system[2] from human operations, and the skillfulness calling mechanism using a voice input device. Then, the task will be divided into basic operations on the basis of the above-mentioned skillfulness knowledge base, and operations which should be carried out by humans will be indicated. Next, the humans will operate the master slave manipulator, teaching box, etc., based on the indication, robots will be controlled with restrictive and compliant operations, and the task will be carried out.

4. Experimental Example

An experiment for the following two cases was conducted, and the two sets of results were compared and studied. In one case, a column inserted into a hole was gripped and extracted solely by the use of a master slave manipulator in order to verify the effectiveness of the skillfulness superposition, while in the other case, the column was handled using the skillfulness superposition. At the beginning of this experiment, the former case had a low success rate (three times out of six were failures), while the latter case suffered no failures. In addition, after the work was carried out on a stable basis, the time required to grip and extract the column from the hole was measured. As a result, there were differences between the use and non-use of the skillfulness superposition in respect to the success rate and time required for the task until skill was attained, but after the skill level was reached, there were no remarkable differences

between them. The time required for the skill level to be reached was short since the task was simple.

As shown below, the effectiveness of the skillfulness superposition can be summarized based on the above-mentioned results: 1. The effectiveness of the skillfulness superposition can be recognized until skill is reached when complex work is involved. The skillfulness superposition is also effective for simple work that must be carried out continuously and which involves many and different skills. 2. Some skills are difficult for humans to acquire. If these skills are realized with software and robots, the effectiveness of the skillfulness superposition will become greater.

5. Postface

Coordination between humans and robots is an important subject for a teleoperating system. This paper shows coordination methods in relation to levels of skillfulness. Based on this philosophy, it is believed that if skills difficult for humans to acquire are prepared for robots, working capabilities surpassing those of the operator's bare hand can be realized.

References

1. "Research and Development of Robots Engaged in Extremely Dangerous Environments," Outline of Research Results for Fiscal 1985, Electrotechnical Laboratory, 1985, p 13.

2. Sato and Hirai, "Understanding Behaviors and Teleoperation Support Based on This Understanding," Prepublication of the 4th Robot Academic Society Science Lecture Meeting, 1985, p 507.

Study of Operation Properties, Radio Wave Delay Time of Teleoperated Manipulator

[Article by Kenji Hiraishi, Haruki Ayata, Kazuo Nakamura, Nobuaki Takanashi and Noriko Terada of NEC Corporation]

[Text] 1. Preface

Manipulator systems are teleoperated in space. When such a manipulator system is studied, the influence of the data transmission delay time on the manipulator system cannot be ignored. The following is a study of a manipulator system, from the standpoint of the operation properties, when this delay time exists.

2. Delay Time and Operation Properties

Table 1 shows the relationship between the delay time and operation form of the manipulator to be teleoperated. It is said that the delay time of human reactions varies depending on the individual, but generally ranges

Table 1. Delay Time and Operational Form of Teleoperated Manipulator

WS:WORK SITE CS:CONTROL SITE

通信回路 1.	運用形態 5.	運用例 6. WS / CS	遅延時間 14. 住復	備 考 15.
直接回路 2.	(WS)──(CS)	静止軌道──地上 7. 宇宙基地──宇宙基地 9.近傍 / 10 11 低地球軌道──地上 (可視時間のみ適用) 12	0.25〜1.25 sec	WSとCSが可視域にならなければならないため、低地球軌道の場合には、運用時間の制限あり 16.
3. TDRS中継 直接受信	(TDRS) (WS) (CS)	低地球軌道──地上 (可視域外でも適用) 13	0.75〜1.6 sec	CSはTDRSから直接受信可能な場所に無ければならない 17.
4. TDRS中継 TDRS局間山	(TDRS) (WS) (TDRSS)─(CS)	低地球軌道──地上 (可視域外でも適用)	0.75〜2.0 sec	CSとTDRS局間の通信回路が衛星回線の場合には更に遅延時間が増大 18.

Key:
1. Telecommunications line
2. Direct line
3. TDRS relay direct receiving
4. TDRS relay by way of TDRS station
5. Operational form
6. Example of operation
7. Geostationary orbit
8. Ground
9. In vicinity of space station
10. Space station
11. Low earth orbit
12. (Operation only while visible)
13. (Operation even outside visible areas
14. Delay time reciprocation
15. Remarks
16. In the case of a low earth orbit, the operating time is limited because WS and CS must be in visible areas
17. CS must be located where it can receive direct information from TDRS
18. When the telecommunications line used between the CS and TDRS station is a satellite circuit, the delay time will be increased further

from 0.2 to 0.4 sec. Of course, delay elements exist in control systems related to humans. In addition to this delay time, when a manipulator system teleoperated in space is studied, as shown in Table 1, the delay time of the telecommunications lines between the working side and operation side cannot be ignored. A delay time is also generated when processing data on radio wave propagation distance and transmitting-receiving systems.

The following is a study of the system configuration for the case when such a delay time exists in the system. Figure 1 presents information on sensors and the control level hierarchy for use in this study.

The MAN IN THE LOOP refers to humans producing controlled variables based on the information on images and inner force senses. It can be said that the system form of the teleoperation according to the telepresence of

such a MAN IN THE LOOP relies on humans in respect to a hierarchy of at least two or three levels, as shown in Figure 1. A delay time of 1 to 2 seconds transfers a sense of unnaturalness and incompatibility to the operators
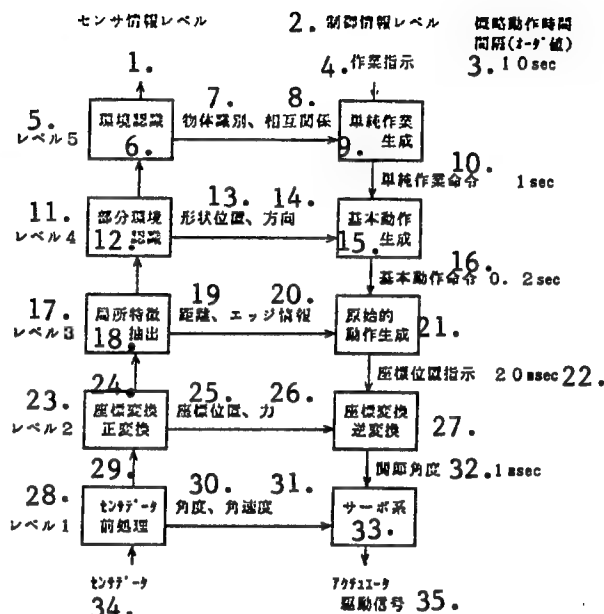

Figure 1. Sensor Information and Control Level Hierarchy

Key:
1. Sensor information level
2. Control information level
3. Approximate operating time interval (order value)
4. Indication of work
5. Level 5
6. Recognition of environment
7. Discrimination of objects
8. Correlation
9. Formation of simple tasks
10. Instructing simple tasks
11. Level 4
12. Recognition of partial environment
13. Position of shape
14. Direction
15. Formation of basic operation
16. Instructing basic operation
17. Level 3
18. Extraction of local features
19. Distance
20. Edge information
21. Formation of primitive operation
22. Indication of position of coordinate
23. Level 2
24. Coordinate transformation and positive transformation
25. Coordinate position
26. Force
27. Coordinate transformation and inverse transformation
28. Level 1 29. Pretreatment of sensor data
30. Angle
31. Angular velocity
32. Angle of joints
33. Servo system
34. Sensor data
35. Actuator driving signal

since the approximate operation delay time interval at level two to three is about 0.02 sec.

The bilateral control which feeds inner force senses back to the operators is very effective when the task is carried out minutely using a teleoperation system, but it is possible for the systems to become unstable when a delay time exists. Also, with regard to the visual information, it is suggested that the sense of incompatibility caused by such a delay time can be removed from the workers through indicators foreseen by computer simulation. However, when an unforeseen accident occurs in orbit, this philosophy cannot cope with the accident and problems will arise. For example, when obtaining precise images to foresee complex working environments, the computer processing time required to produce these images will cause a delay time to occur.

3. Study of Partially Autonomous Property

In order to solve these problems and to lighten the burden on the operators, it is necessary that complete reliance not be placed on direct operations according to the real time of these operators, but that a system be

Figure 2. Example of Configuration of Autonomously Teleoperated System

Key:
1. Work side
2. Communications system
3. Operation side
4. Local AI
5. Main AI
6. Local knowledge base
7. Basic operation formation system
8. Main knowledge base
9. Recognition of partial environment
10. Formation of primitive operation
11. Simulator
12. Pretreatment of sensor data
13. Actuator controller
14. Operator I/F section
15. Sensor
16. Actuator
17. Work object
18. Human

studied instead in which the work is carried out autonomously to some extent. In other words, the working side should have a local looping control system within the overall control loop so that when the operator gives a certain sign to the working side at a certain level, the work will be carried out autonomously. In this way, the controlling method is used to reduce the direct control held by the operators and to increase the rate of autonomous operations. This controlling method is referred to as "Supervisory Control," and is effective when delay time exists. The more both the operating and working sides have interfaces at the high level-control hierarchy, the higher the autonomous degree will be. If it is possible to indicate a basic operation level or a simple task level (a level of about 4 or 5 in Figure 1), the operation properties will be improved. Figure 2 shows an example of such a partially autonomous system configuration.

4. Summary

As mentioned previously, when an unignorable delay time exists in a teleoperated manipulator system, it is believed to be desirable, from the standpoint of operation properties, for supervisory control to have interfaces with both the operating and working sides at the basic operation or simple task level. In order to do so, the manipulator on the working side must be high-functioning and autonomous. We plan to study this system further.

References

1. Miller, H., et al., "Space Application of Automation: Robotics and Machine Intelligence Systems," NASA-CR-162081, 1982.

Graphic Simulator Intervening Space Teleoperation System

43065013W Tokyo PROCEEDINGS OF THE 32ND SPACE SCIENCES & TECHNOLOGY CONFERENCE in Japanese 26-28 Oct 88, No 3F4 pp 720-721

[Article by Kazuo Machida, Yoshitsugu Toda and Toshiaki Iwata of the Electrotechnical Laboratory]

[Text] 1. Preface

The graphic simulator offers very effective operation interfaces with space robots. This kind of simulator is outside of the control loop and has been used to train operators and to examine arm orbits. Sheridan, et al., attempted to use such a simulator as a predictor to compensate for the delay in communication time in the teleoperation loop. The authors of this article, however, have already adopted a simulator in a teleoperation system, indicating non-operations through the correct opening and closing of the control loop and demonstrating a concept whereby the operation efficiency is increased through edit functions.[1]. The following is a report of the trial operation.
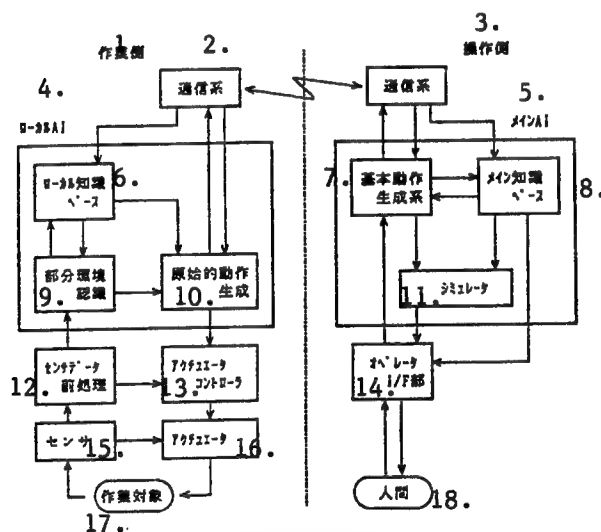
2. Concept and Configuration of Graphic Simulator Intervening Teleoperation System

A real-time graphic simulator is adopted in this system's master slave manipulator. The purpose of the system is to safely and efficiently execute tasks by reversely reproducing the order and interactive task edit and by using graphic images as media. It is believed that this technology combines teleoperation and an autonomous robot. Figure 1 shows the correlation between the teleoperation mode, the intervention of the simulator and the autonomous mode. Human intervention task planning is a prominent part of this concept. The operator indicates, edits and debugs the necessary movement of the arms on the simulator, transmits the obtained sequence to the slave system, and makes the slave system execute this sequence. In this case, if the sequence is used interactively or is batched on-line against the slave system, it will be possible to operate flexible robots. Deficiencies in AI can be readily compensated for by conducting supervisory and intervention work during the autonomous task planning.
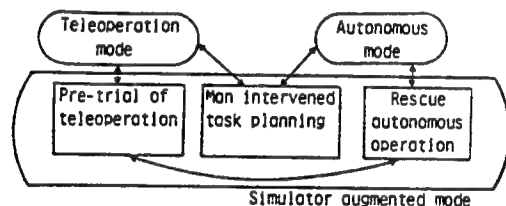
Figure 1. Conceptual Relationship of Simulator Augmented Mode

Figure 2 shows the configuration of the developed system. The respective subsystems are combined as dispersion systems employing microprocessors by means of serial telecommunication lines utilizing optical fiber cables. The structures of the master arm and the slave arm differ, but are generalized. Both arms have general-purpose simulators and standardized telecommunication lines. The operator carries out the operating work by using an actual master arm while observing the movement of the slave arms as shown on a three-dimensional graphic display. Actual time interference is determined on the simulator side, and virtual force is fed back to the master arm based on this judgment. Figure 3 [not reproduced] shows an example of a display image.

3. Edit

The edit is a key module for efficiently operating this system. Figure 4 shows a block diagram of its functions. The working orbit planned on the display by an operator is stored in a buffer memory, and is edited interactively by means of the key module. The reproduction is available in two kinds. One is an image reproduction only for display images, while the other is a slave reproduction executed with slave arms. The following method is used to edit the orbit. The orbit is reproduced reversely or forward on the display, is stopped properly, and is overwritten by using programs or the master arm. This is similar to a method in which the editing and reproducing is carried out by means of video tape recorders and word processors. The reverse function in slave reproduction is effective when a robot is returned to its original position in order to correct the failures caused by autonomous control. In addition, the reproduction speed is variable. When the work must be carried out carefully, slave arms with low follow-up speed capabilities must be used or, if
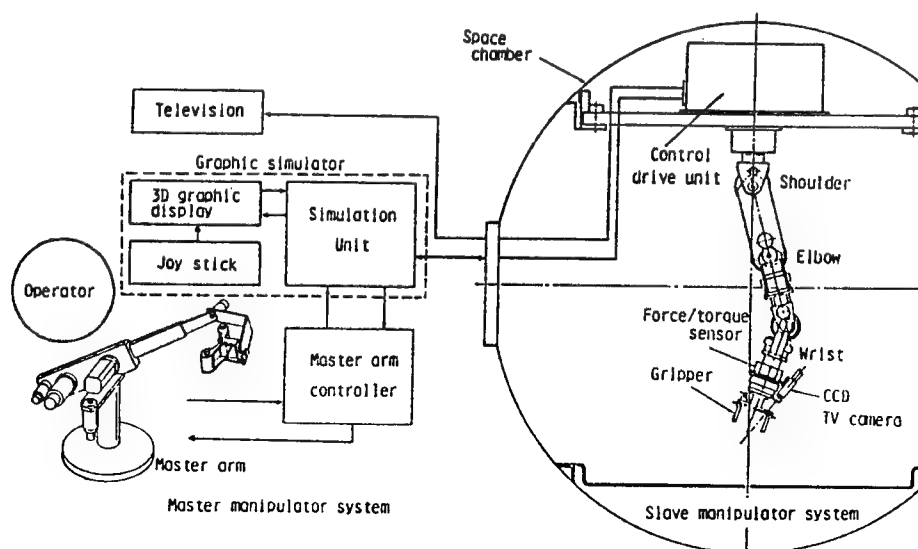

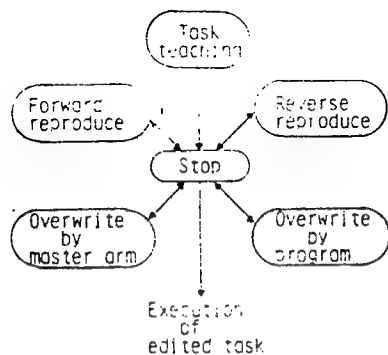**Figure 2. Block Diagram of Graphic Simulator Augmented Teleoperation System**

Figure 4. Task Editing Module

a payload with large mass must be handled, the reproduction will be low. In the reverse case, the reproduction speed is increased depending on the situation.

4. Conclusion

We have seen our way clear to flexibly carrying out teleoperation work by conducting experiments on reproduction, editing and the indication of simple work with this system. This flexible teleoperation system cannot cope with complex work since the processor capacity in the current system is restricted. However, most of the functions obtained by using this method are essentially necessary for teleoperated robots in space, and it is expected that these functions will be developed further in the future.

References

1. Machida, Toda and Iwata, "Real Time Graphic Simulator for Manipulator and Its Application," the 3rd Space Station Lecture Meeting, 1987.

Ground Tester for Space Robot Technologies (2)

43065013x Tokyo PROCEEDINGS OF THE 32ND SPACE SCIENCES & TECHNOLOGY CONFERENCE in Japanese 26-28 Oct 88, No 3F5 pp 722-723

[Article by Yasuo Shinomiya, Shinichiro Nishida and Akiko Kumagai of Komukai Works, Toshiba Corporation]

[Text] 1. Preface

It is anticipated that work in space will be carried out by means of satellites equipped with manipulators. The data transmission time delay between ground and space can be cited as one of the elements representing a problem when these satellites (space robots) are teleoperated from the ground. The time delay lowers the operation efficiency and causes malfunctions to occur. Telepresence/teleoperation technology is regarded as a method for reducing the above influence.

We have studied this technology and its ground tester, have made a portion of the ground tester on a trial basis, and have conducted experiments by using this part.

2. Telepresence/Teleoperation Technology

We are studying the use of a predicted-screen display method, together with hybrid control of position and force, in order to realize telepresence/teleoperation technology.

(1) Predicted-Screen Display Method (See Figure 1)

Pictures in the vicinity of manipulators are transmitted from space robots to the ground, but it is impossible to obtain these pictures in real time on the ground because of the delay in data transmission.

If the reaction of these space robots to operation signals is anticipated and displayed through simulations conducted on the ground, the operation will be carried out based on this reaction image. Accordingly, it will be possible to avoid erroneous operations and increase the operation efficiency.
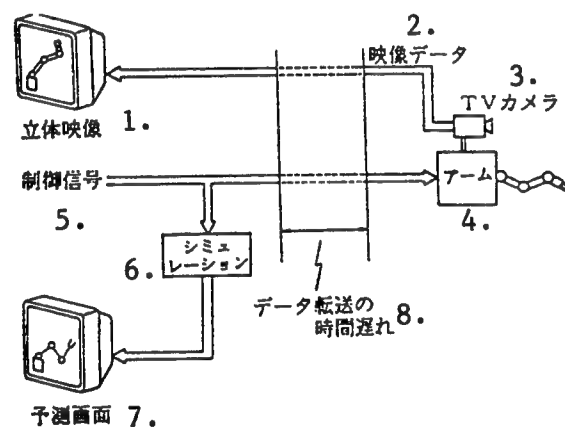

Figure 1. Indication on Predicted Screen

Key:
1. Stereoscopic image
2. Image data
3. TV camera
4. Arm
5. Control signal
6. Simulation
7. Predicted screen
8. Time delay of data transmission

(2) Hybrid Control of Position and Force (See Figure 2)

Unknown obstacles on the predicted screen may conflict with the operator's expectations. These mis-operations are controlled locally by means of the hybrid control of position and force. If this method of control is used, constraint conditions can be determined in accordance with the work contents. In addition, the use of this method will prevent objects from being subjected to excessive force and will prevent operating directions from becoming erroneous.
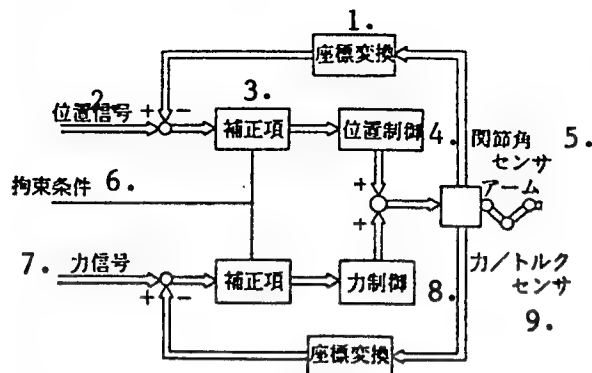
according to the arms mounted on the chaser satellites, and to conduct function-checking tests.

A three-joint arm fixed on the base has been made on a trial basis, and can be controlled, including the time delay, while observing stereoscopic images and by using a joy stick.

4. Test of Hybrid Control of Position and Force

A test was conducted to check the hybrid control of position and force by using the above-mentioned ground tester. Figure 4 shows an example of the test results.

Usual control system: Speed control—directions of x-, y- and rotation axes.

Hybrid control system: Position control—direction of y-axis, and force control—directions of x- and rotation axes.

Contents of test: The arm is moved while stroking the wall in the direction of the y-axis in accordance with commands given by means of the joy stick.

Test results: The functions of the hybrid control system were checked. It was confirmed that the efficiency was higher than that of the usual control system.

5. Postface

The functions of the hybrid control of position and force were checked by using the ground tester for space robot
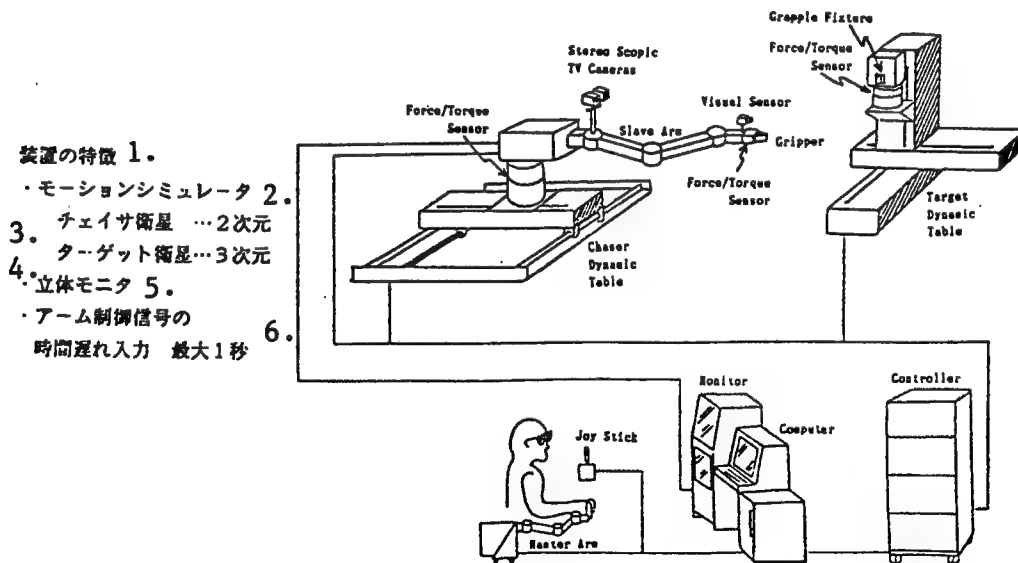

Figure 2. Hybrid Control System

Key:
1. Coordinate transformation
2. Position signal
3. Correction item
4. Position control
5. Joint angle sensor arm
6. Restricted condition
7. Force signal
8. Force control
9. Force/torque sensor

3. Ground Tester

As shown in Figure 3, the configuration of the ground tester has been designed based on the results of studying the telepresence/teleoperation technology. The purposes of this tester are to simulate the tracking and acquisition operations of target satellites two-dimensionally

Figure 3. Ground Tester

Key:
1. Features of ground tester
2. Motion simulator
3. Chaser satellite—two-dimensional
4. Target satellite—three-dimensional
5. Stereoscopic monitor
6. Input of time delay of arm control signal (1 sec max)
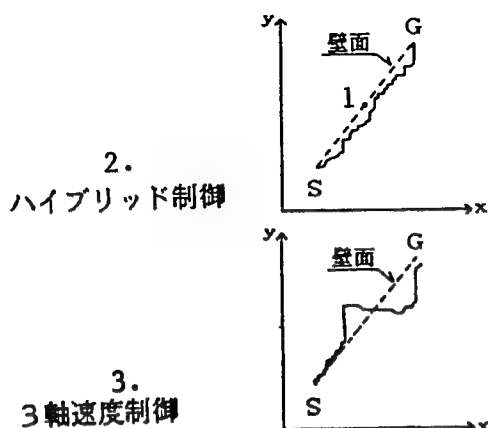
Figure 4. Test Results (Arm Tip Position)
(time delay: 1 sec)

Key:
1. Wall surface
2. Hybrid control
3. Three-axial speed control

technologies. As a next-stage test, we plan to check the performance of the hybrid control system, including the time delay.

References

1. Shinomiya, Y., Nishida, S., Kumagai, A., "The Ground Test Facilities of Space Robots Technology (1)," ISTS, 1988.

Development of Space Master Slave System

[Article by Kiyoshi Gomomoi, Katsumi Nakajima, Masaaki Uenishi, Osamu Noro and Osatake Miki of the Robot Project Laboratory, Kawasaki Heavy Industries, Ltd., Nobuyoshi Muroi of the Space Development Laboratory, Kawasaki Heavy Industries, Ltd.]

[Text] 1. Preface

Using skilled robot manipulators to replace humans is necessary for assembling structures in orbit and replacing units. The teleoperated master slave system is regarded as a means of handling such manipulators. The bilateral master slave system[1] with a different structure is excellent in respect to the operation properties of the master arm as well as the operation of various manipulators in orbit.

The authors have devised a space master arm with high functioning capabilities in a weightless state, have made a ground master arm with operation properties almost equal to those of the space master arm, and have constructed a bilateral master slave system.

The following is a report of the results of tests of the master arm and the bilateral master slave system with a different structure.

2. Devising Master Arm with High Operation Characteristics

Up to now, care has been taken to use low friction, low inertia and gravity balance in order the increase the operation characteristics of the ground master arm. Gravity balance is not necessary for the master arm used in space, but in addition to the low friction and low inertia, we have tried to make uniform the mass characteristics of the operation and the master arm operating range. In this way, the operator can carry out the work smoothly, without experiencing anisotropy. Figure 1 shows the distribution of mass ellipsoids of the devised space-use master arm. The length of the major and
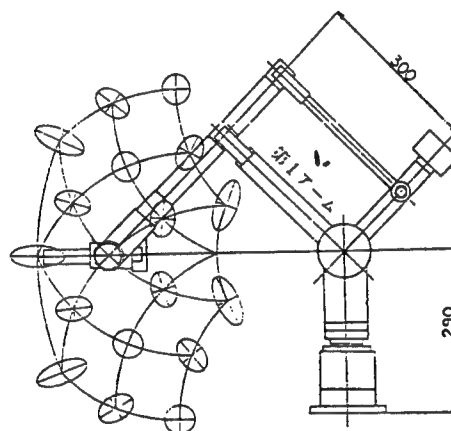

Figure 1. Distribution of Mass Ellipsoids
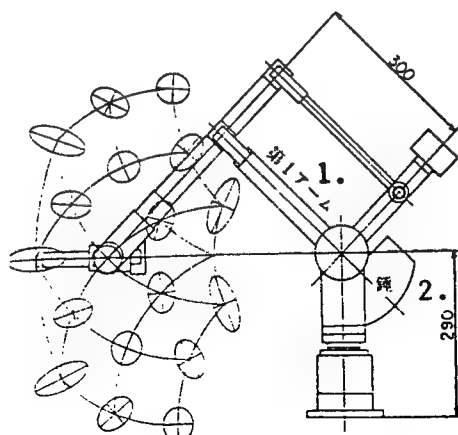**(Space Master Arm)**

Key: 1. 1st arm

Figure 2. Distribution of Mass Ellipsoids
(Ground Master Arm)

Key: 1. 1st arm   2. Weight

minor axes of these ellipses corresponds to the square root of the tip mass, and the mass crossing at right angles to the surface of paper is uniform for almost the same size. Figure 2 shows the distribution of mass ellipsoids of the ground master arm designed so that the mass characteristics are almost the same as those of the above space master arm. A weight of 14 kg is installed below the first arm of the ground master arm so that it experiences a weightless state, but when compared with the space master arm, there is little change in the main axis or in the volume of the mass ellipsoids. Therefore, if this ground master arm is used, it will become possible to simulate the operation of the space master arm. Figure 3 [not reproduced] shows an overall view of the ground master arm made on a trial basis.[2]

3. Configuration of Master Slave System with Different Structure

Three methods of controlling the bilateral master slave system have been studied for a long time. They are termed the "symmetrical," "force reverse transmitting," and "force feedback" control methods. The configuration of this system is designed so that four control methods, including a unilateral control method, can be compared and studied. It is also possible to determine the expansion and reduction of positions and force freely and to change the slave arm standard operating point. The control system consists of a 68020 central processing unit [CPU] and two 68000 CPUs. The former is in charge of calculating the coordinate transformation of position/force, and is also in charge of the signal processing work of a six-axis force sensor, while the latter is in charge of the servo-calculation of the master arm/slave arms.

4. Bilateral Control Test

Figure 4 shows the results of conducting a test of the force reverse transmitting control system to determine whether or not the force imposed on the slave arm is
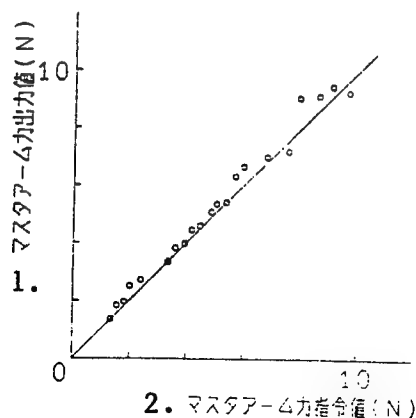

Figure 4. Test of Response of Master Arm Force
Key:
1. Master arm output value (N)
2. Master arm force command value(N)

transmitted precisely to the master arm. It is believed that the force sense is almost satisfactory since the error against the command value is within 10 percent.

5. Postface

We have devised a space-use master arm with excellent operation properties, and have made a master arm which can be used to simulate the space master arm on the ground. In addition, we have constructed a comprehensive bilateral master slave system employing the master arm, and have checked to ensure that the force is transmitted to the master arm precisely. In the future, we plan to improve the operation properties of this system by adding a partially autonomous function, etc.

References

1. Arai and Nakano, "Bilateral Master Slave Control Among Manipulators with Different Structures," JAPAN ROBOT JOURNAL, Vol 4 No 5, 1986 pp 3-13.

2. Gomomoi and Nakajima, "Development and Design of Master Arm with Omnidirectional and Iso-Inertial Mass," scheduled to be printed in compilation C of the JOURNAL OF THE JAPAN MECHANICAL ENGINEERING ASSOCIATION.

Study of Hand Controller for Robots

[Article by Shinichiro Nishida, Ryo Okamura and Yasuo Shinomiya of the Komukai Works, Toshiba Corporation]

[Text] 1. Preface

In order to safely and precisely carry out the required tasks while teleoperating space robots in accordance with the situation, it is important to develop a highly functional operating device (hand controller appropriate for use in space robots). The following is a report of the results of studying this hand controller, a configuration of the orthogonal coordinate-type hybrid master as an optimum form, and the control system.

2. Premise for Study

The operating device was studied assuming the following items:

• The operating device can generally be used for arbitrary arms with six degrees of freedom.
• The correspondence of the operating device to the double arms shown in Figure 1 was studied based on the philosophy that it will be used as an EVA substitute.
• Care was taken with regard to weight and operation space when considering installing the operating device on a space station.
• A wide range of tasks were assumed, extending from precise work to tasks involving large mass objects.
• Remote control was assumed to be based on the main information generated by images from a TV camera installed on the arm base (Figure 2 not reproduced.)
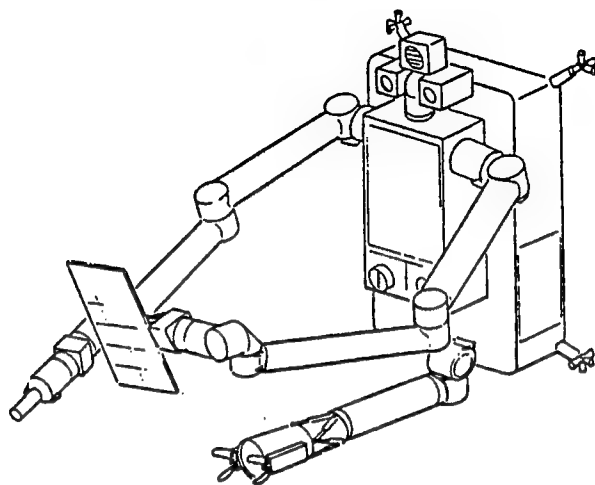
Figure 1. Double-arm EVA Robot

3. Study of Systems as Operating Devices

The systems listed in Table 1 are generally regarded as the operating devices through which humans give instructions for robot movement. The following results have been obtained from experiments on the operation of manipulators. Agravity is simulated in these experiments.

- It is important to use natural contact with human senses in the assembly and combining work requiring skill. An inner force sense is particularly important for such work.
- When large mass objects are handled, a smaller inner force sense will simplify the operation.
- Visual information is important at all times.

When the above items are taken into consideration, it is preferable that the operating device have a driving mechanism with six degrees of freedom or more in order for the inner force senses to be transmitted to humans, and another mechanism enabling the position and speed commands to be switched by one-touch operation. The basic configurations shown in Table 2 are cited as mechanisms realizing three-dimensional operations.

Table 1.
Main Operation Device Systems

Classification	Example of System
On-off mechanism	Switch and keyboard
Pointer mechanism	Mouth, touch panel, track ball
Passive mechanism	Joystick and lever
Active mechanism	Robot mechanism and gripping section

There is little danger caused by excessive operations in the isomorphic M/S where the relationship between the degrees of freedom of the master and slave arms and the coordinates is similar because changes in operation

Table 2. Example of Basic Configuration of Three-Dimensional Operation Mechanism

方式 1.	構成図 2.	手首位置設定 3. 自由度	特異変形 (手首:分離) 4.	座標変換 (先端→関節) 5.
直交座標 タイプ 6.		T-T-T 並進:3 7. 回転:0 8.	0	演算量:0 9.
円筒座標 タイプ 10.		R-T-T 並進:2 11. 回転:1 12.	1	演算量:小 13.
極座標 タイプ 14.		R-R-T 並進:1 15. 回転:2 16.	1	演算量:中 17.
多関節 タイプ 18.		R-R-R 並進:0 19. 回転:3 20.	2 肘伸び姿勢 を含む 21.	演算量:大 22.

Key:
1. Type
2. Block diagram
3. Setting of wrist position and degree of freedom
4. Specific attitude (wrist: separate)
5. Coordinate transformation (tip → joint)
6. Orthogonal coordinate type
7. Translation: 3
8. Rotation: 0
9. Amount of calculation: 0
10. Cylindrical coordinate type
11. Translation: 2
12. Rotation: 1
13. Amount of calculation: small
14. Polar coordinate type
15. Translation: 1
16. Rotation: 2
17. Amount of calculation: medium
18. Articulated type
19. Translation: 0
20. Rotation: 3
21. Including elongation attitude of elbow
22. Amount of calculation: great

possibilities accompanying the operations in both are equivalent. When such a relationship is not similar (different coordinates or different structure), the changes differ and areas with low operation possibilities exist independently. Therefore, areas with low operation properties exist widely in movable ranges.

Accordingly, general-purpose operating devices must have a low specific attitude and low change of operation possibilities depending on the position. The orthogonal coordinate system is an optimal operating device since its position requires no specific attitude and a small
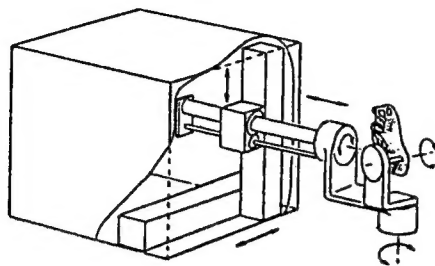
Figure 3. Hybrid Master

amount of calculation is necessary for coordinate transformation. Three axes which command the attitude at the tope intersect at a point on the gripping section. Figure 3 shows a hybrid master constructed according to the previously-mentioned premises. This hybrid master is of the panel-fitting type.

4. Control Method

With regard to the hybrid master studied, force is controlled to control the inner force senses, and the position and speed commands can be switched by one-touch operation. Also, a function for making both functions coexist is useful for the hybrid master. Figure 4 shows a control system for the master (about a certain axis).
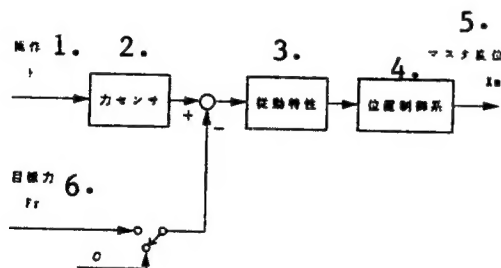

Figure 4. Hybrid Master Control System

Key:
1. Operation
2. Force sensor
3. Slave characteristics
4. Position control system
5. Master displacement
6. Target force

The RMRC position and speed control system is optimal for controlling the slave. Such RMRC control is used in the Japan Experiment Module Remote Manipulator System [JEMRMS] main arm. A wide range of operations, as well as skilled operations, can be commanded, regardless of the arm length, while switching the position and speed commands.

5. Summary

We have studied an operating device appropriate for use in space robots, and have studied the construction and control method of the orthogonal-type hybrid master as an optimal system.

References

1. "Developing M/S Manipulator," NIKKEI MECHANICAL, 23 Apr 1984, pp 49-55.

Development of Hand Controller for Space Robots

[Article by Yasuo Shinomiya, Susumu Ito, Nobuto Matsuhiraku and Makoto Asakura of Toshiba Corporation]

[Text] 1. Preface

The Japan Experimental Module [JEM]'s manipulator consists of a main arm and subarm, and the subarm is controlled with a master slave control system. Up to now, operations have been carried out with the same type of master, having good operating intuition. We have developed and trial manufactured an orthogonal-type master of a different type due to the outfitting properties in the pressurized cabin and the narrowness of the operating space, and have studied the operation properties of this master. It is possible to use this master as a six-axis hand controller even when using a speed command mode, and to use the main arm and subarm together.

2. Photograph 1 [not reproduced] shows the exterior of the six-axis hand controller made on a trial basis. Figure 1 shows the configuration of the degrees of freedom of the six-axis hand controller. This controller is of the orthogonal coordinate type, employs ball screws in three direct-acting axes, and has a stroke of 150 mm. The wrist attitude is devised so that the intersection point of the three axes is in the center of the gripping section and the amount of calculation of coordinate transformation is reduced. Also, the gripping section is equipped with a switch for opening and closing the hand and one for changing the mode. In addition, although unnecessary in space, the empty weight has been compensated for by using a constant force spring and a counter weight in order to conduct ground tests.

When this controller is used as a master arm, the position and the attitude can be commanded individually to the slave arms. The recognition of the overall shape of the slave arms is inferior to that of the same type of master arm alone, but general-purpose master arms with good operation properties can be obtained.

It is possible to use the controller as a speed system like a joystick so that the controller commands the speed in proportion to the displacement or force from the equilibrium position.
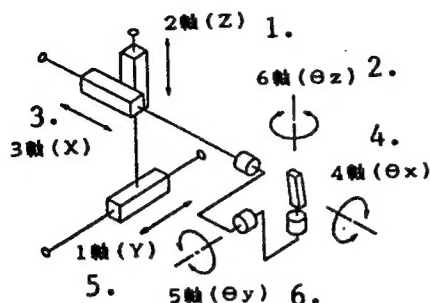
Figure 1. Configuration of Degree of Freedom of Master

Key:
1. Two-axis (Z)
2. Six-axis (θz)
3. Three-axis (X)
4. Four-axis (θx)
5. One-axis (Y)
6. Five-axis (θy)

Figure 2. Control Block Diagram

Key:
1. Master
2. Torque sensor
3. Motor
4. Encoder
5. Force feedback ratio
6. Compensation for empty weight
7. Slave
8. Ratio of expansion and contraction of displacement
9. Order transformation

3. Slave Arm

A vertically articulated arm with basically the same structure as that of the subarms was used as the slave arm. Photograph 2 [not reproduced] shows the exterior of the slave arm. Table 1 gives the basic specifications for a six-axis hand controller consisting of a master arm and slave arms. The empty weight of these slave arms is compensated for by the use of a computer.

**Table 1.
Specifications of Manipulator**

	Slave	Master
Structure	Articulated type	Orthogonal coordinate type
Degrees of freedom	6 + 2 (hand)	6
Arm length	1 m	0.5 m
Tip load	50 N	25 N/0.45 Nm
Tip speed	60 cm/s	40 cm/s
Hand	Parallel opening and closing, snap	Opening and closing switch

4. Control Method

A torque sensor is installed on each axis to control the master arm and slave arms. Force feedback-type bilateral control is carried out as well. Deviations are found and controlled by transforming a standard coordinate system through coordinate transformation since the master arm and slave arms differ in respect to form. Figure 2 shows a control block diagram for this case.

Control modes are shown below, and can be changed with a gripper switch.
(1) Position command mode (master and slave modes)
(2) Position-speed command mode (position: speed command, and attitude: position command)
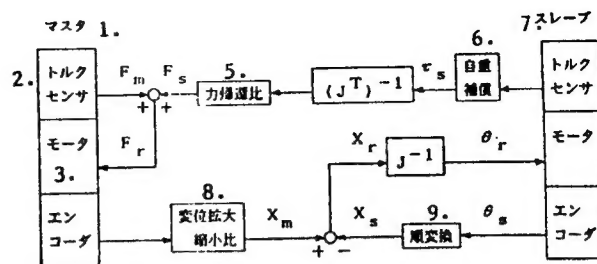(3) Speed command mode (joystick mode)

In addition, movement of origin, displacement/(speed) scale conversion and the setting/change of force feedback ratio are cited as auxiliary functions. The master arm has a small operating area of 150 mm. Such small operating areas are effective for wide working areas of slave arms.

5. Experiment on Demonstration of Operation Properties

Several kinds of experiments were conducted to demonstrate and check the operation properties of this six-axis hand controller. As an example of the subarm operation, an experiment involving the assembly of an antenna and one on engaging a clearance of 0.1 mm were conducted by using a teleoperation system through a stereoscopic TV. Good results were obtained from both experiments.

In addition, an experiment on gross movement was conducted by using a speed command mode, and the positioning work was carried out satisfactorily by using the position-speed command mode mentioned in (2) rather than the full speed command mode in (3). However, instead of using the 10-meter-main arm of the JEMRMS, a slave arm of the same length was used in this experiment. Therefore, it is believed to be necessary to carry out evaluations by using a very long arm equivalent in length to the main arm in the future.

6. Summary

We have developed a compact and orthogonal coordinate-type six-axis hand controller with high outfitting properties, and have obtained satisfactory operation results with respect to the force feedback-type master and slave control and position-speed command joint-use-type control. This controller is promising because, except for its gripping section, it will have dimensions of 30 cm^2 or less and a weight of 10 kg or less. We have proposed the adoption of this controller in the operation devices used to make the main arm and subarms of the JEMRMS uniform, because we have judged the controller to be optimal for these operation devices.

Foreign Broadcast Information Service (FBIS) and Joint Publications Research Service (JPRS) publications contain political, economic, military, and sociological news, commentary, and other information, as well as scientific and technical data and reports. All information has been obtained from foreign radio and television broadcasts, news agency transmissions, newspapers, books, and periodicals. Items generally are processed from the first or best available source; it should not be inferred that they have been disseminated only in the medium, in the language, or to the area indicated. Items from foreign language sources are translated; those from English-language sources are transcribed, with personal and place names rendered in accordance with FBIS transliteration style.

Headlines, editorial reports, and material enclosed in brackets [ ] are supplied by FBIS/JPRS. Processing indicators such as [Text] or [Excerpts] in the first line of each item indicate how the information was processed from the original. Unfamiliar names rendered phonetically are enclosed in parentheses. Words or names preceded by a question mark and enclosed in parentheses were not clear from the original source but have been supplied as appropriate to the context. Other unattributed parenthetical notes within the body of an item originate with the source. Times within items are as given by the source. Passages in boldface or italics are as published.

SUBSCRIPTION/PROCUREMENT INFORMATION

The FBIS DAILY REPORT contains current news and information and is published Monday through Friday in eight volumes: China, East Europe, Soviet Union, East Asia, Near East & South Asia, Sub-Saharan Africa, Latin America, and West Europe. Supplements to the DAILY REPORTs may also be available periodically and will be distributed to regular DAILY REPORT subscribers. JPRS publications, which include approximately 50 regional, worldwide, and topical reports, generally contain less time-sensitive information and are published periodically.

Current DAILY REPORTs and JPRS publications are listed in *Government Reports Announcements* issued semimonthly by the National Technical Information Service (NTIS), 5285 Port Royal Road, Springfield, Virginia 22161 and the *Monthly Catalog of U.S. Government Publications* issued by the Superintendent of Documents, U.S. Government Printing Office, Washington, D.C. 20402.

The public may subscribe to either hardcover or microfiche versions of the DAILY REPORTs and JPRS publications through NTIS at the above address or by calling (703) 487-4630. Subscription rates will be provided by NTIS upon request. Subscriptions are available outside the United States from NTIS or appointed foreign dealers. New subscribers should expect a 30-day delay in receipt of the first issue.

U.S. Government offices may obtain subscriptions to the DAILY REPORTs or JPRS publications (hardcover or microfiche) at no charge through their sponsoring organizations. For additional information or assistance, call FBIS, (202) 338-6735,or write to P.O. Box 2604, Washington, D.C. 20013. Department of Defense consumers are required to submit requests through appropriate command validation channels to DIA, RTS-2C, Washington, D.C. 20301. (Telephone: (202) 373-3771, Autovon: 243-3771.)

Back issues or single copies of the DAILY REPORTs and JPRS publications are not available. Both the DAILY REPORTs and the JPRS publications are on file for public reference at the Library of Congress and at many Federal Depository Libraries. Reference copies may also be seen at many public and university libraries throughout the United States.

NOTICE

JPRS will soon begin publication of a new report in the Worldwide series: ENVIRON-MENTAL ISSUES. The report will compile open-source material from all parts of the world on a wide range of environmental topics, ranging from localized pollution problems to global ecological concerns, in all their political dimensions.

Current DAILY REPORTs and JPRS publications are listed in *Government Reports Announcements* issued semimonthly by the National Technical Information Service (NTIS), 5285 Port Royal Road, Springfield, Virginia 22161 and the *Monthly Catalog of U.S. Government Publications* issued by the Superintendent of Documents, U.S. Government Printing Office, Washington, D.C. 20402.

The public may subscribe to either hardcover or microfiche versions of the DAILY REPORTs and JPRS publications through NTIS at the above address or by calling (703) 487-4630. Subscription rates will be provided by NTIS upon request. Subscriptions are available outside the United States from NTIS or appointed foreign dealers. New subscribers should expect a 30-day delay in receipt of the first issue.

U.S. Government offices may obtain subscriptions to the DAILY REPORTs or JPRS publications (hardcover or microfiche) at no charge through their sponsoring organizations. For additional information or assistance, call FBIS, (202) 338-6735, or write to P.O. Box 2604, Washington, D.C. 20013. Department of Defense consumers are required to submit requests through appropriate command validation channels to DIA, RTS-2C, Washington, D.C. 20301. (Telephone: (202) 373-3771, Autovon: 243-3771.)